Compte rendu de la
ONZIÈME RENCONTRE
DE MORIOND
Flaine - Haute-Savoie (France) 29 Février - 12 Mars 1976

VOL. II

INTERACTIONS FAIBLES ET PHYSIQUE DES NEUTRINOS

J. TRAN THANH VAN

SOUS LE HAUT PATRONAGE DE

- INSTITUT NATIONAL DE PHYSIQUE NUCLEAIRE ET DE PHYSIQUE DES PARTICULES
- COMMISSARIAT A L'ENERGIE ATOMIQUE
- LABORATOIRE DE L'ACCELERATEUR LINEAIRE
- LABORATOIRE DE PHYSIQUE THEORIQUE ET HAUTES ENERGIES
- LABORATOIRE DE PHYSIQUE THEORIQUE ET PARTICULES ELEMENTAIRES

PUBLICATION SUBVENTIONNEE PAR LE C.N.R.S.

La deuxième session de la Onzième Rencontre de Moriond sur
« Interactions faibles et Physique des neutrinos »
était organisée par

J. Trân Thanh Vân

R. Turlay

et J. Iliopoulos

Secrétariat permanent :

Rencontre de Moriond

Laboratoire de Physique Théorique et Particules Elémentaires
Bâtiment 211 - Université de Paris-Sud
91405 ORSAY (France)
Tél. 941.73.72 - 941.73.66

Proceedings of the

ELEVENTH RENCONTRE DE MORIOND

Flaine - Haute-Savoie (France) February 28 - March 12, 1976

VOL. II

WEAK INTERACTIONS AND NEUTRINO PHYSICS

edited by

J. TRAN THANH VAN

SPONSORED BY

- INSTITUT NATIONAL DE PHYSIQUE NUCLEAIRE ET DE PHYSIQUE DES PARTICULES
- COMMISSARIAT A L'ENERGIE ATOMIQUE
- LABORATOIRE DE L'ACCELERATEUR LINEAIRE
- LABORATOIRE DE PHYSIQUE THEORIQUE ET HAUTES ENERGIES
- LABORATOIRE DE PHYSIQUE THEORIQUE ET PARTICULES ELEMENTAIRES

AND BY THE C.N.R.S. FOR PUBLICATION

The Second Session or the Eleventh Rencontre de Moriond on
Weak Interactions and Neutrino Physics
was organized by

J. Trân Thanh Vân

R. Turlay

and J. Iliopoulos

Secrétariat permanent :

Rencontre de Moriond

Laboratoire de Physique Théorique et Particules Elémentaires
Bâtiment 211 - Université de Paris-Sud
91405 ORSAY (France)
Tél. 941.73.72 - 941.73.66

AVANT - PROPOS

La Rencontre de Moriond qui s'est tenue du 29 février au 12 mars 1976 à Flaine (Haute-Savoie), est la onzième d'une série commencée en 1966.

La première Rencontre a eu lieu à Moriond dans des chalets savoyards où les physiciens, expérimentateurs et théoriciens, partageaient non seulement leurs préoccupations scientifiques, mais aussi les tâches culinaires et les travaux ménagers. Elle regroupait principalement les physiciens français travaillant dans les interactions électromagnétiques. Au cours des Rencontres suivantes, venait s'ajouter à la session sur les interactions électromagnétiques, une session sur les interactions fortes à hautes énergies.

Le but principal de ces Rencontres est d'une part, de faire le point sur les récents développements de la physique contemporaine, et d'autre part, de promouvoir une collaboration effective entre expérimentateurs et théoriciens dans le domaine des interactions électromagnétiques et des particules élémentaires. Par ailleurs, la durée relativement longue de la Rencontre et le faible nombre des participants, doivent permettre à la fois une meilleure connaissance humaine entre les participants et une discussion approfondie et détaillée des communications présentées.

Ce souci de recherche et d'expérimentation de nouvelles formes de communication, de nouveaux terrains d'échange et de dialogues, qui depuis l'origine anime les Rencontres de Moriond, nous a

amenés, il y a six ans, à susciter la création pour les biologistes de la première Rencontre de Méribel sur la Différenciation Cellulaire qui se tient en même temps et dans les mêmes locaux que la première session de la Rencontre de Moriond. Des séminaires communs ont été organisés afin d'étudier dans quelle mesure les méthodes d'analyse utilisées en physique pouvaient être appliquées à certains problèmes qui se posent en biologie. Ces conférences ainsi qu'une table ronde sur les problèmes actuels de la Biologie ont suscité de nombreuses discussions "informelles", animées et enrichissantes entre biologistes et physiciens. Ces échanges font espérer qu'un jour peut-être, les problèmes, pour le moment si complexes, posés en Biologie, donneront naissance à de nouvelles méthodes d'analyse ou à de nouveaux langages mathématiques.

La première session de la onzième Rencontre de Moriond (29 février au 6 mars 1976), est consacrée aux interactions hadroniques à hautes énergies. G. KANE, L. MONTANET ainsi que B. et F. SCHREMPP m'ont aidé à l'élaboration du programme de la Rencontre.

La seconde session (6 au 12 mars 1976) est consacrée aux interactions faibles et à la physique des neutrinos, et la coordination est assurée par R. TURLAY et J. ILIOPOULOS. Une attention particulière a porté sur la recherche des particules charmées.

Mmes Geneviève BEUCHEY et Marie-Thérèse PILLET, et Mlle M. ROUSSELLE ont dépensé beaucoup de temps et d'efforts pour la réussite de cette Rencontre.

Au nom de tous les participants, nous les remercions.

J. TRAN THANH VAN

FOREWORD

The Rencontre de Moriond held at Flaine - Haute-Savoie (France) from February 29 to March 12, 1976, was the eleventh such Meeting.

The first one was held in 1966 at Moriond in the French Alps. There, Physicists - experimentalists as well as theoricians - not only shared their scientific preoccupations but also household chores. That Meeting grouped essentially French physicists interested in electromagnetic interactions. At following Meetings a session on high energy strong interactions was added to the electromagnetic one.

The main purpose of these Meetings is to discuss recent developments of contemporary physics and to promote effective collaboration between experimentalists and theoricians in the field of electromagnetic interactions and elementary particles. Besides, the length of the Meeting coupled with the small number of participants favours better human relations as well as a more thorough and detailed discussion of the contributions.

This concern for research and experimentation of new channels of communication and dialogue which from the start animated the Moriond Meetings, incited us, six years ago, to organize a simultaneous Meeting of biologists on Cellular Differentiation at Meribel-les-Allues. Common seminars were organized to study to what extent analytical methods used in physics could be applied to some biological problems. They led us to hope that biological problems, at present

so complex, may give birth in the future to new analytical methods or new mathematical languages.

The first session of the eleventh Rencontre de Moriond (February 29 - March 6, 1976) is devoted to high energies hadronic interactions. G. KANE, L. MONTANET, Barbara and F. SCHREMPP have given me their help in setting the program of the Rencontre.

The second session (March 6 - 12, 1976) was devoted to Weak Interactions and Neutrino Physics and the coordination was assumed by R. TURLAY and J. ILIOPOULOS.

Ms. G. BEUCHEY, M.T. PILLET and M. ROUSSELLE devoted much of their time and energy to the success of this Meeting.

On behalf of the participants I thank them.

J. TRAN THANH VAN

PARTICIPANTS

ALITTI Jean	D.Ph.P.E. Saclay, BP 2, 9II90 Gif sur Yvette, France
BAULIEU Laurent	Physique Théorique, E.N.S., 75231 Paris, France
BERTHELOT André	D.Ph.P.E. , C.E.N. Saclay, BP 2, 9II90 Gif sur Yvette,France
BERTLMANN Reinhold	Institut for Theor. Physics, Univ. of Vienna, I090 Vienna, Austria
BLUM Daniel	Laboratoire de l'Accélérateur Linéaire, 91405 Orsay, France
BOYER Christian	Laboratoire de Physique Théorique et Particules Elémentaires, 91405 Orsay, France
BRISSON Violette	L.P.N.H.E., Ecole Polytechnique, 9II20 Palaiseau, France
CLELAND Wilfred	Dept of Physics, Univ. of Pittsburgh, Pittsburgh, PA. 15260, U.S.A.
COIGNET Guy	CERN, 1211 Genève 23, Suisse
COUNIHAN Martin	CERN, 1211 Genève 23, Suisse
CUNDY Donald	CERN, 1211 Genève 23, Suisse
DAR Arnon	Laboratoire de Physique Théorique et Particules Elémentaires, 91405 Orsay, France
DIAMOND Ronald	Physics Dept, Univ. of Michigan, Ann Arbor, Michigan, U.S.A.
DONOHUE Jack	Physique Théorique, Univ. de Bordeaux, 33170 Gradignan,France
DRUKIER Andrzej	Physique des Solides, 91405 Orsay, France
DOMINGUEZ Cesarea	Inst. Politecnico Nacional, Apartado Postal 14-740, Mexico 14, D.F.
GAILLARD Mary	CERN, 1211 Genève 23, Suisse
GAILLARD Jean-Marc	CERN, 1211 Genève 23, Suisse
GIAZOTTO Alberto	INFN, Via Vecchia Livornese, S. Piero A Grado, Pisa, Italy
BODEK Arie	Enrico Fermi Inst. Univ. of Chicago, Chicago, IL 60637,U.S.A.
GOULIANOS Konstantinos	The Rockefeller University, New York, NY 1002, U.S.A.
HAYOT Fernand	D.Ph.T., C.E.N. Saclay, BP 2, 9II90 Gif sur Yvette,France

ILIOPOULOS Jean	Laboratoire de Physique Théorique, E.N.S., 75231 Paris,France
JAEKEL Marc-Thierry	Laboratoire de Physique Théorique, E.N.S., 75231 Paris,France
JAFFRE Michel	Laboratoire de l'Accélérateur Linéaire, 91405 Orsay, France
KANG Kyungsik	Brown Univ.Providence, RI 02912, U.S.A.
KINGSLEY Roger	Rutherford Lab. Chilton, Didcot, Oxon, OX11 0QX, England
LIPKIN Harry	Dept of Physics, Weizmann Institute of Science, Rehovot,Israel
MANOLESSOU-CRAMMATICOU	D.Ph.T. C.E.N. Saclay, BP 2, 91190 Gif sur Yvette, France
MERLO Jean-Pierre	D.Ph.P.E., C.E.N. Saclay, BP 2, 91190 Gif sur Yvette, France
MEYER Joachim	CERN, 1211 Genève 23, Suisse
MUSSET Paul	CERN, 1211 Genève 23, Suisse
NACHTMANN Otto	Institute for Theor. Physics, Univ. of Heidelberg, Germany
NANOPOULOS Demeter	Laboratoire de Physique Théorique, E.N.S., 75231 Paris,France
NAROSKA Beate	CERN, 1211 Genève 23, Suisse
ORR Robert	CERN, 1211 Genève 23, Suisse
PARISI Giorgio	Laboratori Nazionali Frascati, 00044 Frascati, Italy
PETIAU Pierre	Ecole Polytechnique, L.P.N.H.E., 91120 Palaiseau, France
PORTH Paul	CERN, 1211 Genève 23, Suisse
RENARDY Jean-François	D.Ph.P.E., C.E.N. Saclay, BP 2, 91190 Gif sur Yvette, France
RIESTER Jean-Louis	Centre de Recherches Nucléaires, 67037 Strasbourg, France
ROMANO Francesco	CERN, 1211 Genève 23, Suisse
ROSS Graham	CERN, 1211 Genève 23, Suisse
ROUSSET André	D.G.R.S.T., 35 rue St Dominique, 75700 Paris, France
SAKURAI	CERN, 1211 Genève 23, Suisse
SAUVAGE Gilles	Laboratoire de l'Accélérateur Linéaire, 91405 Orsay, France
SHEN Benjamin	CERN, 1211 Genève 23, Suisse
STEINBERGER	CERN, 1211 Genève 23, Suisse
SUTER Henry	CERN, 1211 Genève 23, Suisse
RUBBIA Carlo	CERN, 1211 Genève 23, Suisse

THEWS Robert	Physics Dept, Univ.of Arizona, Tucson, AZ 8572I, U.S.A.
TITTEL Klaus	69 Heidelberg, Inst. für Hochenenergiephysik, Germany
TURLAY René	D.Ph.P.E., Saclay, BP 2, 9II90 Gif sur Yvette, France
VALENT Galliano	Laboratoire de Physique Théorique et Hautes Energies, Univ. Paris VII, 2 place Jussieu, 7522I Paris, France
VAN DAM Petrus	Ecole Polytechnique, LPNHE, 9II20 Palaiseau, France
WILLIAMS W.S.C.	Dept of Nuclear Physics, Univ. of Oxford, Oxford OXI 3RH,Englan
WILLUTZKI Hans	CERN, I2II Genève 23, Suisse
TRAN THANH VAN	Laboratoire de Physique Théorique et Particules Elémentaires, 9I405 Orsay, France

Secrétariat :

BEUCHEY Geneviève	D.Ph.P.E./S.E.E., CEN Saclay, B.P. 2 91190 Gif-sur-Yvette (France)
PILLET Marie-Thérèse ROUSSELLE Monique	Laboratoire de Physique Théorique et Particules Elementaires, Bât. 211, Université de Paris-Sud, 91405 Orsay (France)

CONTENTS

I. DEEP INELASTIC SCATTERING

O. NACHTMANN	"The parton model revisited"	17
W.S.C. WILLIAMS	"Deep inelastic muon scattering"	43
W.S.C. WILLIAMS	"Hadron production in inelastic muon scattering at 147 GeV"	58
G. COIGNET	"Experimental program planned at S.P.S. by the European Muon Collaboration"	67
G. PARISI	"An introduction to scaling violations"	83

II. NEUTRINO INTERACTIONS

M. JAFFRE	"Charmed particle search in the Gargamelle neutrino experiment"	115
D.C. CUNDY	"The production of $\mu^- e^+$ events in high energy neutrino interactions"	123
D.C. CUNDY	"A study of inclusive strange particle production by neutrinos interacting in hydrogen at FNAL"	127
R.N. DIAMOND	"Recent results on ν-p and $\bar{\nu}(H_2 - N_e)$ Interactions in the Fermilab 15' Bubble Chamber"	133
M.K. GAILLARD	"Aspects of charm"	147

III. MISCELLANEOUS

A. DAR	"How to investigate future energy domains of particle physics with present accelerators ?"	183

C.A. DOMINGUEZ	"Modified Adler sum rule and violation of charge symmetry"	203
D.V. NANOPOULOS	"CP violation, Heavy fermions and all that"	209
A. GIAZOTTO	"Latest results on the axial vector form factor"	229
F. HAYOT	"More than four quark flavors and vector-like models"	237
K. KANG	"Five quark model with flavour-changing neutral current and dimuon events"	245

IV. NEUTRAL CURRENTS

V. BRISSON	"Neutral currents in Gargamelle"	253
A. BODEK	"Experimental studies of neutral currents with the Fermilab narrow band neutrino beam"	267
K. GOULIANOS	"Experimental study of exclusive neutral current reactions and search for μe-pairs at BNL"	283
J.J. SAKURAI	"Eight questions you may ask on neutral currents"	299

THE PARTON MODEL REVISITED

Otto NACHTMANN

Institut für Theoretische Physik
der Universität Heidelberg

Abstract : The basic concepts of the parton model are briefly recalled. In the framework of this model we discuss then the main features of the structure of the nucleons as revealed by the deep inelastic lepton nucleon scattering experiments.

Résumé : Les notions fondamentales du modèle des partons sont rappelées brièvement. Après, nous exposons dans le cadre de ce modèle, les résultats principaux concernant la structure des nucléons qui ont été obtenus par les expériences sur la diffusion profondément inélastique des leptons sur des nucléons.

CONTENTS.

I. INTRODUCTION.

II. KINEMATICS AND GENERAL PARTON CONCEPTS.

III. ELECTRON NUCLEON SCATTERING.

IV. NEUTRINO NUCLEON SCATTERING INVOLVING CHARGED CURRENTS.

V. NEUTRAL CURRENT INTERACTIONS.

VI. NAIVE EXPECTATIONS FOR PRODUCTION OF CHARMED PARTICLES.

I. INTRODUCTION.

The idea to consider hadrons as bound states of pointlike constituents, partons, introduced by Feynman [1], and its application to lepton hadron scattering, initiated by Bjorken and Paschos [2], proved to be enormously successful. The famous SLAC-MIT experiments on deep inelastic electron nucleon scattering and the neutrino experiments done at CERN with Gargamelle told us a lot about hadrons and strong interactions. A brief summary of what we think to have learnt would be as follows :

(i) The experimental verification of (approximate) Bjorken scaling behaviour shows that strong interactions at short distances are weakened and that therefore the parton concept makes sense.

(ii) Comparison of electron and neutrino scattering data reveals that partons which couple to the electromagnetic and weak currents have spin 1/2 and carry fractional charges of the Gell-Mann Zweig quarks [3].

(iii) A fast moving nucleon looks like a jet of fast quarks plus an infinite sea of slow quarks and antiquarks. Roughly half of the momentum of the nucleon is carried by partons other than quarks, probably "gluons".

In these talks which are addressed to experimentalists, I intend to discuss on an elementary level how this information is obtained from the data. We will give a rapid survey of kinematics, the general parton model ideas, then we will discuss in more detail neutrino reactions via charged and neutral currents.

II. KINEMATICS AND GENERAL PARTON CONCEPTS.

We are interested in deep inelastic lepton-nucleon scattering described by the diagram of Figure 1.

$$\ell(k) + N(p) \to \ell'(k') + X(p') \qquad (2.1)$$

Specifically, we will treat the following reactions :

$$
\begin{aligned}
&e + N \to e + X \\
&\nu_\mu + N \to \mu^- + X \\
&\bar{\nu}_\mu + N \to \mu^+ + X \\
&\nu_\mu + N \to \nu_\mu + X \\
&\bar{\nu}_\mu + N \to \bar{\nu}_\mu + X
\end{aligned}
\qquad (2.2)
$$

The relevant kinematic variables are listed in the Table.
The lepton masses will be neglected throughout these talks.
The metric and γ-matrix conventions follow Bjorken and Drell.

VARIABLE	MEANING
$E = \frac{pk}{M}$	Energy of the initial lepton.
$E' = \frac{pk'}{M}$	Energy of the final lepton.
θ	Scattering angle of the leptons.
$q = k - k'$	Four momentum transfer.
$Q^2 = -q^2 = 4\,E\,E'\sin^2\frac{\theta}{2}$	Four momentum transfer squared.
$\nu = \frac{pq}{M} = E - E'$	Energy transfer.
$y = \nu/E$	Fractional energy transfer.
$x = \omega^{-1} = Q^2/2M\nu$	Bjorken's scaling variable.
$P = \frac{M\nu}{Q}$	Momentum of the nucleon in the Breit frame.

TABLE : Kinematic variables for lepton hadron scattering.
Noncovariant variables refer to the laboratory frame if not otherwise stated.

The range of the kinematic variables is as follows :

$$Q^2 \geq 0 \qquad \nu \geq Q^2/2M$$

$$0 \leq x \leq 1 \qquad 0 \leq y \leq 1 \tag{2.3}$$

where we have assumed $E >> M$ in the second line (see Figure 2).

We will discuss the reaction eq. (2.1) only in the Bjorken limit $\nu \to \infty$, $Q^2 \to \infty$, $x = Q^2/2M\nu$ fixed. It is then convenient to consider the Breit frame where the energies of the initial and final lepton are equal and the four momentum of the nucleon and the four momentum transfer are given by :

$$p^\lambda = (\sqrt{P^2 + M^2}, 0, 0, P)$$

$$q^\lambda = (0, 0, 0, -Q)$$

$$P = M\nu/Q \tag{2.4}$$

In the Bjorken limit $P \to \infty$, i.e. we deal with a fast moving nucleon and hope to be able to apply parton ideas.

The two basic assumptions of the parton model are :

(i) A fast moving nucleon looks like a box of free partons all travelling in nearly the same direction as the nucleon and sharing its momentum.

(ii) The cross section for deep inelastic lepton nucleon scattering is the incoherent sum of the cross sections of the partons weighted with the probability to find the partons inside the nucleon. In the scattering the partons are to be considered as free, pointlike particles, i.e. we assume the validity of the impulse approximation.

A deep inelastic lepton hadron scattering event in the parton picture is shown in Figure 3.

It is now easy to do calculations since the whole labour is reduced to computing cross sections for point particles. Consider first electron nucleon scattering and assume that we have several parton species labelled

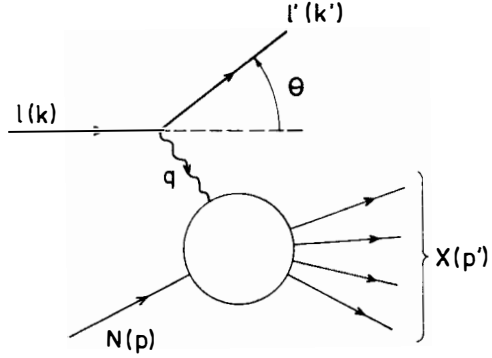

Fig. 1 Lepton nucleon scattering. The four momenta of the particles are indicated in brackets

Fig. 1

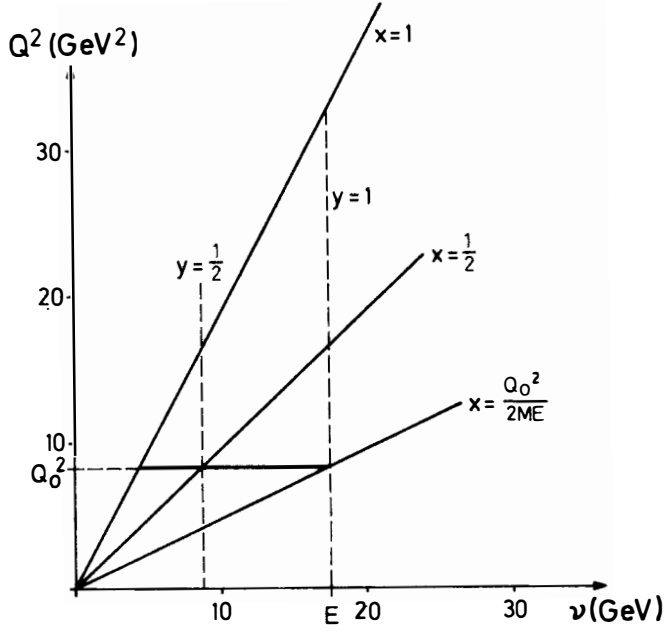

Fig. 2 Kinematic domain for lepton nucleon scattering

Fig. 2

by i which have charges e_i, distribution functions $N_i(x)$ (*) and spin 0 or 1/2. The cross section is then given by :

$$\frac{\partial^2\sigma}{\partial x \partial y}(eN \to eX) = \frac{8\pi\alpha^2}{Q^4} ME$$

$$\{ \frac{1}{2} x \sum_{\text{spin } 1/2} e_i^2 N_i(x) \left[1 + (1-y)^2\right] + x \sum_{\text{spin } 0} e_i^2 N_i(x) (1-y)\} \qquad (2.5)$$

where α is the fine structure constant and we have again assumed E >> M. The sums run over spin 0 or spin 1/2 partons as indicated.

Turning next to neutrino nucleon scattering we assume that we can describe it by an effective current × current interaction :

$$L_{eff} = -\frac{G}{\sqrt{2}} \{ \bar{\mu}\gamma^\lambda(1-\gamma_5)\nu_\mu \, J_\lambda^+ + \bar{\nu}_\mu\gamma^\lambda(1-\gamma_5)\mu \, J_\lambda^- + \bar{\nu}_\mu\gamma^\lambda(1-\gamma_5)\nu_\mu \, J_\lambda^N \} \qquad (2.6)$$

where G is Fermi's constant and $J_\lambda^\pm$, J_λ^N are the weak hadronic charged and neutral currents. If a quark pair q, q' contributes a piece :

$$\bar{q}'\gamma_\lambda(C_V - C_A\gamma_5)q \qquad (2.7)$$

to any of these currents we will obtain a contribution to the cross section as follows : cross section : $\frac{\partial^2\sigma}{\partial x \partial y}(\nu_\mu N \to \ell' X)$, contribution from q and $\bar{q}'$:

$$\frac{G^2 ME}{\pi} \{ \frac{x}{2} \left[N_q(x)(C_V + C_A)^2 + N_{\bar{q}'}(x)(C_V - C_A)^2\right] + \frac{x}{2} \left[N_q(x)(C_V - C_A)^2 + N_{\bar{q}'}(x)(C_V + C_A)^2\right](1-y)^2 \} \qquad (2.8)$$

cross section : $\frac{\partial^2\sigma}{\partial x \partial y}(\bar{\nu}_\mu N \to \bar{\ell}' X)$

(*) $N_i(x)dx$ is the number of partons of species i with momentum (in units of the nucleon momentum) between x and x + dx.

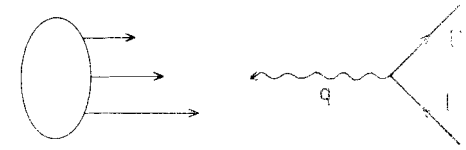

Nucleon

(a)

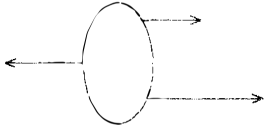

(b)

Fig. 3 Collision of a nucleon with a lepton in the parton model; (a) parton state before, (b) after the collision. Only partons carrying a fraction $x = Q^2/2M\nu$ of the momentum of the nucleon contribute to the scattering for given Q^2 and ν.

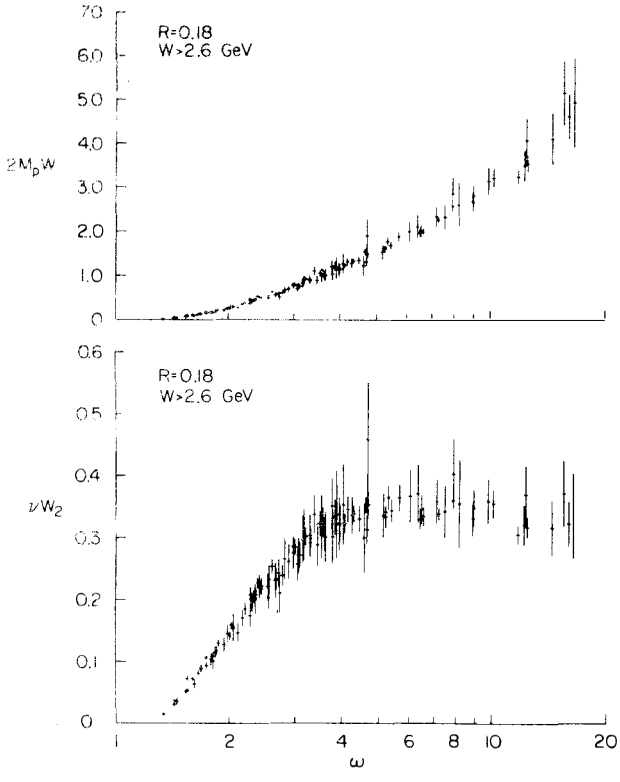

Fig. 4 Experimental results for the structure functions of the proton[4)]

contribution from q and $\bar{q}'$:

$$\frac{G^2 ME}{\pi} \{ \frac{x}{2} [N_q(x)(C_V + C_A)^2 + N_{\bar{q}'}(x)(C_V - C_A)^2] (1-y)^2$$

$$+ \frac{x}{2} [N_q(x)(C_V - C_A)^2 + N_{\bar{q}'}(x)(C_V + C_A)^2] \} \qquad (2.9)$$

Note that the roles of the quark q and the antiquark $\bar{q}'$ are interchanged when going from neutrino to antineutrino scattering.

This is all we need as formulas and we can now turn to a discussion of the experimental results interpreted in terms of the parton model.

III. ELECTRON NUCLEON SCATTERING.

The most important information obtained from electron nucleon scattering is that the structure functions for both the proton and the neutron scale to perhaps ± 15 % as predicted by the naive parton model [4], [5], [6] :

$$2MW_1(\nu, Q^2) = F_1(x) = \sum_{\text{spin } 1/2} e_i^2 N_i(x)$$

$$\nu W_2(\nu, Q^2) = F_2(x) = x \sum_{\text{spin } 1/2} e_i^2 N_i(x) + x \sum_{\text{spin } 0} e_i^2 N_i(x) \qquad (3.1)$$

where the sums run over spin 0 and spin 1/2 partons as indicated. Some experimental results are shown in Figures 4 and 5.

The data of Figures 4 and 5 covers roughly the following kinematic region :

$$1 \text{ GeV}^2 \lesssim Q^2 \lesssim 15 \text{ GeV}^2$$

$$6.75 \text{ GeV}^2 \lesssim M^2 + 2M\nu - Q^2 \lesssim 25 \text{ GeV}^2 \qquad (3.2)$$

The second important point which we learn from the data is that there are few if any charged spin 0 partons in the nucleon. If we neglected all non asymptotic terms, the experimental results would imply [6] :

$$\sum_{\text{spin } 0} e_i^2 N_i(x) / \sum_{\text{spin } 1/2} e_i^2 N_i(x) \simeq 0.17 \qquad (3.3)$$

But we surely must allow for non asymptotic terms at present energies and if we do so everything is quite compatible with no spin 0 partons at all, an alternative which is much more appreciated by theorists.

The third result which we can read out of the experimental data concerns the number of partons in the nucleon. Let us assume that there is a finite number of partons in the nucleon, i.e. that the distribution functions satisfy :

$$\sum_i \int_0^1 dx\, N_i(x) = \text{finite} \tag{3.4}$$

This clearly implies that $N_i(x)$ cannot be as singular as $1/x$ for $x \to 0$ (note that all N_i's must be positive), and therefore we find from eq. (3.1) :

$$F_2(x) \xrightarrow[x \to 0]{} 0 \tag{3.5}$$

Looking at Figure 4 we see that such a behaviour is clearly not indicated by the data which instead suggests for $x \to 0$ ($\omega \to \infty$) :

$$F_2(x) \longrightarrow \text{const} \neq 0 \tag{3.6}$$

Such a behaviour if confirmed by further experiments would imply an infinite number of charged partons in the nucleon.

IV. NEUTRINO NUCLEON SCATTERING INVOLVING CHARGED CURRENTS.

To discuss neutrino nucleon scattering we have to adopt a model which specifies how the weak current acts on the partons. The simplest model is the Gell-Mann Zweig quark model [3] where the electromagnetic and weak charged currents are expressed in terms of the fundamental quark fields u, d, s (up, down, strange) as follows :

$$\begin{aligned} J_\lambda^{em} &= \tfrac{2}{3}\,\bar{u}\gamma_\lambda\, u - \tfrac{1}{3}\,\bar{d}\gamma_\lambda\, d - \tfrac{1}{3}\,\bar{s}\gamma_\lambda\, s \\ J_\lambda^{+} &= \bar{u}\gamma_\lambda\,(1-\gamma_5)d \\ J_\lambda^{-} &= \bar{d}\gamma_\lambda\,(1-\gamma_5)u \end{aligned} \tag{4.1}$$

where we have neglected the Cabibbo angle.

Inserting in our formulae eqs. (2.8) and (2.9), we find for the neutrino and antineutrino cross sections per nucleon on a target consisting of an equal amount of protons and neutrons :

$$\frac{\partial^2\sigma}{\partial x \partial y}(\nu_\mu N \to \mu^- X) = \frac{G^2 ME}{\pi}\{ xN(x) + x\bar{N}(x)(1-y)^2 \}$$

$$\frac{\partial^2\sigma}{\partial x \partial y}(\bar{\nu}_\mu N \to \mu^+ X) = \frac{G^2 ME}{\pi}\{ xN(x)(1-y)^2 + x\bar{N}(x) \} \qquad (4.2)$$

where $N(x)$ and $\bar{N}(x)$ are the distribution functions of quarks and antiquarks in the nucleon. More specifically :

$$N(x) = N_u(x) + N_d(x)$$

$$\bar{N}(x) = N_{\bar{u}}(x) + N_{\bar{d}}(x) \qquad (4.3)$$

where $N_u(x)$, $N_d(x)$ ... are the distribution functions for "up", "down", ... quarks in the proton. (The distribution functions of the neutron are obtained from those of the proton by a charge symmetry operation).

IV.1 : The y-distributions :

Now we discuss some important points concerning the y-distributions.

(i) Since the charged weak currents have a pure V-A structure quarks give a constant term in the neutrino and a $(1-y)^2$ term in the antineutrino cross section. For antiquarks the situation is reversed.

(ii) For y=0 neutrino and antineutrino cross sections become equal. This equality for y=0 must, in fact, hold whenever the charged weak currents are related by a charge symmetry operation in the usual way :

$$P_I^{-1} J_\lambda^+ P_I = -J_\lambda^-$$

$$P_I = e^{i\pi I_2} \qquad (4.4)$$

(remember that we have set the Cabibbo angle to zero). This we can see from eqs. (2.7), (2.8) and (2.9). If the current J_λ^+ contains a contribution :

$$J_\lambda^+ \sim \bar{q}'\gamma_\lambda (C_V - C_A\gamma_5)q \qquad (4.5)$$

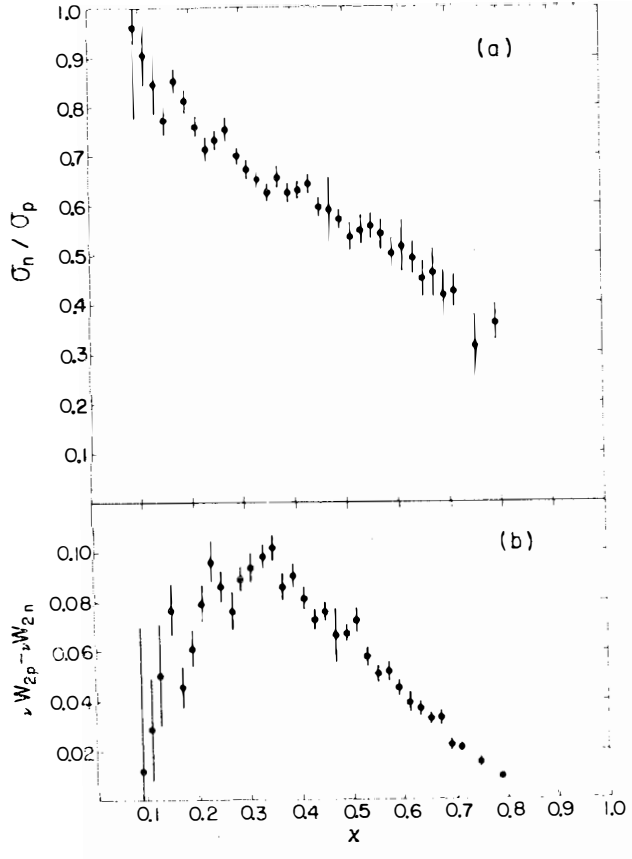

Fig. 5 Experimental results for the structure functions of the neutron compared to those of the proton

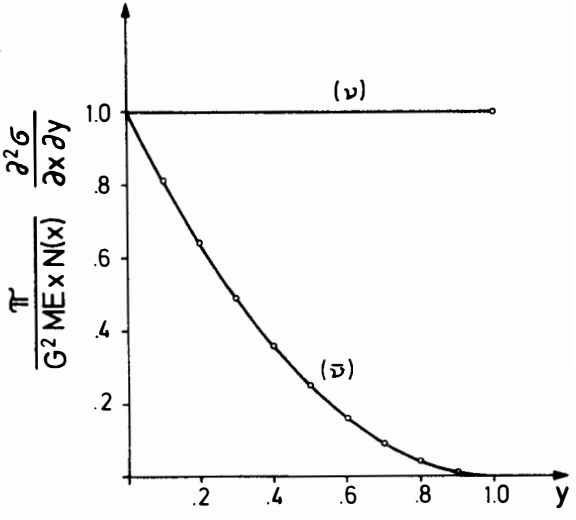

Fig. 6 The y-distributions for neutrino and antineutrino events expected if there are no antiquarks $\bar{u}$, $\bar{d}$ in the nucleon

from a quark pair q', q then eq. (4.4) implies a contribution to J_λ^- of the form :

$$J_\lambda^- \sim -\bar{q}_I' \gamma_\lambda (C_V - C_A\gamma_5) q_I \tag{4.6}$$

from the charge symmetric pair q_I', q_I :

$$P_I^{-1} q P_I = q_I$$

$$P_I^{-1} q' P_I = q_I' \tag{4.7}$$

From eqs. (2.8) and (2.9), we find then the following contributions to the neutrino and antineutrino cross sections for y=0 :

$$\frac{\partial^2\sigma}{\partial x \partial y}(\nu_\mu N \to \mu^- X)\Big|_{y=0} \sim \frac{G^2 ME}{\pi} x\left[N_q(x) + N_{\bar{q}'}(x)\right](C_V^2 + C_A^2)$$

$$\frac{\partial^2\sigma}{\partial x \partial y}(\bar{\nu}_\mu N \to \mu^+ X)\Big|_{y=0} \sim \frac{G^2 ME}{\pi} x\left[N_{q_I}(x) + N_{\bar{q}_I'}(x)\right](C_V^2 + C_A^2) \tag{4.8}$$

But, our target consists of an equal amount of protons and neutrons, i.e. it is charge symmetric and therefore we find an equal amount of quarks q and q_I and likewise $\bar{q}'$ and $\bar{q}_I'$. This shows indeed that :

$$\frac{\partial^2\sigma}{\partial x \partial y}(\nu_\mu N \to \mu^- X)\Big|_{y=0} = \frac{\partial^2\sigma}{\partial x \partial y}(\bar{\nu}_\mu N \to \mu^+ X)\Big|_{y=0} \tag{4.9}$$

if the weak current transforms under a charge symmetry operation as shown in eq. (4.4). We note that the argument remains true if we include spin 0 partons which couple to the weak current.

(iii) If there are no antiquarks $\bar{u}$ and $\bar{d}$ in the nucleon, then the y-distributions for neutrino and antineutrino scattering have a simple behaviour as shown in Figure 6.

The Gargamelle group has extracted the distribution functions N(x) and $\bar{N}(x)$ from the data [7]. (Figure 7).

If the whole picture which we have developed so far is consistent and continues to hold for energies higher than those attainable with Gargamelle, we expect to see the simple y-distributions shown in Figure 6 for neutrino and antineutrino events for fixed $x \gtrsim 0.2$. For $x \lesssim 0.2$ the Gargamelle data implies a sizeable antiquark content in the nucleon with must

reflect itself in a change in the y-distributions. The type of y-distribution expected for $x \lesssim 0.2$ is shown in Figure 8. Even if we do not believe the Gargamelle data we can infer from our discussion of the electromagnetic structure functions in section III the following. Whenever :

$$xN(x) \xrightarrow[x \to 0]{} \text{const.} \neq 0 \tag{4.10}$$

there must be an infinite number of quarks and antiquarks in the nucleon and for $x \to 0$ the y-distributions for neutrino and antineutrino events must be of the type shown in Figure 8, and for very small x they must even become equal since eq. (4.10) implies :

$$\lim_{x \to 0} N(x)/\bar{N}(x) = 1 \tag{4.11}$$

If the electromagnetic structure functions satisfy :

$$F_2^{em}(x) \xrightarrow[x \to 0]{} \text{const.} \neq 0 \tag{4.12}$$

we certainly would expect the neutrino structure function to satisfy eq. (4.10).

IV.2 : The total cross sections :

Next we consider the total neutrino nucleon cross sections. Integrating over x and y we obtain from eq. (4.2) :

$$\sigma^{(\nu)}(E) = \frac{G^2 ME}{\pi} \{ \langle xN \rangle + \frac{1}{3} \langle x\bar{N} \rangle \}$$

$$\sigma^{(\bar{\nu})}(E) = \frac{G^2 ME}{\pi} \{ \frac{1}{3} \langle xN \rangle + \langle x\bar{N} \rangle \} \tag{4.13}$$

$$\langle xN \rangle = \int_0^1 dx\, xN(x)$$

$$\langle x\bar{N} \rangle = \int_0^1 dx\, x\bar{N}(x) \tag{4.14}$$

Remember that x is the longitudinal momentum of the parton in units of the longitudinal momentum of the nucleon. Therefore $\langle xN \rangle$ and $\langle x\bar{N} \rangle$ are the fraction of the total longitudinal momentum of the nucleon carried by quarks u, d and antiquarks $\bar{u}$, $\bar{d}$.

We observe that our parton theory predicts a linear rise of the

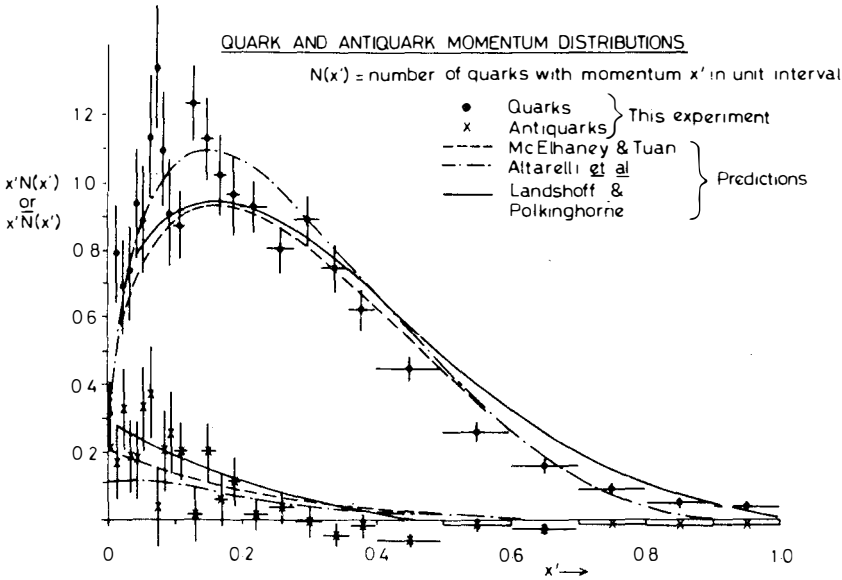

Fig. 7 Quark and antiquark distribution functions N(x') and N̄(x') (x' = $Q^2/(2Mν + M^2)$) from ref. 7)

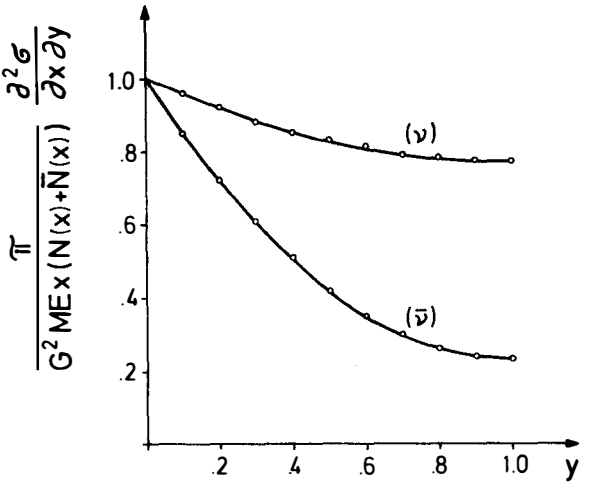

Fig. 8 The y-distributions for neutrino and antineutrino events expected for a ratio N̄(x)/N(x) = 0.30

total cross sections with the energy of the incident neutrino. This is beautifully confirmed by experiment [8], [9] (compare Figure 9).

Putting in the experimental numbers for the total cross sections, we can determine $\langle xN \rangle$ and $\langle x\bar{N} \rangle$. We find :

$$\langle xN \rangle = 0.46 \pm 0.02$$

$$\langle x\bar{N} \rangle = 0.03 \pm 0.01 \tag{4.15}$$

The data on electron nucleon scattering on the other hand allow us to estimate also the amount of momentum carried by s and $\bar{s}$ quarks since :

$$\int_0^1 dx x(F_1^{ep}(x) + F_1^{en}(x)) = \frac{5}{9} \langle xN \rangle + \frac{5}{9} \langle x\bar{N} \rangle + \frac{2}{9} \langle x(N_s + N_{\bar{s}}) \rangle \tag{4.16}$$

The experimental values [4], [5] :

$$\int_0^1 dx x F_1^{ep}(x) = 0.167 \pm 0.008$$

$$\int_0^1 dx x F_1^{en}(x) = 0.126 \pm 0.006 \tag{4.17}$$

lead to :

$$\langle x(N_s + N_{\bar{s}}) \rangle = 0.10 \pm 0.06 \tag{4.18}$$

Adding up all the momentum carried by quarks we find that roughly half of the momentum is still missing and must be attributed to other partons. This could be either gluons or quarks which are still inoperative at low energies. Discarding the latter alternative we find for the momentum carried by gluons :

$$\langle xN_G \rangle = 0.41 \pm 0.05 \tag{4.19}$$

We add a warning not to take these numbers too seriously since we have completely neglected the longitudinal contribution. Inclusion of such a contribution which can be shown to be small also in neutrino scattering would not effect $\langle xN \rangle$ and $\langle xN_G \rangle$ much but could change the other numbers by a substantial amount.

IV.3 : The charges of the partons :

If we neglect the antiquark and strange quark contributions to the longitudinal momentum of the nucleon altogether, we find :

$$\sigma^{(\nu)}(E) = \frac{G^2 ME}{\pi} \langle xN \rangle$$

$$\sigma^{(\bar{\nu})}(E) = \frac{G^2 ME}{\pi} \frac{1}{3} \langle xN \rangle$$

$$\int_0^1 dx x(F_1^{ep}(x) + F_1^{en}(x)) = \frac{5}{9} \langle xN \rangle \qquad (4.20)$$

The naive numbers 1/3 and 5/9 are quite close to the experimental values [4], [5], [8], [9] :

$$\frac{\sigma^{(\bar{\nu})}(E)}{\sigma^{(\nu)}(E)} = 0.38 \pm 0.02$$

$$\frac{\int_0^1 dx x(F_1^{ep}(x) + F_1^{en}(x))}{\pi\sigma^{(\nu)}(E)/(G^2 ME)} = 0.62 \pm 0.04 \qquad (5/9 \simeq 0.56) \qquad (4.21)$$

A ratio of 1/3 for the antineutrino to neutrino cross sections is characteristic of a target consisting of no antiquarks but only quarks interacting via a V-A current. The number $5/9 = (2/3)^2 + (1/3)^2$ is characteristic of the fractional charges of the quarks. For integral charges we would expect 5/9 to be replaced by 1 which would be in contradiction with experiment (eq. (4.21)). Can we therefore conclude that integral charges for quarks are excluded ?

The correct answer to this question requires somewhat more subtle reasoning. In writing down eq. (4.20) we have assumed that quarks have isospin 1/2 and what we can therefore conclude from eq. (4.21) is that the experiments on deep inelastic electron and neutrino nucleon scattering exclude quarks with integral charges and isospin 1/2. This is even true if we allow for antiquark contributions [10].

In general, we have to argue roughly as follows. The neutrino cross section measures the value of the isospin raising operator of the partons, the electron cross section the charge squared of the partons :

$$\sigma^{(\nu)} \propto |I_+|^2$$

$$\sigma^{(e)} \propto Q^2 \qquad (4.22)$$

Experimentally one finds :

$$Q^2 < |I_+|^2 \tag{4.23}$$

this means : either we insist on isospin 1/2 for partons, i.e. $|I_+|^2 = 1$, then we must have fractional charges, or we insist on integral charges, $Q^2 = 1$, then we must allow for partons with isospin > 1/2, e.g. isospin 1 which gives $|I_+|^2 = 2$.

This rough argument can be made completely rigorous [10]. Together with H. Kühnelt I made a systematic investigation of parton models with integral charges [11]. It urned out that the data on deep inelastic scattering is compatible with integrally charged partons. But if we also insist that the theory produces the correct value for the amplitude of $\pi^\circ \to 2\gamma$ decay we predict for electron positron annihilation into hadrons :

$$\frac{\sigma(e^+e^- \to \text{hadrons})}{\sigma(e^+e^- \to \mu^+\mu^-)} \geq 22 \tag{4.24}$$

This is far beyond the present experimental value and therefore we conclude that the deep inelastic scattering data combined with the other experimental information mentioned requires unambiguously fractional charges for the partons. These could be the true charges or only effective charges which govern the scattering below some "color" threshold as would be the case in the Han-Nambu model [12], [13].

IV.4 : Sum rules :

Charge, strangeness and baryon number conservation require the total number of u minus $\bar{u}$, d minus $\bar{d}$ and s minus $\bar{s}$ quarks in the proton to be as in the naive three quark model :

$$\begin{aligned}
&\int_0^1 dx(N_u(x) - N_{\bar{u}}(x)) = 2 \\
&\int_0^1 dx(N_d(x) - N_{\bar{d}}(x)) = 1 \\
&\int_0^1 dx(N_s(x) - N_{\bar{s}}(x)) = 0
\end{aligned} \tag{4.25}$$

For the distribution functions $N = N_u + N_d$ and $\bar{N} = N_{\bar{u}} + N_{\bar{d}}$ which can be obtained from experiments on a charge symmetric target this implies the Gross-Llewellyn Smith sum rule [14] :

$$\int_0^1 dx(N(x) - \bar{N}(x)) = 3 \tag{4.26}$$

This sum rule which is sensitive to the quark charges is well satisfied by the Gargamelle data which leads to a value 3.0 ± 0.6 [7] for the integral in eq. (4.26).

A second sum rule which follows from eq. (4.25) is Adler's neutrino sum rule [15]. To discuss this sum rule we integrate the neutrino and antineutrino cross sections eq. (4.2) for fixed incident neutrino energy E and fixed Q^2 over the allowed kinematic region in ν (compare Figure 2). We find easily :

$$\frac{d\sigma^{(\nu)}}{dQ^2}(\nu) = \frac{G^2}{2\pi}\int_\nu^1 dx\left[N^{(\nu)}(x) + \bar{N}^{(\nu)}(x)\left(1 - \frac{\nu}{x}\right)^2\right]$$

$$\frac{d\sigma^{(\bar{\nu})}}{dQ^2}(\nu) = \frac{G^2}{2\pi}\int_\nu^1 dx\left[N^{(\bar{\nu})}(x)\left(1 - \frac{\nu}{x}\right)^2 + \bar{N}^{(\bar{\nu})}(x)\right] \tag{4.27}$$

$$\nu = Q^2/2ME$$

where we have for the moment distinguished the distribution functions N, $\bar{N}$ appearing in the neutrino and antineutrino cross sections. For $\nu \to 0$, this leads to :

$$\lim_{\nu\to 0}\left[\frac{d\sigma^{(\nu)}}{dQ^2}(\nu) - \frac{d\sigma^{(\bar{\nu})}}{dQ^2}(\nu)\right]$$
$$= \frac{G^2}{2\pi}\lim_{\nu\to 0}\left\{\int_\nu^1 dx\left[N^{(\nu)}(x) + \bar{N}^{(\nu)}(x) - N^{(\bar{\nu})}(x) - \bar{N}^{(\bar{\nu})}(x)\right]\right.$$
$$\left. + \frac{3}{2}\nu\,(N^{(\bar{\nu})}(\nu) - \bar{N}^{(\nu)}(\nu))\right\} \tag{4.28}$$

For our charge symmetric target we have of course $N^{(\nu)} = N^{(\bar{\nu})}$, $\bar{N}^{(\nu)} = \bar{N}^{(\bar{\nu})}$, and since the sum rules eq. (4.25) or alternatively the Pomeranchuk theorem require :

$$\lim_{\nu\to 0}\nu\,(N(\nu) - \bar{N}(\nu)) = 0 \tag{4.29}$$

we find :

$$\lim_{\nu\to 0}\left[\frac{d\sigma^{(\nu)}}{dQ^2}(\nu) - \frac{d\sigma^{(\bar{\nu})}}{dQ^2}(\nu)\right] = 0 \tag{4.30}$$

in agreement with the Gargamelle data [7]. On an arbitrary mixture of protons

and neutrons as target we would find :

$$\lim_{\nu \to 0} \left[\frac{d\sigma^{(\nu)}}{dQ^2}(\nu) - \frac{d\sigma^{(\bar{\nu})}}{dQ^2}(\nu) \right] = -\frac{G^2}{\pi} 2 \langle I_3 \rangle \tag{4.31}$$

where $\langle I_3 \rangle$ is the mean value of the third component of the isospin operator. We note that inclusion of a charmed quark in the conventional scheme (see section VI) would leave eq. (4.30) practically unchanged.

V. NEUTRAL CURRENT INTERACTIONS.

We will now turn to neutrino scattering involving neutral currents :

$$\begin{aligned} \nu_\mu + N &\to \nu_\mu + X \\ \bar{\nu}_\mu + N &\to \bar{\nu}_\mu + X \end{aligned} \tag{5.1}$$

We will discuss these reactions in the framework of the Salam-Ward-Weinberg model [16], extended to hadrons in the Glashow-Iliopoulos-maiani scheme [17]. In this model, there are four quarks : u, d, s, c (c for charm) and the weak neutral current is written in terms of quark fields in the following way :

$$\begin{aligned} J_\lambda^N = & \bar{c}\gamma_\lambda \left(\frac{1}{2} - \frac{4}{3} z - \frac{1}{2}\gamma_5\right) c \\ & + \bar{u}\gamma_\lambda \left(\frac{1}{2} - \frac{4}{3} z - \frac{1}{2}\gamma_5\right) u \\ & + \bar{d}\gamma_\lambda \left(-\frac{1}{2} + \frac{2}{3} z + \frac{1}{2}\gamma_5\right) d \\ & + \bar{s}\gamma_\lambda \left(-\frac{1}{2} + \frac{2}{3} z + \frac{1}{2}\gamma_5\right) s \end{aligned} \tag{5.2}$$

where $z = \sin^2 \theta_w$ and θ_w is the Weinberg angle.

The cross sections for the reactions eq. (5.1) are now easily derived from our formulae of section II. We will again consider a target with equal number of protons and neutrons. To simplify the discussion we will now neglect the antiquark, strange and charmed quark content of the nucleon altogether. As we have seen in section IV this should be a valid approximation for $x \gtrsim 0.2$. The cross sections per nucleon are then :

$$\frac{\partial^2\sigma}{\partial x \partial y}(\nu_\mu N \to \nu_\mu X) = \frac{G^2 ME}{\pi}\,\frac{x}{2}\,N(x)\,\{\,(1-2z+\frac{10}{9}z^2)+\frac{10}{9}z^2(1-y)^2\,\}$$

$$\frac{\partial^2\sigma}{\partial x \partial y}(\bar{\nu}_\mu N \to \bar{\nu}_\mu X) = \frac{G^2 ME}{\pi}\,\frac{x}{2}\,N(x)\,\{\,(1-2z+\frac{10}{9}z^2)(1-y)^2+\frac{10}{9}z^2\,\} \qquad (5.3)$$

We note that for $z \neq 0$ the current (eq. (5.2)) is not of a pure V-A type, therefore, both neutrino and antineutrino cross sections contain a constant and a $(1-y)^2$ term even in the approximation of neglecting antiquarks in the nucleon.

The total cross sections are easily derived from eq. (5.3). We find :

$$\sigma^{(\nu)}(E) = \frac{G^2 ME}{\pi}\,\langle xN\rangle\,(\frac{1}{2}-z+\frac{20}{27}z^2)$$

$$\sigma^{(\bar{\nu})}(E) = \frac{G^2 ME}{\pi}\,\frac{1}{3}\,\langle xN\rangle\,(\frac{1}{2}-z+\frac{20}{9}z^2) \qquad (5.4)$$

Now, we consider the ratios of neutral current to charged current cross sections neglecting antiquarks also for the charged current cross section. Eqs. (4.20) and (5.4) lead then immediately to :

$$R^{(\nu)} = \frac{\sigma(\nu_\mu N \to \nu_\mu X)}{\sigma(\nu_\mu N \to \mu^- X)} = \frac{1}{2}-z+\frac{20}{27}z^2$$

$$R^{(\bar{\nu})} = \frac{\sigma(\bar{\nu}_\mu N \to \bar{\nu}_\mu X)}{\sigma(\bar{\nu}_\mu N \to \mu^+ X)} = \frac{1}{2}-z+\frac{20}{9}z^2$$

$$0 \leq z \leq 1 \qquad (5.5)$$

This shows that the ratios $R^{(\nu)}$ and $R^{(\bar{\nu})}$ are constrained to lie on a curve as shown in Figure 10.

The experimental value [18], which should in fact be somewhat shifted due to certain cuts applied to the data, is quite consistent with the simple model discussed above and gives a Weinberg angle $\sin^2\theta_w \simeq 0.4$. The data also seems to exclude a pure V-A or V+A structure for the weak neutral current but is quite compatible with pure V or pure A.

VI. NAIVE EXPECTATIONS FOR PRODUCTION OF CHARMED PARTICLES.

In this last section we will discuss what one expects for the production of charmed particles (assuming that they exist) in the naive parton model. We work again within the framework of the Glashow-Iliopoulos-Maiani scheme [17], where the charged weak currents in eq. (2.6) are expressed in terms of quark fields as follows :

$$J_\lambda^+ = \bar{u}\gamma_\lambda(1-\gamma_5)(\cos\theta_C d + \sin\theta_C s) + \bar{c}\gamma_\lambda(1-\gamma_5)(-\sin\theta_C d + \cos\theta_C s)$$

$$J_\lambda^- = (J_\lambda^+)^\dagger \qquad (6.1)$$

where θ_C is the Cabibbo angle.

Now we can once more use our general formulae of section II to get the cross sections for the $\Delta C \neq 0$ production of charmed particles by neutrinos and antineutrinos. For a charge symmetric target we find :

$$\frac{\partial^2\sigma}{\partial x \partial y}(\nu_\mu + N \to \mu^- + X(C=+1)) = \frac{G^2 ME}{\pi}$$

$$\{ xN(x)\sin^2\theta_C + 2xN_s(x)\cos^2\theta_C + 2x\bar{N}_c(x)(1-y)^2 \} \qquad (6.2)$$

$$\frac{\partial^2\sigma}{\partial x \partial y}(\bar{\nu}_\mu + N \to \mu^+ + X(C=-1)) = \frac{G^2 ME}{\pi}$$

$$\{ 2xN_c(x)(1-y)^2 + x\bar{N}(x)\sin^2\theta_C + 2x\bar{N}_s(x)\cos^2\theta_C \} \qquad (6.3)$$

Comparing with eq. (4.2) we note the following points :

(i) We expect the distribution functions $N_c(x)$, $N_{\bar{c}}(x)$, $N_s(x)$, $N_{\bar{s}}(x)$ to be similar in shape to $\bar{N}(x)$ (see Figure 7). Therefore $\Delta C \neq 0$ charmed particle production for $x \gtrsim 0.2$ should occur only in neutrino scattering and at a rate of $\sim \sin^2\theta_C = 0.04$ compared to normal neutrino events. There can of course always be associated production of charmed particles in either neutrino or antineutrino scattering via the conventional $\Delta C = 0$ currents.

(ii) For $x \lesssim 0.2$ $\Delta C \neq 0$ production is expected to occur both in neutrino and antineutrino scattering. If we neglect the c and $\bar{c}$ quark content of the nucleon, the y-distribution of these $\Delta C \neq 0$ events will be constant for both neutrino and antineutrino scattering. If the y-distributions for $\Delta C = 0$ neutrino and antineutrino events had the simple form of Figure 6, i.e. if

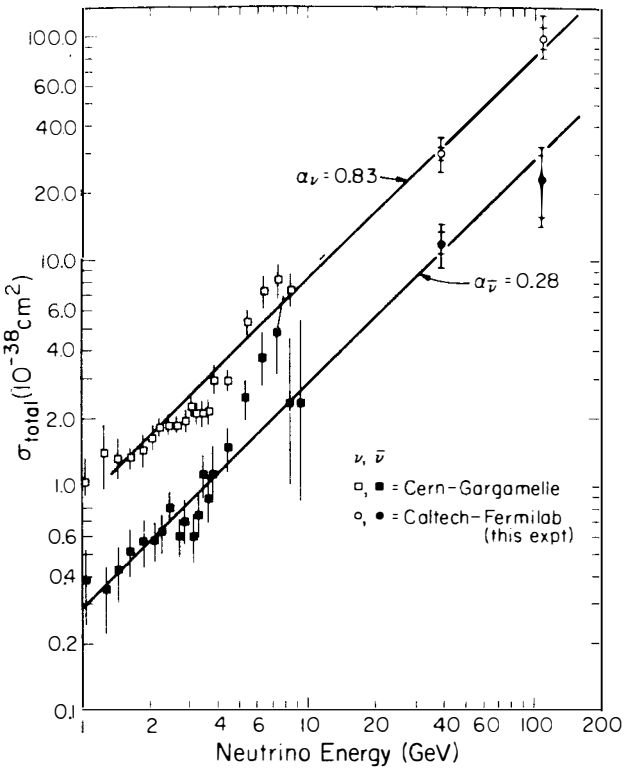

Fig. 9 Total cross sections for neutrino and antineutrino nucleon scattering via charged currents (from ref. 9)

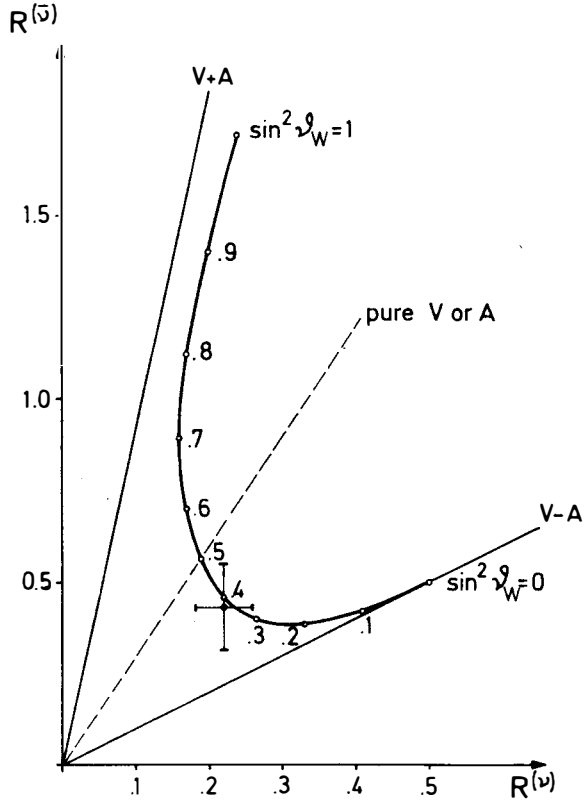

Fig. 10 Plot of the ratios $R^{(\nu)}$ versus $R^{(\bar\nu)}$. The line is the prediction of the simple model discussed in the text. The experimental point is from ref. 18)

$\bar{N}(x) = 0$, then an additional constant term in the y-distribution for antineutrino events could be interpreted as evidence for $\Delta C \neq 0$ production. But we know that $\bar{N}(x) \neq 0$ (see Figure 7) and therefore it is difficult to disentangle the effects of conventional antiquarks from $\Delta C \neq 0$ production in the y-distributions.

(iii) What about the equality of the neutrino and antineutrino cross sections at $y = 0$? From eqs. (4.2), (6.2) and (6.3) we find above charm threshold :

$$\left.\frac{\frac{\partial^2\sigma}{\partial x \partial y}(\bar{\nu}_\mu N \to \mu^+ X)}{\frac{\partial^2\sigma}{\partial x \partial y}(\nu_\mu N \to \mu^- X)}\right|_{y=0} = \frac{N(x) + \bar{N}(x) + 2(N_c(x) + N_{\bar{s}}(x))}{N(x) + \bar{N}(x) + 2(N_{\bar{c}}(x) + N_s(x))} \qquad (6.4)$$

But we expect $N_c(x) + N_{\bar{s}}(x) \sim N_{\bar{c}}(x) + N_s(x)$; therefore no large deviation of this ratio from one is expected in the conventional charm model.

(iv) The total $\Delta C \neq 0$ production cannot be more than 10 - 15 % of the $\Delta C = 0$ production if we assume scaling in the latter case, since the neutrino and antineutrino cross sections show no apparent change in slope when going from low to high energies (see Figure 9). If dimuon events [19] arise from leptonic or semileptonic decays of charmed particles, the corresponding branching ratios must be rather big to account for the observed ~ 1 % dimuon events.

With these remarks, I would like to close this introduction to the parton model. I hope that you are now as eager as myself to hear from experimentalists the latest news of where the simple picture which I have sketched for you is confirmed by the data and where it needs possibly radical modification.

ACKNOWLEDGEMENTS.

The author would like to thank the organizers of the XIth Rencontre de Moriond for their kind invitation.

REFERENCES.*

[1] R.P. FEYNMAN, Phys. Rev. Letters 23, 1415 (1969).

[2] J.D. BJORKEN and E.A. PASCHOS, Phys. Rev. 185, 1975 (1969).

[3] M. GELL-MANN, Phys. Letters 8, 214 (1964).
G. ZWEIG, CERN reports TH-401, 412 (1964) (unpublished).

[4] G. MILLER et al., Phys. Rev. D5, 528 (1972).

[5] A. BODEK et al., Phys. Rev. Letters 30, 1087 (1973).

[6] E.D. BLOOM in proceedings of the 6th international symposium on electron and photon interactions at high energies, H. ROLLNIK and W. PFEIL (ed.), North Holland, Amsterdam, London (1974).

[7] H. DEDEN et al., Nucl. Phys. B85, 269 (1975).

[8] T. EICHTEN et al., Phys. Rev. Letters 46B, 274 (1973).

[9] B.C. BARISH et al., Phys. Rev. Letters 35, 1316 (1975).

[10] O. NACHTMANN, Phys. Rev. D5, 686 (1972).

[11] H. KÜHNELT and O. NACHTMANN, Nucl. Phys. B88, 41 (1975).

[12] M.Y. HAN and Y. NAMBU, Phys. Rev. 139, B 1006 (1965).

[13] H.J. LIPKIN, Phys. Rev. Letters 28, 63 (1972).

[14] D.J. GROSS and C.H. LLEWELLYN SMITH, Nucl. Phys. B14, 337 (1969).

[15] S.L. ADLER, Phys. Rev. 143, 1144 (1966).

[16] A. SALAM and J.C. WARD, Phys. Letters 13, 168 (1964).
S. WEINBERG, Phys. Rev. Letters 19, 1264 (1967).
A. SALAM in : Elementary Particle Theory, ed. N. SVARTHOLM (ALMQUIST and FORLAG, Stockholm, 1968).

[17] S. GLASHOW, J. ILIOPOULOS and L. MAIANI, Phys. Rev. D2, 1285 (1970).

[18] F.J. HASERT et al., Nucl. Phys. B73, 1 (1974).

[19] A. BENVENUTI et al., Phys. Rev. Letters 35, 1199, 1203, 1249 (1975).

---

* Due to limited time available for preparing these lectures, the list of references is very incomplete. The author apologizes to all those whose work is not mentioned.

DEEP INELASTIC MUON SCATTERING

W.S.C. Williams,
Department of Nuclear Physics,
University of Oxford.

Abstract : Results from two experiments at the Fermilab on deep muon-nucleon inelastic scattering are reviewed. The measurements give the structure function νW_2 in the range $1 < \omega < 1000$ and $0.2 < q^2 < 50$ $(GeV/c)^2$. There is evidence that at $\omega < 6$ the structure function decreases as q^2 increases. At high ω the evidence for an increase of νW_2 with q^2 may indicate a scaling violation or a slower turn-on of scaling as q^2 increases from zero than has been found at SLAC.

Résumé : Cet article passe en revue les résultats de deux expériences réalisées au Fermilab sur la diffusion inélastique profonde muon-nucléon. Ces résultats donnent les valeurs de la fonction de structure νW_2 dans les gammes $1 < \omega < 1000$ et $0.2 < q^2 < 50(GeV/c)^2$. Ils montrent que pour $\omega < 6$ la fonction de structure diminue au fur et à mesure que q^2 augmente. Pour un ω élevé, il est apparu qu'il y a accroissement de νW_2 en même temps que de q^2. Ceci peut indiquer une violation de l'invariance d'echelle ou, par rapport à celle découverte a SLAC, une emergence plus lente du "scaling" lorsque q^2 augmente à partir de zéro.

Two experimental programs to study deep inelastic muon-nucleon scattering have been completed at the Fermilab. One is known as E.26 and is a collaboration between the Universities of Cornell, Michigan State, California at San Diego and the Lawrence Berkeley Laboratory. The other is known as E.98 and is a collaboration between the Universities of Chicago, Harvard, Illinois and Oxford. I am associated with E.98 and in Fig. 1 I list the names of the collaborators. Some results from E.26 have been published and the names of the collaborators may be obtained from these papers[1, 2, 3].

University of Chicago	Harvard University
H.L. Anderson	B.A. Gordon
R.M. Fine	W.A. Loomis
R.H. Heisterberg	F.M. Pipkin
H.S. Matis	S.H. Pordes
L.W. Mo	W.D. Shambroom
L.C. Myrianthopoulos	L.J. Verhey
S.C. Wright	R. Wilson
University of Illinois	**University of Oxford**
W.R. Francis	V.K. Bharadwaj
R.G. Hicks	N.E. Booth
T.B.W. Kirk	G.I. Kirkbride
	T.W. Quirk
	A. Skuja
	M. Staton
	W.S.C. Williams

Fig. 1 E.98 Collaborators.

Let me start by defining the kinematic quantities and the structure functions. A μ^+ of energy-momentum E, p is incident on a nucleon of mass M, scatters inelastically to energy-momentum E', p' at angle θ. The kinematic quantities that I shall use are:-

The energy transfer $\nu = E - E'$

The four momentum transfer $q^2 \simeq 4EE'\sin^2\theta/2$

As far as the muon is concerned q^2 and ν completely define the collision. The differential cross-section for the process can be written

$$\frac{d^2\sigma}{dq^2 d\nu} = \frac{4\pi\alpha^2}{q^4} \frac{E'}{E} \{W_2 \cos^2\frac{\theta}{2} + 2W_1 \sin^2\frac{\theta}{2}\},$$

where α is the fine structure constant. W_1 and W_2 are structure functions characteristic of the nucleon and they are functions of the two independent variables q^2 and ν. The Bjorken hypothesis of scale invariance is that in the limits $\nu \to \infty, q^2 \to \infty$, νW_2 and MW_1 are no longer functions of the two independent variables q^2 and ν but only a function of the ratio ν/q^2. In deep inelastic muon scattering we have become accustomed to thinking not about ν/q^2 but the dimensionless $2M\nu/q^2 \equiv \omega$ (the neutrino researchers prefer $x = 1/\omega$). So Bjorken scaling is the statement

$$\lim_{q^2 \to \infty,\ \nu \to \infty} W_2(q^2,\nu) = f(\omega)$$

Strictly we cannot measure W_1 and W_2 separately without making cross-section measurements at two energies. However, the effect of W_1 is small as the data I shall discuss are at small angles. The effect of W_1 is included by making an assumption which connects W_1 and W_2. Consider the ratio of W_1 to W_2 which can be expressed

$$\frac{W_1}{W_2} = (1 + \frac{\nu^2}{q^2}) (1 + R)$$

where $R = \sigma_L/\sigma_T$ is the ratio of photoabsorption cross-sections for longitudinal and transverse photons[6]. The data are analysed to obtain values of W_2 assuming $R = 0.18$, the value obtained in experiments at SLAC[7]. The results are not sensitive to any reasonable value of R assumed.

Fig. 2A shows lines of constant ω on the parts of the q^2, ν plane which are accessible to experiments using the 150 GeV muon beam presently available at the Fermilab.

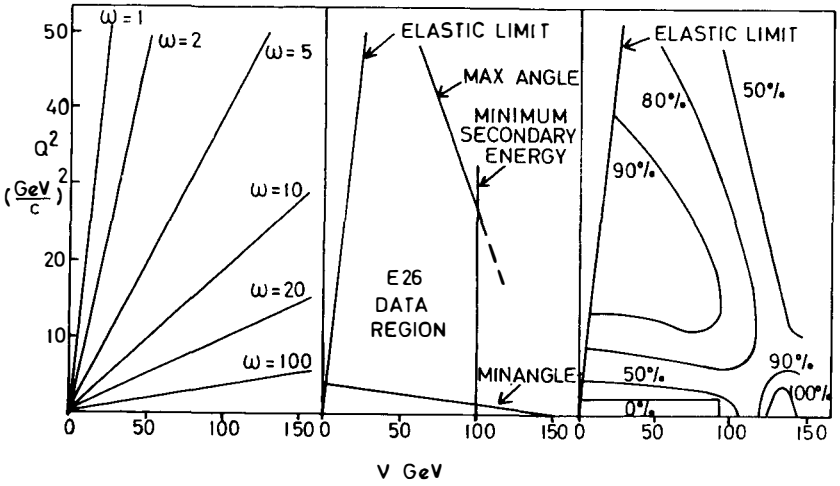

Fig 2A Fig 2B Fig 2C

Fig. 2(A). Lines of equal ω on the q^2-ν plane. (B) the E.26 data region on the q^2-ν plane at 150 GeV. The region is defined by the elastic limit (ω = 1), the maximum and minimum angles and the requirement that the secondary muon energy is greater than one third the primary energy. (C) Some contours of equal acceptance on the $q^2\nu$ plane for E.98.

The objectives of E.26 were to test the Bjorken scaling hypothesis in muon-nucleon scattering at the energies available at the Fermilab using a heavy target in order to achieve the high luminosity necesary to reach large q^2. The experiment uses a thick iron target and the secondary muon momentum is measured in solid iron toroidal magnets. This arrangement immediately implies that the resolution on kinematic quantities is limited and that no information can be obtained about the secondary hadrons produced. The experiment was run under the following conditions:-

Beam Energy GeV	150	56
Integrated Beam Muons	1.5×10^9	4×10^9
Target g cm^{-2} Fe	622	233
Luminosity cm^{-2}	5.6×10^{35}	5.6×10^{35}

The apparatus accepted secondary muons scattered at angles between 11 and 65 mradians and with energies greater than $\frac{1}{3}$ the incident energy. Scaling was tested by two methods: (1) A direct comparison of the data obtained at the two energies. (2) A comparison of actual yields against yields calculated using a Monte Carlo model of the apparatus and the scaling function νW_2 determined at SLAC.

The objectives of E.98 were to measure the structure function νW_2 for hydrogen and deuterium targets and to obtain information on the secondary hadrons produced in muon scattering, again at the Fermilab energies. The experiment used a liquid hydrogen or deuterium target and the momentum of secondary particles was measured using a 7.5 Tesla-metre air magnet. Secondary positive muons of energy greater than 15 GeV/c and charged hadrons of momentum greater than 6 GeV/c are detected. The experiment was run under the following conditions:

Beam Energy GeV	147	147
Integrated Beam Muons	1.84×10^{10}	2.10×10^{10}
Target g cm^{-2}	D_2 20.1	H_2 8.4
Luminosity cm^{-2}	2.4×10^{35}	1.1×10^{35}

The total luminosity is less than one third of that obtained with a solid target in E.26. The scaling function νW_2 was calculated from yields, acceptance, luminosity, etc., and radiative corrections were made.

Fig. 2B shows the E.26 acceptance region on the same scale as Fig. 2A and Fig. 2C shows some equal acceptance curves for E.98. E.26 has results inside $1 < q^2 < 40$(GeV/c) and $1 < \omega < 50$.

E.98 has results inside $1 < q^2 < 50(GeV/c)^2$ and $1 < \omega < 1000$. Notice, however, that at any ω, the actual range of q^2 is limited by kinematics and acceptance.

The E.26 results have been published[1,2]. Fig. 3 shows the data in bins of ω as a function of q^2. The vertical scale is such that it gives the ratio of the observed yield to the Monte Carlo predicted yield. So the scale is the rate $r = \nu W_2$ (E.26)/νW_2 (SLAC) with all the effects of experimental resolution folded in. All results should be 1.0 within error if scaling holds with the same value of νW_2 as at SLAC energies. Note the

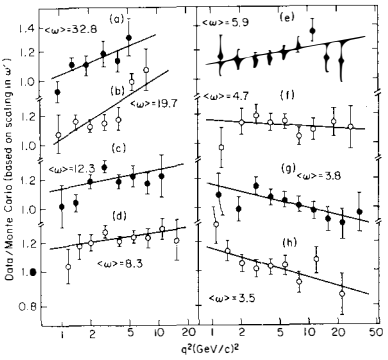

Fig. 3. Ratio of observed yield to monte carlo predicted yield for E.26. The ratio is plotted versus q^2 for eight bins of ω.

character of the scaling violation indicated by this data:

1. At $\omega < 6$ νW_2 decreases as q^2 increases.
2. At $\omega > 6$ νW_2 increases as q^2 increases.

These effects have been parametrised as follows. In each bin of ω the data are fitted with

$$\ell n\ r = c_\omega + b_\omega \ell n\frac{q^2}{3}.$$

Then the values of b_ω have been fitted with

$$b_\omega = a\ \ell n(\frac{\omega}{\omega_o}).$$

This gives $a = 0.099 \pm 0.018$ and $\omega_o = 6.1(+3.9, -2.4)$ with $\chi^2/DF = 6/4$. This means that the data can be represented by

$$\ell n(\nu W_2(q^2,\omega)) \simeq \ell n(\nu W_2(3,\omega)) + 0.099\ \ell n(\frac{q}{3})\ \ell n(\frac{\omega}{6.1}). \qquad (1)$$

Systematic errors raise the uncertainty on a; $a = 0.099 \pm 0.040$.

The E.98 results I shall discuss are those for the deuterium target and the structure function is that for deuterium divided by two. Fig. 4 shows these values of νW_2 per nucleon in bins of ω as a function of q^2. Note the following features:

1. $1 < \omega < 3$: νW_2 decreases as q^2 increases.
2. $5 < \omega < 11$: consistent with a constant νW_2.
3. $11 < \omega < 60$: νW_2 might be increasing with q^2.

These features have the same character as those found in E.26 although not so obvious. To test this quantitatively we fit the data with

$$\nu W_2(q^2,\omega) = \nu W_2(q_o^2,\omega)\ [1 + a\ \ell n(\frac{q^2}{q_o^2})\ \ell n(\frac{\omega}{\omega_o})]. \qquad (2)$$

This fit is done only for data with $q^2 < 2$ and that means $1 < \omega < 60$. We fix $q_o^2 = 3(GeV/c)^2$ and $\omega_o = 6$ as suggested by the E.26 results. The fit requires two stages:-

1. $\nu W_2(q_o^2,\omega)$ is found by fitting data in the range $2 < q^2 < 4(GeV/c)^2$ and $3 < \omega < 60$ with a polynomial in 1-x where $x = 1/\omega$.

$$\nu W_2(q_o^2,\omega) = \sum_{n=3}^{5} a_n(1-x)^n$$

2. Data in the full range of q^2 and ω is then fitted to find the a of Eq. 2. [This form is not quite the same as that used in E.26 (Eq.1) but is the same as far as the value of a is concerned.] The value obtained is $a = 0.11 \pm 0.04$.

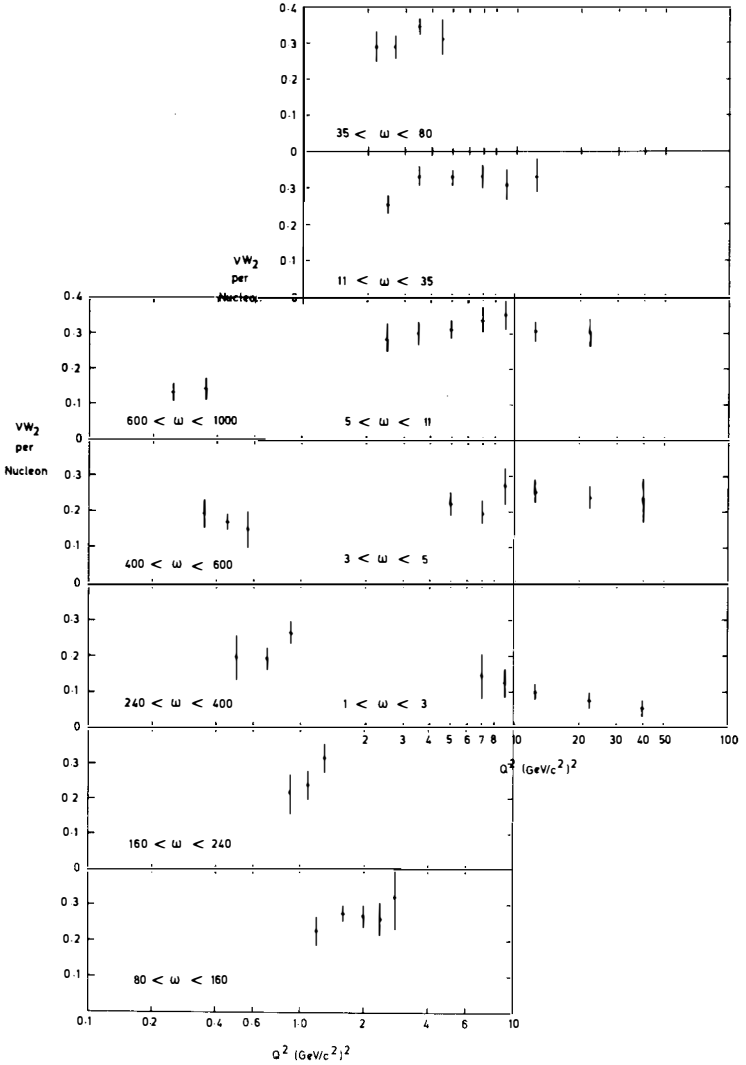

Fig. 4 Values of νW_2 per nucleon versus q^2 in various ω bins for deuterium at 147 GeV. E.98 data.

This result should be compared with the E.26 result a = 0.099±0.018. Thus the first conclusion from the E.98 data is that the data do not disagree with the scaling violation claimed by E.26.

Notice in Fig. 4 that at large ω our q^2 ranges contract and decrease. Thus in the fit described has been restricted to data with ω < 60 for which $q^2 > 2(\text{GeV/c})^2$.

Although there is some suggestion of scaling violations, the data are not inconsistent with a constant νW_2 in every ω bin. We therefore assume that the data is in the deep inelastic region and the Bjorken scaling holds. We combine all the data in each

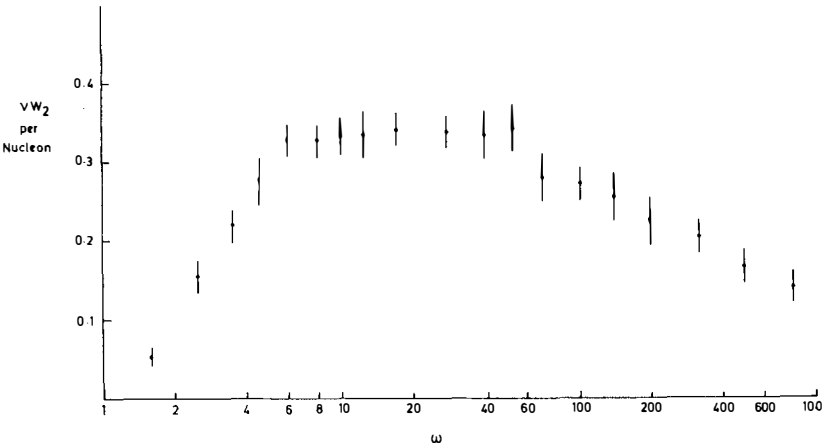

Fig. 5. E.98 data from deuterium at 150 GeV. The structure function νW_2 per nucleon versus ω.

ω bin and plot νW_2 as a function of ω, Fig. 5. Notice that νW_2 is decreasing beyond ω = 80. But in these bins the average q^2 is decreasing rapidly as ω increases (see Figs. 2A, 2B and 4). To understand this we must note that

1. νW_2 must $\to$ 0 as $q^2 \to 0$, so νW_2 must "turn-on" as q^2 departs from zero.

2. Stein et al[4] have investigated how νW_2 turns on and have found, for SLAC energies

$$\nu W_2(q^2,\omega) = \nu W_2(q^2 = \infty,\omega)\,[1 - W^{el}(q^2)]$$

where $W^{el}(q^2) = \dfrac{G_E^2(q^2) + \tau G_M^2(q^2)}{1 + \tau}$, $\tau = \dfrac{q^2}{4M^2}$ and G_E and G_M are the electric and magnetic elastic scattering form factors. This means that at SLAC energies turn-on is complete within a few percent by $q^2 = 1.5$ (GeV/c)^2.

Let us take a closer look at this turn-on, firstly in the E.26 data. I am indebted to Lou Hand and his colleagues for permission to show these results. Fig. 6 shows their values of r ($F_2(q_2)$/0.662 on this figure) for their data with $\omega > 10$ as a

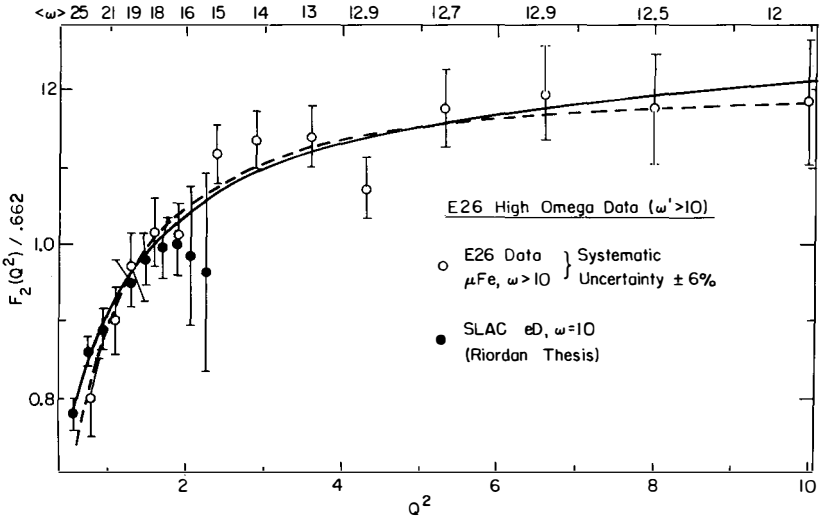

Fig. 6 E.26 results. Ratio of yield observed to Monte Carlo predicted yield using SLAC deuterium results versus q^2 averaged over all $\omega > 10$.

function of q^2. Above $\omega > 10$ νW_2 could be constant as $q^2 \to \infty$ so plotting all the data in this way gives a handle on the q^2 turn on. Fig. 6 shows evidence of a continued rise beyond $q^2 = 1$ $(GeV/c)^2$. This could mean

1. Turn-on is occurring more slowly than at SLAC energies and only becomes constant at large q^2.

or

2. Turn-on is the same as at SLAC energies but scale violation is occurring as $\ell n q^2$.

The solid line in Fig. 6 is a function which scales ultimately:

$$r = \sum_{i=1}^{2} A_i \left(\frac{\beta_i}{1+\beta_i} + \frac{\beta_i}{(1+\beta_i)^2} \right) \text{, where } \beta_i = \frac{q^2}{m_\rho^2}, \beta_2 = \frac{q^2}{M_2^2} .$$

Now we turn to the E.98 results. We plot all the data for

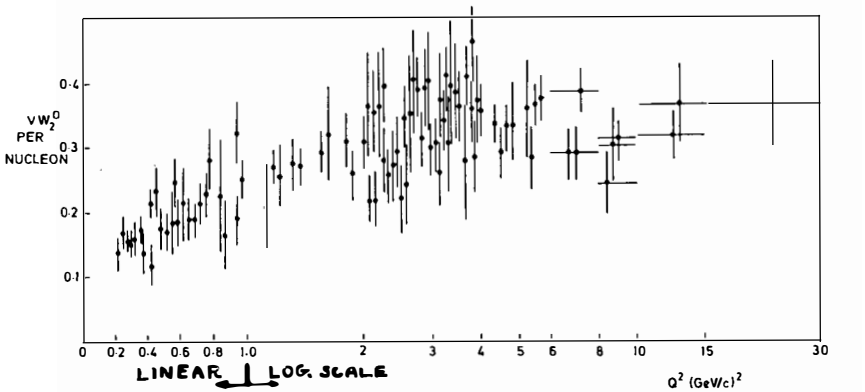

Fig. 7 E.98 data. The structure function per nucleon for deuterium versus q^2 for all $\omega > 10$.

$\omega > 10$ as a function of q^2 (Fig. 7). This result could be interpreted as evidence that turn-on is not complete much before $q^2 = 3$ $(GeV/c)^2$. We try to fit the data with a function

$$\nu W_2(q^2,\omega) = f(\omega)g(q^2),$$

where $g(q^2 \to \infty) = 1$. Because our large ω data has a strong correlation between q^2 and ω the fit must be done in two stages. We take all our data with $q^2 > 2$ for which presumably $g(q^2) \simeq 1$ and fit a function,

$$f(\omega) \equiv \nu W_2(q^2 > 2,\omega) = \sum_{n=3}^{5} a_n(1 - x)^n, \quad x = 1/\omega.$$

Then all the data are used to find $g(q^2)$ assuming

$$\nu W_2(q^2,\omega) = f(\omega)g(q^2),$$

with $$g(q^2) = A\left(\frac{\beta}{1+\beta} + \frac{\beta}{(1+\beta)^2}\right), \qquad \beta = \frac{q^2}{\Lambda^2}.$$

Adjusting Λ^2 and A to fit we find:

$$A = 1.0248 \pm 0.0164,$$

$$\Lambda^2 = 0.9407 \pm 0.0708 \ (\mathrm{GeV/c})^2,$$

$$\chi^2/DF = 198/156.$$

We now go back to all the data and refit with

$$\nu W_2(q^2,\omega) = \left[\sum_{n=3}^{5} a_n(1-x)^n\right]\left[\frac{\beta}{1+\beta} + \frac{\beta^2}{(1+\beta)^2}\right]$$

asjusting a_3, a_4, a_5, keeping $\beta = q^2/0.94$.

This gives

$$f(\omega) \equiv \nu W_2(q^2 \to \infty,\omega) = 0.3446(1-x)^3 + 1.239(1-x)^4 - 1.252(1-x)^5,$$

with $\chi^2/DF = 250/149$.

This fit gives $\nu W_2(q^2 \to \infty, \omega \to \infty) = 0.332$. But, of course, this must not be taken too seriously. The fit procedure is designed to find a fit which will give scaling in the limit $q^2 \to \infty$. However, the data are not inconsistent with scaling plus a q^2 turn-on.

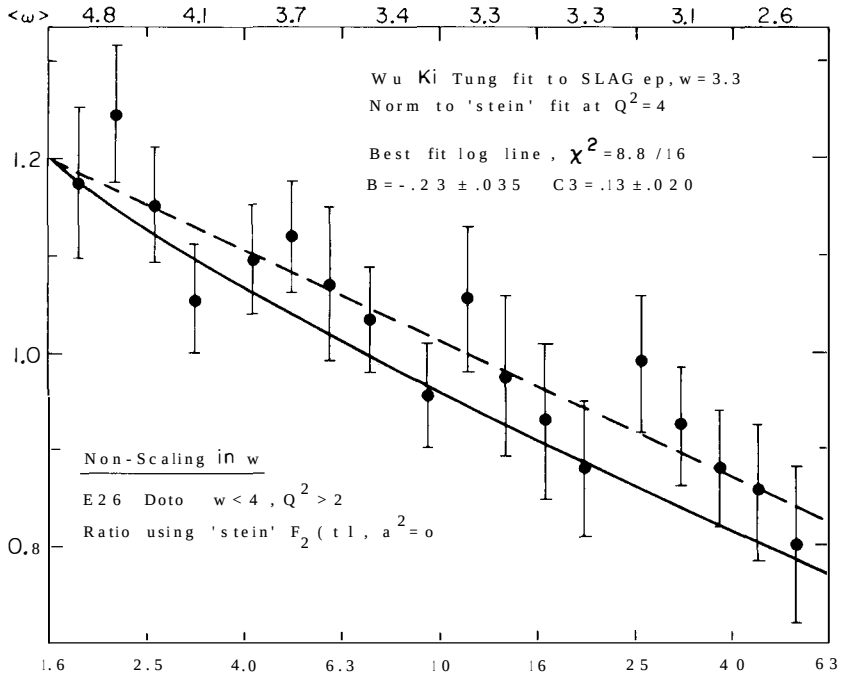

Fig. 8 E.26 data. Ratio of yield observed to monte carlo predicted yield versus q^2 for low ω (measured $\omega < 4$). B is the slope of the best straight line fit (logarithmic in q^2. Dotted line.) The solid line is an extrapolation of Wu-ki Tung's fit to SLAC data[8] using asymptotic freedom type formula in which the scaling violation is logarithmic.

Finally, let us go back and look at the low ω data again. Fig. 8 shows the results of a more recent analysis of the E.26 data. Data with $\omega < 4$ is plotted so as to show the ratio of yield to predicted yield using the Stein et al fit[4] to the deuterium structure function. In this figure the average ω varies from point

to point but plotting the ratio ensures the variation with ω is removed and reveals the dependence on q^2. This curve is further evidence for a low ω scaling violation. To help convince you

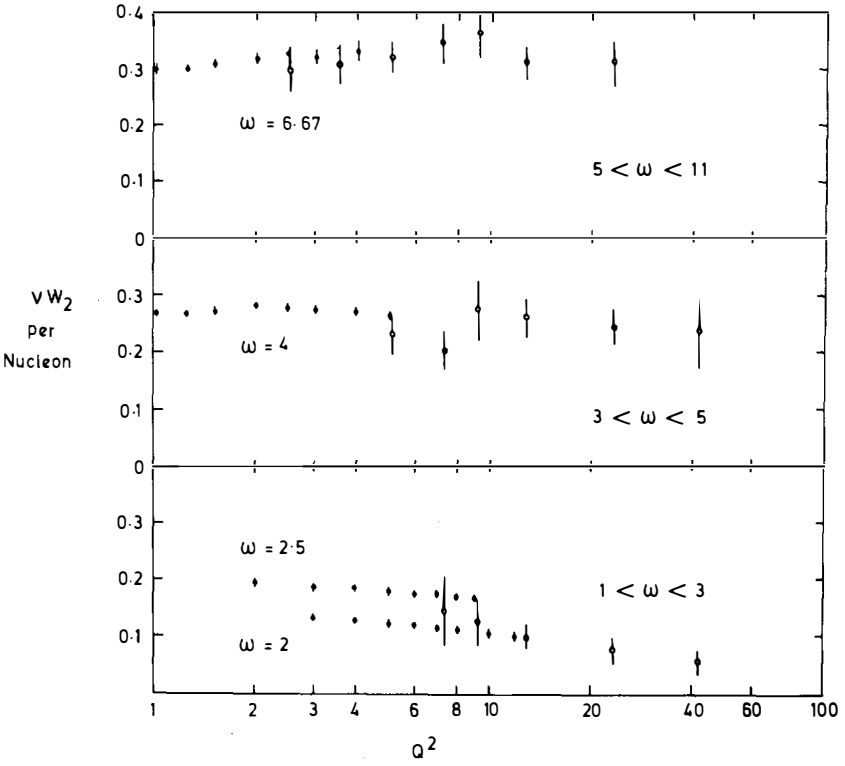

Fig. 9 E.98 and MIT/SLAC data (5) for the structure function νW_2 per nucleon for deuterium versus q^2. The open circles are E.98 data. The closed circles are MIT/SLAC data.

Fig. 9 shows the E.98 data again plotted with results on the deuterium structure function obtained at SLAC energies by Riordan

et al[5]. Their results are in much finer ω bins but the decrease with increasing q^2 that they observed matches well with that found in E.98.

What are the conclusions?

1. There is clear evidence for scaling violation at ω less than 6. The structure function νW_2 decreases by about 50% in the bin $1 < \omega < 3$ as q^2 increases from 5 to 50 $(GeV/c)^2$.
2. At high ω the situation is not so clear. There is certainly a turn-on of νW_2 with q^2 but the data is consistent either with turn-on by $q^2 \simeq 1.5$ (GeV/c) followed by a very slow rise associated with a scaling violation, or with a slower turn-on which is not complete until about $q^2 = 3$ $(GeV/c)^2$.

Obviously more data is required. Unfortunately at the energies presently available (up to 220 GeV) or within sight (300 GeV at the SPS or 700 GeV at FNAL with the "energy saver") the range of q^2 available at high ω is limited. For example to reach $q^2 = 2$ $(GeV/c)^2$ at $\omega = 1000$ will require incident muons of more than 1.1 TeV!

At the Fermilab E.98 runs again as E.398 and will take data this summer at 225 GeV. E.26 returns as E.319 with an improved apparatus.

REFERENCES

1. Y Watanabe et al, Phys. REv. Letters, 35, 898 (1975).
2. C. Chang et al, Phys. Rev. Letters, 35, 901 (1975).
3. D.J. Fox et al, Phys. Rev. Letters, 33, 1504 (1974).
4. S. Stein et al, SLAC-PUB-1528, (Jan. 1975).
5. E.M. Riordan et al, SLAC-PUB-1635 (Aug. 1975).
6. L.N. Hand, Phys. Rev. 129, 1834 (1963).
7. G. Miller et al, Phys. Rev. D5, 528 (1972).
8. Wu-ki Tung, Phys. Rev. Letters, 35, 490 (1975).

HADRON PRODUCTION IN INELASTIC MUON SCATTERING AT 147 GeV.

W.S.C. WILLIAMS
Department of Nuclear Physics
University of Oxford

Abstract : Results are presented on inclusive hadron production spectra in inelastic scattering of muons by nucleons at 147 GeV.

Résumé : Presentation de resultats sur les spectra inclusifs de la production d'hadron dans la diffusion inélastique de muons par des nucleons à 147 GeV.

I will present data from the E98 experiment at the Fermilab. The collaborators are given in Fig. 1 of my talk on deep inelastic muon scattering at this meeting.

The interest lies now with the hadrons produced by the absorption of the virtual photon exchanged between the scattered muon and the target nucleon. This photon transfers four-momentum q^2 and energy ν. The total centre of mass energy squared of the photon-nucleon system is

$$S = M^2 + 2M\nu - q^2 \simeq 2M\nu.$$

We refer the production of hadrons to the axis defined by the direction of the virtual photon ($\vec{q}$) and we use (q^2,s) to represent the total photon-nucleon cross-section at the photon kinematic point defined by q^2 and s. The invariant differential cross-section for inclusive single hadron production is $Ed^3\sigma(q^2, s)/dp^3$. Then, assuming azimuthal isotropy

$$\frac{E}{\sigma(q^2,s)} \frac{d^3(q^2,s)}{dp^3} = \frac{1}{\sigma(q^2,s)} \frac{1}{\pi} \frac{E}{(P^2_{max} - P^2_T)^{\frac{1}{2}}} \frac{d^2\sigma}{dP^2_T dx'}$$

centre of mass quantities

where

P_{max} = maximum possible momentum of any hadron in the centre of mass.

P_T = momentum of the hadron transverse to $\underline{q}$.

P_L = momentum of the hadron along $\underline{q}$.

x' = a Feynman scaling variable,

$$= \frac{P_L}{(P^2_{max} - P^2_T)^{\frac{1}{2}}}$$

The invariant differential cross-section is sometimes factorised

$$\frac{E}{\sigma} \frac{d^3\sigma}{dp^3} = F(x') G(P_T).$$

although it is not clear that this is possible. It follows that we integrate over P_T to obtain a longitudinal structure function:

$$F(x',q^2,s) = \frac{1}{\sigma(q^2,s)} \frac{1}{\pi} \int_0^\infty dp^2_T \frac{E}{(P^2_{max} - P^2_T)^{\frac{1}{2}}} \frac{d^2\sigma(q^2,s)}{dp^2_T dx'}.$$

The transverse momentum distribution in an x' range is given by the function

$$G(p^2_T, q^2 s) = \frac{1}{\sigma(q^2, s)} \frac{1}{\pi} \int_{x'_1}^{x'_2} dx' \frac{d^2\sigma}{dp^2_T dx'} .$$

Hydrogen data have been published [1] and Fig. 1 shows the results for $F(x', q^2, s)$ as a function of x' for various regions of q^2 and s.

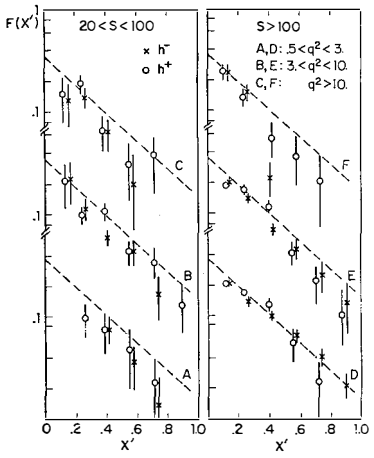

Fig. 1. Longitudinal structure function for inclusive hadron production for various regions of q^2 and s.

The statistics are limited but there is no obvious variation from region to region and the data is consistent with a universal curve of the form

$$f(x') = 0.35 \exp(-3.25x')$$

which is also a good representation of data obtained at lower energies, Dakin et al [2].

The deuterium data have now been analysed and this allows a subtraction to obtain neutron target data. Fig. 2 shows the N^+/N^- (positive to negative hadron ratio) as a function of ω for proton and neutron targets. The solid

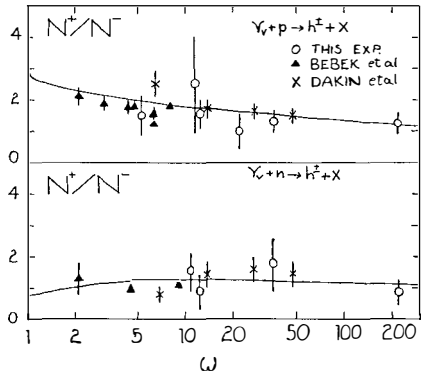

Fig.2. Ratios of positive to negative hadron numbers as a function of ω for proton and neutron targets in this and other experiments. The solid lines are the fits mentioned in the text. The x' cuts are $0.4 < x' < 0.85$ for this experiment and for Dakin et al[2], $0.3 < x' < 0.7$ for Bebek et al [4].

line is a fit by Dakin and Feldman [3] based on a simple quark model of the nucleons.

All other neutron and proton data are indistinguishable and are combined to give results for the average nucleon.

Fig. 3 shows F(x') versus x' for inelastic muon, neutrino and anti-neutrino scattering and for e^+e^- annihilation. The results are not identical but remarkably similar for the various processes.

The data have been fitted with the following form

$$\frac{E}{\sigma}\frac{d^3\sigma}{dp^3} = A(x') \exp\left[\frac{-2b(x')\,P_T^2}{1+[1+P_T^2/M^2(x')]^{\frac{1}{2}}}\right]$$

where

A(x') is the longitudinal x' distribution at $P_T = 0$,

$b(x') \approx 1/\langle P^2_T \rangle$,

M(x') is to fix up the fact that the distribution is not a pure exponential in P^2_T.

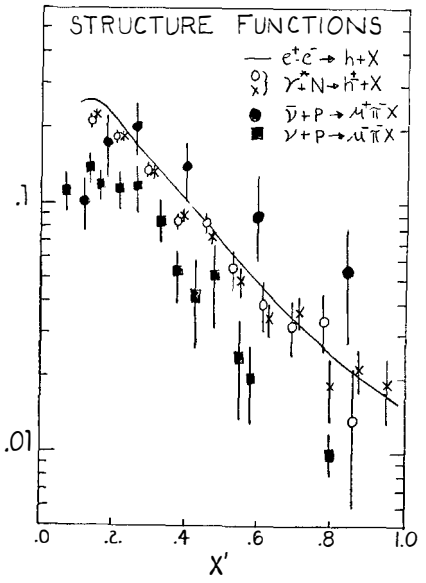

Fig. 3. The longitudinal structure for inclusive hadron production in this experiment (virtual photons, γ^* at $s \approx 200$ GeV^2) and in other processes (e^+e^- annihilation at $s=50$ GeV^2 and neutrino and anti-neutrino interactions at $10<s<100$ GeV^2)

Fig. 4 shows the results for A(x'), b(x'), $\langle P_T \rangle$ and also a curve of $G(P^2_T)$ in three bins of x'. We have seen that the longitudinal distribution is similar to other reactions. The variation of $\langle P_T \rangle$ is typical of secondary hadron production in all processes: an increasing $\langle P_T \rangle$ as x' increases. M(x') does not vary rapidly with x' and has a mean value of about 0.45 GeV.

The data has been examined for the effects of anisotropy in the azimuth defined by the scattering plane of the muon. Such anisotropy will occur generally as a result of the transverse component of the virtual photon polarization. However, in a spin $\frac{1}{2}$ parton model such anisotropies do not occur. Within statistics our data are consistent with azimuthal isotropy.

We conclude that

(1) Photon induced inclusive hadron distributions consistent with a simple spin $\frac{1}{2}$ parton model of nucleons.

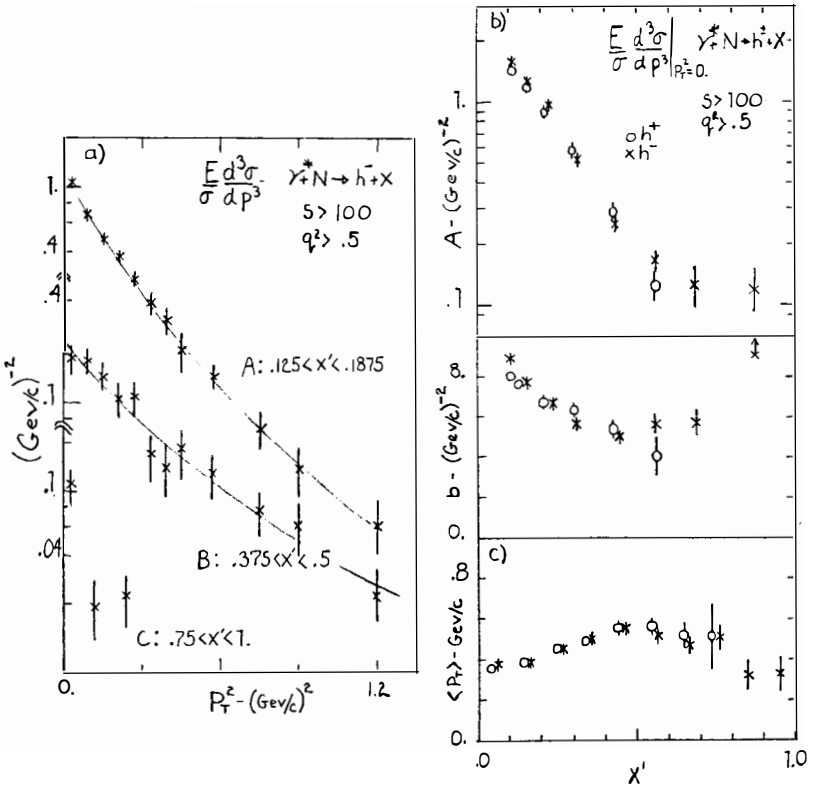

Fig. 4. Results on the coefficients A(x'), b(x') and on $\langle P_T \rangle$ as a function of x'. Also shown are curves of $G(P^2_T)$ in three bins of x'.

(2) Independent of model productions, inclusive hadron distributions in muon inelastic scattering have properties similar to hadron-hadron interactions after removing leading particle effects.

Let me complete this talk by saying a little about exclusive rho-meson production.

$$\mu^+ \rightarrow \mu^+ + \gamma^*$$

$$\gamma^* + p \rightarrow \rho^\circ + p$$

$$\rho^\circ \rightarrow \pi^+ + \pi^-$$

We do not see the recoil proton so we select events by the following criteria:-

(1) The final state contains a μ^+, one positive and one negative hadron (h^+, h^-),

(2) the vertex is inside the target volume,

(3) the missing energy is 0 ± 3.5 GeV.

Then the spectrum of invariant mass of the h^+h^- system is calculated assuming

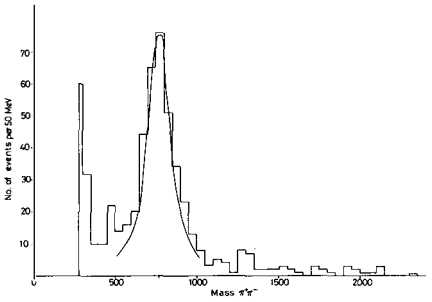

Fig.5. Mass spectrum of +- pairs assumed to be $\pi^+\pi^-$. The peak at 280 MeV is due to e^+e^- wrongly identified. The rho peak is clearly visible at 750 MeV.

that the hadrons are pions. Fig.5 shows an example of such a distribution. The rho peak is clear. The low energy peak is due to e^+e^- wrongly identified as $\pi^+\pi^-$. They are removed by requiring:-

(4) The h^+h^- opening angle is greater than 5 mr.

In addition events are selected by requiring:-

(5) The four-momentum transfer squared (t) to the proton is less than 0.6 $(GeV/c)^2$.

This leaves 184 events in hydrogen. These are treated in the following way

(1) In each q^2,s bin calculate $\frac{d\sigma(q^2,s)}{dmdt}$.

(2) Integrate over m by fitting a relativistic p-wave Breit-Wigner so as to obtain $\frac{d\sigma(q^2,s)}{dt}$. These distributions are shown in Fig.6.

(3) The dσ/dt distributions are fitted with e^{+bt} and this gives $b = 6.6 \pm 0.6$ GeV^{-2} for $q^2 < 1$.

(4) Integrate over t to obtain $\sigma(q^2,s)$. The result showing σ as function of q^2 is shown in Fig.7.

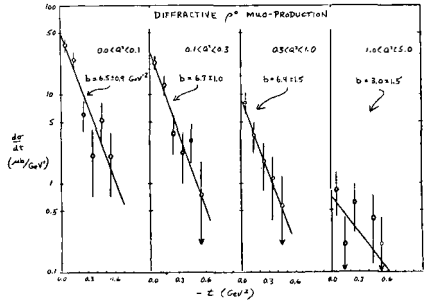

Fig.6. Values of $\frac{d\sigma}{dt}$ versus t for four ranges of q^2.

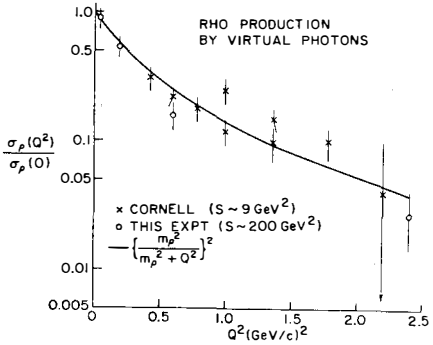

Fig.7. Values of $\sigma(q^2,s)$ as a function of q^2 for this experiment ($s \simeq 200$ GeV^2) and for data obtained at Cornell at s=9 GeV^2.

(5) Extrapolate to $q^2 = 0$ to obtain the total cross-section for real photons for the reactions $\gamma + p \rightarrow \rho^\circ + p$. The result is shown in Fig.8. The solid curve is a prediction from a vector dominance

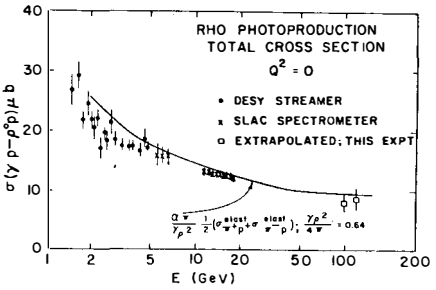

Fig.8. Values of the total photoproduction cross-section for rho-mesons measured at DESY, SLAC and derived from the data of this experiment.

model and which obtains the ρ°-proton cross-section from pion-proton cross-sections using a simple quark model.

(6) The angular distribution of ρ° decay gives $R_\rho = \sigma_L/\sigma_T$ where σ_L and σ_T are the rho production cross-sections by longitudinal and transverse virtual photons. In addition, it gives δ the phase between the L and T amplitudes. Results have large errors and are consistent with R_p being small or zero and $\delta = 90° \pm 40°$.

References

(1) W.A. Loomis et al, Phys. Rev. Letters 35, 1483 (1975).

(2) J.T. Dakin et al, Phys. Rev. D.10, 1401 (1974).

(3) J.T. Dakin and G.J. Feldman, Phys. Rev. 8D, 2862 (1973)

(4) C.J. Bebek et al, Phys. Rev. Letters, 34, 75º (1975).

EXPERIMENTAL PROGRAM PLANNED AT S.P.S. BY THE EUROPEAN MUON COLLABORATION

G. COIGNET
Laboratoire d'Annecy de Physique des Particules
B.P. 909 - 74019 Annecy-le-Vieux, France.

Abstract: The properties of the CERN SPS muon beam, which is expected to come in operation in early 1978, are given. The apparatus now being constructed is briefly described. The wide range of physics that can be investigated is then reviewed.

Résumé: Les caractéristiques du faisceau de muons du CERN SPS, qui doit entrer en opération au début de 1978, sont présentées. L'appareillage, actuellement en construction, est décrit. Le vaste programme de physique qui pourra être investigué est ensuite passé en revue.

The purpose of this contribution is to give an idea on what is going on in the preparation of the experimental program proposed[1] by the European Muon Collaboration (E.M.C.).

THE CERN SPS BEAM

The layout of the proposed beam[2] is presented in Fig. 1. It consist of four sections.

The front end section accepts and selects a beam of parent π's and K's from a primary target on which a 400 GeV/c proton beam is directed. Parent π's and K's are allowed to decay in a long FODO (strong FOcussing DefOcussing) channel which contains, with minimum losses, both parent π's and the wide momentum band of decay μ's ($0.57\ p_o(\pi) \leq p(\mu) \leq p_o(\pi)$). This results in a large particle flux. A beryllium absorber attenuates the unwanted hadrons by a factor $\simeq 10^8$. The desired band of muon momenta, and also of muon helicities, is selected by a series of vertical bending magnets. In this back end part, the off momentum muons are deflected away laterally with the help of magnetic collimators. The addition of scintillator hodoscope detectors in the focussing spectrometer just in front of the experimental area, allows the measurement of the momenta of individual muons to $\sim \pm 0.5\%$.

The expected characteristics of the beam are:

- wide energy range: $50 < E(GeV) < 300$
- very high intensity: $>10^8$/burst at 200 GeV/c, (see Table 1)
- large area: radius <5 cm for 99% containment,
  r.m.s. radius = 1.5 cm with $\Delta\theta_H = \pm 0.25$ mrad
  $\Delta\theta_V = \pm 0.45$ mrad
  $\frac{\Delta p}{p} = \pm 4.5\% \rightarrow \pm 0.5\%$ with beam hodoscopes
- low halo: few % level in 4 x 4 m^2 with R > 6 cm
- good purity: $\pi/\mu < 10^{-6}$
- high polarization: variable from +70% to -70%, with an intensity drop of less than a factor 3.

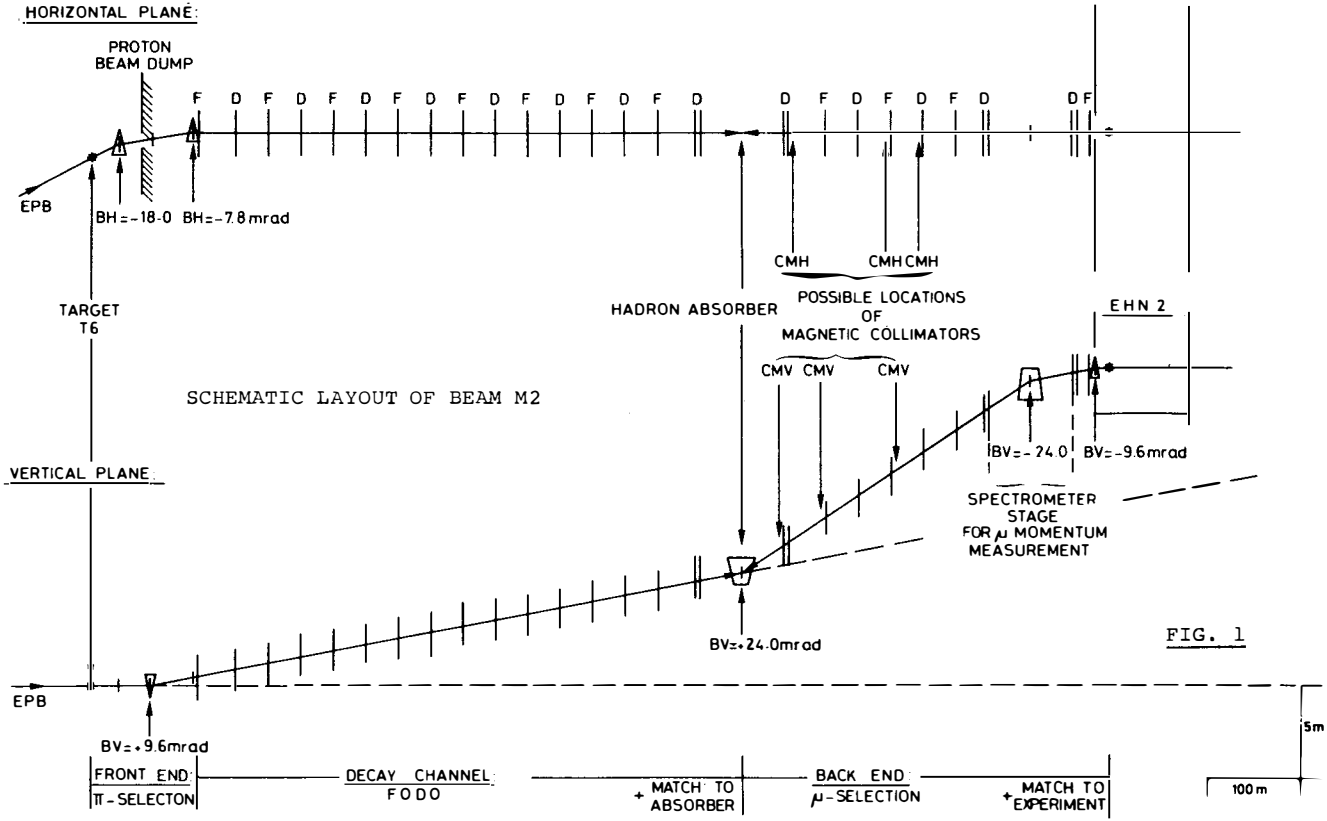
HORIZONTAL PLANE
PROTON BEAM DUMP
F D F D F D F D F D F D F D F D D F D F D F D F D D F
EPB
BH=-18.0
BH=-7.8mrad
CMH
CMH CMH
TARGET T6
HADRON ABSORBER
POSSIBLE LOCATIONS OF MAGNETIC COLLIMATORS
EHN 2
CMV CMV CMV
SCHEMATIC LAYOUT OF BEAM M2
BV=-24.0
BV=-9.6mrad
VERTICAL PLANE
SPECTROMETER STAGE FOR μ MOMENTUM MEASUREMENT
BV=+24.0mrad
EPB
BV=+9.6mrad
FRONT END π-SELECTON
DECAY CHANNEL FODO
+ MATCH TO ABSORBER
BACK END μ-SELECTION
+ MATCH TO EXPERIMENT
5m
100m

FIG. 1

THE EXPERIMENTAL SET-UP

The forward spectrometer (Fig. 2), which will be used for all experiments, consists of:

- A Dipole Magnet of 4 Tesla-metre, with 1 m high x 2 m wide aperture.
- Drift Chambers before (W_1 - W_2) and after (W_3 - W_7) the magnet. They are of variable size and variable resolution (0.3 mm to 1 mm). Each chamber is made of 6 or 8 planes with different orientation of the sensitive wires.
  Multiwire proportional chambers in the magnet are used to give easier matching of track segments in the lever arms before and after the 4 Tm magnet.
  The chambers are not sensitive in the beam region.
- A magnetised iron muon identifier made of a 2 m thick iron block. This block is magnetised so as to bend vertically (i.e. in the non bending plane of the dipole magnet) the muons which cross it, thus allowing an estimation of their momentum.
- Trigger scintillation hodoscope counters H_1 - H_4 equipped with coincidence matrices, are used to define particles with:
  - an angle $\theta > \theta_{MIN}$ to eliminate low q^2 events and prevent flooding the data acquisition system,
  - a momentum $p > p_{MIN}$ to reduce to a tolerable level the $\pi \rightarrow \mu$ decay background.

A is a halo veto counter, required in anticoincidence in the trigger. B_1, B_2 are beam hodoscopes, each consisting of 3 planes, inclined at 60°, made of 60 elements 2mm wide. These are equipped with TDC's and will be used to help the vertex reconstruction. For low intensity ($<10^7$/sec) experiments they could be used to give a beam veto requirement in the trigger. With a typical target position (2.5 m from the upstream edge of the magnet) the forward spectrometer accepts particles scattered, with a momentum larger than 15 GeV/c, in an angular range θ_{MIN} (~0.5°) $< \theta <$ 9°. The expected resolutions are then: $\Delta\theta = \pm 0.45$ mrad and $\Delta p = \pm 10^{-4} p^2$.

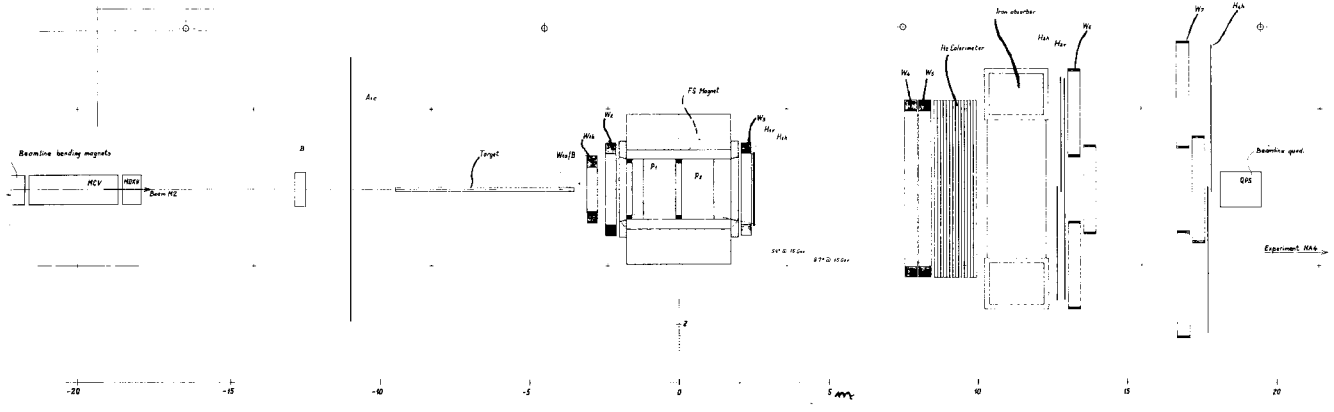

THE FORWARD SPECTROMETER

FIG. 2

Two types of target will be used, according to the experiments:

- A 6 m long hydrogen target.
- A heavy target of Sampling Total Absorption Counter type.

A 1 m long longitudinally polarized protons target is under study.

Two threshold Čerenkov counters, placed one in front of the magnet, the other after the magnet, will allow π - (K-p) separation between 7 to 25 GeV/c and π - K - p separation from 25 to 50 GeV/c. The H_2 hodoscope is of calorimeter type, 18 radiation lengths of Pb and 5.6 collision lengths of Fe: it will help to separate particles both neutral, (n, K^o) from (π^o, γ), and charged, hadrons from μ.

Two movable electron-photon detectors (1.2 x 1.3m^2) made of lead scintillator sandwiches (5 rad length), multiwire proportional chambers, and lead glasses (8 x 8 x 40 cm^2) will also be used for specific studies.

DEEP INELASTIC SCATTERING

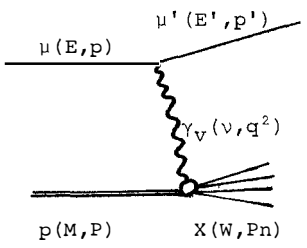

with the kinematical variables

$q^2 = (p-p')^2 = -Q^2$; negative mass^2 of γ_V.

$\nu = \frac{q \cdot P}{M} = E - E'$; γ_V energy.

$\omega = \frac{2M\nu}{Q^2} = \frac{1}{x}$

$W = (M^2 + 2M\nu + q^2)^{\frac{1}{2}}$

and θ the muon scattering angle in the lab,

the differential cross-section is written:

$$\frac{d^2\sigma}{dE'd\Omega'} = \left(\frac{4\alpha^2 (E')^2}{Q^4} \cos^2\frac{\theta}{2}\right)\left[W_2(\nu,q^2) + 2W_1(\nu,q^2) \tan^2\frac{\theta}{2}\right]$$

A long series of electron and muon scattering experiments[3] have established the scale invariance, namely that

$$2MW_1 \sim F_1(\omega) \ , \quad \nu W_2 \sim F_2(\omega)$$

In 1975, both new SLAC electron results[4] and FNAL muon results[5] indicated a scaling violation at the 10% level. Many reasons have been suggested to explain this feature and in any case, we need accurate measurements at much larger q^2 and ν values. Fig. 3 shows the kinematical range that can be explored by this experiment. The expected resolutions, depending on running time, can be found in reference 1.

Due to lack of space I shall just mention what else can be done when detecting the scattered muon under specific conditions:

σ_L/σ_T separation (H_2 target), since

$$\frac{d^2\sigma}{dq^2 d\nu} = \Gamma(q^2,\nu)\left[\sigma_T(q^2,\nu) + \varepsilon\,\sigma_L(q^2,\nu)\right]$$

is obtained at fixed q^2 and ν by varying the primary muon energy, i.e. ε, the relative longitudinal γ_ν polarisation.

Virtual compton scattering and wide angle bremsstrahlung interference measurement in order to obtain a new structure function[6] V(x) which is related to the cube of the parton charge. This measurement can be achieved using μ^+ and μ^- beams, and the photon detectors. The asymmetry $A = \frac{\sigma(\mu^+) - \sigma(\mu^-)}{\sigma(\mu^+) + \sigma(\mu^-)}$ is proportional to the interference between Bethe-Heitler and Compton terms.

Neutral weak current and two photon effetcs can be looked at with a heavy target by using beams of distinct charges and helicities. Calculations[7] based on the Weinberg-Salam model show that the biggest effect is expected for the asymmetry

$$A^{+-} = \frac{\sigma_{\mu^+L} - \sigma_{\mu^-R}}{\sigma_{\mu^+L} + \sigma_{\mu^-R}} \sim 10^{-4}\,Q^2 \quad (Q^2 \text{ in } (\text{GeV}/c)^2)$$

where L and R indicate the muon helicity. Should a significant asymmetry be observed, further measurements could be made with muons of the same charge and opposite helicities to separate the neutral current and the two photon effects.

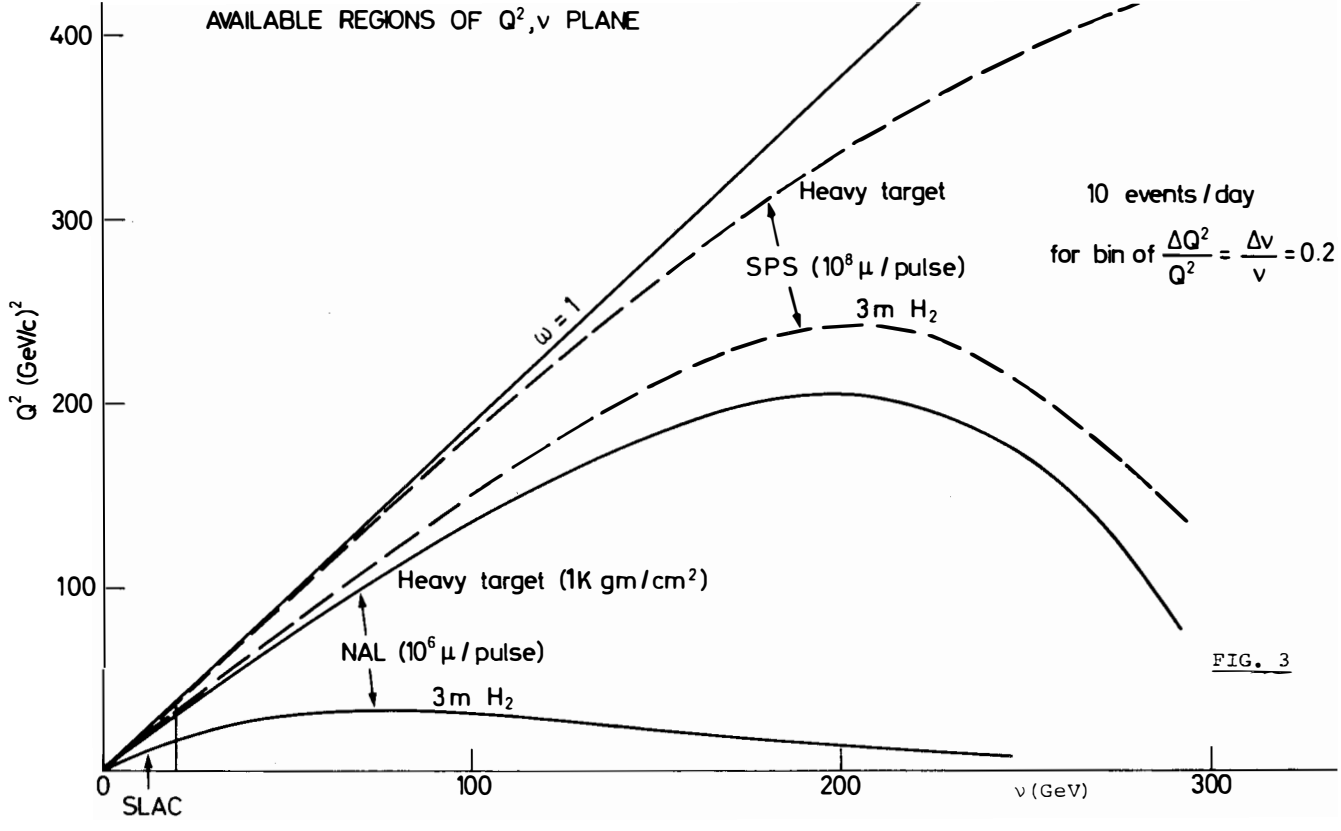
AVAILABLE REGIONS OF Q², ν PLANE
400
300
200
100
0
Q² (GeV/c)²
ω = 1
Heavy target
SPS (10⁸ μ / pulse)
3m H₂
10 events / day
for bin of ΔQ²/Q² = Δν/ν = 0.2
Heavy target (1K gm/cm²)
NAL (10⁶ μ / pulse)
3m H₂
SLAC
100
200
ν (GeV)
300

FIG. 3

Determination of the structure function $G_1(\nu,q^2)$ using the polarized beam and the longitudinally polarized target to measure the asymmetry parameter

$$A = \frac{\frac{d^2\sigma}{d\Omega' dE'}(\uparrow\downarrow) - \frac{d^2\sigma}{d\Omega' dE'}(\uparrow\uparrow)}{\frac{d^2\sigma}{d\Omega' dE'}(\uparrow\downarrow) + \frac{d^2\sigma}{d\Omega' dE'}(\uparrow\uparrow)} = 2\tan^2\frac{\theta}{2}\left[\frac{(E + E'\cos\theta)\, MG_1 + q^2 G_2}{W_2 + 2W_1 \tan^2\theta/2}\right]$$

where $\uparrow\downarrow(\uparrow\uparrow)$ means that the beam and the target polarization are parallel (antiparallel). The experiment is difficult since the actual measured asymmetry is typically 0.1 x A due to the facts that beam and target are not 100% polarized and that the target is not free hydrogen: but it is the unique way to have informations on the spin dependent structure function G_1, G_2 being expected to be small. For 300 hours running time, the error on A is estimated to be in the ±3%, ±5% range.

HADRON PRODUCTION

If the violation of scaling is interpreted as being due to a new threshold effect, then it is of first importance to look at associated hadronic production both in deep inelastic and multimuon experiments.

Even if the explanation is not correct, there is a whole field of physics to be studied, namely the global comparison of virtual photon induced reactions with photon and hadron induced ones. The high flux of this virtual photon beam (10^5 - 10^6 per burst depending on ν) allows this comparison.

Among the measurements to be performed are:

- Inclusive spectra of neutral and charged hadrons.
- Particle correlations.
- Vector meson production: ρ, ω, Φ, ρ' and higher masses...

The forward spectrometer has a good acceptance for hadrons produced with $x > 0$, not a too high p_T, and W values less than 7 GeV. The expected resolutions in W and ω, will be respectively $\Delta W < 1$ GeV and $\Delta\omega < 0.5$ GeV.

The addition of a vertex detector[1] inside a dipole magnet, will allow the extension of the acceptance for $x < 0$

and larger p_T values, i.e. extend the hadronic production study into the target fragmentation region. (This part of the detector is not approved at the moment).

MULTIMUON PRODUCTION

The production of a final state containing two or three muons is of great interest since it allows the search for new particles:

CHARM. If charm exists the single or double semileptonic decay of pair of charmed particles will give a rather high contribution to the 2μ or 3μ trigger events. Using the generalised Vector Dominance Model[9] the Ψ contribution can be estimated to ≈1% of the γp total cross section. Taking this conservative value and assuming a semi-leptonic branching ratio[10] of charmed particles of 10% we obtain

$$\text{for a } 2\mu \text{ trigger} \quad \frac{\sigma(\mu p \to \mu D\bar{D} + X \;\; \hookrightarrow \mu + \ldots)}{\sigma(\mu p \to \mu + \text{any})} \simeq 2 \times 10^{-3}$$

$$\text{for a } 3\mu \text{ trigger} \quad \frac{\sigma(\mu p \to \mu D\bar{D} + X \;\; \hookrightarrow \mu + \ldots \;\; \hookrightarrow \mu + \ldots)}{\sigma(\mu p \to \mu + \text{any})} \simeq 10^{-4}$$

corresponding respectively to 10 events/burst and 0.5 event/burst for 100% acceptance and 10^8 muons incoming on a 6 m H_2 target. In both cases the events include hadrons and the mean missing energy carried by the neutrinos must be small.

Ψ and other vector mesons. The cross sections and expected rates can be estimated by using as input the measured photoproduction cross section from FNAL[11] at $E\gamma \simeq 100$ GeV

$\sigma(\gamma p \to \Psi \;\; \hookrightarrow \mu^+\mu^- + X = 20 \pm 5$ nbarns/nucleus. Assuming that the process is dominated by a V.D.M. type graph where the virtual Ψ is elastically scattered on the nucleus, a A dependence of the cross section and using the Williams-Weizsäker approximation[12]

to relate the photoproduction cross section and the corresponding muo-production cross section by nearly real photons, we find

$$\sigma(\mu p \to \underset{\mu^+\mu^-}{\psi} + X) = 6 \times 10^{-35}\,cm^2; \quad \sigma(\mu Fe \to \underset{\mu^+\mu^-}{\psi} + X) = 3.4 \times 10^{-33}\,cm^2$$

The corresponding rates for 10^8 μ/burst (E_μ=200 GeV) and 100 hours running time are: 6300 with a 6 m H_2 target, 1.2×10^5 with a 1 m Fe target.

This high rate production will be very useful for calibration purposes. The acceptance[13] for masses as large as 15 GeV/c^2 is high (40%). The possibility of finding new vector mesons is directly related to their leptonic decay branching ratios.

HEAVY LEPTONS. The heavy lepton pair production can be computed using Q.E.D. graphs. The heavy lepton is assumed then to decay via $L^\pm \to \mu^\pm + \nu + \bar{\nu}$.

The calculations done by G. Menessier and used by P. Payre[13] for coherent and quasi elastic scattering, indicate that the main contribution comes from the space-like photon graph. The cross sections and corresponding rates on hydrogen and iron targets are indicated in Table 2. The heavy lepton events will be characterized by a large missing neutrino energy ($E_{\mu_1} + E_{\mu_2} + E_{\mu_3} < E_{beam}$) and pratically no hadronic energy.

The detection of electrons will be useful since the ratio $R = \frac{L \to e\nu\bar{\nu}}{L \to \mu\nu\bar{\nu}}$ determines the heavy lepton type.

B^o Heavy photon. B^o, the hypotetical massive spin 1 boson of electromagnetic interactions proposed by Lee and Wick[14], is mainly produced with a space-like leptonic propagator. From Linsker[15] calculations, cross sections taking into account coherent, quasi elastic and inelastic production have been estimated[13]: The cross sections and expected rates on hydrogen and iron targets are indicated in Table 3, for $5 < M_{B^o}(GeV/c^2) < 13$.

TABLE 1

INTENSITY AND HALO

PARENT ENERGY (GeV)	MUON ENERGY (GeV)	MUON SIGN	INTENSITY PER 10^{12} INT.PROT.*	HALO LEVEL R>6 cm %
300	280	+	1.4×10^{7}	3.3±0.5
		-	2.8×10^{6}	
220	200	+	1.2×10^{8}	1.0±0.2
		-	3.3×10^{7}	
140	120	+	3.1×10^{8}	2.6±0.3
		-	1.4×10^{8}	
200	120	+	7.1×10^{7}	3.3±0.8
		-	2.3×10^{7}	

* 3×10^{12} protons incident on 50 cm of Be $\approx 10^{12}$ interacting protons.

TABLE 2 - HEAVY LEPTON PRODUCTION CROSS SECTIONS AND RATES

Lepton Mass M (GeV/c^2)	6 m H_2 σ(cm^2)	Rates	1 m Fe σ(cm^2)	Rates
.5	85. x10^{-36}	8900		
1.0	8.4x10^{-36}	880	9.9x10^{-34}	35000
1.5	1.8x10^{-36}	190	5.6x10^{-34}	4700
2.0	4.8x10^{-37}	50	2.4x10^{-35}	840
3.0	4.5x10^{-38}	4.7	1.5x10^{-36}	51
4.0			8.1x10^{-38}	3

TABLE 3 - B^O PRODUCTION CROSS SECTIONS AND RATES

B^O Mass M (GeV/c^2)	6 m H_2 σ(cm^2)	Rates	1 m Fe σ(cm^2)	Rates
5	72. x10^{-36}	7600	28.10x10^{-34}	99500
7	16. x10^{-36}	1700	4.67x10^{-34}	16500
10	1.7x10^{-36}	180	5.7 x10^{-37}	2020
13	0.1x10^{-36}	10	4.0 x10^{-36}	140

The cross sections are given per nucleus and the rates are computed assuming 100% acceptance, $10^8\mu$/burst at 200 GeV, during 100 hours. The expected mass resolutions are respectively ± 16 MeV/c^2 for the H_2 target and ± 150 MeV/c^2 for the Fe target.

Electromagnetic tridents give a negligible contribution to this μ-μ mass range. However, low mass tridents represent a severe background at the trigger level. They will be suppressed by requiring a minimum angle and a minimum momentum for the two muons (low p_T cut), the overall acceptance remaining quite good.

CONCLUSIONS

The aim of the E.M.C. in designing the apparatus was to achieve extreme flexibility to cover the widest range of physics: this need for flexibility seems to be even more important since the recent developments in the field of new particles.

The apparatus now in construction will offer many possibilities (different targets, various triggers, particle identification, hadronic and electromagnetic energy measurements...) for doing exciting physics in 1978.

I gratefully acknowledge Drs. J.J. Aubert, J.H. Field, E. Gabathuler and P. Payre for very useful discussions. I want to thank Dr. R. Orr for reading the manuscript, and Mrs. A. Mazzari for her quick and accurate typing.

REFERENCES

1) Proposed Experiments and equipment for a programme of muon physics at the SPS by the European Muon Collaboration CERN/SPSC/74-78, SPSC P.18.
   - The European Muon Collaboration consists of some 50-60 physicists from France, Germany, Italy and the United Kingdom.
2) R. CLIFFT and N. DOBLE CERN/SPSC/74-12.
3) For a summary, see for example E. BLOOM, review talk in Proc. of the 6th International Symposium on Electron and Photon Interactions at high energies, BONN (1973) p. 227.
4) S. STEIN et al. SLAC-PUB-1528, 1975 and Phys.Rev. D12, 1884 (1975).
5) C. CHANG et al. Phys. Rev. Lett. 35, 901 (1975).
6) S.J.BRODSKY, J.F. GUNION and R.L. JAFFE Phys. Rev. D6, 2487 (1972).
7) S.M. BERMAN and J.R. PRIMACK SLAC-PUB-1360.
   M. SUZUKI LBL preprint, October 1973.
   C.P. KORTHALS-ALTES et al. Marseille preprint, CNRS 74/P-594
   C.H. LLEWELLYN-SMITH and D.V. NANOPOULOS, CERN TH.1850 (1974).
8) J. KUTI and V.F. WEISSKOPF Phys. Rev. D4, 3418 (1971).
9) D. SCHILDKNECHT, DESY 73/21 (1973).
10) M.K. GAILLARD, B.W. LEE and J.L. ROSNER Rev. Mod. Phys. 47, 277 (1975).
11) W. LEE et al. Contribution to the 7th International Symposium on Electron and Photon Interactions at high energy - STANDFORD (1975).
12) P. KESSLER Nuovo Cimento 53, 809 (1960).
13) P. PAYRE Thèse de troisième cycle - ORSAY (1975).
14) T.D. LEE and G.C. WICK Phys. Rev. D2, 1033 (1970).
15) R. LINKSER Phys. Rev. D5, 1709 (1972).

AN INTRODUCTION TO SCALING VIOLATIONS

G. PARISI
Laboratori Nazionali di Frascati
Frascati (Italy)

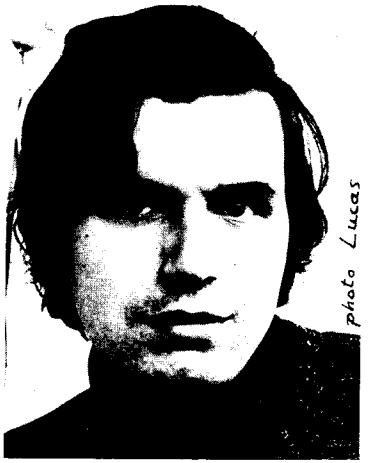

Abstract: The theory of scaling violations in deep inelastic scattering is presented using the parton model language; intuitive physical arguments are used as far as possible. In the comparison between theory and experiments particular attention is payed to the consequences of the opening of the threshold for charm production.

Resumé : On utilise ici le language du modèle a partons pour exposer la théorie de la violation de la loi d'échelle dans la diffusion très inélastique, en employant autant que possible des argumenta intuitifs. On compare ensuite théorie et donnés expérimentales en étudiant avec attention particulière les conséquences de l'overture du seuil pour produire du charm.

1. - INTRODUCTION(x)

ὅσων ὄψις ἀκοὴ μάθησις, ταῦτα ἐγὼ προτιμέω (o)
(Heracleitus)

I think that deep inelastic scattering is one of the best processes which can be used to test our theoretical understanding of strong interactions. The success of the Bjorken scaling law and the ability of the parton model to explain the experimental data are the main historical motivations for our present belief in the quark model.

It has now been realized that the naive quark-parton model is inconsistent and that small violations of the scaling law must be present: more accurate data seem to agree with this conclusion. The standard theoretical arguments which are used to study scaling violations are mainly based on sophisticated field theory techniques such as Wilson expansion at short distances and on the light cone, anomalous dimensions, bilocal operators.... All this theoretical machinery has been essential to derive unambigous and correct results, however we have departed from the physically intuitive approach which makes the standard parton model so appealing.

In this introduction to the violations of the scaling law, we try to recover the physical interpretation of the theory; to this end the language of the parton model will be used to derive and interpret the theoretical results. We hope that this paper will partially fill the gap between the conclusions of the parton model (which are physically motivated but incorrect) and the conclusions of a field theoretical analysis (which are correct but whose intuitive interpretation has been lost somewhere(+).

2. - THE PARTON MODEL

Let us briefly review the main ideas which are behind the parton model[6] in order to understand how they must be modified to account for the violations of the Bjorken scaling law.

(x) - Part of the results presented here have been obtained by the author in collaboration with G. Altarelli and R. Petronzio[1-3].

(o) - The things of which there is seeing and hearing and perception, these do I prefer.

(+) - This point of view is not new: a similar approach has been advocated by Polyakov[4] and by Kogut and Susskind[5].

In a deep inelastic process an highly virtual photon of mass Q^2 interacts with the pointlike constituents (partons) of the hadron. In the Breit frame the photon carries no energy and the proton has a momentum P proportional to $(Q^2)^{1/2}$. For high Q^2, P is large and the proton looks like a highly Lorentz contracted pancake; the time (τ) of interaction is proportional to $(Q^2)^{-1/2}$. For small τ we can safely suppose that the photon scatters incoherently on each parton; the cross section for deep inelastic scattering depends on the parton distribution seen when we look inside the hadron with a resolution time τ.

The cross section for longitudinaly (σ_L) and transverse (σ_T) polarized photons can be written using two independent structure functions[7]: $F_1(x, Q^2)$, $F_2(x, Q^2)$, x being equal to $2M\nu/Q^2$.

For spin 1/2 partons:

$$F_2(x, Q^2) = \Sigma_i e_i^2 \, x N_i(x, \tau) , \qquad \tau = (Q^2)^{-1/2} , \tag{2.1}$$

where $N_i(x, \tau)$ is the number of partons of the i-th type, having charge e_i and carrying longitudinal momentum xP; σ_L/σ_T is proportional to $\langle p_\perp^2 \rangle / Q^2$, where $\langle p_\perp^2 \rangle$ is the mean squared value of the transverse momentum carried by the partons.

This is quite general: we have only assumed that the electromagnetic current couples to point-like constituents and that the final state interaction does not change total cross sections at very high energies: after the interaction with the photon the system evolves in time with its own hamiltonian.

The Bjorken scaling law follows from the assumption that:

$$\lim_{\tau \to 0} N(x, \tau) = N(x) \neq 0 . \tag{2.2}$$

In very short times partons cannot modify their distribution inside the hadron: they move slowly and they can be considered free on a short time scale.

Two main assumptions are thus involved in the derivation of the Bjorken scaling law:

a) The hadron interacts with an highly virtual photon via some point-like constituents (partons). Final state interactions can be neglected.

b) The constituents cannot change their momentum too fast: their interactions can be neglected in the limit $\tau \to 0$.

However what is the rationale for these assumptions? In any reasonable quantum field theory in 4 dimensional space-time the first one is valid, the second one is false[8-9].

For example in quantum electrodynamics the validity of both assumptions would imply that the radiative corrections scale with the energy and are the same both for $e\bar{e}$ and $\mu\bar{\mu}$ scattering. Anyone working in high energy physics knows that this is not the case and that radiative corrections show a logaritmic dependence on E/m.

If the first hypothesis is true, even in presence of scaling violations the parton model inequalities in deep inelastic scattering (e.g. $1/4 \leq \leq F_2^n(x,Q^2)/F_2^p(x,Q^2) \leq 4$) are unchanged. The failure of the second hypothesis implies that the Bjorken scaling law is no more valid and that more complicated scaling laws are satisfied. These new scaling laws depend on the detailed dynamics of the strong interactions and their verification would be quite important.

Before discussing what happens in the strong interaction case, I want to clear up the situation in a more familiar case, i.e. quantum electrodynamics. This will be done in sections 3 and 4. In section 5 I will present the theoretical results based on a coloured gauge theory of strong interactions. In sections 6 and 7 I will compare the theoretical results with the experimental data on electron and neutrino scattering.

3. - THE COSTITUENTS OF THE ELECTRON

ἐν δὲ μέρει κρατέουσυ περυπλομένοιο κύκλοιο, καὶ φθίνει εἰς ἄλληλα καὶ αὔξεται ἐν μέρει αἴσης (x)

(Empedocles)

Pure quantum electrodynamics is a good place to study the violations of the Bjorken scaling law. They show up in very simple and familiar formulae: the equivalent number of photons in an electron on energy E (momentum P = E) is:

$$N_\gamma(x,P) \simeq \frac{\alpha}{2\pi}\frac{4}{x}\ln(P/m_e) + O(\alpha^2) , \qquad (3.1)$$

(x) - In turn they (elements) get the upper hand in the revolving cycle, and perish into one another and increase in the turn appointed by their fate.

where x is the fraction of longitudinal momentum carried by the photon. If we interpret $1/P \simeq (1/Q^2)^{1/2}$ as the resolution time τ, we obtain that the equivalent number of photons in the electron is :

$$N_\gamma(x,\tau) = \frac{\alpha}{2\pi}\frac{4}{x}\ln(1/m_e\tau) + O(\alpha^2) \quad , \quad \tau m_e \ll 1 . \tag{3.2}$$

This quantity goes to infinity when $\tau \to 0$ and the assumption b) (eq. 2.2) of the last section is violated. Moreover for each photon of momentum xP there must be an electron of momentum $(1-x)P$; the momentum distribution of the electrons inside the electron is :

$$N_e(x,\tau) = \delta(x-1) + \frac{\alpha}{2\pi}\left[\frac{4}{1-x} - 2C\,\delta(x-1)\right]\ln(1/m_e\tau) . \tag{3.3}$$

The constant C is fixed by the condition that the total number of electrons is not changed by the interaction :

$$\int_0^1 N_e(x,\tau)\,dx = 1 . \tag{3.4}$$

Stricly speaking C is logaritmically divergent ($C = 2\int_0^1 \frac{dx}{1-x}$). The two divergences in eq. (3.4) cancel each other.

However eqs. (3.1) and (3.3) cannot be used directly to study the limit $\tau \to 0$: the neglected higher order terms become important when $\alpha \ln \tau \simeq 1$. Let us first study the effect of multiple photon emission (see Fig. 1). The key step is to concentrate one's attention on the time derivative of the number of electrons ; the variable $L = -2\ln(m_e\tau)$ is introduced for convenience.

From eq. (3.3) we find :

$$\frac{dN_e(x,L)}{dL} = -\frac{1}{2}\frac{dN_e(x,\tau)}{d\ln\tau} = \frac{\alpha}{2\pi}\frac{2}{1-x} - C\,\delta(x-1) = \frac{\alpha}{2\pi}P_{ee}(x) . \tag{3.5}$$

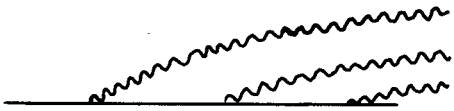

fig.1

FIG. 1 -A typical diagram contributing to multiple photon emission.

Eq. (3.5) suggests that the transition probability for electron bremsstrahlung is independent of L. However the electron distribution is L dependent: the change in time of the electron distribution must be the product of the transition probability p and the actual electron distribution at "time" L. One is led to the following "master" equation:

$$(3.6) \qquad \frac{dN_e(x,L)}{dL} = \frac{\alpha}{2\pi}\int_x^1 \frac{dy}{y} N_e(y,L)\, p_{ee}(x/y) =$$

$$= \frac{\alpha}{2\pi}\left[-CN_e(x,L) + \int_x^1 N_e(y,L)/(y-x)\, dy\right].$$

The first term arises from the decrease of $N_e(x,L)$ due to the bremsstrahlung of electrons staying at the point x: it is naturally proportional to $N_e(x,L)$. The second term represents the increase in the number of electrons at the point x due to bremsstrahlung of electrons carrying momentum $y > x$, the relative loss of electron momentum being x/y.

Eq. (3.6) can be easily solved by computer; qualitative statements can be made studying the L dependence of the moments:

$$(3.7) \qquad M_e^N(L) = \int_0^1 \frac{dx}{x} x^N N_e(x,L).$$

Substituting eq. (3.6) in the derivative of eq. (3.7) we obtain:

$$(3.8) \qquad \frac{dM_e^N(L)}{dL} = \frac{\alpha}{2\pi}\int_0^1 \frac{dx}{x} x^N N_e(x,L) \int_0^1 \frac{dy}{y} y^N p_{ee}(y) =$$

$$= -\frac{\alpha}{2\pi} M_e^N A_{ee}^N; \qquad A_{ee}^1 = 0 \qquad A_{ee}^N > 0 \ (N > 1),$$

whose solution is:

$$(3.9) \qquad M_e^N(L) = M_e^N(L_o)\exp\left[-\frac{\alpha}{2\pi} A_{ee}^N (L-L_o)\right].$$

M^1 is the total number of electrons in the system and it is a constant. M^2 is the total momentum in P units carried by the electrons and it goes exponentially to zero: the whole momentum is transferred from the electron to the photon system. Increasing L, $N_e(x,L)$ shifts towards $x = 0$ and asymptotically it is concentrated at this point.

Eqs. (3.6-3.9) are valid in the so called leading logaritm approximation (terms proportional to $(\alpha L)^n$ are retained and terms proportional to $\alpha(\alpha L)^n$ are neglected).

The transition probabilities p_{ee} contain higher orders in α; however these new terms are not L dependent and no qualitative conclusion is changed; to neglect them is a good approximation for all values of L if α is not too large.

A similar equation can be written for the photons:

$$\frac{dN_\gamma(x, L)}{dL} = \frac{\alpha}{2\pi} \int_x^1 \frac{dy}{y} N_e(y, L)\, p_{\gamma e}(x/y) . \tag{3.10}$$

The following relation holds:

$$p_{\gamma e}(x) = p_{ee}(1-x) . \tag{3.11}$$

However the situation is not so simple: the photon itself may split in a $e\bar{e}$ pair, each of the new born e or $\bar{e}$ may emit a photon and so on. The whole process is quite similar to the evolution of an electromagnetic shower in lead. A typical diagram is shown in Fig. 2.

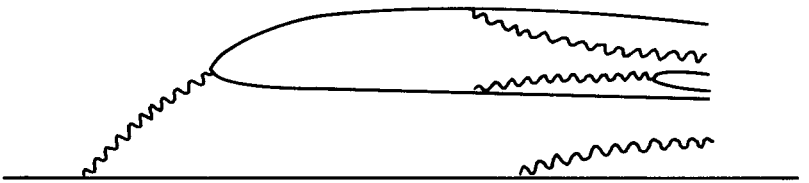

fig.2

FIG. 2 - A typical diagram contributing to the formation of the "shower".

It is clear that we must introduce in the game the distributions of the e, $\bar{e}$ and γ inside the electron; using the same arguments as in the previous case a more complicated master equation can be derived:

$$\frac{dN_e(x, L)}{dL} = \frac{\alpha}{2\pi} \int_x^1 \frac{dy}{y} \left[N_e(y, L)\, p_{ee}(x/y) + N_\gamma(y, L)\, p_{e\gamma}(x/y) \right] ,$$

$$\frac{dN_{\bar{e}}(x, L)}{dL} = \frac{\alpha}{2\pi} \int_x^1 \frac{dy}{y} \left[N_{\bar{e}}(y, L)\, p_{\bar{e}\bar{e}}(x/y) + N_\gamma(y, L)\, p_{\bar{e}\gamma}(x/y) \right] , \tag{3.12}$$

$$\frac{dN_\gamma(x,L)}{dL} = \frac{\alpha}{2\pi}\int_x^1 \frac{dy}{y}\left\{ N_\gamma(y,L)p_{\gamma\gamma}(x/y) + \right.$$
$$\left. + \left[N_e(y,L) + N_{\bar{e}}(y,L)\right] p_{\gamma e}(x/y)\right\} ,$$

where:

$$p_{ee}(y) = p_{\bar{e}\bar{e}}(y) = p_{\gamma e}(1-y) = p_{\gamma\bar{e}}(1-y) ,$$

$$p_{\bar{e}\gamma}(y) = p_{e\gamma}(y) = p_{e\gamma}(1-y) = \frac{1}{2}\left[y^2 + (1-y)^2\right] ,$$

(3. 13)

$$p_{\gamma\gamma}(y) = - C_\gamma \delta(y-1) ,$$

$$C_\gamma = \frac{1}{2}\int dy \left[p_{e\gamma}(y) + p_{\bar{e}\gamma}(y)\right] = \frac{1}{3} .$$

The meaning of these equations is quite clear. The last equation implies that the number of photons which disappear at the point x it is equal to the number of new born $e\bar{e}$ pairs carrying total momentum x. The functions $p_{e\gamma}$ and $p_{\gamma e}$ are related to the longitudinal distributions of bremsstrahlung photons and of Dalitz pair electrons(x).

It is interesting to note that the derivative of the difference of the number of electrons and positrons does not depend on the γ distribution:

(3. 14)
$$\Delta N(x,L) = N_e(x,L) - N_{\bar{e}}(x,L) ,$$

$$\frac{d\Delta N(x,L)}{dL} = \int_x^1 \frac{dy}{y}\Delta N(y,L)\, p_{ee}(x/y) .$$

The L evolution of this difference decouples from that of the other functions. Also this coupled set of equations can be easily solved with a computer: the knowledge of the three functions N_e, $N_{\bar{e}}$ and N_γ at a particular value of L in the region $1 > x > x_m$ allows us to compute them at any value of L, in the same x region.

It is possible to study the behaviour of the moments of the distributions; if one defines a three component vector

---

(x) - The possibility of using these formulae to compute higher order processes in quantum electrodynamics has been suggested by Cabibbo. This technique has been applied to the study of the reactions $e^+e^- \to e^+e^-$ (10) and $e^+e^- \to e^+e^-e^+e^-$ (11).

(3.15) $$M_i^N(L) = \int_0^1 \frac{dx}{x} x^N N_i(x,L)$$ $i = 1 \leftrightarrow e$, $i = 2 \leftrightarrow \bar{e}$, $i = 3 \leftrightarrow \gamma$

one finds :

(3.16) $$\frac{dM_i^N(L)}{dL} = -\frac{\alpha}{2\pi} A_{iK}^N M_K^N(L) ,$$

where A is a three by three matrix. If we denote by λ_a^N and $\vec{u}_a^N$ the three eigenvalues and eigenvectors of A^N, the solution of (3.16) can be written using the vectorial notations as :

(3.17) $$\vec{M}^N(L) = \sum_1^3 a\, M_a^N \vec{u}_a^N \exp -\frac{\alpha}{2\pi}(L-L_o)\lambda_a^N .$$

The quantities M_a^N are fixed by the boundary condition $\vec{M}^N(L)\big|_{L=L_o} = \vec{M}^N(L_o)$.

For N = 2 one of the eigenvalues is 0, reflecting the conservation of the total momentum carried by the constituents. When $L \to \infty$ the distributions of both electrons and photons shifts towards 0, the ratio of the momentum carried by the electrons and the positrons goes to one and the total momentum carried by the "valence" electron goes to zero, while the momentum carried by the sea of $e\bar{e}$ pairs and by the photons goes to a constant. In the limit $L \to \infty$ an equilibrium situation is reached : the momentum lost by the electrons via bremsstrahlung is equal to the momentum refilling due to the creation of Dalitz pairs. The mean value of the momentum carried by each constituent goes to zero and this degradation of momentum is the origin of the progressive concentration of the functions N(x, L) near x = 0. Up to now, we have considered only the distributions in longitudinal momentum. The transverse momentum distribution can be studied using similar techniques ; one finds[12] :

$$\frac{\sigma_L}{\sigma_T} \propto \frac{\langle p_\perp^2 \rangle}{p^2} = \bullet(\alpha) .$$

Unfortunately the situation is not so simple : we have neglected the possibility that an $e\bar{e}$ pair annihilate in a photon which subsequently splits in an $e\bar{e}$ pair and so on. A typical diagram is shown in Fig. 3.

To study this phenomenum a new concept must be introduced : vacuum polarization. The effect of these new diagrams can be accounted for, by the introduction of an effective L dependent coupling constant.

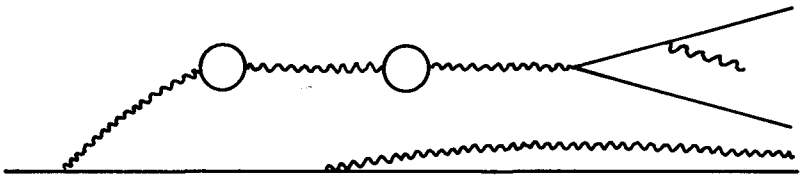

fig.3

FIG. 3 -A typical diagram contributing to vacuum polarization.

We prefer to discuss the consequences of vacuum polarization and to write the final formulae in this section; we postpone to the next section the discussion on the rationale and on the physical meaning for the introduction of an effective time dependent coupling constant. The correct formulae are obtained by substituting α by $\alpha(L)$ in eqs. 3.12 and 3.16. The function $\alpha(L)$ satisfies the differential equation:

$$\frac{d\alpha(L)}{dL} = \beta\alpha^2(L) + \bullet\left[\alpha^3(L)\right] , \qquad L \gg 1 , \tag{3.18}$$

whose solution is:

$$\alpha(L) = \frac{\alpha(L_0)}{1 - \beta(L-L_0)\alpha(L_0)} , \qquad \alpha(L),\ \alpha(L_0) \ll 1 . \tag{3.19}$$

Two different possibilities are open[13]:

a) $\beta > 0$,

b) $\beta < 0$.

In case a) the effective coupling increases with L, also if we start from a small value of α, increasing L we are projected in the strong coupling regime where we cannot justify our approximation of neglecting higher order in α in the transition probabilities p. What will finally happen in this case is still an open problem: no general consensus has been reached on this point.

Case a) is realized in pure QED; the energies at which the perturbative expansion become useless are gigantic: they are of the order of the mass of the universe.

Case b) is better understood: increasing L the effective coupling constant decreases; also if we start from a relative large value of α we finally end up with a small value of $\alpha(L)$ ($\alpha(L) \to -1/\beta L$ when $L \to \infty$). In this kind of theory the large L limit can be controlled using a perturba

tive estimate of the transition probabilities, whatever the value of the coupling constant in the low momentum region.

There is no problem to solve the modified eq. (3.12) by computer. Eq. (3.16) becomes now:

$$\frac{dM_i^N(L)}{dL} = -\frac{\alpha(L)}{2\pi} A_{iK}^N M_K^N(L) \quad , \tag{3.20}$$

whose solution is:

$$\vec{M}^N(L) = \sum_1^3 a \, M_a^N \vec{u}_a^N \left[1 - \beta(L-L_o)\alpha(L_o)\right]^{-\frac{\lambda_a^N}{2\pi\beta}} \quad . \tag{3.21}$$

We now have in our hands the tools which are needed to study the violations of the scaling law in deep inelastic scattering. We are able to compute how the distribution of the pointlike constituents depends on the resolution time. We have seen that when the resolution time goes to zero ($L \to \infty$) a continuous process of interchange of momentum among the bare constituents is present, the laws which regulate this phenomenum can be summarized in the "master" equation (3.12).

4. - VACUUM POLARIZATION

It is a common day experience that salt can be easily dissolved in water but not in oil. This fact is due to the high value of the static dielectric constant $\varepsilon_s = 80$ ($\varepsilon_s = 1$ in vaccum). The force between two charges is:

$$F = \frac{q_1 q_2}{\varepsilon_s} \frac{1}{r^2} \quad , \qquad r \to \infty \quad , \tag{4.1}$$

at large distances. However, at distances smaller than the radius of the water molecule (a), one recovers the more familiar:

$$F = q_1 q_2 \frac{1}{r^2} \quad , \qquad r << d \, . \tag{4.2}$$

It is possible to define a function $\varepsilon(r)$ such that:

$$F = \frac{q_1 q_2}{\varepsilon(r)} \frac{1}{r^2} \quad , \qquad \varepsilon(0) = 1 \, , \quad \varepsilon(\infty) = \varepsilon_s \, . \tag{4.3}$$

This effect arises from the orientation of the water dipoles in presence of an electric field. The scale of the phenomenum is naturally given by d.

Equivalently one would define an r dependent effective charge and write:

(4. 4) $$F = q_1(r)\, q_2(r)\, \frac{1}{r^2} \quad , \qquad q_1(r) = q_1 / \sqrt{\varepsilon(r)} \; .$$

A typical plot of q(r) as function of L is shown in Fig. 4.

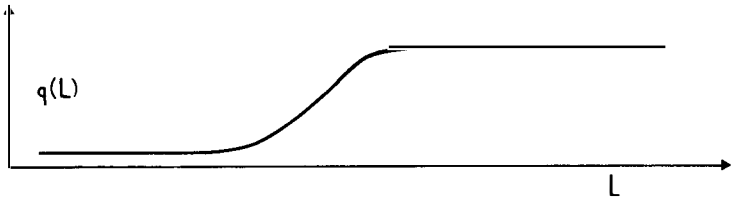

FIG. 4 -The effective charge in water as function of $L = -\ln(r/d)$, r being the distance and d being the radius of water molecules.

The polarization of water decreases the force among Na^+ and Cl^- ions and allows the solution of salt in water: charged ions in water are nearly asymptotically free at large distances while they have a strong interaction at short distances.

A more drammatic effect can be found in metals: here $\varepsilon_s = \infty$ and the effective charge goes to zero exponentially at large distances: the charge is completely shielded.

In quantum electrodynamics the role of water is played by the virtual $e\bar{e}$ pairs which fill the vacuum. The presence of a charge modifies their distribution and produces a polarization of the vacuum which alters the value of the effective charge seen at large distances. The inverse of the mass of the virtual pair corresponds to the radius of water molecules: the shielding effect reaches a constant at distances larger than $1/2\ m_e$. However there is no upper bound to the mass of a virtual pair so that the effective charge changes its value also at very short distances. At distances of order 10^{-100} cm the effective coupling constant becomes of order 1 and non linear phenomena in the electric field are quite important. It is not clear what happens at so short distances, however this problem is not relevant here.

We hope we have clarified why the effective coupling constant in Quantum electrodynamics depends on the distance r and by relativistic invariance also on the resolution time τ. The fact that the force among different (equal) sign charges is attractive (repulsive) implies that in all possible materials, vacuum included, $\varepsilon_s > 1$ and the effective charge at large distances

is smaller than the bare charge: $q(\infty) < q(0)$. We can conceive a world in which the force among charges of the same sign is attractive and among charges of opposite sign is repulsive. We will call the matter of which this world is made up "enantion". The static polarizability of the enantion is always less than 1. Also in this case we can introduce a distance-dependent effective coupling constant: the effective charge seen at large distances is always greater that the bare one:

$$q(\infty) = \frac{q(0)}{\sqrt{\varepsilon_s}} > q(0) \quad . \tag{4.5}$$

Let us chose a particular kind of enantion in which $\varepsilon_s = 0$ and let us suppose that the radius of the molecules has a continous distribution which ranges from zero up to a maximum length d. In this case $q(\infty)/q(0) = \infty$. If the effective charge seen at large distance is finite, the effective charge at very small distance must be equal to zero (see Fig. 5). Two ions in enantion behave as free at short distances while the interaction remains strong at large distances.

Why are we interested in such a devious system? The reason is simple: there are models of strong interactions in which the polarizability properties of vacuum are just the same as those of enantion. These model belong to case b) of section 3 and have a coupling constant which is asymptotically zero at short distance. I think that it is interesting to have a concrete example of a system in which the interaction among pointlike particles fades at short distances.

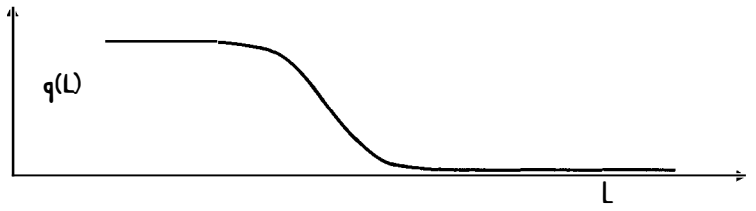

FIG. 5 -The effective charge in enantion as function of $L = -\ln(r/d)$, r being the distance and d being the maximum radius of enantion molecules.

5. - THE STRUCTURE OF STRONG INTERACTIONS

τέσσαρα γὰρ πάντων ῥιζώματα πρῶτον ἄκουε[x]
(Empedocles)

In the most popular model of strong interactions the hadrons are composed of 4 quarks (p, n, λ and p')[14]; the three different colours of quarks interact via the exchange of an octet of coloured gluons. Electromagnetic and week currents are colour singlets; the theory is invariant under the group SU(3) colour.

The effective coupling constant of the theory satisfies the equation[15-17]:

$$\frac{d\alpha(L)}{dL} = -\frac{25}{12\pi}\alpha^2(L) + O(\alpha^3) \qquad (L = \ln Q^2)\,, \tag{5.1}$$

whose solution is:

$$\alpha(L) = \frac{\alpha(L_o)}{1 + \frac{25}{12\pi}(L - L_o)\alpha(L_o)}\,. \tag{5.2}$$

The situation is the same as in enantion. Although the coupling constant of strong interactions is large at distances of order $1/m_\pi$, it is possible that at rather shorter distances it becomes smaller and smaller and that a perturbative approach can be used in the deep inelastic region. If this is the case, it is possible to obtain sharp predictions for the breaking of the Bjorken scaling law for very high Q^2.

We denote by $N_{q_i}(x, L)$ $i = 1, 4$, $N_{\bar{q}_i}(x, L)$ $i = 5, 8$ and $N_g(x, L)$ respectively, the longitudinal momentum distributions of quarks, antiquarks and gluons inside an hadron. The L dependence of these distribution functions can be computed using the transition probabilities for the processes: $q \to q + g$, $g \to q + \bar{q}$ and $g \to g + g$. The first two are present also in quantum electrodynamics, while the third is peculiar to non abelian gauge theories.

The following master equation holds:

$$\frac{dN_{q_i}(x, L)}{dL} = \frac{\alpha}{4\pi}\int_x^1 \frac{dy}{y}\left[p_{qq}(x/y)N_{q_i}(y, L) + p_{qg}(x/y)N_g(y, L)\right], \tag{5.3}$$

(x) - Hear first the four roots of all things.

$$\frac{dN_g(x,L)}{dL} = \frac{\alpha}{4\pi}\int_x^1 \frac{dy}{y}\left[p_{gg}(x/y)N_g(y,L) + p_{gq}(x/y)\sum_1^8 N_{q_i}(y,L)\right],$$

where

$$p_{qq}(y) = \frac{4}{3}\left[\frac{4}{(1-y)_+} - \delta(y-1) - 2 - 2y\right],$$

$$p_{gq}(y) = \frac{4}{3}\left[\frac{2(1-y)^2+2}{y}\right],$$

(5.4)

$$p_{qg}(y) = \frac{3}{16}\left[2(1-y)^2 + 2y^2\right],$$

$$p_{gg}(y) = 3\left[\frac{4}{(1-y)_+} + \frac{4}{y} + 4y(1-y)\right] - 2\delta(y-1),$$

$\frac{1}{(1-y)_+}$ is a distribution defined by:

$$\int_x^1 \frac{dy}{y}\frac{1}{(1-\frac{x}{y})_+}N(y) = \ln(1-x)N(x) + \int_x^1 \frac{dy}{y}\frac{1}{1-\frac{x}{y}}\left[N(y) - N(x)\right]. \quad (5.5)$$

The following consistency conditions are satisfied:

$$p_{qq}(y) = p_{gq}(1-y),$$

$$p_{qg}(y) = p_{qg}(1-y), \quad (5.6)$$

$$p_{gg}(y) = p_{gg}(1-y).$$

Eqs. (5.3-5.5) can be directly derived from the standard results of ref. (18-20) using the technique employed in ref. (21).

Higher orders in α have been neglected. σ_L/σ_T is of order α and is therefore asymptotically zero.

Let us try to use these formulae to compute the violations of the scaling law in deep inelastic scattering on nucleons.

Electron and neutrino deep inelastic scattering gives us very good information on the x distribution of quarks inside the nucleon, however no in

formation is available on the gluon distribution; we only know that gluons must be present in the nucleon: they carry about 0.48 of the total momentum. Unfortunately the theoretical predictions for scaling violations depend on the form of the gluon distribution. Two phenomena contribute to the scaling violations: firstly the shift of the quark and antiquark distributions due to gluon bremsstrahlung, secondly the creation of quark-antiquark pairs. Only the second process depends on the distribution of gluons. However it is quite reasonable that the sea will be negligible for x near to one ($x > 0.5$). Model independent conclusions can be reached only in this region.

If we want to be more quantitative we can try to put upper and lower bounds on the scaling violations using two extreme models of gluon distributions.

The first unreasonable possibility is that the gluons are concentrated at $x = 0$; $N_g(x, L) = 0.48\,\delta(x)/x$.

In this case the L derivative of the structure function is[21]:

$$(5.7)\qquad \frac{dF_2(x,Q^2)}{d\ln q^2} = \frac{\alpha(Q^2)}{3\pi}\left\{\left[3 + 4\ln(1-x)\right]F_2(x,Q^2) + x\int_x^1 dy\left[\left(-2\left(1+\frac{x}{y}\right) + \frac{4}{1-\frac{x}{y}}\right)F_2(y,Q^2) - \frac{4F_2(x,Q^2)}{1-\frac{x}{y}}\right]\right\}.$$

The value of the effective coupling constant $\alpha(Q^2)$ appears as a factor. Using as input[22]

$$(5.8)\qquad F_2^p(x) = (1-x)^3\left[1.274 + 0.5989(1-x) - 1.675(1-x)^2\right]$$

we obtain curve I of Fig. 6 for $\alpha(Q^2) = 0.4$. Notice that for such an high value of α corrections coming from the higher order terms may not be completely negligible. In this case we have neglected the gluon contribution which is positive: curve I is a lower bound on the derivative.

A physical motivated upper bound can be obtained supposing that the gluon distribution is proportional to the quark distribution in the region x near to one: for example we can assume that the x distribution is exactly $1.92(1-x)^3/x$. In this case one obtains the curve III of Fig. 6. In the region

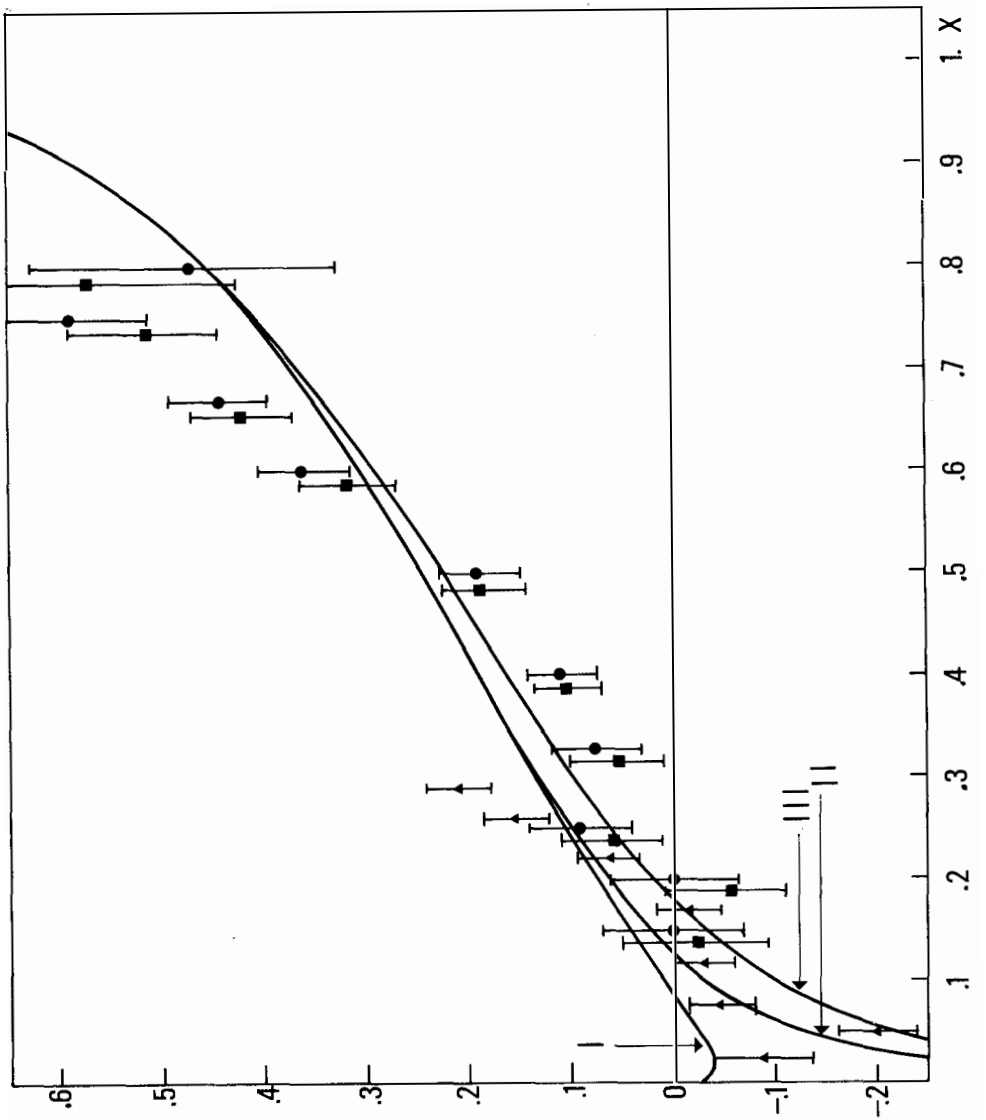

FIG. 6 - Curve I, II and III are respectively the predictions for $-\partial \ln F_2^p(x, Q^2)/\partial(\ln Q^2)$ assuming respectively, I the concentration of all gluons at $x = 0$, II an educated guess for the gluon distribution, and III a distribution $(1-x)^3$ for the gluons; the same predictions are obtained for the neutron with an accuracy of 0.02; $\alpha = 0.4$ has been assumed. (●) and (●) are respectively the experimental points for proton and deuterium[27]; (▲) are the experimental points for iron[28].

of large x there is no significant difference between the two curves for the two extreme choices of the gluon distribution. The difference is concentrated in the region of low x and it is due to the increase of the sea.

An educated guess for the gluon distribution can be obtained as follows: suppose that at a low value of L only p and n quarks are present in the proton. Using the master equation (5. 3) one can compute the quark, antiquark and gluon distributions for all values of L. If we impose the constraint that, at a particular value of L, the structure functions coincide with eq. (5. 8) we are able to fix the quark and gluon distributions at that particular L. Without entering into the details of how it can be done, we show directly the results: the predictions for the derivative of the structure functions are represented by curve II of Fig. 6.

A consistency check[2] of this model can be done comparing the predicted quark and antiquark distributions with the experimental data coming from neutrino and antineutrino scattering at Gargamelle. The agreement is not bad (see Fig. 7): notice that we have no free parameter and that we have used as input only data coming from deep inelastic electron scattering.

It seems to me that the predicted antiquark distribution is too concetrated near $x = 0$ (better data are needed to prove this conclusion); it is reasonable to suppose that the predicted gluon distribution has the same defect and that we are understimating the number of gluons in the large x region. My personal conclusion is that the correct prediction is between curve II and III. The ambiguity due to our ignorance of the gluon distribution is not large and sharp predictions can be made in the real asymptotic region.

Similar results can be obtained for the neutron structure functions. The difference among curves I, II and III for the neutron and the proton would hardly be observable in Fig. 6. It is always less than 0. 02.

These predictions are done in the region of very high Q^2 where $\alpha(Q^2)$ and M^2/Q^2 are small numbers. In the next section we shall see that in the intermediate Q^2 region where actual experiments are done, extra ambiguities are present which make the comparison between theory and experiments less straightforward.

6. - THE COMPARISON WITH EXPERIMENTS

ἁμαρτίης αἰτίη ἡ ἀμαθίη τοῦ χρέσσονος[x]
(Democritus)

When precise data on deep inelastic e-p scattering appeared in 1970 it was clear that violations of the Bjorken scaling were present[24]. These violations disappeared when the variable x' was used[25]; x and x' are asymptotically equal; the difference is only relevant at "low" values of Q^2. The amount and the very existence of scaling violations depends on the choice of the "correct" variable.

Up to now no strong theoretical argument has been found which allows a choice between x or x' or any other similar variable. However the choice of the "best" variable can be done using the experimental data plus a theoretical criterion of what we mean by the "best" variable.

In 1970 an experimental proof of Bjorken scaling was strongly desirable and the "best" variable was the one for which Bjorken scaling was better satisfied. In 1975 it was discovered that it is impossible to find a variable for which the Bjorken scaling law is satisfied both for proton and neutron deep inelastic scattering[26]. The experimental observation of scaling violations in the proton at fixed x' ($0.5 < x' < 0.7$) (see Fig. 8) suggests the use of a variable different from x', on the contrary the lack of scaling violations in the neutron at fixed x' would imply that x' is the "best" variable (see Fig. 9).

It is possible to use a new scaling variable x_{1975} for the proton and the old x' for the neutron, and this may be a simple phenomenological way to summarize the data. I think that it would be quite hard to find a theoretical justification in the framework of the parton model for the use of two different scaling variables: the criterion that the "best" variable must minimize the violations of Bjorken scaling, has led us to a dead end.

A new criterion is needed: we propose that the best variable should be such that scaling violations are the same for the neutron and the proton, at least in the large x region. If we use the experimental data[27,28] to com-

---

(x) - The cause of errors is ignorance of better.

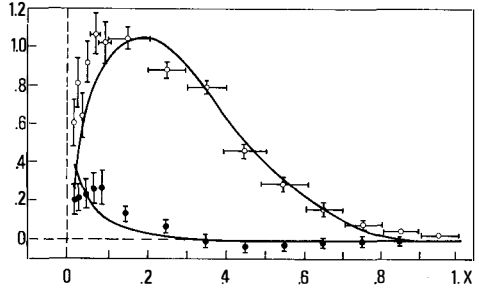

FIG. 7 -Our predictions for the amount of quarks (♦) and antiquarks (♦) in an isospin zero target are presented together with the experimental values extracted from neutrino and antineutrino scattering[23].

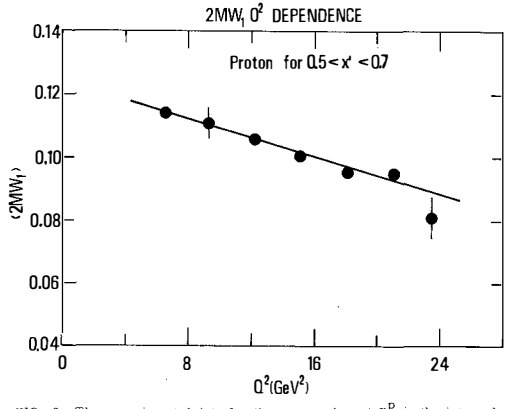

FIG. 8 - The experimental data for the mean value of F_1^p in the interval $0.5 \leq x' \leq 0.7$ plotted against Q^2.

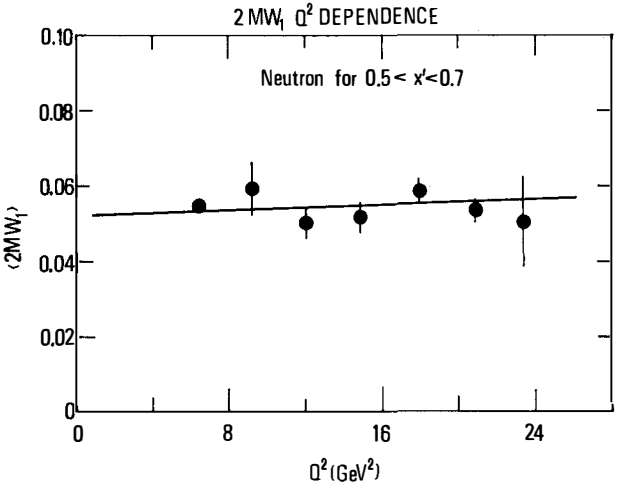

FIG. 9 - The experimental data for the mean value of F_1^n in the interval $0.5 \leq x' \leq 0.7$ plotted against Q^2.

pute the logaritmic derivative of the proton and of the neutron structure functions at fixed x, we find that they are roughly equal (see Fig. 6).

How is it possible that the two logaritmic derivatives at fixed x are equal and those at fixed x' are different? The answer can be easily found using the identity:

$$\left.\frac{\partial \ln F}{\partial Q^2}\right|_{x'} = \left.\frac{\partial \ln F}{\partial Q^2}\right|_{x} + \left.\frac{\partial \ln F}{\partial x}\right|_{Q^2} \cdot \left.\frac{\partial x}{\partial Q^2}\right|_{x'} . \tag{6.1}$$

In the x region we are interested in, one find that:

$$\frac{\partial \ln F_2^n}{\partial x} \simeq 1.2 \frac{\partial \ln F_2^p}{\partial x} . \tag{6.2}$$

Any change of variable modifies the Q^2 derivative of the neutron data more strongly than the proton data.

The variable x (and not x') satisfies the new criterion we have proposed, and we are going to use it in the rest of the paper (see Fig. 6). We stress that, if our intuition is wrong and if the predicted scaling violations must be compared with the derivative of the experimental data at fixed x', the present experimental evidence excludes that the observed scaling violations come from the mechanism described in this paper. However the data are not accurate enough to fix unambigously which is the best variable: any variable not too far from x would also satisfy our criterion within the experimental errors. The problem of the best variable arises from the existence of scaling violations due to the finite mass of the nucleons and of the quarks; these violations disappear asymptotically, however in the low Q^2 region it is impossible to disentangle the scaling violations which die as Q^2 is increased, from those which survive in the limit $Q^2 \to \infty$. The theory of these mass dependent scaling violations is practically lacking: the situation can be clarified in the framework of the so called covariant parton model of Landshoff and Polkingorne[29], unfortunately the analysis has not been carried out in detail.

Another problem is present: our asymptotic predictions do not distinguish among F_1 and F_2 (σ_L is asymptotically zero), however at present energies the logaritmic derivative of F_1 is systematically larger than that

of F_2 [27, 30]. Now it is not clear which function should be compared with the theoretical predictions: the chosen function must satisfy the requirement of minimizing the scaling violations due to finite mass effects.

The observed Q^2 dependence of the function F_2 can be well fitted using $\alpha = 0.4$ (see Fig. 6); a similar agreement between theory and experiment would be obtained using F_1 instead of F_2: in this case we would get $\alpha = 0.5$.

I would like to conclude that the observed scaling violations can be accounted for by interactions among partons with a coupling constant of order 0.4 - 0.5 in the few GeV^2 range. However there is still another effect which increases the error on the value of α: the large value of the coupling constant changes rather drastically with Q^2. The data in the central x region have $\langle Q^2 \rangle$ 3-6 GeV^2, while the data at x near to 1 have $\langle Q^2 \rangle$ 8-12 GeV^2.

In principle changing Q^2, we should also change the value of the effective coupling constant; in this particular instance this is not true because we are changing both Q^2 and x together. The effect we are talking about, is of the same order of magnitude as the neglected terms proportional to α^2 in the transition probabilities p (eq. (5.4)). We must realize that eq. (5.3) is asymptotically correct also if we substitute $\alpha(Q^2)$ by $\alpha(Q^2/(1-x))$; eq. (5.1) implies:

$$\alpha(Q^2/(1-x)) \simeq \alpha(Q^2) - \frac{25}{12\pi} \ln(1-x)\, \alpha^2(Q^2) \quad . \tag{6.3}$$

The difference is of order α^2. Notice that $\langle (1-x)Q^2 \rangle$ is roughly constant in a wide x region in the SLAC sample.

The effect of the neglected second order terms has not been computed at the present moment; it can be easily be of order of 30%, expecially in the region $x \sim 1$ where higher order contributions are expected to be enhanced. Terms proportional to α^2 are not negligible because our preferred value for the coupling constant is not small; they will distort the theoretical predictions in the region $x \sim 1$ and they will also change the Q^2 dependence of the moments of the structure function for N very large.

In our theoretical predictions we have also neglected the effect of the Q^2 dependence of the r. h. s. of eq. (5.7); the error we have introduced is

rather small and can be easily corrected using the data themselves and not their scaling fit (5. 8) in the r. h. s. of eq. (5. 7).

If I take care of all these ambiguities, I would estimate:

$$0.25 \leq \alpha(6\ \mathrm{GeV}^2) \leq 0.5 \,. \tag{6.4}$$

Correspondly:

$$0.4 \leq \alpha(1\ \mathrm{GeV}^2) \leq 1.2 \,. \tag{6.5}$$

The determination of the value of α is based mainly on the SLAC data. If high quality data coming from an high energy μ beam becomes available in the future for a large interval of Q^2, the determination of α can be improved. I hope that at that time the theoretical ambiguities will be solved: the transition probabilities will be computed at order α^2 and the scaling violations due to the finite mass of the proton will be understood.

7. - SCALING VIOLATIONS AND THE SEARCH FOR CHARM

The parton model gives rather interesting predictions when it is applied to neutrino and antineutrino induced reactions. In this paper we concentrate our analysis on the charged current processes; a similar analysis can be done for the case of neutral currents. If only V-A currents are present, we find:

$$\sigma_\nu = \frac{2G^2 M E_\nu}{\pi}\left[M_q^\nu + \frac{1}{3}M_{\bar{q}}^\nu\right], \quad \sigma_{\bar{\nu}} = \frac{2G^2 M E_{\bar{\nu}}}{\pi}\left[M_{\bar{q}}^{\bar{\nu}} + \frac{1}{3}M_q^{\bar{\nu}}\right] \tag{7.1}$$

$$\langle y\rangle_\nu = \frac{1}{2}\,\frac{6M_q^\nu + M_{\bar{q}}^\nu}{6M_q^\nu + 2M_{\bar{q}}^\nu}, \qquad \langle y\rangle_{\bar{\nu}} = \frac{1}{4}\,\frac{M_q^{\bar{\nu}} + 6M_{\bar{q}}^{\bar{\nu}}}{M_q^{\bar{\nu}} + 3M_{\bar{q}}^{\bar{\nu}}},$$

where σ denotes total cross section and y is the ratio between the neutrino (the antineutrino) energy and the energy given to the hadron system E_h: $y = E_h/E^\nu$. M_q^ν and $M_{\bar{q}}^\nu$ ($M_q^{\bar{\nu}}$ and $M_{\bar{q}}^{\bar{\nu}}$) are respectively the effective momentum carried by the quarks and the antiquarks which interact with the neutrino (with the antineutrino).

In the 4 quark model different results hold below and above the threshold for creation of charmed particles in the final state; below threshold

we find:

$$(7.2)\qquad M_q^{\nu} = \cos^2\theta_c M_n^2 + \sin^2\theta_c M_{\lambda}^2 \ , \qquad M_q^{\bar{\nu}} = M_p^2 \ ,$$

$$M_{\bar{q}}^{\bar{\nu}} = \cos^2\theta_c M_{\bar{n}}^2 + \sin^2\theta_c M_{\bar{\lambda}}^2 \ , \qquad M_{\bar{q}}^{\nu} = M_{\bar{p}}^2 \ .$$

Above threshold, transitions involving the p' quark are switched on:

$$(7.3)\qquad M_q^{\nu} = M_n^2 + M_{\lambda}^2 \ , \qquad M_q^{\bar{\nu}} = M_p^2 + M_{p'}^2 \ ,$$

$$M_{\bar{q}}^{\bar{\nu}} = M_{\bar{n}}^2 + M_{\bar{\lambda}}^2 \ , \qquad M_{\bar{q}}^{\nu} = M_{\bar{p}}^2 + M_{\bar{p}'}^2 \ .$$

It is commonly assumed that the quark distributions inside the nucleon can be divided into a valence contribution, an SU(3) symmetric sea of quarks and antiquarks and a charmed sea. If the target has isospin zero we get:

$$(7.4)\qquad M_p^2 = \frac{V^2}{2} + S^2 \ , \quad M_n^2 = \frac{V^2}{2} + S^2 \ , \quad M_{\lambda}^2 = S^2 \ , \quad M_{p'}^2 = C^2 \ ,$$

$$M_{\bar{p}}^2 = S^2 \ , \qquad M_{\bar{n}}^2 = S^2 \ , \qquad M_{\bar{\lambda}}^2 = S^2 \ , \quad M_{\bar{p}'}^2 = C^2 \ .$$

If we neglect the sea, no antiquarks are present in the nucleon: the antineutrino over neutrino total cross section ratio is below threshold:

$$(7.5)\qquad R \equiv \sigma_{\bar{\nu}}/\sigma_{\nu} = 1/3\cos^2\theta_c \simeq 0.35 \ .$$

At Gargamelle energies $R = 0.39$[23]; only a small contamination of antiquarks is present in the nucleon at low energy. The x distributions of quarks and antiquarks are shown in Fig. 7: the mean value of x of antiquarks ($\langle x_S \rangle$) is much smaller than that of the valence quarks ($\langle x_V \rangle$). The data suggests that at $Q^2 = 1\ \mathrm{GeV}^2$ (the mean value of Q^2 in the Gargamelle experiment is about $1\ \mathrm{GeV}^2$) the following relations hold:

$$(7.6)\qquad V^2 = 0.46 \ , \quad S^2 = 0.01 \ , \quad C^2 = 0 \ , \quad G^2 = 0.48 \ .$$

Obviously the data give no information about the amount of charmed quarks present in the proton; for simplicity I have assumed that the charmed

component of the proton can be neglected in the low Q^2 region. The conser vation of the total momentum implies the sum rule

$$V^2 + 6\,S^2 + 2\,C^2 + G^2 = 1 \quad , \tag{7.7}$$

which has been used to fix the momentum carried by the gluons (G^2).

Violations of the Bjorken scaling law are due to the presence of a threshold for charm production and to the Q^2 dependence of the quark distri butions. The first effect is characteristic of neutrino scattering. It will be shown here that both effects are needed to explain the observed violations of the scaling law in neutrino deep inelastic scattering: in the framework of the 4 quark model it is not simple to fit the experimental data neglecting the Q^2 dependence of the parton distributions.

The Q^2 dependence of the momentum carried by each component of the proton can be easily computed: proceeding as in section 3 we can derive from eqs. (5.3-4) an equation having the same form as eq. (3.20); its solution is[3]:

$$\begin{aligned}
V^2(Q^2) &= B_8\, G^{-32/75} \quad , \\
S^2(Q^2) &= \frac{3}{56} + \frac{1}{14} B_o G^{-56/75} + \left(\frac{1}{24} B_{15} - \frac{1}{6} B_8\right) G^{-32/75} \quad , \\
C^2(Q^2) &= \frac{3}{56} + \frac{1}{14} B_o G^{-56/75} - \frac{1}{8} B_{15} G^{-32/75} \quad , \\
G^2(Q^2) &= \frac{4}{7} - \frac{4}{7} B_o G^{-56/75} \quad ,
\end{aligned} \tag{7.8}$$

where

$$G(Q^2) = 1 + \frac{25}{12\pi}\, \alpha(\mu^2) \ln Q^2/\mu^2 \quad . \tag{7.9}$$

The constants B_o, B_8 and B_{15} can be fixed by requiring that eq. (7.6) be satisfied at $Q^2 = 1\ \mathrm{GeV}^2$.

In Fig. 10 the results have been plotted for $\alpha(1) = 0.5$, as functions of Q^2. Since G is a slowly varying function of Q^2 we can compute G from an effective Q^2 value

$$Q^2_{Eff} = 2\,M\,E\,\langle xy \rangle \quad , \tag{7.10}$$

where $\langle xy \rangle$ is the average value of xy, which is different for neutrino and antineutrino. At fixed energy E neutrino data involve larger value of

Q^2_{Eff} than antineutrino data.

Our predictions for the momentum carried by the charmed quarks must be taken cum grano salis: the effects of the large mass of the charmed quarks has not been taken into account. A more precise analysis would be needed to study effects that depend crucially on the amount of charmed quarks in the proton.

The cross sections and the y distribution below and much above the threshold for charm production can be easily computed.

The effects of the threshold may be simulated by a simple θ function in the mass W of the produced hadronic system:

$$\sigma_T(x,y) \simeq \sigma_B(x,y) + \sigma_C(x,y)\,\theta(W - W_T) \quad , \tag{7.11}$$

where σ_B is the cross section below the threshold for charm production, σ_C is the asymptotic cross section for producing a charmed final state and W_T is an effective threshold mass. Simple kinematical arguments, due to Barnett, suggest that:

$$W_T^2 = m_{p'}^2/\langle x \rangle \quad , \tag{7.12}$$

where $m_{p'}$ is the mass of the charmed quark and $\langle x \rangle$ is the mean value x of the quarks from which the p' is produced. Charm is produced by neutrinos mainly out of valence quarks, by antineutrinos out of sea quarks. Using $m_{p'} = 2$ GeV, $\langle x_V \rangle = 0.25$ and $\langle x_S \rangle = 0.13$ we estimate:

$$W_T^{\nu} \simeq 4 \text{ GeV} \quad , \qquad W_T^{\bar{\nu}} \simeq 5.5 \text{ GeV} \quad . \tag{7.13}$$

The higher value of the effective threshold for antineutrino is caused by the exoticity of the hadronic final state (B = 1, C = -1).

In Figs. 11 and 12 we show our predictions for $\langle y \rangle_{\nu}$ and R respectively for various values of W_T and a. The data for $\langle y \rangle_{\bar{\nu}}$ come from the HPWF collaboration. For simplicity the same threshold has been used for neutrino and antineutrino.

When $a = 0$ the scaling violations due to the strong interactions are absent and when $W_T = \infty$ the charm threshold never opens. It is apparent that both $a \neq 0$ and $W_T < \infty$ are needed to fit the data for $\langle y \rangle_{\bar{\nu}}$; in this

case R is predicted to rise with E. If the momentum carried by each quark were Q^2 independent, R would stay almost constant and be insensitive to the charm threshold; in fact the increased proportion of momentum carried by the sea makes R to behave as in Fig. 12. While this prediction is not supported by the published data of the Caltech group[32] (although not excluded within quoted errors) a sharp rise of R has been reported by the HPWF group[33, 34].

In the infinite energy limit very simple predictions are obtained:

$$(7.14) \qquad \sigma_\nu = \sigma_{\bar\nu} = \frac{G^2 M E}{\pi} \frac{2}{7} \quad , \qquad \langle y \rangle_\nu = \langle y \rangle_{\bar\nu} = \frac{7}{16} \quad .$$

If scaling violations were absent, eq. (7.6) implies that the fraction $\Delta\sigma/\sigma$ of charmed final states would not exceed 10% even at infinite energy. The predictions with scaling violations included are shown in Fig. 13. If charmed particle have an average branching ratio into muons of the order of 5% to 10%, the observed yield of events with muons of opposite charge is obtained[35, 36].

Dimuons with equal charge[35] may come from the production of a charmed quark-antiquark pair in an event with $\Delta C = 0$. A very rough estimate of the order of magnitude of the cross section for the creation of two charmed particles is:

$$(7.15) \qquad \sigma_{C\bar C} \simeq C^2 \sigma_T \quad .$$

A careful study of the effects due to the high p' mass would be needed to understand if this mechanism may explain the observed yield of equal sign dimuons. It is also possible that the equal sign dimuons come from the decay of a massive b quark[37] produced out of a p' quark.

A distinctive feature of the scaling violations due to the strong interaction is that the x distributions of quarks and antiquarks shift toward zero with increasing Q^2. This effect has been observed in electroproduction and should also be observed in neutrino production. Predictions for the behaviour of the structure functions at fixed x can be made using the same techniques as in section 5. However it may be convenient to concentrate on global quantities such as $\langle x \rangle$.

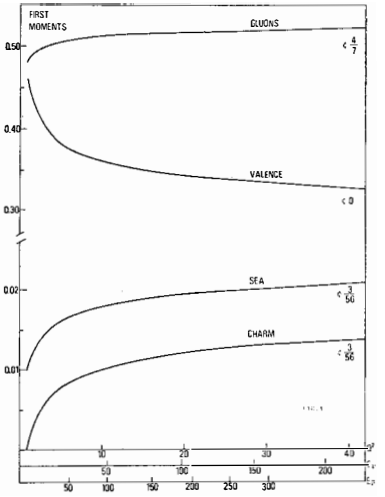

FIG. 10 - Momenta carried by the gluons, the valence quarks, the SU(3) symmetric sea and the charmed sea. The arrows indicate the asymptotic values. $G + 2V + 6G + 2C = 1$ is identically satisfied. The curves have been computed using $\alpha(1\ GeV^2) = \alpha = 0.5$.

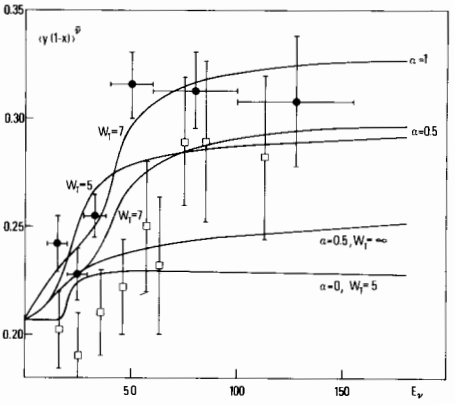

FIG. 11 - Average value of $y_{\bar{\nu}}$ for different values of α and W_T, the effective invariant mass for charm threshold. $\alpha = 0$ corresponds to Q^2 independent parton distributions. $W_T \to \infty$ corresponds to neglecting effects for charm production. Both effects seem to be needed to reproduce the data. α is the coupling constant at $Q^2 = 1\ GeV^2$. The experimental points are taken from ref. (31).

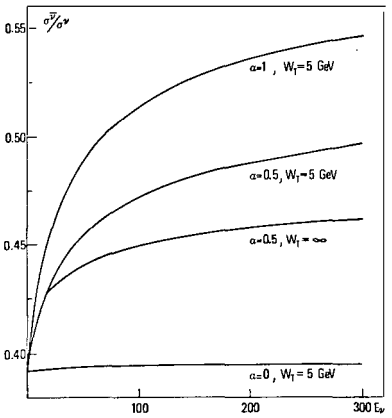

FIG. 12 - The ratio $\sigma^{\bar{\nu}}/\sigma_{\nu}$ for different values of $\alpha(1\ \mathrm{GeV}^2)$ and W_T, the effective invariant mass for charm threshold.

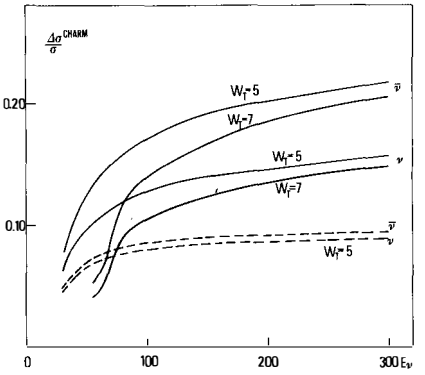

FIG. 13 - The prediction for the fraction $\Delta\sigma/\sigma$ of charmed final states for neutrino and antineutrino. The dashed line is obtained with Q^2 independent parton distributions, the full lines are obtained assuming $\alpha = 0.5$ at $Q^2 = 1\ \mathrm{GeV}^2$; W_T is the effective invariant mass for charm production.

Evolution equations like eq. (7. 8) can be written also in this case[3]. This problem will not be studied here: the interested reader can find a careful treatment of this and of many other phenomena concerning scaling violations in neutrino scattering in the paper of Altarelli presented at this Rencontre de Moriond[38].

8. - CONCLUSIONS

In this paper we have shown that in relativistic quantum field theory the breaking of the Bjorken scaling law can be understood in terms of successive fragmentations of the partons. The parton model relations among electron, neutrino and antineutrino scattering are preserved, provided we use Q^2 dependent parton distributions.

The scaling violations observed in deep inelastic electron scattering can be understood using a strong interaction coupling constant of the order 0. 4 in the few GeV range. Using this value for the strong interaction coupling constant we compute the scaling violations in neutrino and antineutrino scattering. The most interesting prediction is a large increase in the momentum carried by the sea of antiquarks with increasing energy. The mean value of y in antineutrino scattering and the ratio of the total antineutrino and neutrino cross sections are consequently affected. Without this effect it is hard to understand the present experimental data in the framework of the 4 quark model. It appears that a correct treatment of the violations of the Bjorken scaling law is a necessary ingredient in any successfully analysis of neutrino scattering at present energies.

The author is really grateful to R. K. Ellis for a critical reading of the manuscript.

REFERENCES

(1) - G. Parisi and R. Petronzio, A dynamical approach to deep inelastic scattering, Rome preprint 617 (1975); to be published on Nuovo Cimento.

(2) - G. Parisi and R. Petronzio, On the breaking of Bjorken scaling, Rome preprint; submitted to Physics Letters B.

(3) - G. Altarelli, G. Parisi and A. Petronzio, Charmed quarks and asymptotic freedom in neutrino scattering, Rome preprint, submitted to Physics Letters B.

(4) - A. M. Poliakov, Sov. Phys. -JEPT 32, 296 (1971).

(5) - J. Kogut and L. Susskind, Phys. Rev. D9, 697 (1971).

(6) - S. D. Drell, D. J. Levy and T. M. Yan, Phys. Rev. 187, 2159 (1970).

(7) - We use the same notation as G. Altarelli, Riv. Nuovo Cimento 4, 335 (1974).

(8) - G. Parisi, Phys. Letters 42B, 114 (1972).

(9) - G. Parisi, Serious difficulties with canonical dimensions, Frascati report LNF-72/94 (1972).

(10) - N. Cabibbo and M. Rocca, CERN preprint Th 1974.

(11) - N. Cabibbo and G. Parisi (unpublished).

(12) - D. Bailin, A. Love and D. V. Nanopoulos, Lett. Nuovo Cimento 9, 501 (1974).

(13) - K. Symanzik, Lett. Nuovo Cimento 6, 420 (1973).

(14) - S. L. Glashow, J. Iliopoulos and L. Maiani, Phys. Rev. D2, 1285 (1970).

(15) - G. 't Hooft, Marseille Conference 1972 (unpublished).

(16) - H. D. Politzer, Phys. Rev. Letters 30, 1346 (1973).

(17) - D. J. Gross and W. Wilzek, Phys. Rev. Letters 30, 1343 (1973).

(18) - H. Georgi and H. D. Politzer, Phys. Rev. D9, 416 (1974).

(19) - D. J. Gross and W. Wilczek, Phys. Rev. D9, 980 (1974).

(20) - A. Zee, F. Wilzeck and S. L. Treiman, Phys. Rev. D10, 2881 (1974).

(21) - G. Parisi, Phys. Letters 43B, 207 (1973); 50B, 367 (1974).

(22) - G. Miller et al., Phys. Rev. D5, 528 (1972).

(23) - CERN-Gargamelle collaboration, Phys. Letters 46B, 274 (1973).

(24) - D. Wilson, Review talk presented at the Kiev Conference (1970).

(25) - E. D. Bloom and F. J. Gilman, Phys. Rev. Letters 25, 1140 (1970).

(26) - R. Taylor, Review talk presented at the Stanford Conference (1975).

(27) - A. Bodek et al., SLAC Publ. 1445 (1975).

(28) - C. Chang et al., Phys. Rev. Letters 35, 901 (1975).

(29) - N. Cabibbo, G. Parisi, M. Testa and A. Verganelakis, Lett. Nuovo Cimento 4, 569 (1970).

(30) - E. M. Riordan, Phys. Letters 52B, 249 (1973).

(31) - A. Benvenuti et al., Further data on the high-y anomaly in inelastic antineutrino scattering, Preprint HPWF 76/1 (1976).

(32) - B. C. Barish et al., Phys. Rev. Letters 35, 1316 (1975).

(33) - A. K. Mann, Talk presented at this Rencontre.

(34) - C. Rubbia, Talk presented at this Rencontre.

(35) - A. Benvenuti et al., Phys. Rev. Letters 35, 1199, 1203 and 1249 (1975).

(36) - B. G. Barish et al., Cal. Tech. Report 58-485 and 68-510 (1975).

(37) - H. Harari, SLAC-Pub-1589 (1975).

(38) - G. Altarelli, Talk presented at this Rencontre.

CHARMED PARTICLE SEARCH IN THE GARGAMELLE NEUTRINO EXPERIMENT

M. JAFFRE

Laboratoire de l'Accélérateur Linéaire
Université de PARIS-SUD, Bâtiment 200
91405 Orsay (France)

Abstract : A total of 18000 neutrino interactions between 1 and 12 GeV have been analysed for search of semi-leptonic decays of charmed particles. 2 events ($\mu^- e^+ V^\circ$ + ...) have been found. The probability that they can be due to background is less than 10^{-3}.

Résumé : 18000 interactions de neutrino d'énergie comprise entre 1 et 12 GeV ont été analysées pour la recherche de désintégrations semi-leptoniques de particules charmées. 2 événements ($\mu^- e^+ V^\circ$ + ...) ont été trouvés. La probabilité qu'ils soient du bruit de fond est inférieure à 10^{-3}.

Recently the existence of neutral currents has been evidenced by several experiments (1). However, the weak neutral currents seem to conserve strangeness, unlike charged currents.

This fact cannot be explained without addition of new quantum numbers. The simplest way is to extend the symmetry SU_3 to SU_4. The new quantum number is called charm (C) (2).

In the quark parton model, we can write the weak charged current as :

$$J_\mu = \bar{p}\gamma_\mu(1+\gamma_5)\ (n\cos\theta_c + \lambda\sin\theta_c) + \bar{p}'\gamma_\mu(1+\gamma_5)(\lambda\cos\theta_c - n\sin\theta_c)$$

Charmed particles can be produced in neutrino interactions :

. on valence quark the reaction is :

$\nu n \to \mu^- p'$ factor $\sin^2\theta_c$ final state C = 1, S = 0

. on sea-quarks the reactions are :

$\nu\lambda \to \mu^- p'$ factor $\cos^2\theta_c \times \alpha_\lambda$ final state C = 1, S = +1

$\nu p' \to \mu^- \bar{\lambda}$ factor $\cos^2\theta_c \times \alpha_{p'}$ final state C = 1, S = 1

($\bar{\lambda}$) ($\bar{\lambda}$) (p') (p')

α_λ, $\alpha_{p'}$, are the fractions of the momentum carried by λ and p' quarks.

Charmed particles can decay semi-leptonically (like kaons) as :

$p' \to \lambda + \ell^+ + \nu_\ell$ final state S = -1, C = 0

In the final state, we expect two leptons of opposite charge and one (S = -1) or two (S = 1, S = -1) strange particles.

I - SEARCH FOR CHARMED PARTICLES IN GARGAMELLE

Electrons are unambiguously recognised among the other tracks in Gargamelle. But, the detection efficiencies for $K^\pm$, $\Sigma^\pm$ and Σ° are small, so the selection has been performed only for reactions involving K°_S and Λ°, and only for the charged decay modes :

Finally we have searched events of the type $\mu^- e^+ \nu^\circ + X$ in Gargamelle filled with heavy freon.

Data collection

About 400 000 pictures taken in ν-beam in 1971 and 1972 have been scanned for the topology above, and 300 000 new pictures have been taken during last year with a ν flux increased by a factor 3, due to the CERN PS booster.

Analysis

The analysis is performed by 7 Laboratories : Aachen-Bruxelles-CERN-Ecole Polytechnique (Paris)-Milan-Orsay and U.C. London

Until now only 50 % of the whole sample has been analysed for the peculiar topology ($\mu^- e^+ \nu^\circ + \ldots$)

Cuts

We have applied the following cuts to events we are looking for :

- fiducial volume of 3 m^3
- positron energy $E_{e^+} > 200$ MeV

Results

We have found 2 events satisfying the above criteria (3). These 2 events correspond to 18 000 observed ν-interactions with visible deposited energy greater than 1 GeV, in the same fiducial volume.

One new event has been found in the last sample of data. However our background calculations will correspond to the first 2 events.

We have reported the principal caracteristics of the 3 events in the Table I.

TABLE I : $\mu^- e^+ \nu^\circ$

p_{μ^-} GeV/c	p_{e^+} GeV/c	E_{vis} GeV	W	P_T	X_{vis}	Y_{vis}
.150 ± .002	.250 ± .050	3.15	2.1	.55	.04	.94
1.060 ± .150	.895 ± .250	3.4	1.9	1.1	.46	.69
.920 ± .080	.750 ± .200	5.1	2.7	.8	.42	.82

II - WHAT ARE THE PRINCIPAL SOURCES OF BACKGROUND ?

1 - $\bar{\nu}_e$ interactions :

Due to the contamination of ν beam, $\bar{\nu}_e$ interactions can be a source of background if a π^- is produced at the vertex and is not recognized, simulating a μ^- candidate.

This background is obtained by multiplying the expected number of $\bar{\nu}_e$ events by the probability of observing a μ^- candidate and a V° in the final state.

In order to calculate this probability we used the events (obtained in antineutrino beam) which gave a similar configuration :

$$\bar{\nu}_\mu N \rightarrow \mu^+ \pi^- V^\circ + X$$
$$\qquad\qquad\quad \hookrightarrow \text{not recognized}$$

We found 4 events in a sample of 2430 events $\bar{\nu}_\mu N \rightarrow \mu^+ X$. We corrected for the different shapes of the fluxes of $\bar{\nu}_e$ and $\bar{\nu}_\mu$.

The $\bar{\nu}_e$ flux in a neutrino beam is very low ; the rate of the $\bar{\nu}_e$ events, using the $\bar{\nu}_\mu/\nu_\mu$ cross section ratio is $7\ 10^{-5}$.

Finally, the background of $\bar{\nu}_e$ interactions is $(2.5 \pm 1.5)\ 10^{-3}$ event.

2 - Asymmetric Dalitz pair and close gamma rays :

An asymmetric Dalitz pair or an attached γ ray can simulate an e^+ at the vertex.

We defined a total asymmetry when the length of one of the electrons is less than 5 mm.

Theoretical calculations and experimental study of a sample of 260 γ's of energy greater than 200 MeV gave a probability $P = (1.1 \pm 0.7)$ % to observe only the e^+ of the pair. From the distribution of length of the γ's, or theoretical calculations the probability of materialization at the vertex ($d < 5$ mm) has been found to be (4.2 ± 1.3) %.

On a sample of 6129 ν_μ events, 25 γ of energy greater than 200 MeV correlated to 53 $\mu^- V^\circ$ candidates were observed ; this yields a background of $(3.3 \pm 2.4)10^{-2}$ event.

3 - Semi-leptonic decays of hadrons

The positron at the vertex could be due to decays of K and π.

- $K^{\circ}_{L} \rightarrow \pi^{-} e^{+} \nu_{e}$

The detection efficiency for K° is 0.26 ± 0.03. We have observed 1 event with an associated production $K^{\circ}V^{\circ}$ over 6129 ν_{μ} events. Over the total sample, we then expect 2.3 $K^{\circ}_{Le_3}$ decays associated to a V°.

Using the K°_{s} spectrum, which is roughly constant between 0.3 and 2 GeV we have found that the probability for a K°_{L} to decay at less than 1 cm from the vertex is $4\ 10^{-4}$.

The background arising from this decay is $8\ 10^{-4}$ event

- $K^{+} \rightarrow e^{+} \pi^{\circ} \nu_{e}$

K^{+} decay in flight may simulate an e^{+} emitting bremsstrahlung γ rays.

The detection efficiency for K^{+} is 0.30 ± 0.09. We have observed 11 events with an associated production $K^{+}V^{\circ}$ over 6129 ν_{μ} events.

The probability of the configuration has been calculated by a Monte Carlo method, taking into account the K^{+} spectrum and the following cuts which are very conservative:

- angle $K^{+}e^{+} < 20°$
- both angles $e^{+}\gamma(\pi^{\circ}) < 20°$
- K^{+} decay length < 30 cm

Finally, we have estimated this background to be less than $5\ 10^{-3}$ event.

III - CORRELATION BETWEEN e^{+} AND V°

Other observations contribute to believe our background calculations, and prove a strong correlation between e^{+} and V°.

1. $\mu^{-} e^{-} V^{\circ}$

The asymmetry ($\gamma \rightarrow e^{-}$) is bigger than the asymmetry ($\gamma \rightarrow e^{+}$) because of Compton effect and e^{+} annihilation. From observed γ rays it was measured : (4.2 ± 1.3) % instead of (1.1 ± 0.7) %.

If the 2 events were due to background we should expect 8 events of the type :

$$\mu^{-}\ e^{-}\ V^{\circ}$$

None has been observed ; this is in agreement with the expected background from ν_{e} interactions and asymmetric

attached γ rays, which amounts to 0.2 event.

2. $\mu^- e^+$ (without V°)

The rate of production of observed V° in neutrino interactions is (.9 ± .1) %.

On a smaller sample ($\sim$ 50 % of the statistics) we have found 4 events ($\mu^- e^+$ ...), if the positron and the V° were uncorrelated we should expect 7 10^{-2} ($\mu^- e^+$ V°) in the whole sample. The probability that the 2 ($\mu^- e^+$V°) observed are compatible with that expected number is less than 5 10^{-3}.

This indicates a great correlation between the postitron and the V°.

The 4 events ($\mu^- e^+$ ...) can be explained by :

. $\mu^- e^+$ V° events in which the V° is not detected :
1.5 event

. expected background (asym. attached γ, $\bar{\nu}_e$) :
2 events

There caracteristics are listed in Table II.

TABLE II : $\mu^- e^+$ without V°

p_{μ^-} GeV/c	p_{e^+} GeV/c	E_{vis}	W	x_{vis}	y_{vis}
2.650 ± .260	2.6 ± .9	$\sim$ 15	4.7	.09	.82
4.2 ± .32	1.89 ± .8	$\sim$ 7			
2.35	.888	3.3	1.4	.32	.29
1.985 ± .194	.473	3.1	1.5	.33	.39

IV - CONCLUSION

We have observed 2 events $\mu^- e^+$ V°. All the possible sources of background have been taken into account. Our calculations lead to a total background of (4 ± 2) 10^{-2} event. Other observations confirm our confidence in the background calculations. We did not observe any $\mu^- e^-$ V° event, and the number of $\mu^- e^+$ events is low, as expected if the e^+ and the V° are correlated.

The interpretation of the 2 events as semi-leptonic decay of charmed particles is very attractive.

Due to the π^+/p ambiguity, the V°'s are ambiguous Λ and K°. Assyming the V° to be a Λ(K°) the mass of the Λe^+(K°e^+) system in GeV/c is 1.24 ± 0.02 (0.65 ± 0.03) for the first event and 1.91 ± 0.17 (1.57 ± 0.20) for the second. These numbers are lower limits for the masses of the $\Lambda e^+\nu$ (K°$e^+\nu$) system.

REFERENCES

1 - F.J. Hasert et al - Phys. Letters 46B (1973) 121
F.J. Hasert et al - Phys. Letters 46B (1973) 138
La physique du neutrino à haute énergie, Paris March 1975

2 - B.J. Bjorken and S.L. Glashow, Phys. Letters 11 (1964) 255.
D. Amati, H. Bacry, J. Nuyts and J. Prentki, Il Nuovo Cimento X 34 (1964) 1732.
S.L. Glashow, J. Iliopoulos and L. Maïani, Phys. Rev. D2 (1970) 1285

3 - H. Deden et al. Phys. Letters 58B (1975) 361.
J. Blietschau et al, Phys. Letters 60B (1976) 207.

,

THE PRODUCTION OF $\mu^- e^+$ EVENTS

IN HIGH ENERGY NEUTRINO INTERACTIONS

Berkeley-CERN-Hawaii-Wisconsin E28 Collaboration

D.C. Cundy
CERN, Geneva, Switzerland

Abstract: Using a Ne-H_2 mixture in the FNAL bubble chamber, exposed to the wide band neutrino beam, a search has been made for events containing both a muon and an electron. To date 10 events of this type have been found and the characteristics and implications of these events are discussed.

Résumé: Des interactions ayant en même temps un muon et un électron dans l'état final, ont été recherchés dans la chambre à bulles de FNAL remplie d'un mélange Ne-H_2 et exposé au faisceau neutrino à bande large. A ce jour, 10 événements de ce type ont été trouvés, leurs caractéristiques et leurs implications sont décrites.

The E28 experiment consists of 100,000 pictures taken in the 15' FNAL bubble chamber using a filling of 20% Ne in hydrogen. The density was $\sim$ 0.3 gm/cm^3 and the radiation length $\sim$ 100 cm. The exposure took place in the wide band neutrino beam, and the event rate for charged-current events was found to be $\sim$ 1 event/ 8 pictures.

The aim of the experiment was to look for di-lepton events of the type μe, as a direct comparison to the recently observed di-muon events.

The bubble chamber was complemented by an external muon identifier (E.M.I.). The punch through probability for a pion was a few percent and hence it is very difficult to detect dimuon events at $\sim$ 1% rate. However it does allow good muon identification for single muon events.

The electron, positron tracks are identified either by seen bremsstrahlung, trident production or sudden energy loss. The only way to obtain the electron detection efficiency is to use the electron-pairs produced along with the neutrino interactions. Preliminary results indicate that it is $\sim$ 25 - 50%.

A summary of the 10 $\mu^- e^+$ events found so far is shown in table 1. One notices that some information is lacking on some events, however this can be excused if one considers the vast distance that this collaboration covers.

These 10 events come from the scanning of $\sim$ 30,000 pictures. Thus giving a corrected rate of $\sim$ 1.4%. The error on this rate is probably a factor of 2 due to the problem of the electron detection efficiency.

1. BACKGROUNDS

There are two main sources of background (a) Asymmetric Dalitz pairs and very close converted γ-rays, (b) $\bar{\nu}_e$ events giving rise to e^+.

(a) Asymmetric Dalitz Pairs : The mean charge multiplicity of these events is $\sim$ 5, implying $\sim$ 2 - 3 π^o's/event. Hence, one expects $\sim$ 0.03 Dalitz pairs/event (experimentally find 0.04 $\pm$ 0.01). Assuming that an electron of 5 MeV can be recognized in these pictures, then the probability that e^+e^- pair will appear only as an e^+ is $\sim$ 0.003. Therefore, one concludes that the asymmetric Dalitz background rate is $\sim 10^{-4}$/event. The rate for very close asymmetric converted γ-rays is expected to be the same.

(b) $\bar{\nu}_e$ events : The ratio of $\bar{\nu}_e/\nu_\mu$ flux is $\sim 10^{-3}$. The cross section ratio $\sigma_{\bar{\nu}}/\sigma_\nu \sim 0.3$. Hence, the global e^+ production from this source is 4×10^{-3}. However, when one takes into account the fact that the majority of these events will have fast e^+'s (i.e. $(1-y)^2$ distribution) then a background rate of $\sim 10^{-3}$ is estimated.

Other backgrounds due to K^+, K^o leptonic decays are in the 10^{-5} region. Hence, the conclusion is that the observation of events with $\mu^- e^+$ is a real effect and that the background levels are only about 10% of the observed signal.

2. EXCESSIVE K^o PRODUCTION

One immediately remarks from table 1 that 9 out of the 10 events have a K^o_s. This would lead to the conclusion that on average ~ 2.5 K^o's are produced in these interactions.

One obvious explanations of these events is that they are due to leptonic decays of a new particle

$$D \rightarrow K^o e^+ \nu$$

The range of the masses M_{Ke} would imply a mass $M_D \sim 2 - 3$ GeV.

It is also interesting to speculate if these events are due to the same process as the dimuon events.

If we assume that they are, then as the dimuon events had $p_{\mu^+} > 5$ GeV, and the $\mu^- e^+$ events have $P_{e^+} < 5$ GeV, the total production rate of dilepton events is 4% of the charged-current rate, and the majority of these would seem to have a visible K^o_s.

It is interesting to remark the neutrino experiment in hydrogen E_{45} observed a visible K^o_s rate of 3% !

TABLE 1

	W_1 1	W_2 2	W_3 3	B_1 4	C_1 5	C_2 6	C_3 7	W_4 8	W_5 9	W_6 10
E_{vis} GeV	34	11	26	28	100	21	32			
μ^- identified p/GeV/c	EMI 14	3	EMI 22	9	EMI 9	EMI 14	12			
e^+ identified p/GeV/c	B-C 2	B-T 1.1	B 2.2	T 5.3	B-C 5.3	C 1.2	B 17.7			
Strange Particle p/GeV/c	K^o_s 6.3	K^o_s 3.1	K^o_s 1.8	K^o_s 5.6	$K^o_s + K^o_L$ int 38.0	$K^o_s 2\pi^o$ .4	K^o_s 1.05	$K^o_s 2\pi^o 2K^o_L$		$3V^o$
$m_{K^o e^+}$ GeV	1.3	.9	1.1	.7	2.1	1.04	2.1			
y_{vis}	.6	.7	.2	.6	.9	.3	.6			
x_{vis}	.003	.1	.9	.2	.05	.02	.2			
W_{min}(GeV)	6	4	1.3	5	13	3.7	5.5			

Topology

1) $\mu^- e^+ K^o 2\pi^- 3\pi^+ \pi^o$ 4pn
2) $\mu^- e^+ K^o 2\pi^- \pi^+ \pi^o p$
3) $\mu^- e^+ K^o$
4) $\mu^- e^+ K^o \pi^- \pi^+ \pi^o p$
5) $\mu^- e^+ K^o K^o_L p\pi^{\pm} 3\pi^o n$
6) $\mu^- e^+ \pi^- \pi^+ p$ $7\gamma(K^o_s)$
7) $\mu^- e^+ K^o_s n$

Electron recognition: B - bremsstrahlung
C - curling
T - trident

A STUDY OF INCLUSIVE STRANGE PARTICLE PRODUCTION BY NEUTRINOS INTERACTING IN HYDROGEN AT FNAL

FNAL-Hawaii-Berkeley-Michigan E45 Collaboration

D.C. Cundy
CERN, Geneva, Switzerland

Abstract: About 500 charged-current events produced by neutrinos above 10 GeV were used to study strange particle production, $\Delta S = -\Delta Q$ interactions and the possible existence of charmed particles.

Résumé: Environ 500 événements de type courant chargé produits par des neutrinos d'énergie supérieure à 10 GeV ont été analysés en vue de l'étude de la production de particules étranges, des interactions avec $\Delta S = -\Delta Q$ et de l'existence éventuelle de particules charmées.

This report deals with analysis of 76,000 photographs using the 300 GeV wide band beam at FNAL. The average proton intensity was 7×10^{12} protons/pulse. 3000 events of possible neutral origin were picked up at the scanning stage. However, a large number of these events are due to low energy hadronic debris from neutrino events occuring upstream of the bubble chamber. Hence, only the 650 events in which the visible momentum (P_x) along the ν beam direction was greater than 10 GeV/c were retained. From a study of the neutron induced background it was estimated that this reduced sample contained only a few percent of non-neutrino induced events. As the external muon identifier was essentially not used in this experiment, one has to resort to an algorithm for the definition of charged-current events and the selection of the muon.

The muon is choosen as the negative leaving track which has the highest transverse momentum with respect to the neutrino direction. In order to be classed as a charged-current event the momentum of the "muon" must be on the opposite side of the neutrino direction than the remaining hadron momentum vector.

This algorithm, together with a 10 GeV/c P_x cut, was estimated to obtain a charged-current neutrino sample that contained only a few percent of neutral currents.

In this experiment essentially all the neutral energy in the event is missed, but it is still possible to obtain a good estimation of the neutrino energy. If one makes the approximation that the projection of the charged hadron momentum vector unto the ν-μ plane represents the true hadron momentum vector, it is then possible, using momentum balance with the muon, to obtain the neutrino energy.

The error in the neutrino energy is obviously a function of the neutrino energy and the kinematic configuration . The error formula is:

$$\frac{\delta E}{E} \propto \frac{P_T}{\sqrt{mE}} \left[\frac{y}{2x(1-y)} \right]^{\frac{1}{2}}$$

where P_T is the missing momentum out of the $\nu\mu$ plane, E is the neutrino energy, $x = \frac{q^2}{2m\nu}$, $y = \frac{\nu}{E}$ (i.e. the Bjorken scaling variables).

Note that $\frac{\delta E}{E}$ decreases as $\frac{1}{\sqrt{E}}$ and has an asymptotic value of $\sim$ 7%.

Note also the pathological behaviour at $x = 0$ and $y = 1$.

Using this energy estimation it is possible to evaluate total cross sections, x distributions and y distributions. These are certainly compatible with scaling, but the corrections due to the energy estimation are so large that the statistics must be increased by an order of magnitude before any detailed comparison can be attempted.

The behaviour of the hadron vertex was found to be as expected from strong interactions. As this data has now been published (Phys. Rev. Letters 36 (1976) 639) it will not be discussed in this written report.

1. INCLUSIVE STRANGE PARTICLE PRODUCTION

This experiment is essentially blind to the identification of charged kaons, and can only be considered to give information on the reaction

$$\nu + p \rightarrow \mu^- + V^{o}\text{'s} + X^{++}$$

In a sample of 530 events with $P_x > 10$ GeV/c, and classed as charged current events, the following V^o events were found:

Type	Number of events > 10 GeV/c P_x
K^o_s	16
$\Lambda^o(\Sigma^o)$	16 + 1 (Σ^o)
$\Lambda^o K^o_s$	3
$\bar{\Lambda}$	1

The global characteristics of these events, such as the energy distribution, x, y distributions show no marked differences within the limited statistics, with respect to the normal charged-current events. Fig. 1 shows the observed V^o cross section relative to the charged-current cross section as a function of W (ie the mass of hadronic system). As expected it rises slowly with energy and does not seem to show any marked difference from that observed in electromagnetic interactions.

2. LIMITS OF $\Delta S = -\Delta Q$ REACTIONS

In these events it is possible to search for $\Delta S = -\Delta Q$ interactions of the type

$$\nu p \rightarrow \mu^- \Lambda^o X^{++}$$

with no other strange particle produced.

In order to do this, one has of course to subtract the background from the associated production events

$$\nu p \rightarrow \mu^- \Lambda^o K^+ + X^+$$

$$\nu p \rightarrow \mu^- \Lambda^o K^o + X^{++}$$

3 associated production events of the type $K_s^o \Lambda^o$ were observed.

Taking account of the detection efficiency of K_s^o and assuming $\frac{\Lambda^o K^+}{\Lambda^o K^o} = 1$ then the expected number of single Λ^o events from associated production is 15 compared with the 17 observed. To get an upper limit for $\Delta S = - \Delta Q$ reactions in this channel one considers that the 3 $K^o \Lambda^o$ events are a 90% upward fluctuation from 0.82 $K^o \Lambda^o$ events. In this way one obtains:

$$\left| \frac{\Delta S = - \Delta Q}{\text{total}} \right| < 3.6\% \qquad E_\nu > 10 \text{ GeV}$$

Note that this is for channels involving Λ^o's only, and therefore cannot exclude large violations involving only K^o's etc. However, it is certainly a high upper limit because there are indications from the Gargamelle experiment that $\frac{\Lambda^o K^+}{\Lambda^o K^o} > 1$.

3. SEARCH FOR CHARMED PARTICLES

Charmed particles, if they exist, are expected to be produced in the following reactions:

1) $\nu p \rightarrow \mu^- B_c X$

- $\rightarrow \Lambda + \pi$'s — Charmed
- $\rightarrow K^o p + \pi$'s — Baryons

2) $\nu p \rightarrow \mu^- M_c X$

- $\rightarrow K^o + \pi$'s — Charmed Mesons

All possible particle combinations and charge states were investigated and no possible signal greater than 7 events above background were observed. Preliminary results give limits:

$$\sigma_{B_c} \times \text{B.R.} \; (\Lambda\pi\text{'s}) \lesssim 2\%$$

$$(pK^{o}\pi\text{'s}) \lesssim 4\%$$

$$\sigma_{M_c} \times \text{B.R.} \; (K^{o}\pi\text{'s}) \lesssim 4\%$$

Note no 3 C event of the type $\mu^{-}\Lambda\pi^{+}\pi^{+}\pi^{+}\pi^{-}$ claimed by B.N.L. has been observed. In the same sample of film 28 Δ^{++} were produced by neutrinos above 5 GeV. Thus the limits on charmed baryon production is about $\sin^2\theta_c \; \sigma_{\Delta^{++}}$ and therefore still leaves the possibility of the discovery of these states open.

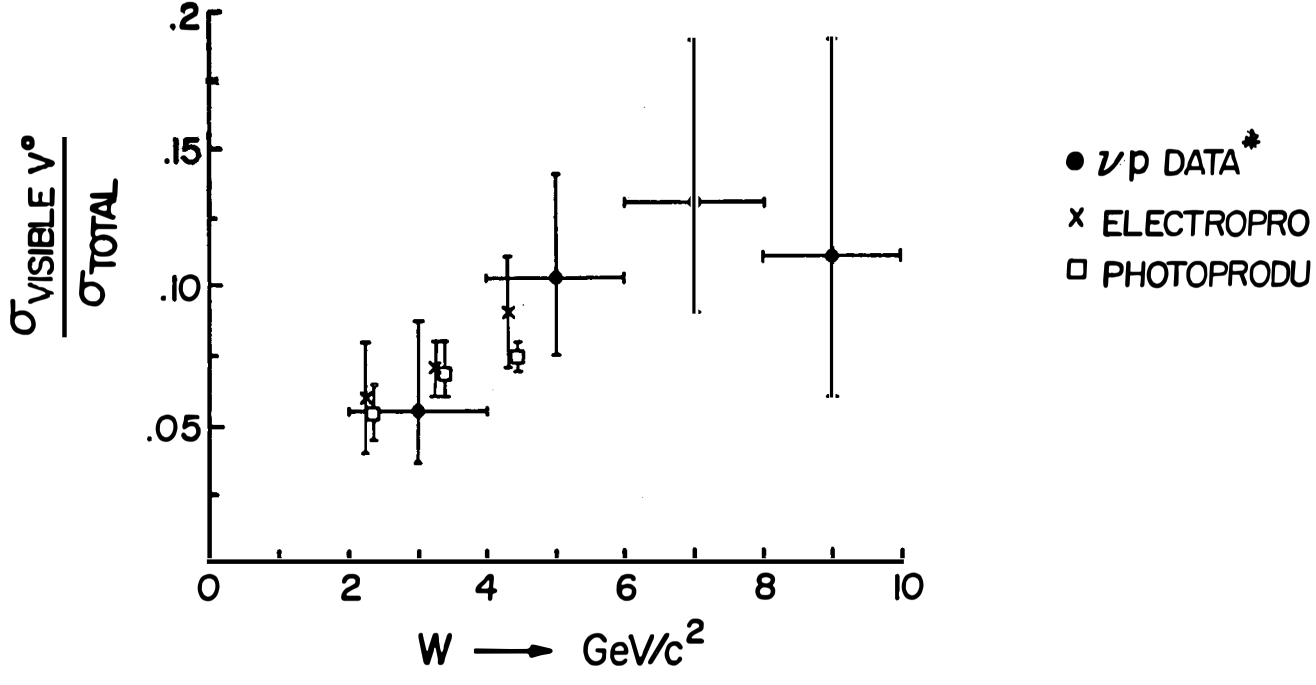
$\frac{\sigma_{\text{VISIBLE V}^0}}{\sigma_{\text{TOTAL}}}$
.2
.15
.10
.05
0
2
4
6
8
10
W ⟶ GeV/c²
● νp DATA*
× ELECTROPRO
□ PHOTOPRODU

Recent Results on ν-p and $\bar{\nu}$-(H_2-N_e) Interactions in the Fermilab 15' Bubble Chamber

R. N. Diamond
Physics Department
University of Michigan
Ann Arbor, Michigan 48109

The ratio of neutral to charged current events in ν-p interactions in the Fermilab 15' bubble chamber is obtained with the aid of an external muon identifier. The three-constraint reaction $\nu p \rightarrow \mu^- \pi^+ p$ is investigated for $\Delta^{++}(1236)$ production and momentum transfer and angular distributions are presented. Preliminary results from $\bar{\nu}$ interactions in a 21% N_e-H_2 mixture are also presented. Within the limited statistics the y distribution for small x shows a flattening at high energies.

Résumé

Le rapport de courants neutres sur courants chargés, observé dans la chambre-à-bulles à quinze pieds au Fermilab, est obtenu avec l'aide d'un "External Muon Identifier" (appareil autour de la chambre pour l'identification électronique des muons). La réaction $\nu p \rightarrow \mu^- \pi^+ p$ est examinée pour chercher la production du $\Delta^{++}(1236)$ et les distributions angulaires et distributions t sont montrées. Resultats préliminaires provenant des réactions $\bar{\nu}$ dans un mélange Ne-H_2 (21%) sont également donnés. En tenant compte de statistique limité, la distribution y à petit x montre un aplatissment à haute énergie.

I would like to present some results from the Fermilab 15' bubble chamber on νp interactions and $\bar{\nu}$ interactions in a 21% atomic mixture of H_2 and N_e. The ν-p data comes from a 62 K frame exposure out of an approved 300 K and has become a 4-way collaboration. Groups from the University of Michigan and Fermilab have been joined by groups from Lawrence Berkeley Laboratory and the University of Hawaii, who built and operated the external muon identifier (EMI).

The neutral current results presented below are preliminary in nature since we are only beginning to incorporate EMI information with bare bubble chamber results. A full understanding of the EMI and its geometric and kinematic acceptance is still lacking. When this understanding is obtained we hope to present the inclusive distributions which will tell us about the space-time structure of the weak neutral current interaction.

For the present statistical analysis we use both the EMI and the kinematic event reconstruction method described in Ref.1. We look for events with 3 or more prongs and consider the reaction $\nu p \rightarrow \mu^- x^{++}$. According to this method the highest transverse momentum negative is chosen as the muon and events are classified as opposite-side (OS) or same-side (SS), depending on whether the total hadron vector lies on the opposite (same) side of the assumed neutrino direction as does the muon. We estimate on the basis of Monte Carlo calculations that 95% of the charged current events are OS, muon correctly chosen, while only $\sim$ 40% of neutral current and neutral hadron events are classified as OS events. The SS events therefore, constitute an enriched sample of neutral current events. The EMI is used to estimate the fraction of SS events which are charged current events and which because of measuring inaccuracy or because of a neutral hadron component with relatively

large transverse momentum happen to populate the same-side data sample.

The EMI is a single-plane of 1m x 1m multiwire proportional chambers mounted behind the 15' bubble chamber. The total area is 23 m^2. Between the EMI chambers are ~ 4-5 pion interaction lengths of zinc and copper. Tracks are extrapolated from the bubble chamber into the EMI and hits in the projected EMI chamber are examined for the best match. The following is an over simplication[2], but in essence two numbers are calculated for each track: one, the probability P_μ that because of multiple Coulomb scattering a muon would have a hit in the EMI farther from the extrapolation point than the hit actually obtained; and two, the probability P_h that a hadron would give a closer hit than the one obtained. For this neutral current analysis we require that P_μ be greater than 10% and that P_h be less than 10%.

We define the ratio R' to be

$$R'_{10} = \left(\frac{\#NC}{\#CC}\right) \Sigma P_x \text{ (hadrons)} > 10 \text{ GeV/c}$$

The number of neutral current (NC) events in the data sample is

$$\#NC = (NO\ \mu\text{'s} - \text{background})/\epsilon ,$$

where $NO_{\mu's}$ = number of events with no muon candidate (because of decay or interaction) + number of SS events which have no muon fit in the EMI,

background = events due to neutral hadrons, and anti-neutrinos, and

ϵ = fraction of all NC events which appear in the same side sample.

The number of charged current (CC) events in the data sample is

$$\#CC = f\ (CC_{OS} + CC_{SS}) - CC_{NC}$$

where $CC_{OS} + CC_{SS}$ = number of charged current events in

both the OS and SS data samples as determined by the EMI,

f = fraction of CC events with hadron momentum greater than the ΣP_x cut, and

CC_{NC} = the number of neutral current events (SS+OS) which because of hadronic punch through in the EMI give $P_\mu > .10$ and which have ΣP_x for the remaining hadrons greater than the cut. (A negligible number).

In order to obtain $(CC_{OS} + CC_{SS})$ one must correct the number of events found by the EMI efficiency. This efficiency is determined by:

geometric acceptance ($\Sigma P_x > 5$ GeV)	87%
chambers not on	99%
P_μ cut	90%
	77.5%

The fraction f is determined from the data and for $\Sigma P_x > 5$ GeV/c is $\sim$ 70%.

The background in the SS sample due to antineutrinos has been estimated by Monte Carlo calculations, the charged current antineutrino rate being consistant with these calculations. The neutral hadron rate has been estimated to be 1.4 ± 1.0% of the OS sample for incident neutrons and less than 1.2 ± 1.2% for incident K_L^0's. Figure 1 shows how the neutron rate was obtained. The beam mass was calculated assuming the final state $pp\pi^-$. For those events with $.8 < M^2_{beam} < .95$ (GeV/c^2) the momentum distribution was plotted. Scaling by the ratio of total neutron cross section to the cross section for $np \rightarrow pp\pi^-$ the histogram labelled "predicted neutron rate" is obtained. This distribution is extrapolated to large neutron momentum and the number of neutron events which mimic neutrino events and satisfy the various cuts imposed on the neutrino data is estimated by Monte Carlo. The

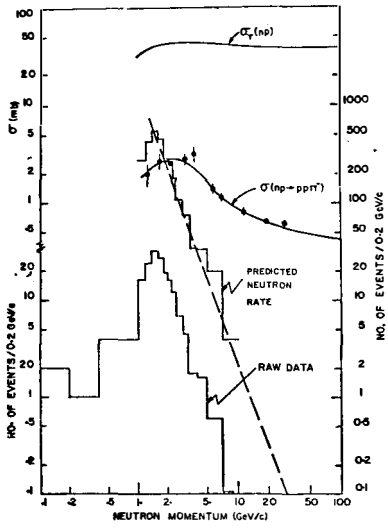

Figure 1

K°_L contamination is estimated by a similar extrapolation procedure assuming the same momentum distribution for K°_L as for K°_S produced in νp interactions, and assuming that all events with a V° with $4 < \Sigma P_x < 8$ GeV/c come from K°_L interactions. This extrapolation gives an upper limit of 1.2 ± 1.2% of the total OS sample.

We have only to evaluate ϵ, the fraction of neutral current events which appear in the same side and then substitute into our expression for R' to obtain the neutral current ratios for events with hadron momentum greater than same cutoff. Now

$$\epsilon = \epsilon' + P(1-\epsilon')$$

where ϵ' = fraction of NC events with no muon candidate

P = fraction of NC events with a muon candidate which appear in the same side sample.

The same side sample also contains some CC events. Let α be the fraction of CC events in the SS sample and #SS be the number of events in the SS sample. It turns out that 20% of the SS events have no muon candidate, i.e.

$$\epsilon' (\#NC) = .2 (\#SS)$$

and Monte Carlo calculations show that $P \cong 0.6$ and $\alpha \cong 0.05$.

Therefore $$(\#SS) = \frac{\epsilon'(\#NC)}{.2} = \epsilon'(\#NC) + P(1-\epsilon')(\#NC) + \frac{\alpha(\#NC)}{R'}$$

Assuming $R' = 0.3$ we have

$$\epsilon' = 0.167 \quad \text{and} \quad \epsilon = .667.$$

The data sample for which the EMI was working reliably has 160 CC events with hadron momentum greater than 10 GeV/c. The corresponding number of

no μ events = 40 ± 6,

neutron induced events = 4.9 ± 3.2,

K_L^o induced events = 4.0 ± 4.0, and

antineutrino induced events = 3.0 ± 3.0

This yields $R'_{10} = 0.25 \pm 0.09$

If we do the same analysis for events with $P_{hadron} > 5$ GeV/c, we get $R'_5 = 0.30 \pm 0.13$

One can use the Weinberg Salam Model[3] to estimate the neutral current ratio for the entire broad band neutrino beam. In doing this we assume that the multiplicity distributions are the same in neutral current and charged current events. The ratios one obtains by these corrections are

$R = 0.29 \pm 0.11$ for $\Sigma P_x > 10$ GeV/c

and $R = 0.34 \pm 0.15$ for $\Sigma P_x > 5$ GeV/c.

The errors are purely statistical; they do not reflect the uncertainties in the models which have been assumed.

We turn now to the Δ^{++} production in the neutrino film and use kinematic fitting to isolate the three constraint reaction $\nu p \to \mu^- \pi^+ p$. Out of 78,000 pictures and $\sim$ 550 CC events above 10 GeV $\sim$ 45 3-C fits to this reaction are obtained. The fits are generally not ambiguous with $np \to \pi^- pp$ or $\nu p \to \mu^- k^+ p$, though there may be a small number of antineutrino events $\bar{\nu} p \to \mu^+ \pi^- p$. These will not affect the Δ^{++} results since the '$\pi^+ p$' mass will be large. The $\pi^+ p$ mass distribution is shown in figure 2. It is dominated by a peak at $\sim$ 1.25 GeV/c^2, but there are clearly events at high mass. We consider events with $\pi^+ p$ mass less than 1.4 GeV/c^2 to be Δ^{++}'s.

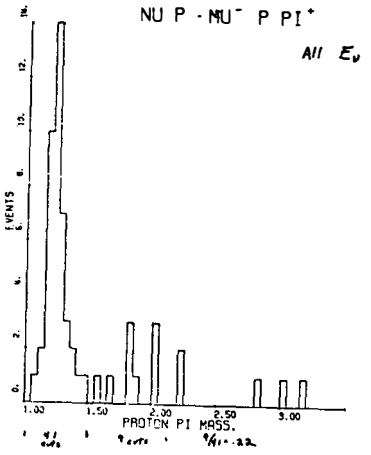

Figure 2

The neutrino energy distribution for the Δ^{++} events is shown in figure 3, and should be compared to the distribution in figure 4, which is the total charged current energy distribution divided by the energy. If the cross section is proportional to neutrino energy the distribution in figure 4 should be the neutrino flux shape, and if Δ^{++} production is independent of energy (therefore a constant fraction of the flux), the distributions in figures 3 and 4 should be the same. While the two distributions are consistent, the evidence is not compelling.

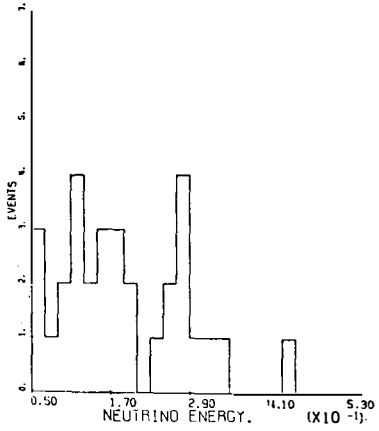

Figure 3

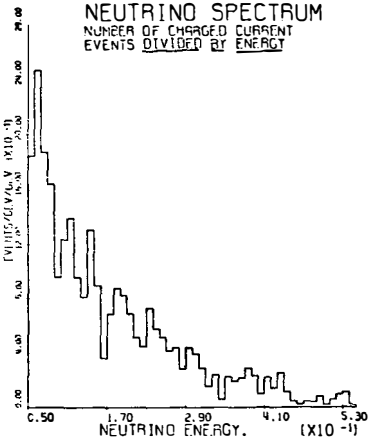

Figure 4

In figure 5 we show the Q^2 distribution for the Δ^{++} events. We note that there are a number of events at high Q^2, but figure 6 which is a scatter plot of Q^2 vs. E_ν, indicates that these high Q^2 events are not a particularly high energy phenomenon.

Curve 1 in figure 5 is a prediction for 20 GeV neutrinos due to Adler[4]. It is based on a fit to the Argonne neutrino data and uses the value $M_A = 0.96$ for the mass parameter in the axial vector form factor. Curve 1 is an attempt at an absolute normalization while curve 2 is curve 1 multiplied by an arbitrary factor of 2 to allow for our uncertainty in the normalization. The Q^2 distribution thus appears to be consistent with the Adler prediction.

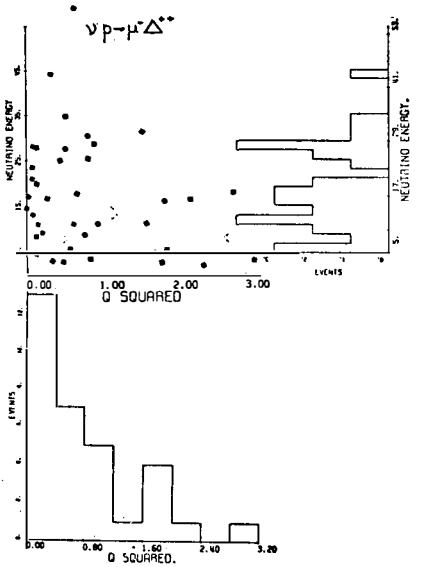

Figure 5

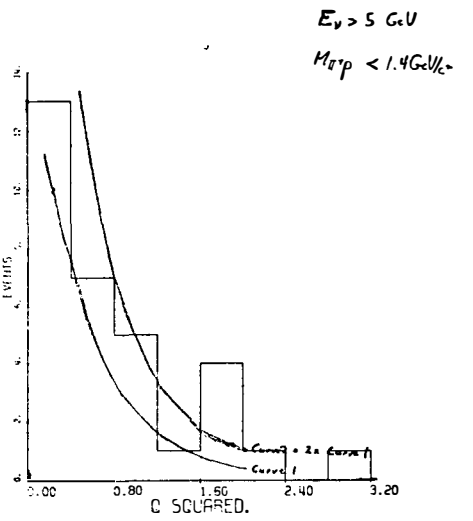

Figure 6

Lastly we show the Gottfried-Jackson angular distributions for diagram 7. In the π^+p center of mass system θ is defined to be the angle between the proton and the ω^+ direction and Φ the angle between the normals to the μ-ν plane and π^+p plane. The θ-Φ scatter plot in figure 8 also contains the projections. We note the flat cos θ distribution which we consider an indication of resonance production. A non-resonant angular distribution might have a strong forward-backward peaking. The Φ distribution seems to peak at 0°, indicating that the π^+p plane and μ-ν planes

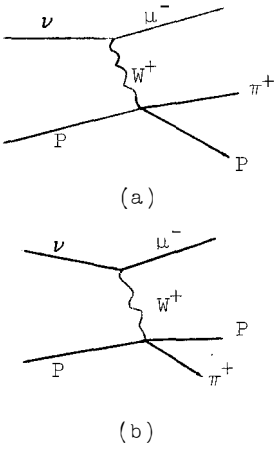

figure 7

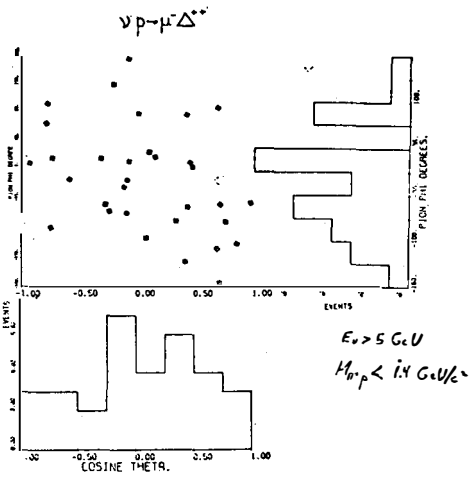

figure 8

tend to be aligned and that the particular orientation of figure 7a with the π^+ in the muon direction is preferred. We do not understand the effect.

Clearly more statistics are needed in order to give more detailed quantitative results. We have on hand approximately 100K pictures of neutrinos produced by 400 GeV/c protons and using a two-horn broad band beam. We hope to have four times the number of events and to be able to report on these data before the end of the year. The experiment has been approved for 300K pictures.

The antineutrino experiment which the Michigan bubble chamber group is participating in is a collaboration with Fermilab and two Soviet groups, ITEP in Moscow and Serpukhov. The collaboration is quite spread out but communication has been fairly good with weekly exchange of telex messages and quarterly group meetings. Most of the 50K pictures exposure of the 15' bubble chamber has been scanned and measured, but there is still a careful scrutiny of some exotic looking events and a systematic

search for dilepton events to be done.

The chamber was filled with a 21% atomic mixture of N_e in H_2 giving a radiation length of ~ 1.2 m, the mean γ ray conversion probability being ~ 50%. All events with two or more prongs were scanned for and at some of the labs one prong events were also found. The efficiency for the one prongs is quite low, however. The EMI was operating well during the exposure and has been relied on for muon identification. The muon is taken to be the highest momentum positive track which gives an acceptable fit in the EMI (muon probability > 0.04, hadron probability < 0.1).

We have only begun the analysis of the $\bar{\nu}$ data and have not for example settled on a kinematic reconstruction method. The procedure of transverse momentum balance used in the νp data may work well, but Fermi motion in Ne may make for unacceptable errors. We have to study this and other procedures to determine what works well. The method which we have temporarily adopted is correct on the average, but we might, by another method, be able to reduce the errors.

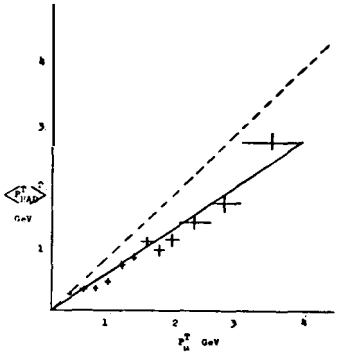

Figure 9

In figure 9 we plot the mean transverse momentum of the hadrons, charged secondaries plus neutral conversions, relative to the $\bar{\nu}$ against the muon transverse momentum. Since there are missing neutral hadrons we obtain a curve which lies below the 45° line of transverse momentum balance. We find that transverse momentum can be balanced if we set $(P_T)^{\text{total}}_{\text{had}}$, the total hadron momentum transverse to the $\bar{\nu}$, equal to

$$(P_T)^{total}_{had} \cong 1.3 \langle P_T \rangle^{vis}_{had}$$

where $\langle P_T \rangle^{vis}_{had}$ is the mean visible hadron transverse momentum. For each event we can scale the hadron longitudinal momentum by this factor and add the muon longitudinal momentum in order to get $E_{\bar{\nu}}$. Empirically, however, it is found that a larger fraction of the total hadron momentum is missing for events with relatively low visible hadron momentum than for events with high hadron momentum. The expression actually used to compute $E_{\bar{\nu}}$ is

$$E_{\bar{\nu}} = 1.25 \times |P_x^{had} + 0.5 \text{ GeV/c}| + P_x^{\mu}$$

where P_x^{μ} and P_x^{had} are respectively the visible longitudinal muon and hadron momentum.

We use the expression above to calculate the scaling variable $y = \nu/E_{\bar{\nu}} = (E_{\bar{\nu}} - E_{\mu})/E_{\bar{\nu}} = (E_{had} - M_P)/E_{\bar{\nu}}$, the fraction of antineutrino energy transferred to the hadrons. There has been considerable interest generated in the antineutrino y distributions, because of a reported flattening of the distribution at high energy for low values of the x scaling variable by the HPWF[5] collaboration. At this time we choose not to show the x distributions as potentially distorting effects of the kinematic reconstruction method are larger here than for the y distributions.

The following cuts were imposed on the data:

1. E_{μ}, the muon energy be greater than 3 GeV in order to avoid EMI efficiency,
2. ν, the energy transfer to the hadron system, be greater than 1 GeV in order to remove events which might be sensitive to the reconstruction method.
3. $E_{\bar{\nu}}$, the reconstructed antineutrino energy be greater than 10 GeV in order to assure good EMI acceptance and to reduce

hadronic background events.

Approximately 650 events survive the cuts. Cut 1 removes events at high y for low $E_{\bar{\nu}}$ and cut 2 removes events at low y for low $E_{\bar{\nu}}$. The geometric acceptance of the EMI for positive muons generated within the bubble chamber fiducial volume has been computed by Monte Carlo as a function of x and y at fixed neutrino energy. The y distributions have been corrected for this acceptance. Certain data points have not been plotted in the y distributions if the data cuts and EMI acceptance imply a correction factor for the raw data in excess of 50%.

Figures 10-13 show the corrected y distributions for both low $E_{\bar{\nu}}$ and high $E_{\bar{\nu}}$ for all x and for x less than 0.1. There is an indication of a flattening of the y distribution at high $E_{\bar{\nu}}$ and low x, but with low statistical significance. The HPWF data reported at the 1975 Palermo conference is plotted for com-

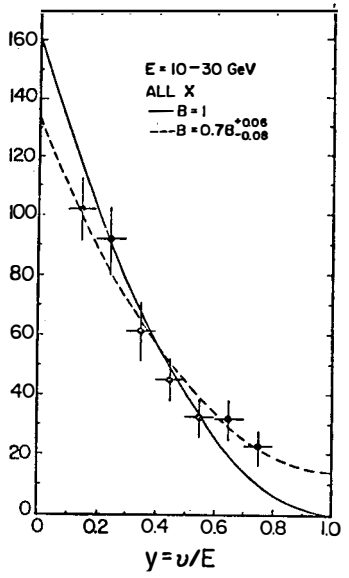

Figure 10

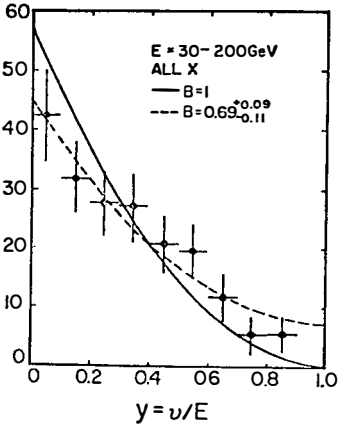

Figure 11

parison. Also plotted are curves of the form

$$\frac{dN}{dy} \sim [(1-y+y^2/2) - B(y)(1-y/2)]$$

which assume the validity of the Callan-Gross relation[6]. The

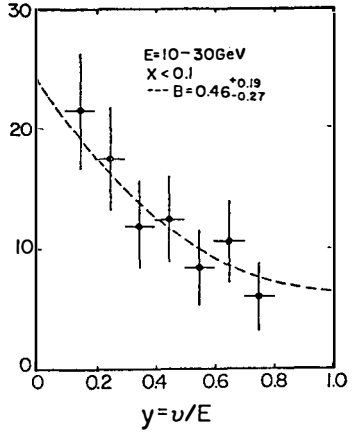

Figure 12

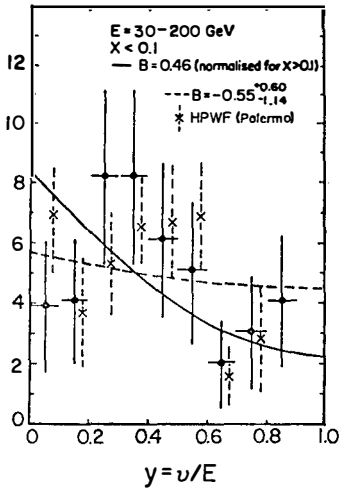

Figure 13

parameter B in the quark parton model is defined by the relation

$$\frac{1-B}{2} = \bar{Q}/(Q+\bar{Q})$$

where Q and $\bar{Q}$ represent the fraction of nucleon momentum carried by the quark and antiquark respectively.

Table I shows the values of B obtained from fits to the y distributions for different x bins and different energies. There is a weak tendency for the B values to increase as $x \to 1$ indicating that the antiquarks are not likely to be found at high x. A fit to the total $\bar{\nu}$ data sample gives $B = 0.80 \pm 0.05$ which is consistent with previous measurements[5,7,8].

TABLE OF FITTED B-VALUES

	E=10-30	E=30-200	E=10-200
ALL X	$0.78^{+0.06}_{-0.08}$	$0.69^{+0.09}_{-0.11}$	$0.74^{+0.06}_{-0.06}$
X=0-0.1	$0.46^{+0.19}_{-0.27}$	$-0.55^{+0.60}_{-1.14}$	$0.19^{+0.21}_{-0.29}$
X=0.1-0.2	$0.78^{+0.13}_{-0.18}$	$0.73^{+0.19}_{-0.28}$	$0.76^{+0.11}_{-0.14}$
X=0.2-0.4	$0.75^{+0.12}_{-0.15}$	$0.84^{+0.09}_{-0.16}$	$0.79^{+0.08}_{-0.11}$
X=0.4-	$0.95^{+0.05}_{-0.09}$	$1.00^{+0.0}_{-0.04}$	$1.00^{+0.0}_{-0.07}$

References

(1) J. W. Chapman et al., preprint submitted tp Phys. Rev.

(2) See for example V. Stenger, U. Hawaii Internal Report #11-75.

(3) See S. Weinberg, Rev. Mod. Phys. 46, 255 (1974).

(4) P. Schreiner and F. von Hippel, Phys. Rev. Lett. 30, 339 (1973).

(5) B. Aubert et al., Phys. Rev. Lett. 33, 984 (1974).

(6) C. G. Callan and D. J. Gross, Phys. Rev. Lett. 22, 156 (1969)

(7) T. Eichen et al., Phys. Lett. B46 #2, 274 (1973).

(8) S. J. Barish et al., ANL Preprint, submitted to Phys. Rev. Lett.

ASPECTS OF CHARM

Mary K. GAILLARD

CERN, Geneva

and

Laboratoire de Physique Théorique et
Particules Elémentaires*, Orsay

Abstract : By way of introduction the theoretical and phenomenological motivations for the Weinberg-Salam-GIM model are recalled. We then discuss in some detail the characteristics of charmed particle production in neutrino interactions.

Résumé : En guise d'introduction, nous rappelons les bases théoriques et phénoménologiques sur lesquelles repose le modèle Weinberg-Salam-GIM. Ensuite, nous examinons les effets prévus de la production du charme dans les expériences neutrino

* Laboratoire associé au CNRS.

I wish to discuss in some detail the expected signatures for charmed particles in neutrino interactions, with respect to both inclusive experiments (the characteristics of dimuon events and threshold effects in X and Y distributions) and exclusive experiments where hadrons are identified in the final state. But first I must define what I mean by charm, and I would also like to convey the reasons for which so many theorists believe in it.

1 - WHAT IS CHARM ?

As far as strong interactions are concerned, charm is a new, conserved quantum number associated with the introduction of a fourth quark :

$$(u, d, s) \rightarrow (u, d, s, c) \tag{1.1}$$

where u, d and s are the ordinary Gell-Mann-Zweig quarks : "up", "down" ($I = 1/2$, $S = 0$, $I_3 = + 1/2, - 1/2$), and "strange" ($I = 0$, $S = -1$). The implicit implication is that charmed quarks will bind with each other and with ordinary quarks, so that a spectroscopy of new hadrons emerges [1] :

$$SU(3) \rightarrow SU(4) \tag{1.2}$$

However, the compelling arguments for charm appear within the context of weak interactions [2], where the charmed quark serves to complete a "weak isodoublet", and to achieve lepton-quark symmetry : charged currents are built from two left-handed lepton doublets :

$$E = \begin{pmatrix} \nu_e \\ e^- \end{pmatrix}_L \qquad M = \begin{pmatrix} \nu_\mu \\ \mu^- \end{pmatrix}_L \tag{1.3}$$

and two left-handed quark doublets :

$$Q = \begin{pmatrix} u \\ d_c \end{pmatrix}_L \qquad Q' = \begin{pmatrix} c \\ s_c \end{pmatrix}_L \tag{1.4}$$

where d_c and s_c are the Cabibbo rotated d and s quarks :

$$\begin{aligned} d_c &= d \cos\theta_c + s \sin\theta_c \\ s_c &= s \cos\theta_c - d \sin\theta_c \end{aligned} \tag{1.5}$$

2 - WHY CHARM ?

Charm was introduced in 1964 by a variety of authors [3] for a variety of reasons, but the important point was made by [2] Glashow, Ilopoulos and Maiani (GIM) who noted that the introduction of the charmed quark suppresses the amplitudes for strangeness changing processes induced by higher order weak interactions. The coupling of quarks to the charged intermediate boson is given by :

$$\mathcal{L}_{W^{\pm}} = W^{+}(\bar{u}_L \gamma_\mu d_{c_L} + \bar{c}_L \gamma_\mu s_{c_L}) + \text{h.c.} \qquad (2.1.a)$$

which can be written equivalently as :

$$\mathcal{L}_{W^{\pm}} = W^{+}(\bar{u}_{c_L} \gamma_\mu d_L + \bar{c}_{c_L} \gamma_\mu s_L) + \text{h.c.} \qquad (2.1.b)$$

with :

$$\begin{aligned} u_c &= u \cos\theta_c - c \sin\theta_c \\ c_c &= c \cos\theta_c + u \sin\theta_c \end{aligned} \qquad (2.2)$$

Then we see that by successive emission of W-bosons (Figure 1), we can have : $s \to c_c \to s$ or $d \to u_c \to d$

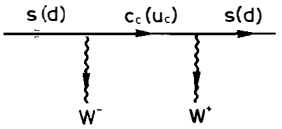

FIG. 1 : Successive weak boson emission from a quark line : the orthogonality of the Cabibbo-GIM quarks ensures that $\Delta S = 0$ if $\Delta Q = 0$.

but there is no way to induce $s \leftrightarrow d$, because s and d couple to orthogonal states. This statement is of course only true in the limit of (u, c) mass degeneracy. For a finite mass difference the combination of u and c emitted at the s vertex does not remain coherent, and the $s \leftrightarrow d$ amplitude is non-zero. However, the potential difficulty arises only when the W-loop is closed (Figure 2) ; then the amplitude resulting from Feymann integration gives a contribution which is a priori larger than permitted by experimental observation. As the leading (i.e., too large) contribution is independent of the mass of the intermediary quark, the GIM mechanism sufficiently suppresses the

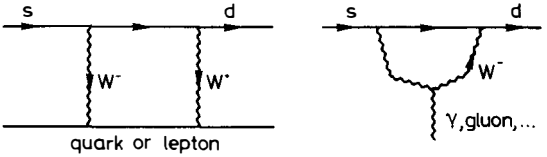

FIG. 2 : Diagrams which induce large amplitudes for $\Delta S \neq 0$, $\Delta Q = 0$ transitions if only one quark is exchanged.

amplitude even in the presence of mass splitting.

No one took the GIM model too seriously at the time it was proposed. For one thing the theory was unrenormalizable ; one was arguing about cancellations in infinite integrals. Secondly, it was perhaps not obvious at the time that arguments based on free quark amplitudes were relevant to hadron physics. Now that the possibility of a renormalizable theory of weak interactions has become a reality, and deep inelastic scattering experiments have taught us that free quark amplitudes probably are relevant, the charm hypothesis becomes much more compelling.

Rather than re-review the theory in logically ordered detail, I would simply like to impress upon you the way in which the requirements of renormalizability on the one hand, and the facts of observed phenomenology on the onther hand, form a closed, self-consistant picture in the context of the Weinberg-Salam-GIM model. This is illustrated diagrammatically in Figure 3. Let me underline the salient features.

a) The triangle anomaly [4] is a rather obscure theoretical point, but it cannot be ignored if the theory is to be renormalized. There is an infinity which arises in the calculation of a triangle diagram (Figure 4) involving a closed fermion loop with one axial and two vector couplings. In a V-A theory this can be removed only if the couplings are such that the sum over all fermion types vanishes (up to mass-dependent terms). In the $SU(2)_{Left} \times U_1$ model of Weinberg and Salam [5], this condition requires that the left-handed fermion charges sum to zero*.

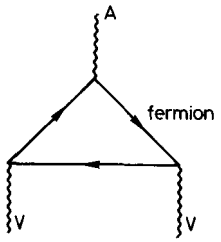

FIG. 4 : Diagram giving rise to the "triangle anomaly".

* The lepton-quark symmetry thus imposed is not required in vector-like theories [7].

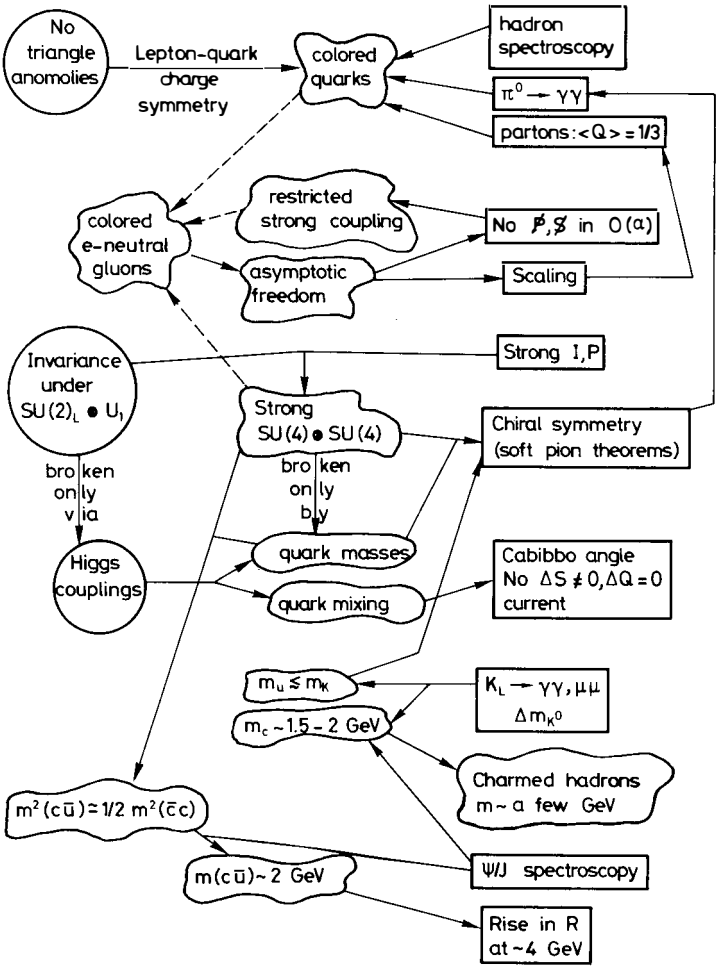

FIG. 3 : Diagrammatical representation of the consistancy between the requirements of renormalizability (circles) and observed phenomenology (rectangles) in the Weinberg-Salam-GIM model.

If quarks have an (average) charge which is fractional - as required by the deep inelastic data discussed by Nachtmann [6] - one finds that color must be introduced to insure the cancellation of anomolies. But color was already needed to make the simple quark model for hadron spectroscopy compatible with Fermi statistics [8], and, for example, to understand the $\pi^\circ \to \gamma\gamma$ decay rate [9] (in the context of approxiamte chiral symmetry).

b) The general requirement of renormalizability is that all interactions be invariant with respect to the weak interaction gauge group - assumed here to ba $SU(2)_L \times U_1$. Together with the observed strong interaction symmetries - parity and ordinary isotopic spin - this requirement implies that strong interactions must be invariant under chiral $SU(4) \otimes SU(4)$:

- SU(4) because the weak invariance is :

$u \leftrightarrow d_c$
$c \leftrightarrow s_c$

while the strong invariance is :

$u \leftrightarrow (d = \cos\theta_c\, d_c - \sin\theta_c\, s_c)$

so any quark mixing must leave the strong interactions invariant.

- Chiral* SU(4) because the weak interaction symmetry mixes only left-handed components, so a separate invariance under right and left transformations is needed.

c) It has been shown [10] that the phenomenological requirement that parity and strangeness violations be absent from hadronic interactions in order α can be insured if the strong interactions are mediated by gauge bosons which are neutral with respect to the electromagnetic and weak charges.

One of the very restricted class of interactions which satisfies both b) and c), and one which is natural in a color quark theory, is one where strong interactions are mediated by a color-octet of electrically neutral vector gluons. If the gluon couplings are invariant under color gauge

---

* Vector-like theories [7] require only invariance under ordinary SU(4) - or rather SU(n).

transformations (Yang-Mills couplings), the theory is asymptotically free [11], giving the only known field theoretical basis for approximate scaling in deep inelastic lepton-hadron scattering. Furthermore, in my understanding, the proof of c) is rigorous only in an asymptotically free theory.

d) The physical quark masses are induced by the Higgs coupling which in fact induces a quark mass matrix, mixing fermion states of equal charge, thus giving rise to the Cabibbo angle via the s, d (or equivalently c, u) mixing. On the other hand, the fact that states degenerate in charge are also degenerate with respect to the third component of "weak isospin" (see Eqs. (1.3) and (1.4)) insures that the neutral currents remain diagonal in fermion fields after diagonalization of the mass matrix : the primary neutral currents corresponding to "weak isospin" :

$$J^{I_3^W} \sim \bar{u}u - \bar{d}_c d_c + \bar{c}c - \bar{s}_c s_c = (\bar{u}u + \bar{c}c) - (\bar{d}d + \bar{s}s) \qquad (2.3.a)$$

and to "weak hypercharge" :

$$J^{Y^W} \sim \bar{u}u + \bar{d}_c d_c + \bar{c}c + \bar{s}_c s_c = (\bar{u}u + \bar{c}c) + (\bar{d}d + \bar{s}s) \qquad (2.3.b)$$

are invariant under the Cabibbo rotation. So $\Delta S = 0$ if $\Delta Q = 0$, as required by phenomenology.

e) Explicit calculations [12] of the free quark diagrams discussed above (Figures 1 and 2) yield compatibility with the phenomenology of rare K-decays and the neutral kaon mass difference only if the "up" quark is light on a hadronic scale - which together with the chiral invariance imposed by renormalizability on the strong couplings, gives a theoretical basis for approximate chiral SU(2) and the success of soft pion theorems* - and if the charmed quark is much heavier (but with $m_c \ll m_W$). The latter is certainly in agreement with phenomenology, since the persistant invisibility of charmed hadrons is the best indication that SU(4) is badly broken !

We have sketched how the Weinberg-Salam-GIM theory is not only consistant** with the phenomenology of normal hadrons - but almost requires such

---

* A recent example being the determination of g_A via pion photoproduction reported here [13].

** None of the above arguments is effected by a proliferation of fermion doublets, as discussed by Nanopoulos [14], as long as $N_{\text{leptons}} = N_{\text{quark flavors}}$ in accordance with a).

features as approximate scaling and chiral symmetry. What about new phenomena ?

The calculation [12] of the K_L, K_S mass difference yielded an estimate for the charmed quark mass :

$$m_c \simeq 1.5 \text{ GeV} \tag{2.4}$$

No one dared take this result too literally, and the effects of strong interactions on the free quark calculation are still under dispute [15], but the fact is that the observed ψ/J spectroscopy [16], consistant with that of a non-relativistic fermion-anti-fermion bound state system, indeed suggests a mass in the neighbourhood of (2.4). Furthermore, using the simple form of SU(4) symmetry breaking - i.e., via quark masses alone - one may naïvely extrapolate the Gell-Mann-Okubo mass formulae to predict from the J/ψ mass of 3 GeV a charmed hadron ground state (0^- meson) at about 2 GeV. This coincides remarkably with the rise in the ratio :

$$R = \frac{(e^+e^- \to \text{hadrons})}{\sigma(e^+e^- \to \mu^+\mu^-)} \tag{2.5}$$

observed [16] at a center of mass energy $\sqrt{s} \simeq 4$ GeV. These numerical coincidences between observed phenomena and naïve theoretical predictions may be a practicle joke of nature, but they are certainly suggestive.

3 - NEUTRINO PRODUCTION OF CHARM : ELEMENTARY EXPECTATIONS :

In this section we shall summarize the simple parton model predictions for charm discussed by Nachtmann [6], and comment on the effects of thresholds and on the expected semi-leptonic branching ratio, which determines the expected di-lepton yield. In subsequent sections we shall take up more specific issues relevant to the experimental data presented at this meeting.

3-1 : The parton model :

As discussed by Nachtmann [6], the content of the physical nucleon in terms of ordinary quark and anti-quark partons may be extracted from low energy electroproduction and neutrino data. If $P_i(x)$ is the probability for finding a parton of type i with momentum fraction x in the proton, we define :

$$u(x) = x\, P_u(x), \quad \int_0^1 dx\, u(x) \equiv u, \text{ etc } \ldots \tag{3.1}$$

and :

$$r = (\bar{u} + \bar{d})/(u + d) \tag{3.2}$$

is the relative anti-parton content of the nucleon. The analysis of data from Gargamelle [17] suggests that :

$$r \simeq 0.1 \tag{3.3}$$

with anti-partons confined to the small x region :

$$\bar{u}(x),\ \bar{d}(x) \to 0, \quad x \sim (0.1 - 0.2) \tag{3.4}$$

a result which is in accord with theoretical prejudice [18]. A similar analysis is made for electroproduction, where the e-parton cross section is proportional to the parton squared charge :

$$\sigma^{e\ Z(I=0)} \sim \frac{5}{9}\left[u + \bar{u} + d + \bar{d}\right] + \frac{2}{9}(s + \bar{s}) \tag{3.5}$$

By comparing the experimental values for (3.5) with ν and $\bar{\nu}$ cross sections, one can in principle extract the relative $s + \bar{s}$ content of the nucleon. The data [17], [19] are compatible with $s + \bar{s} \simeq 0$, but a 20 % strange parton content is not ruled out. Intuitively one expects that :

$$s,\ \bar{s} \lesssim \bar{u},\ \bar{d} \tag{3.6}$$

and that the s, $\bar{s}$ distribution will also be confined to small x.

Now let us naïvely extend these ideas to charmed particle production. The important elementary scattering processes are :

$$\nu_\mu + d \to \mu^- + c, \qquad \sigma \sim \sin^2\theta_c\left[\bar{d}(x) + s(x)\right] \tag{a}$$

$$\left.\begin{aligned} \nu_\mu + s &\to \mu^- + c, \qquad \sigma \sim 2\cos^2\theta_c\ s(x) \qquad (b)\\ \bar{\nu}_\mu + \bar{s} &\to \mu^- + \bar{c}, \qquad \sigma \sim 2\cos^2\theta_c\ \bar{s}(x) \qquad (c) \end{aligned}\right\} \to 0, \quad x \gtrsim 0.1 \tag{3.7}$$

where we have assumed an I=0 nuclear target. From the above discussion we see that these two contributions may be comparable :

$$\frac{2s}{u+d} = \frac{2\bar{s}}{\bar{u}+\bar{d}} \lesssim 10\ \%, \quad \sin\theta_c \simeq 5\ \% \tag{3.8}$$

The $\bar{\nu}\bar{d}$ cross section is suppressed by both the Cabibbo angle and the sea factor and is negligible. If the nucleon has any charm content it must be considerably less that the s-content (to be compatible with the strong Zweig suppression of the ψ/J relative to the ϕ), and the processes :

$$\begin{aligned} \nu_\mu + \bar{c} &\to \mu^- + \bar{s}, \bar{d} \\ \bar{\nu}_\mu + c &\to \mu^+ + s, d \end{aligned} \qquad (3.9)$$

are further suppressed by a $(1 - y)^2$ factor relative to (3.7 b.,c.) ; we shall neglect this contribution. Then we expect that (sufficiently above threshold), charm production will be characterized by [20] :

a) A flat y-distribution.

b) A component with a valence x-distribution for ν's, contributing roughly 5 % to the total ν cross section.

c) A possibly comparable component confined to small x and which contributes equally to ν and $\bar{\nu}$ cross sections, and is thus relatively enhanced by the factor ~ 3 in $\bar{\nu}$ reactions.

These expectations are illustrated [21] in Figure 5 where the y-distribution has been cut-off at a threshold value (see next section). However, before confronting these predictions with the data, we should comment on their domain of validity.

3-2 : Threshold effects :

In order to produce a system of invariant mass m_o, we must have $W \geq m_o$; this implies :

$$E \geq m_o^2/2m, \quad y \geq m_o^2/2mE, \quad x \leq 1 - m_o^2/2mE_y \qquad (3.10)$$

As a new mass threshold is passed, its presence will first appear in the high y, low x region, thus distorting the distributions described above. Furthermore, we hardly expect the parton picture to be a reasonable description in the baryon resonance region for W ; the results discussed above are relevant for $W \gtrsim 2$ GeV. For charmed particle production, the lowest baryon state may have a mass of about 2.5 GeV. Then the threshold energy is :

$$E_c \gtrsim 3 \text{ GeV} \qquad (3.11)$$

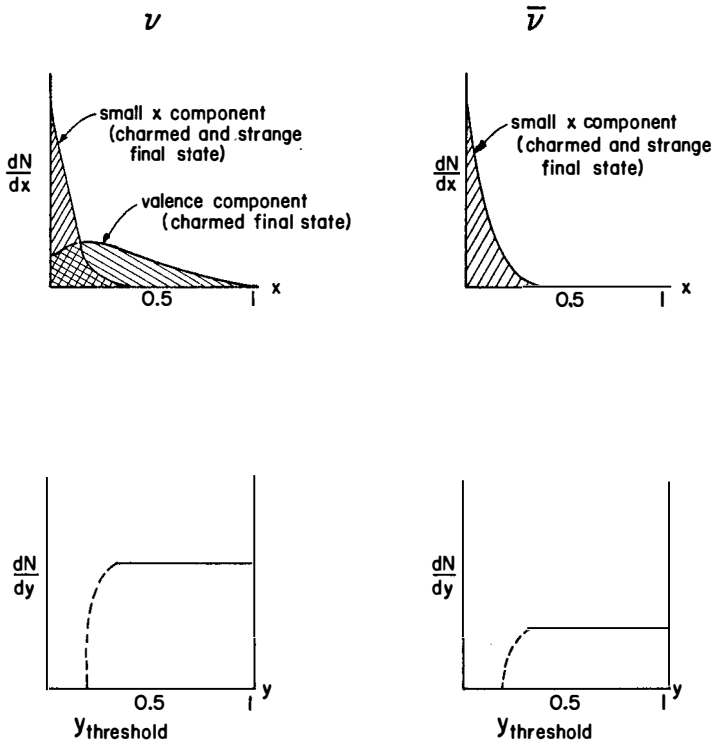

FIG. 5 : Expected x and y distributions for neutrino production of charmed particles [21].

However, the charm "resonance region" may extent to 3 or 4 GeV. Thus if we want to cover a reasonable region of the x, y plane in the scaling region, say $1 > y > 0.5$, $0 < x < 0.5$ for $W^2 > (10\text{-}15)$ GeV we require :

$$E_c^{(sc.)} \gtrsim (20\text{-}30) \text{ GeV} \tag{3.12}$$

i.e. a considerably higher threshold is required for effective scaling. One then has to guess as to how the scaling threshold might be approached. What has been done by most authors is simply to multiply the parton distributions by a θ-function :

$$d\sigma \rightarrow d\sigma\, \theta(W - W_c) \tag{3.13}$$

where $W_c \simeq$ a few GeV is the anticipated effective scaling threshold in W.

Another related problem is that in the parton model described above, the quarks were treated as massless. It is generally believed that ordinary quarks are (effectively) light on the scale of ordinary hadron masses ; $m_{u,d,s} \lesssim$ a few hundred MeV. However, the charmed quark apparently has an effective mass of 1.5-2 GeV (c.f. eq. (2.4) and above discussion). There has recently emerged some field theoretical justification [22] for an approach [23] which simply takes the parton model literally for massive quarks. This alters the kinematics in such a way that the scaling variable x is redefined by :

$$x \to x' = x + m_c^2/2m_N E_\nu y \tag{3.14}$$

if all but the charmed quark mass are neglected. It happens moreover that the charmed quark mass is on a scale similar to the expected masses of the charmed hadrons. We saw in section 2 that the presumed mass of the 0^- ground state is about 2 GeV, and bubble chamber data, to be discussed later, suggest for the lowest baryon state :

$$m_{C_o^+} \simeq (2.2\text{-}3)\ \text{GeV}, \quad C_o^+ = (cud,\ 1/2^+) \tag{3.15}$$

If m_c is replaced by W_c in eq. (3.14), one obtains a smooth extrapolation [24] to the scaling region with the condition $x' < 1$ ensuring the correct threshold cut off.

3-3 : Leptonic branching ratio for charmed particle decay :

In order to estimate dilepton yield due to charm production by neutrinos, an estimate of the leptonic branching ratio is necessary. In terms of quarks, the dominant decay processes are expected to be :

$$\text{Non-leptonic} : c \to s\, u\, \bar{d} \qquad \text{Ampl.} \sim G_F \cos^2 \theta_c \tag{3.16}$$

$$\text{Leptonic} : c \to s\, \ell^+ \nu \qquad \text{Ampl.} \sim G_F \cos \theta_c \tag{3.17}$$

These are a priori comparable in magnitude. However from our experience with strange particle decays we expect that the non-leptonic amplitude may be effectively enhanced by the strong interactions, i.e. by gluon exchange. This can be qualitatively understood as follows. For the lepton decay (Figure 6.a), the momentum transfer carried by :

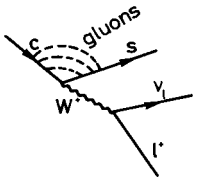

FIG. 6.a : Strong interaction corrections to semi-leptonic quark decay.

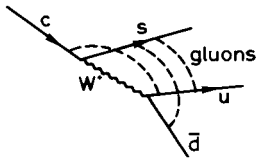

FIG. 6.b : Strong interaction corrections to non-leptonic quark decay.

the intermediate boson is always the invariant mass of the lepton pair :

$$q^2 = (p_\ell + p_\nu)^2 << m_W^2$$

so the effective coupling is always weak :

$$\text{Ampl.} \sim g^2/(m_W^2 - q^2) \sim G_F$$

However, for the non-leptonic case the gluon exchange diagram of Figure 6.b allows for contributions from W's carrying high momentum, which might attenuate to some extent the mass suppression factor in the W-propagator. The effect can be calculated in an asymptotically free field theory where colored quarks are assumed to couple strongly though the exchange of an octet of colored gluons. One finds [25] that the effective fermi coupling constant is modified by a logarithmic factor :

$$G_F \to G_{eff} = G_F\left[1 + b\ \ell n(m_W^2/\mu^2)\right]^\gamma \qquad (3.18)$$

where μ is a normalization mass and it turns out that :

$$\left.\begin{array}{l}\gamma > 0, \quad G_{eff} > G_F \\ \\ \gamma < 0, \quad G_{eff} < G_F\end{array}\right\} \quad \text{for the } \Delta I = \begin{cases}1/2\\3/2\end{cases} \qquad (3.19)$$

part of the non-leptonic current-current operator. In the GIM model the magnitude of this effect is not sufficient to account for the accuracy of the observed $\Delta I = 1/2$ rule. However there are various arguments leading one to expect a further enhancement of the (1/2)/(3/2) amplitude ratio in the

matrix elements of the current-current operator.* (If there are more than four quarks, the effect in (1.40) is somewhat increased). The same analysis holds for the $\Delta C = 1$ current-current operator responsable for charmed particle decay, with $\Delta I = 1/2(3/2)$ replaced by $\Delta V = O(1)$, V-spin being the $u \leftrightarrow s$ symmetry group. However, the effect may be weakened in this case [26]. The only change in eq. (3.18) in going from strangeness to charm decay is in the choice of the renormalization mass μ, which should be characterized by :

a) The effective masses of the external quarks in the hadron wave function, and

b) The onset of scaling for processes involving the appropriate quantum numbers.

Both criteria suggest $\mu^2_{\Delta c} > \mu^2_{\Delta s}$, thus decreasing the factor in brackets in (3.18) for the charm case.

For strangeness changing decays leptonic branching ratios are typically :

$$B^s_\ell \sim 10^{-3}$$

This is due to a phase space suppression of 3-body-final states as well as to the effective enhancement of non-leptonic rates which is empirically of order :

$$A_s \simeq \sin \theta_c^{-2} \simeq 20$$

For the decays of massive charmed particles, 3-body phase space is irrelevant, so we expect :

$$B^c_\mu = B^c_e = (2 + A_c)^{-1} \tag{3.20}$$

and from the above discussion we expect :

$$A_c < A_s \simeq 20 \tag{3.21}$$

---

* It is relevant to the conclusions below that anologous arguments fail [26] for the case of charm decay.

while the minimum non-leptonic ratio expected is that for a freely decaying quark, i.e. no enhancement. Since the (ud) quark pair in Figure 6.b can carry three colours we obtain :

$$A_c > A_{free} = 3 \tag{3.22}$$

Thus we obtain :

$$5\ \% \lesssim B_\mu = B_e \lesssim 20\ \% \tag{3.23}$$

as the theoretically reasonable range for the leptonic branching ratio.

Now we turn to a discussion of the specific experimental issues.

4 - DILEPTON EVENTS AT HIGH ENERGIES :

Dilepton events have been observed by several groups [27], [28], [29] at Fermilab. In particular, the HPWF Collaboration [27] has observed a dimuon signal with an apparent hadronic invariant mass threshold :

$$W \gtrsim 4 \text{ GeV}$$

and with relative cross sections for E > 40 GeV :

$$\frac{\sigma_\nu(\mu^-\mu^+)}{\sigma_\nu(\mu^-)} \simeq 10^{-2} \qquad \frac{\sigma_{\bar\nu}(\mu^+\mu^-)}{\sigma_\nu(\mu^-\mu^+)} \simeq 0.8 \pm 0.6 \tag{4.1}$$

$$\frac{\sigma_\nu(\mu^-\mu^-)}{\sigma_\nu(\mu^-\mu^+)} \sim 0.1 \qquad \frac{\sigma_\nu(3\mu)}{\sigma_\nu(2\mu)} \lesssim \frac{1}{50} \tag{4.2}$$

As the semi-leptonic charm changing interactions defined by the quark current (2.1) respects a $\Delta C = \Delta Q$ rule, completely analogous to the familiar $\Delta Q = \Delta S$ rule, the production and semi-leptonic decay of a charmed particle will necessarily lead to a $(\mu^-\mu^+)$ state. Let us first consider the "opposite sign" dimuon events. Their spread in invariant mass rules out their interpretation in terms of a decay $X \to \mu^+\mu^-$, and sources such as a heavy lepton or an intermediate boson appear unlikely, particularly because of the observed large energy asymmetry [30] in favor of the $\mu^-(\mu^+)$ for $\nu(\bar\nu)$ induced events. So we shall compare the data with the naïve parton model predictions for charm as discussed previously. For future reference let us remark that in processes involving high momentum transfers characteris-

tic of the deep inelastic scaling region, one expects that the scattered charmed quark is more apt to combine with a single anti-quark to form a charmed meson than with two other quarks to form a charmed baryon. Charmed mesons will cascade to the meson ground state (assumed to be 0^- as for ordinary mesons) which will then decay weakly. Thus we expect $\Delta C \neq 0$ neutrino interactions to produce most abundantly :

$$D^+ \equiv \{(c\,\bar{d}),\ 0^-\}\ ,\quad D^\circ \equiv \{(c\,\bar{u}),\ 0^-\}$$

and probably to a lesser extent, when the charmed quark picks up a strange anti-quark :

$$F^+ \equiv \{(c\,\bar{s}),\ 0^-\}$$

4-1 : Opposite sign dimuons :

The predictions are :

$$\begin{aligned} \sigma_\nu(\mu^-\mu^+) &= B_\mu(\sigma_v + \sigma_s) \\ \sigma_{\bar{\nu}}(\mu^+\mu^-) &= B_\mu\,\sigma_s \end{aligned} \tag{4.3}$$

where B_μ is the muonic branching ratio and σ_v and σ_s are the valence and sea quark contributions, respectively, with :

$$\sigma_s \lesssim 2\,\sigma_v,\quad \frac{\sigma_v}{\sigma_\nu^{TOT}} \simeq \sin^2\theta_c \simeq 0.05,\quad B_\mu = (5\text{-}20)\ \%$$

Therefore we predict :

$$\frac{\sigma_{\bar{\nu}}(\mu^+\mu^-)}{\sigma_\nu(\mu^-\mu^+)} \lesssim \frac{2}{3} \tag{4.4}$$

and :

$$B_\mu\,\sigma_v = B_\mu(\sigma_\nu - \sigma_{\bar{\nu}}) = (0.003 \text{ to } 0.01) \tag{4.5}$$

These expectations are in agreement with the data, eq. (4.1), which are compatible with parameters in the range (assuming always $r_s \lesssim 10\ \%$) :

$$(r_s,\ B_\mu) = (10\ \%,\ 7\ \%) \text{ to } (1\ \%,\ 16\ \%) \tag{4.6}$$

r_s is the relative strange quark content of the nucleon :

$$r_s = 2s/(u+d) = 2\bar{s}/(u+d) \qquad (4.7)$$

If this interpretation is correct, we expect the $\bar{\nu}$ distribution to be confined to small x, while the ν distribution will contain a component characteristic of the valence quark distribution ($< x > \simeq 0.2$). However if threshold effects are important at Fermilab energies, these distributions can be distorted towards the high y, low x region (see Eqs.(3.10)).

The data are displayed in Figure 7, where the rudimentary theoretical curves have been superimposed.*

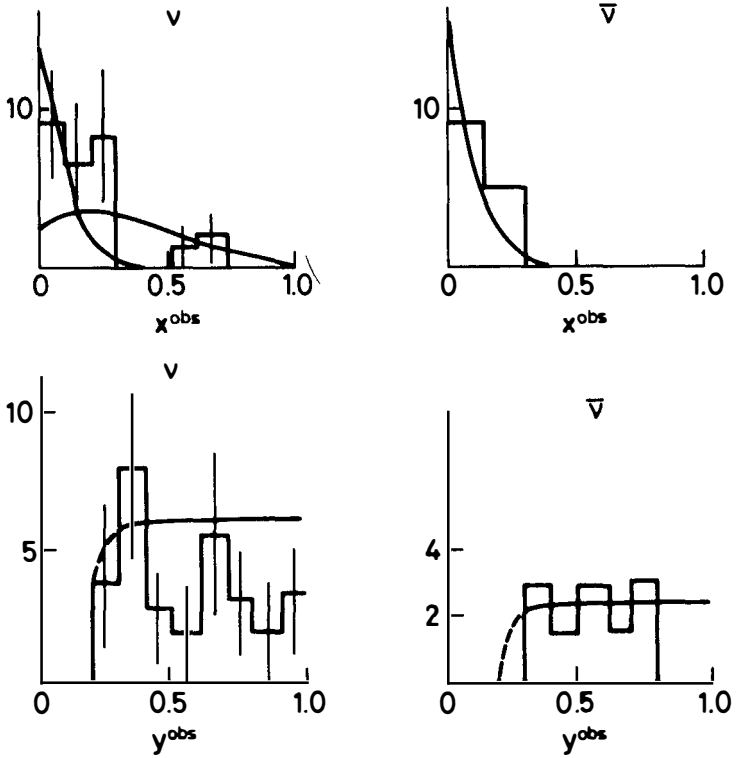

FIG. 7 : The observed x and y distributions for the HPWF dilepton data [27], and the naïve parton model predictions (Fig. 5).

---

* The theoretical curves are plotted against the true x, y variables, which are not actually measured because the incident neutrino energy is unknown, and there is a presumed decay neutrino contributing to the total final state "hadronic" energy. The data are plotted against quantities derived from the observed energy and satisfy $y^{obs} < y$, $x^{obs} > x$.

Comparisons have also been made incorporating threshold corrections in the form [31] of a θ-function, Eq. 3.13, or the smoother [23] correction of Eq. 3.14, but at the present level of the data the comparison is not significantly different, and there is no apparent discrepancy** with the predictions. In particular, the x-distribution for antineutrinos is indeed confined to small x.

One may also attempt to include the decay distributions of the second muon [24], [32]. Results are again in qualitative agreement with the GIM model. In particular the E_-/E_+ asymmetry is well described [32], as opposed to the case for a heavy lepton or W hypothesis. Another interesting comparison is shown in Figure 8, where $k_\perp$ is the component of the μ^+ momentum relative to the (ν, μ^-) plane. The theoretical curves are for V±A induced decays :

$$\text{charm} \rightarrow \text{hadrons} + \mu^+\nu \qquad \text{(n-body)} \tag{4.8}$$

and :

$$P_c \rightarrow \mu^+\nu \qquad \text{(2-body)} \tag{4.9}$$

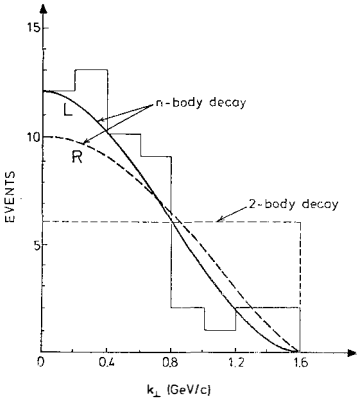

FIG. 8 : Predicted and experimental distributions [32] of μ^+ transverse momentum in ν dilepton events. L and R are for V-A and V+A coupling respectively.

where P_c is a charmed pseudoscalar. The distribution for the general case, Eq. (4.8), is derived from the free quark decay distribution for :

$$c \rightarrow s\ \ell\ \nu$$

(or equivalently the muon decay distribution). The decay (4.8) is "allowed", while in a V±A theory (4.9) is forbidden by helicity conservation. The ratio of allowed to forbidden decays scales as the fourth power of the parent mass. From the measured ratio of $K_{\ell 2}$ to $K_{\ell 3}$ one

** It is pointed out in refs. [23] and [31] that the fit to the neutrino y distribution is somewhat improved if there is a $(1-y)^2$ component as anticipated in vector-like theories [7].

expects [1] for m_F = 2 GeV :

$$\Gamma(F \to \ell\nu)/\Gamma(F \to \ell + \text{all}) < 1.5\ \% \qquad (4.10)$$

The $D \to \ell\nu$ decay is further suppressed by the Cabibbo angle and should be negligible.

4-2 : Same sign dimuons :

The $\Delta C = \Delta Q$ rule led us to predict only opposite sign dimuons in charm decay. However, in spite of the analogous $\Delta S = \Delta Q$ rule for strangeness changing processes, the reaction :

$$\bar{\nu} + N \to \mu^+ + K + X$$
$$\qquad\qquad\quad \hookrightarrow \mu^+ + X'$$

can occur because a decaying neutral kaon loses the memory of its strangeness via $K^\circ \leftrightarrow \overline{K^\circ}$ mixing.

In the GIM model, the analogous $D^\circ \leftrightarrow \overline{D^\circ}$ mixing is expected to be negligible because [33] :

a) The $\Delta C = \Delta S$ rule for Cabibbo favored transitions implies that mixing can occur through strangeness zero intermediate states :

$$D^\circ \to (\text{hadrons})_{S=0} \to \overline{D^\circ} \qquad \text{Ampl.} \sim \sin^2 \theta_c$$

b) Just as the GIM mechanism insures that the $K^\circ \leftrightarrow \overline{K^\circ}$ transition vanishes in the limit of u, c mass degeneracy the $D^\circ \leftrightarrow \overline{D^\circ}$ transition vanishes for d, s degeneracy, which is a much better approximation.

c) Because of the many channels available we expect :

$$\Gamma >> \Delta\Gamma, \Delta m$$

for the two combinations of D° and $\overline{D^\circ}$ which are decay eigenstates. Putting these factors together, one obtains an estimate [34] of about 10^{-4} for "wrong sign" dimuons in semi-leptonic decays.

Then the only mechanism available for the $\mu^-\mu^-$ events in the GIM model is associated production of charm via a charm conserving reaction :

$$\nu + N \to \mu^- + C + \bar{C} + X$$
$$\qquad\qquad\quad \big\lfloor \to \text{hadrons} \qquad \big\lfloor \to \mu^- + \nu + \text{hadrons} \tag{4.11}$$

Since the events occur at a level of about 10^{-3}, this requires :

$$\sigma(\nu N \to C\bar{C} + X)/\sigma_\nu^{TOT} \sim 10^{-3}/B_\mu \simeq (0.6\text{-}1.5) \cdot 10^{-2} \tag{4.12}$$

Is this level unreasonably high ? The extrapolation of fits to ordinary hadron production leads to an estimate of $D\bar{D}$ production at ISR - where much more energy is available - of the order [35] :

$$\sigma(pp \to D\bar{D} + X)/\sigma(pp)^{TOT} \sim 5 \cdot 10^{-4} \tag{4.13}$$

However, much of the cross section and much of the available energy in pp collisions go into leading particle effects which have no analogue in deep inelastic νp reactions. The large $p_\perp$ sector in pp scattering might provide a better means of comparison and the relative D production is expected to increase significantly with $p_\perp$; for example [35] :

$$(D/\pi)_{TOT} \lesssim 10^{-4}, \quad (D/\pi)_{p_\perp > 1\ GeV} \simeq 3 \cdot 10^{-3} \tag{4.14}$$

In any case the associated production interpretation may be tested, as it implies two unambiguous predictions :

a) Trimuon events should occur at a level :

$$\sigma_\nu(3\mu) = B_\mu\, \sigma_\nu(\mu^-\mu^-) \simeq (0.7 \text{ to } 1.6) \cdot 10^{-2}\, \sigma(\mu^-\mu^+) \tag{4.15}$$

The limit in (4.2) is not yet sensitive to this prediction.

b) Dimuon events in leptoproduction :

$$\ell + N \to \ell + C + \bar{C} + X$$
$$\qquad\qquad \big\lfloor \to \text{hadrons} \qquad \big\lfloor \to \ell\nu + \text{hadrons}$$

should occur at a level of roughly :

$$\frac{\sigma_\ell(\ell\ell')}{\sigma_\ell(\ell)} \sim \frac{2\sigma_\nu(\mu^-\mu^-)}{\sigma_\nu(\mu^-)} \sim 2 \cdot 10^{-3} \tag{4.16}$$

with :

$$\sigma_{\ell}(\ell\ell^{+}) = \sigma_{\ell}(\ell\ell^{-})$$

4-3 : High energy (μ e K_s) events :

The data on neutrino induced μ e events at the Fermilab 15 foot bubble chamber will be discussed by Cundy [29]. The observed rate corresponds to a relative cross section of about a per cent. In Figure 9 is a John Ellis plot* of the x and y distributions, again with the curves of Figure 5 superimposed, as well as the shape of the HPWF data [27] (dashed histogram) for comparison.

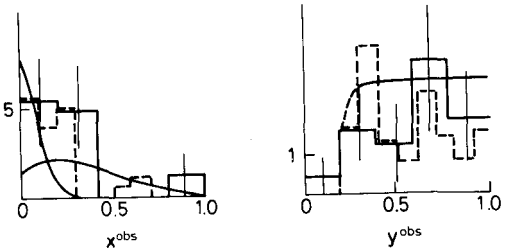

FIG. 9 : John Ellis plot of the observed x and y distributions for the $\mu^{-}e^{+}$ events observed in the 15 foot bubble chamber [29], together with the parton model distributions (Fig. 5) and the HPWF data (dashed lines, see Fig. 7).

The remarkable feature of these events is that all but one has an identified K_s. If one assumes that the dominant mechanism, (in accordance with the $\Delta C = \Delta S$ rule derived from the Cabibbo favored part of the coupling (2.1)) responsible for the observed signature is :

$$\begin{array}{l} \nu_{\mu} + N \rightarrow \mu^{-} + D^{+} + X \\ \qquad\qquad\quad \hookrightarrow e^{+} \nu_{e} + K_{s} \end{array} \qquad (4.17)$$

one may try to guess the mass of the D^{+} from the observed $e^{+}K_s$ distribution. A statistical assumption that on the average the decay products share the parent momentum equally gives :

---

* This nomenclature is intended to absolve the experimentors of responsibility for the plot of Figure 9.

$$m_{D^+} \simeq \sqrt{2} < m_{Ke} > \simeq 2.3 \tag{4.18}$$

for the value $< m_{Ke} > \simeq 1.3$ corresponding to 7 of the events plotted in Figure 9 for which there is an invariant mass measurement. Barger and Phillips [36] have calculated the relation between $< m_{Ke} >$ and the parent mass for a V-A decay matrix element. Their result considerably lowers the estimate (4.18). However they have neglected form factor effects which are expected to be considerably more important for charmed pseudoscalar decays than for K_{e_3} decay. The reason is that the physical region for the squared momentum transfer :

$$m_e^2 \leq t \leq (m_D - m_K^2) \tag{4.19}$$

extends to values not very far from the expected position of a pole in the form factor. Assuming F^*-dominance :

$$F^{+*} \equiv \{(c\bar{s}),\ 1^-\}$$

in analogy with K^* dominance which describes well the form factor in K_{e_3} decay, the V-A matrix element acquires a correction factor :

$$f(t) = (1 - t/m^2_{F^*})^{-1} \tag{4.20}$$

It is expected that the lowest lying charmed vector and pseudoscalar mesons, D, F, D^*, F^*, will be nearly degenerate in mass, separated at most by a few hundred MeV. Then the factor (4.20) can become quite large, enhancing the high t region of phase space. A point-like V-A interaction favors the configuration (helicity allowed) of Fig.10.a, with :

$$t = 0, \quad E_\nu \simeq 1/4\ m_D, \quad m_{Ke} = \sqrt{m_D^2 - 2\ E_\nu\ m_D} \simeq \frac{m_D}{\sqrt{2}} \tag{4.21}$$

while the maximum t configuration is that (helicity forbidden) of Figure 10.b with the kaon at rest and :

$$t = (m_D - m_K)^2, \quad E_\nu \simeq \frac{1}{2}(m_D - m_K), \quad m_{Ke} \simeq \sqrt{m_D\ m_K} \tag{4.22}$$

so the presence of the form factor, which enhances high t configurations, serves to lower the mean value of m_{Ke}.

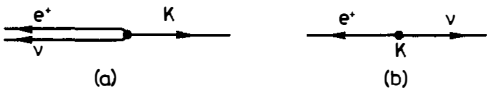

FIG. 10 : Final state configurations for D → Kℓν corresponding to $t = 0$ (a) and $t = t_{max}$ (b).

In Figure 11, we show the mass distribution calculated by Buras [37] assuming a D mass of 2 GeV and an F^* mass of 2.3 GeV. The events are also plotted, two of them lying outside the kinematically allowed region.

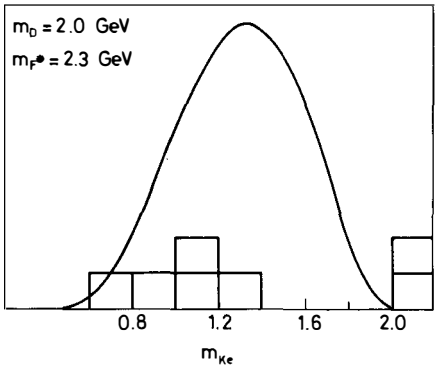

FIG. 11 : Predicted $K_s e^+$ mass distribution [37] for the decay $D \to K_s e^+ \nu$ for m_D = 2 GeV and assuming F^* dominance with m_{F^*} = 2.3 GeV.

However, even if the 3-body decay were the dominant semi-leptonic mode, which it may not be*, the paring of the electron with a K_s is rather arbitrary since several of the events contain more than one identified kaon, and others show a high multiplicity of unidentifiable charged prongs which could include a K from the decay $D^\circ \to K^- e^+ \nu$. This is as it should be ; for charm production from the sea, there is an $\bar{s}$ left behind which will manifest itself by the appearance of an additional strange particle (see Figure 5). (Note however that the event with large x ($x^{obs} = 0.9$) plotted in Figure 9 has only $\mu^- e^+ K_s$ as visible particles in the final state, and is thus compatible with valence production).

---

* Estimates [38] of the $D \to K^* \ell \nu$ rate suggest it may be equally important.

What is in fact puzzling in these events is the rarity of $\mu^- e^+$ events without an identified K_s. If the ν is scattered from a valence quark one expects $\overline{K^o}$ and K^- to occur in roughly equal ratios. Since only half of the $\overline{K^o}$ are K_s, and only 2/3 of these have visible decays, we expect that on the average 1/6 of the events will contain an identified K_s. For charm production from a sea quark, there will be an additional kaon (K^+ or K^o) at the production, and one estimates that about a third of the events will contain a K_s. Allowing for 15 % associated production of kaons in the recoiling hadron system still only gives :

$$\sigma(K_s)/\sigma(\text{charm}) \simeq (27\text{-}29)\ \% \text{ for } r_s = 0.05\text{-}0.1 \qquad (4.23)$$

Hopefully the present data is subject to a statistical or scanning fluke ; otherwise they present a puzzle for any interpretation.

5 : ANOMOLOUS x AND y DISTRIBUTIONS :

If we are correct in attributing the $(\mu^-\mu^+)$ signal to the production and decay of charmed particles which have predominantly non-leptonic decays, we expect accordingly an increment in the total single muon event rate : $\sigma_\nu \to \sigma_\nu + \sigma_\nu^c$:

$$\sigma_\nu^c(\mu^-)/\sigma_\nu(\mu^-) = (B_h/B_\mu)\sigma_\nu(\mu^-\mu^+)/\sigma_\nu(\mu^-) \simeq (4 \text{ to } 13)\ \% \qquad (5.1)$$

for $B_\mu \simeq (16 \text{ to } 7)$ % where B_h is the non-leptonic branching ratio. Recalling that the uncertainty in the presumed value of B_μ is correlated with the uncertainty in :

$$\sigma_{\bar{\nu}}(\mu^+\mu^-)/\sigma_\nu(\mu^-\mu^+) \simeq (1/5 \text{ to } 2/3)$$

and that :

$$\sigma_{\bar{\nu}}^{TOT}/\sigma_\nu^{TOT} \simeq 1/3$$

we find accordingly :

$$\sigma_{\bar{\nu}}^c(\mu^+)/\sigma_{\bar{\nu}}^c(\mu^+) \simeq (2.5\text{-}25)\ \% \qquad (5.2)$$

For ν-production, the charm contribution will not give distributions

which are strikingly different from the dominant contribution, except for a possible enhancement at small x if the sea contribution is important.

Note that the sea contribution to Eq. (5.1) is $\lesssim$ 8 % of σ_{ν}^{TOT} ; however the small x enhancement could be increased by a threshold distortion of the valence contribution, giving still $\lesssim$ 13 %. In the y distributions no significant effect is expected.

Effects of charm production by anti-neutrinos can be much more dramatic ; what we expect is a flattening of the y-distribution at low x, and this indeed is what is observed in the data presented here [39], [40]. Rather than show you data curves which you have seen already, let me as an example, assume a simple parton picture for the estimation of the parameter :

$$B = \frac{q-\bar{q}}{q+\bar{q}} \tag{5.3}$$

which is used by the experimenters in interpreting their data. Specifically we assume :

a) (30 ± 3) % of the u+d distribution lies below x = 0.15 (recall that $\langle x \rangle \simeq 0.2$ for ν-production).

b) The $\bar{u}+\bar{d}$ content is $(\bar{u}+\bar{d})/(u+d) = (10\pm1)$ %, and lies entirely below x = 0.15.

c) For charm production we take two simple hypotheses consistent with the dilepton data (see Eqs. (4.6) and (4.7)).

i. $(r_s, B_h) = (0.1, 0.86)$, and

ii. $(r_s, B_h) = (0.005, 0.80)$

Since the antineutrino sees only the $\bar{s}$-quark, while the neutrino sees the s-quark, the effective values of B above charm threshold will be different (unless the charm sea is as important as the strange sea). Specifically we obtain :

$$B^{\nu} = B^{\bar{\nu}} = \begin{cases} 0.80\text{-}0.83 & \text{(all x)} \\ 0.42\text{-}0.57 & (x \lesssim 0.15) \end{cases}$$

below charm threshold, and :

	(i)	(ii)	
B^{ν} =	0.82-0.85	0.81-0.84	(all x)
	0.64-0.53	0.61-0.48	($x \lesssim 0.15$)
$B^{\bar{\nu}}$ =	0.67-0.70	0.74-0.70	(all x)
	0.16-0.30	0.29-0.43	($x \lesssim 0.15$)

above charm threshold. As threshold effects raise the average value of y, their effect is to raise B^{ν} and lower $B^{\bar{\nu}}$; inclusion of a charm sea has the opposite effect.

The above estimates for B appear compatible with the data presented by Diamond [39], but are perhaps harder to reconcile with that presented by Rubbia [40]. Aside from threshold effects we have ignored all possible scaling violations. We heard from Parisi [41] the type of effect expected in an asymptotically free theory. I would like to mention one other effect which might be important for relatively low momentum transfer : $Q^2 \lesssim 10$ GeV , namely the diffractive process depicted in Figure 12.

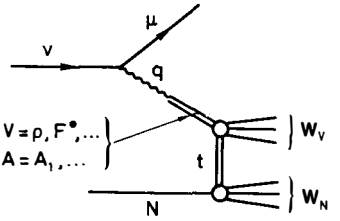

FIG. 12 : Diffractive mechanism for neutrino scattering.

The point is that no one has considered applying the parton model to ordinary hadron production for $Q^2 \lesssim 1$ GeV where the ρ contribution is important. More generally, the contribution from any vector (or axial) meson exchange peaks broadly at $Q^2 = m_V^2$ and falls off for $Q^2 \gtrsim 2\, m_V^2$. For an F^* of mass about 2 GeV, this corresponds to rather high values of Q^2. The differential cross section corresponding to the contribution of a given vector meson is of the form [42] :

$$\frac{d\sigma^{diffr.}}{dt\, dx\, dy} \sim \frac{x(1-x)}{(Q^2 + m_V^2)^2}\; y \left\{ y^2 \frac{d\sigma_T}{dt} + \left(\frac{d\sigma_T}{dt} + \frac{d\sigma_L}{dt} \right) \left(\frac{1-y-m_\mu xy/2E_\nu}{1+2m_\mu x/2E_\nu y} \right) \right\} \qquad (5.4)$$

where σ_T (σ_L) is the cross section for scattering of a transversely (longitudinally) polarized vector meson from a nucleon. This expression does not have the simple x, y dependence characteristic of the parton model. For high energies where Pomeron exchange at the hadronic vertex is expected to be dominant, one expects the V-N cross section to peak at low t :

$$\sigma_{T,L} \sim e^{bt}$$

Through kinematics [43] this is reflected by a distortion of the x, y distribution toward the high y, low x region ; the expected x and y distributions [21] are shown in Figure 13.

FIG. 13 : (x, y) distribution for diffractive production of charmed particles [21].

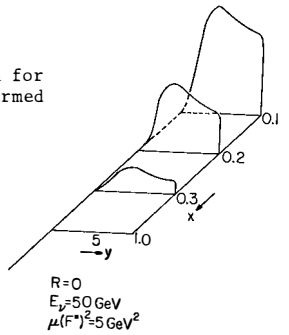

The qualitative features of the diffractive contributions are in many ways characteristic of the parton "sea" contributions :

a) Neglecting V,A interference, they contribute equally to ν and $\bar{\nu}$ scattering and therefore are relatively enhanced by a factor of about 3 in $\bar{\nu}$ interactions.

b) They are important in the low x, high y region. Since in practice the "sea" is observed as a flattening of the $(1-y)^2$ distribution as $y \to 1$ in the low x region of $\bar{\nu}$-scattering :

$$d\sigma^{\bar{\nu}}(x, y) \neq 0 \quad \text{for} \quad y \to 1 \quad \text{if} \quad x \lesssim 0.1$$

the effect is similar to that of a vector meson contribution if Q^2 is in the appropriate range. The difference with the "sea" contribution is that the diagrams of Figure 12 do not scale : as E_ν increases Q^2 increases for fixed x, y, and the effect will disappear unless higher mass resonances become important.

It may be that the transition from the "diffractive" region, $Q^2 \lesssim m_v^2$, to the "scaling" region, $Q^2 \gg m_v^2$, is so smooth that they need not [44] be considered as separate phenomena (indeed we do not advocate adding the two contributions), but this is not necessarily the case. A detailed study of expected distributions, taking into account the experimental energy spectra, would be a useful complement to the expected scaling distributions already in the literature.

The total expected contribution to charm production from diffractive F^* scattering can be fairly reliably estimated. The necessary parameters are the strength of the F^* coupling to the $\Delta S = \Delta C = \pm 1$ hadronic current and the total F^*N scattering cross section. The analogous parameters are known for ρ, ω, ϕ and the J/ψ (we assume $J/\psi = \{(\bar{c}c), 1^-\}$), from e^+e^- annihilation and photoproduction data ; the F^* parameters may be estimated from these using the additive quark model and mass interpolations where necessary. The relative contribution of elastic F^* production ($F^*N \to F^*N$) is shown* in Figure 14 as a function of energy. This is related to the total production cross section by the optical theorem :

$$\frac{\sigma^{e\ell}}{\sigma_{TOT}} \simeq \frac{\sigma_{TOT}}{16\pi b} \simeq 2.5 \, \frac{\sigma_{TOT}(mb)}{16\pi b(GeV^{-2})} \sim 0.07$$

if $\sigma_{TOT}(F^*N) = 5.5$ mb (additive quark model) and $b_{F^*} \simeq 4\ GeV^{-2}$ (from photoproduction data [45] $b_\rho \simeq 8\ GeV^{-1}$, $b_{J/\psi} \simeq 2\ GeV^{-1}$). Then from the curve of Figure 14 we expect a total contribution from F^* production of charm of about 7 % in neutrino interactions and 20 % for antineutrinos, for neutrino energies above 10 GeV.

6 : DILEPTON SIGNATURES NEAR CHARM THRESHOLD :

The last topic I wish to discuss concerns the anticipated characteristics of charm production for energies not far above charm threshold, which are relevant to the dilepton signals observed at Gargamelle [46] and in other CERN PS [47] and Brookhaven experiments [48].

---

* We saw in the talk by Williams (this volume) that the analogous case of elastic leptoproduction of the ρ is in agreement with theoretical predictions based on vector meson dominance.

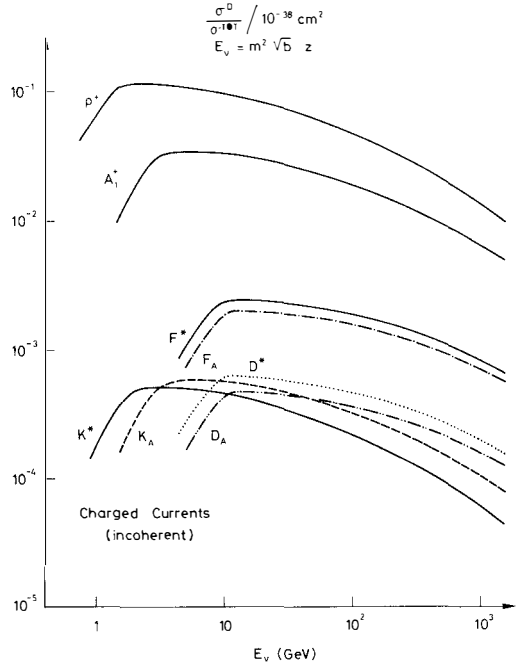

FIG. 14 : Relative ν cross sections for elastic diffractive production of vector mesons. The contribution to the total diffractive cross section for each vector meson is given by :

$$\sigma_{TOT}^{diffr.}/\sigma_{e\ell}^{diffr.} \simeq 0.4\ \pi b m b\ GeV^2/\sigma_{TOT} \quad (VN)$$

(Gaillard et al. [42]).

Provided the charmed baryons are not excessively heavy as compared with charmed mesons, one expects that at low energies the dominant charm changing process should be elastic baryon production. This involves the conversion of one valence quark in the target nucleon into a charmed quark. Thus the allowed processes are :

$$\nu + n(ddu) \rightarrow \mu^- + C^+(cdu) \qquad (6.1)$$

$$\nu + p(uud) \rightarrow \mu^- + C^{++}(cuu) \qquad (6.2)$$

The state $C^+ = (cdu)$ may be in an isotopic spin configuration I = 0 or 1. The mass splitting is related by SU(4) to the $\Sigma(I = 1) - \Lambda(I = 0)$ mass splitting, and one expects [1], in complete analogy to the Σ-Λ case :

$$m_{C_1} > m_{C_0} \tag{6.3}$$

For equal baryon masses the production of the I = 0, $1/2^+$ state C_0^+ is favoured; the production ratios are roughly [49] :

$$C_0^+ \; : \; C_1^+ \; : \; C_1^{+*} \; : \; C_1^{++*} \simeq 1 \; : \; 0.2 \; : \; 0.4 \; : \; 0.35 \; : \; 0.7 \tag{6.4}$$

where 0, 1 is the total isospin and the asterisk denotes a $3/2^+$ state. Moreover, as the C_0^+ is expected to be the lightest state, this will further enhance its relative production rate near threshold. Semi-leptonic decays with $\Delta S = \Delta C = \pm 1$ satisfy the isospin selection rule $\Delta I = 0$, so the decay of the C_0^+ must be to an I = 0 hadronic state :

$$C_0^+ \to \ell^+ \nu + \begin{cases} \Lambda^\circ \\ Y_1^\circ \to \Sigma\pi \\ \vdots \end{cases} \tag{6.5}$$

The lowest available state is significantly favored by phase space which has an $(m_{C_0} - m_Y)^5$ dependence ; for $m_{C_0} \simeq 2.5$ GeV we find :

$$(m_C - m_\Lambda)^5 / (m_C - m_{Y_1^\circ})^5 \simeq 3 \tag{6.6}$$

There is no reliable way to estimate the Y_1° coupling, but in the static SU(8) (= spin and SU(4)) limit, all couplings vanish for transitions to states other than the ground state $1/2^+$ and $3/2^+$ baryons. As the Λ° is the only I = 0 member of the 56-plet, a preponderance of Λ°'s in the final state for charm production near threshold would not be surprising. On the other hand, the $(\Delta m)^5$ phase space factor enhances the otherwise Cabibbo suppressed $\Delta S = 0$ decay ; one estimates [50] (see Figure 15) :

$$\Gamma(C_0^+ \to n\ell\nu) / \Gamma(C_0^+ \to \Lambda\ell\nu) \simeq 1/4 \tag{6.7}$$

Since in the present instance there is some reason to believe that the decay $C^+ \to \Lambda$ eν may be dominant, invariant mass distributions for the Λe system may be more relevant than those for the high energy μ e K_s data discus-

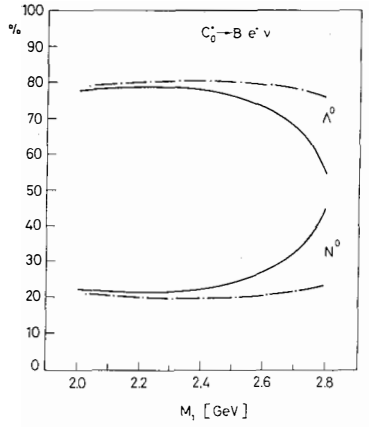

FIG. 15 : The branching ratios [50] (%) as functions of the masses M_1 of the decaying charmed baryon for two values of (m_{F^*}, m_{D^*}) : (2.05 GeV, 2 GeV) solid line and (2.3 GeV, 2.25 GeV) dashed line for $C_0^+ \to Be^+\nu$ (N° is the neutron).

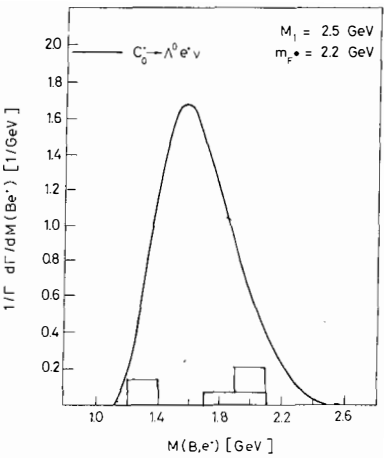

FIG. 16 : The normalized mass distribution [50] $1/\Gamma(d\Gamma/dM(Be^+))$ at fixed M_1 = 2.5 GeV and m_{F^*} = 2.2 GeV for the reaction $C_0^+ \to \Lambda^0 e^+ \nu$. The "$\Lambda^0$"$e^+$ invariant masses for the Gargamelle events are also indicated.

sed above. In Figure 16, we show the expected mass distribution [50] for a parent mass of 2.5 GeV, where a dipole form factor with m_{F^*} = 2.2 GeV has been assumed.

The invariant masses of the Gargamelle events [46], determined under the assumption that the observed V° is a Λ^0, are also indicated in Figure 17. Their average value :

$$< m_{\Lambda e} > \simeq 1.7$$

Suggests a parent mass :

$$m_{C_0^+} \simeq 2.35 \text{ GeV} \qquad (6.8)$$

REFERENCES :

[1] For the anticipated properties of charmed hadrons see M.K. GAILLARD, B.W. LEE and J.L. ROSNER, Rev. Mod. Physics 47, 277 (1975).

[2] S.L. GLASHOW, J. ILIOPOULOS and L. MAIANI, Phys. Rev. D2, 1285 (1970).

[3] Y. HARA, Phys. Rev. 134, B701 (1964).
D. AMATI, H. BACRY, J. NUYTS and J. PRENTKI, Phys. Letters 11, 190 (1964).
B.J. BJØRKEN and S.L. GLASHOW, Phys. Letters 11, 255 (1964).
Z. MAKI and Y. OHNUKI, Progr. Theor. Phys. (Kyoto) 32, 144 (1964).

[4] J. STEINBERGER, Phys. Rev. 76, 1180 (1949).
J.S. BELL and R. JACKIW, Nuovo Cimento 51, 47 (1969).
S.L. ADLER, Phys. Rev. 177, 2426 (1969).
C. BOUCHIAT, J. ILIOPOULOS and Ph. MEYER, Phys. Letters 38B, 519 (1972).

[5] S. WEINBERG, Phys. Rev. Letters 19, 1264 (1967).
A. SALAM, Proceedings of the 8th Nobel Symposium, Stockholm 1968, ed. by N. Svartholm, p. 367 (ALMQUIST and WIKSELLS, Stockholm, 1968).

[6] See the lectures by O. NACHTMANN in this volume.

[7] See the lectures by F. HAYOT, K. KANG and R. KINGSLEY in this volume.

[8] O.W. GREENBERG, Phys. Rev. Letters 13, 598 (1964).
M. GELL-MANN, public communication.

[9] S. ADLER [4], appendix, and published or unpublished remarks by many people.

[10] S. WEINBERG, Phys. Rev. D8, 605 (1973) and Rev. Mod. Phys. 46, 255 (1974).
D.V. NANOPOULOS, Nuovo Cimento Letters 8, 873 (1973).

[11] G. 't HOOFT, unpublished.
D. GROSS and F. WILCZECK, Phys. Rev. D8, 3633 (1973).
H.D. POLITZER, Phys. Rev. Letters 30, 1346 (1973).
M. GELL-MANN and H. LEUTWYLER, Caltech preprint CALT-68-409 (1973).

[12] H.I. VAINSHTEIN and I.B. KHRIPLOVECH, Zh. Eksp. Teor. Fiz., Pes'ma Red. 18, 141 (1973).
E. MA, Phys. Rev. D9, 3103 (1974).
M.K. GAILLARD and B.W. LEE, Phys. Rev. D10, 897 (1974).
V.V. FLAMBAUM, Novosibirsk preprint 75-24 (1975).

[13] See lecture by A. GIAZOTTO in this volume.

[14] See lecture by D.V. NANOPOULOS in this volume.

[15] D.V. NANOPOULOS and G.G. ROSS, Phys. Letters 56B, 279 (1975).
E.B. BOGOMOLNY, V.A. NOVIKOV and M.A. SHIFMAN, Moscow preprint ITEP-42 (1975).
A.I. VAINSHTEIN, V.I. ZAKHAROV, V.A. NOVIKOV and M.A. SHIFMAN, Phys. Letters, 60B, 71 (1975).
M.K. GAILLARD, B.W. LEE and R.E. SHROCK, CERN preprint TH-2066 (1975).

[16] J.J. AUBERT et al., Phys. Rev. Letters 33, 1404 (1974).
J.-E. AUGUSTIN et al., Phys. Rev. Letters 33, 1406 (1974).
G.S. ABRAMS et al., Phys. Rev. Letters 33, 1453 (1974).

[17] Gargamelle Collaboration : see D.C. CUNDY, Proc. XVII Int'l Conf. on High Energy Physics, p. IV-131 (London, 1974).

[18] For a review, see : C.H. LLEWELLYN SMITH, Phys. Reports 3C, 261 (1972).

[19] G. MILLER et al., Phys. Rev. D5, 528 (1972).
J.S. POUCHER et al., Phys. Rev. Letters 32, 118 (1974).

[20] A. De RUJULA, H. GEORGI, S.L. GLASHOW and H.R. QUINN, Revs. Modern Phys. 46, 391 (1974).
G. ALTARELLI, N. CABIBBO and L. MAIANI, Phys. Letters 48B, 435 (1974).

.../...

M.K. GAILLARD, B.W. LEE and J.L. ROSNER, ref. [1].
V. BARGER, T. WEILER and R.J.N. PHILLIPS, "Charm production by partons in neutrino scattering", University of Wisconsin-Madison report COO-441 (1975).

[21] B.W. LEE, "Dimuon events", Fermilab-Conf-75/78-THY (1975).

[22] H. GEORGI and H.D. POLITZER, "Freedom at moderate energies : masses in color dynamics", Harvard preprint, January 1976.

[23] R.M. BARNETT, "Evidence in neutrino scattering for right-handed currents associated with heavy quarks", Harvard preprint, January 1976.

[24] E. DERMIN, "Dimuon distributions due to deep inelastic neutrino production of new hadrons", Oxford preprint (1976).

[25] M.K. GAILLARD and B.W. LEE, Phys. Rev. Letters 33, 108 (1974).
G. ALTARELLI and L. MAIANI, Phys. Letters 52, 351 (1974).

[26] J. ELLIS, M.K. GAILLARD and D.V. NANOPOULOS, Nuclear Phys. B100, 313 (1975).

[27] A. BENVENUTI et al., Phys. Rev. Letters 34, 419 (1975) ; ibid 35, 1199, 1203 and 1249 (1975).

[28] B.C. BARISH, Proc. la physique du neutrino à haute énergie, 18-20 March 1975, Ecole Polytechnique, Paris. (Cal-Tech-Fermilab Collaboration).

[29] See lecture by D. CUNDY in this volume.

[30] A. PAIS and S.B. TREIMAN, Phys. Rev. Letters 35, 1206 (1975).

[31] V. BARGER, R.J.N. PHILLIPS and T. WEILER, "Dimuon production by neutrinos : test of weak current models", SLAC-PUB-1688 (1976).

[32] L.M. SEHGAL and P.M. ZERWAS, Phys. Rev. Letters 36, 399 (1976).

[33] R.L. KINGSLEY, S.B. TREIMAN, F. WILCZECK and A. ZEE, Phys. Rev. D11, 1919 (1975).

[34] J. ELLIS, M.K. GAILLARD and D.V. NANOPOULOS, Ref. TH.2116-CERN (1976), to be published in Nuclear Physics.

[35] M. BOURQUIN and J.-M. GAILLARD, "A simple Phenomenological Description of Hadron Production", CERN preprint, submitted to Nucl. Phys. and private communication.

[36] V. BARGER and R.J.N. PHILLIPS, "Weak Semi-Leptonic Decay Distributions for New Particles", Wisconsin preprint COO-504 (1976).

[37] A. BURAS, private communication. We thank him for providing us with the distribution of Fig. 11.

[38] I. HINCHLIFF and C.H. LLEWELLYN SMITH, "Can Charm Account for Prompt Lepton Production ?". Oxford preprint Ref. 9/76 (1976).

[39] See lecture by R. DIAMOND in this volume.

[40] See lecture by C. RUBBIA in this volume.

[41] See lecture by G. PARISI in this volume.

[42] C.-A. PIKETTY and L. STODOLSKY, Nuclear Phys. B15, 571 (1970).
T. INAMI, Phys. Letters 56B, 291 (1975).
B.A. ARBUZOV, S.S. GERSHTEIN and V.N. FOLOMESHKIN, preprint IHEP 75-11 Serpukhov (1975).
B.A. ARBUZOV, SS. GERSHTEIN, V.V. LAPIN and V.N. FOLOMESHKIN, preprint IHEP 75-25, Serpukhov (1975).
J. PUMPLIN and W. REPKO, Phys. Rev. D12, 1376 (1975).
V. BARGER, T. WEILER and R.J.N. PHILLIPS, "Vector meson dominance calculations for the $\bar{\nu}$ anomaly and dimuon production", Wisconsin preprint COO-456 (1975) ; and Phys. Rev. (to be published).
M.K. GAILLARD, S.A. JACKSON and D.V. NANOPOULOS, Nuclear Phys. B102, 326 (1976).
M.B. EINHORN and B.W. LEE, "Contributions of vector-meson dominance to charmed meson production in inelastic neutrino and antineutrino interactions", FERMILAB-PUB-75/76-THY (1975).

[43] For a quantitative discussion of t_{min} effects, see the Schladming lectures (1976) by the present author.

[44] B.W. LEE, private remarks.

[45] K. BERKELMAN, Proc. 1971 Int'l Symp. on electron and photon interactions at high energies, Cornell University, Ithaca, Ed. N.B. Misty, p. 263 (1971).
B. KNAPP et al., Phys. Rev. Letters 34, 1040 (1975).

[46] See lecture by M. JAFFRE in this volume.

[47] H. FAISSNER, Schladming lectures (1976).

[48] See lecture by D. GOULIANOS in this volume.

[49] R.E. SHROCK and B.W. LEE, Fermilab-PUB-75/80-THY (1975) ; see also J. FINJORD and F. RAVNDAL, Phys. Letters 56B, 61 (1975).

[50] A.J. BURAS, CERN preprint TH.2142-CERN (1976).

HOW TO INVESTIGATE FUTURE ENERGY DOMAINS OF PARTICLE PHYSICS WITH PRESENT ACCELERATORS ?

Y. AFEK, G. BERLAD and G. EILAM

Department of Physics
Technion-Israel Institute of Technology, Haifa, Israel

A. DAR*

Laboratoire de Physique Théorique et Particules Elémentaires
Université de Paris-Sud, 91405 Orsay, FRANCE

Abstract : We summarize evidence which indicates that high energy collisions between particles and nuclei and between heavy ions and target nuclei can be used to investigate future energy domains of particle physics with present accelerators.

* On sabatical leave from the Technion-Israel Institute of Technology, Haifa, Israel.

INTRODUCTION.

When a high energy particle with laboratory momentum p_{lab} collides with a target nucleon at rest, the center of mass energy squared is given approximately by :

$$s \overset{\sim}{=} 2mp_{lab} \tag{1}$$

where m is the nucleon mass. When the target particle is a nucleus of atomic weight A the center of mass energy squared for coherent reactions is A times larger :

$$s_A \overset{\sim}{=} 2mAp_{lab} \overset{\sim}{=} As \tag{2}$$

What is the center of mass energy squared for incoherent reactions in :

a) particle-nucleus collisions at high energies ?

b) nucleus-nucleus collisions at high energies ?

Below we will show evidence that for particle-nucleus collisions at high energies the average center of mass energy squared available for the production of particles is approximately given by :

$$s_{eff} \overset{\sim}{=} A^{1/3}\, s \tag{3}$$

while for high energy nucleus-nucleus collisions it is approximately given by :

$$s_{eff} \overset{\sim}{=} A_1^{1/3}\, A_2^{1/3}\, s \tag{4}$$

where A_1 and A_2 are the atomic weights of the colliding nuclei.

In order to extract this evidence from present available experimental data on high energy particle-nucleus collisions, let us consider the following "coherent Tube Model" for high energy particle nucleus collisions [1] :

THE COHERENT TUBE MODEL [1].

The model is based on two simple assumptions :

- ASSUMPTION (1) :

The interaction of a high energy particle with a target nucleus results from its simultaneous collision with all the nucleons that lie within a tube of cross section σ along its path in the target nucleus. In particular, if there are i nucleons within this tube then the center of mass energy squared for the particle-tube collision is given by :

$$s_i \tilde{=} 2 imp_{lab} \tilde{=} i\ s$$

Assumption (1) can be tested for instance by looking for the production of heavy particles in particle-nucleus collisions at incident energies well below the threshold for their production in particle-nucleon collisions. However, in order to increase the predictive power of assumption (1) we will introduce a second assumption.

- ASSUMPTION (2) :

In the center of mass systems, the particle-tube collision resembles a particle-nucleon collision at the same center of mass energy. (Assumption (2) is motivated by the observation that various quantities which characterize multi-particle production, like the average charge multiplicity, the multiplicity distribution, and the particle spectra and their momentum distributions, are independent of the quantum members of the colliding particles).

Assumptions (1) and (2) can be used to calculate particle-nucleus collisions directly from particle-particle collisions provided one knows the probability p(i, A) that the incident particle encounters exactly i nucleons in an inelastic particle-nucleus collisions. However, p(i, A) can be easily calculated from low energy nuclear models. For instance, from an independent particle model for the target nucleus one obtains :

$$p(i, A) = \frac{\int d^2b \binom{A}{i} \left(\frac{\sigma T}{A}\right)^i \left(1 - \frac{\sigma T}{A}\right)^{A-i}}{\sigma_{in}^{pA}} \qquad (5)$$

where the total inelastic particle-nucleus cross section is approximately given by :

$$\sigma_{in}^{pA} = \int d^2b \left[1 - \left(1 - \frac{\sigma T}{A}\right)^A\right] \qquad (6)$$

T(b) is the nuclear thickness at impact parameter b and is given by :

$$T(b) = \int_{-\infty}^{\infty} dz\ \rho(b, z) \qquad (7)$$

where ρ is the nuclear density function normalized such that $\int \rho(r) d^3r = A$. σ is the total inelastic particle-nucleon cross section.

SUMMARY OF RESULTS.

With the aid of assumptions (1) and (2) one can easily derive the following results :

a) Inclusive cross sections for p + A → c + anything [1-b] :

$$E \frac{d^3\sigma_c^{pA}}{dp^3}(s, E + p_{\parallel}, p_{\perp}) = \frac{\sigma_{in}^{pA}}{\sigma_{in}^{pp}} \sum_{i=1}^{A} p(i, A)\, E \frac{d^3\sigma_c^{pp}}{dp^3} \left(is, i^{1/2}(E + p_{\parallel}), p_{\perp}\right) \qquad (8)$$

where E is the energy of particle c and p is its momentum in the lab system with longitudinal and transverse components, $p_{\parallel}$ and $p_{\perp}$, respectively. For large values of $p_{\perp}$, inclusive cross sections in pp collisions were found [2] to depend only on $p_{\perp}$ and s. Moreover, we have found that expressions like expression (8) are not sensitive to the specific choice of a nuclear model for calculating p(i, A), and that the average over the different tubes can be well approximated by an average tube of thickness $A^{1/3}$ nucleons. Consequently eq. (8) reduces to the simple scaling law :

$$\frac{\sigma_{in}^{pp}}{\sigma_{in}^{pA}} E \frac{d^3\sigma_c^{pA}}{dp^3}(s, p_{\perp}) \simeq E \frac{d^3\sigma_c^{pp}}{dp^3}(s_{eff}, p_{\perp}) \qquad (9)$$

where s_{eff} is given by expression (3). In Figs. (1)-(5), the scaling law (9) is compared with experimental data on inclusive production of $\pi^{\pm}$, $K^{\pm}$, $\bar{p}$ and p at high energies from p, W and Ti targets [2]. Good agreement between theory and experiment is obtained.

Eq. (8) can be written in terms of the laboratory rapidity variable y as :

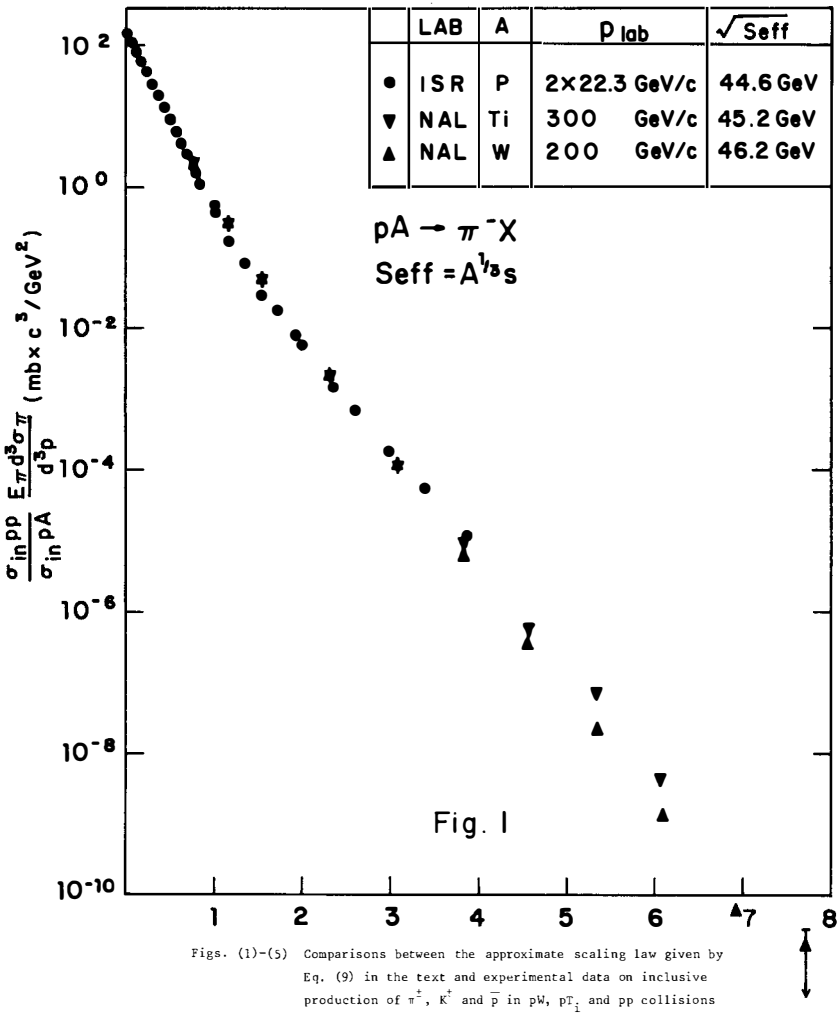

Figs. (1)-(5) Comparisons between the approximate scaling law given by Eq. (9) in the text and experimental data on inclusive production of $\pi^{\pm}$, K^{+} and $\bar{p}$ in pW, pT_i and pp collisions at respectively, $\sqrt{s}$ = 19.4, 22.8 and 44.6 GeV. According to the approximate scaling law all these data should be on the same line since they all have about the same $s_{eff} = A^{1/3} s$.

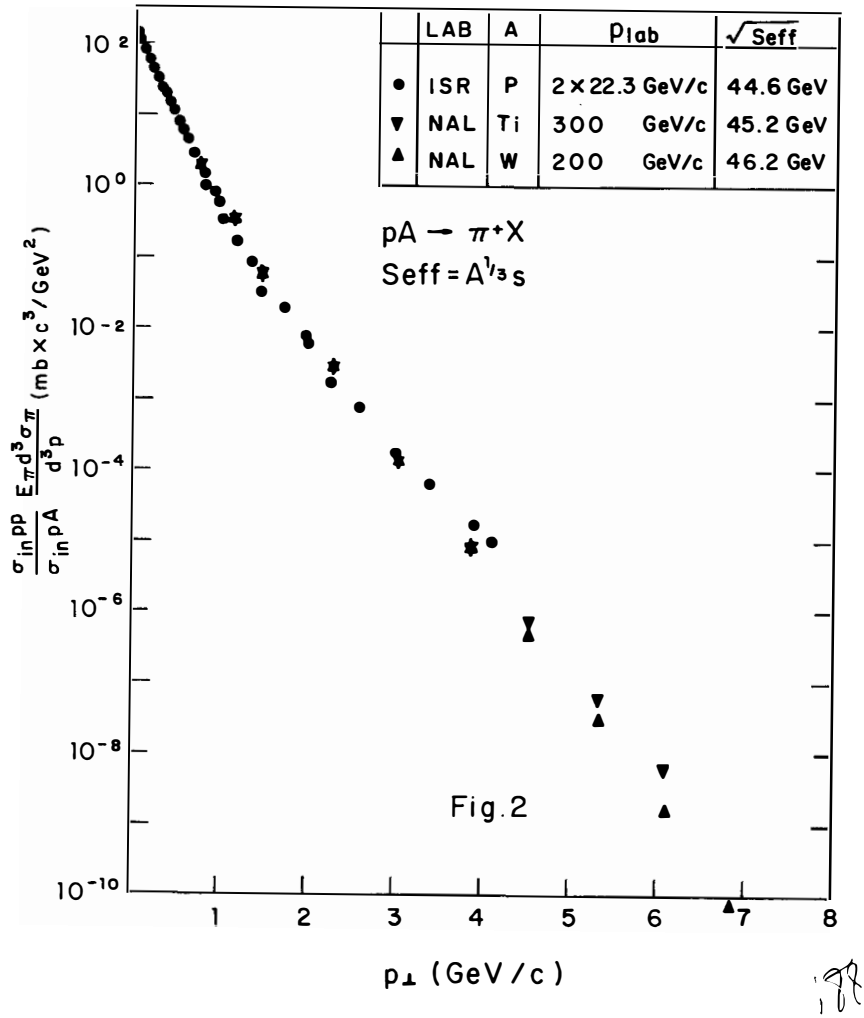
LAB | A | Plab | √Seff
● ISR | P | 2×22.3 GeV/c | 44.6 GeV
▼ NAL | Ti | 300 GeV/c | 45.2 GeV
▲ NAL | W | 200 GeV/c | 46.2 GeV
pA → π+X
Seff = A^1/3 s
Fig.2
$\frac{\sigma_{in}^{pp}}{\sigma_{in}^{pA}} \frac{E_\pi d^3\sigma_\pi}{d^3p}$ (mb×c³/GeV²)
p⊥ (GeV/c)

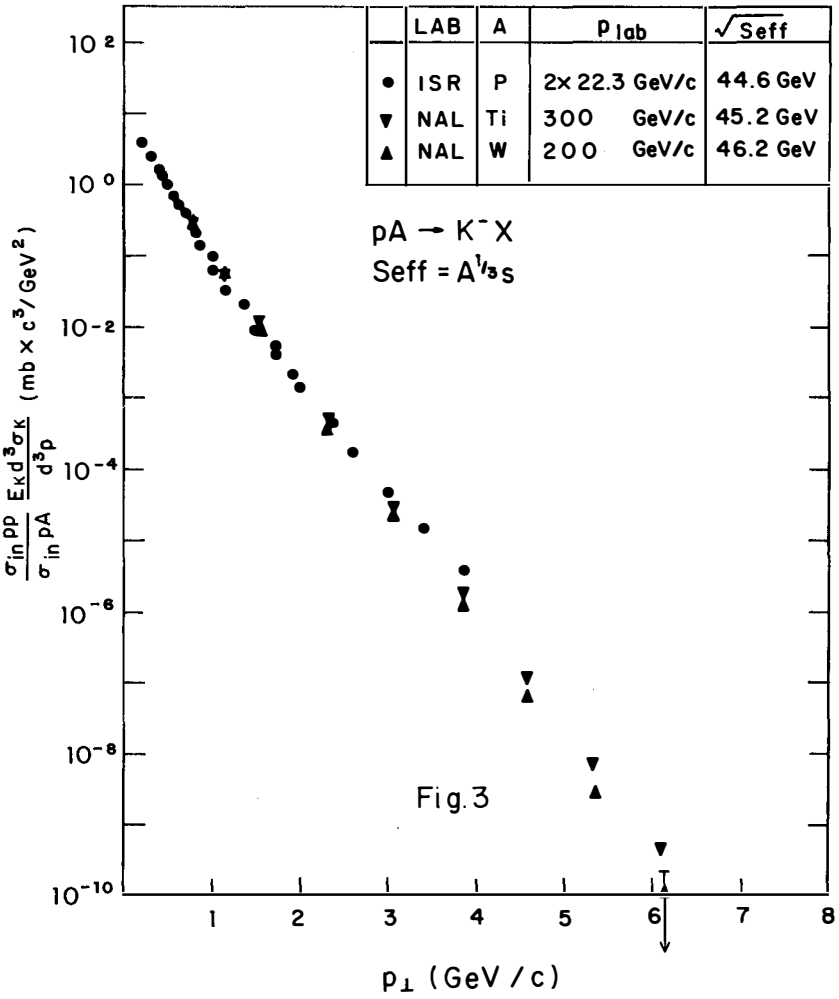
LAB
A
p lab
√Seff
ISR
P
2x 22.3 GeV/c
44.6 GeV
NAL
Ti
300 GeV/c
45.2 GeV
NAL
W
200 GeV/c
46.2 GeV
pA → K⁻X
Seff = A^1/3 s
Fig. 3
10 2
10 0
10-2
10-4
10-6
10-8
10-10
1
2
3
4
5
6
7
8
p⊥ (GeV / c)
σin pp / σin pA Ek d3σk / d3p (mb × c3/ GeV2)

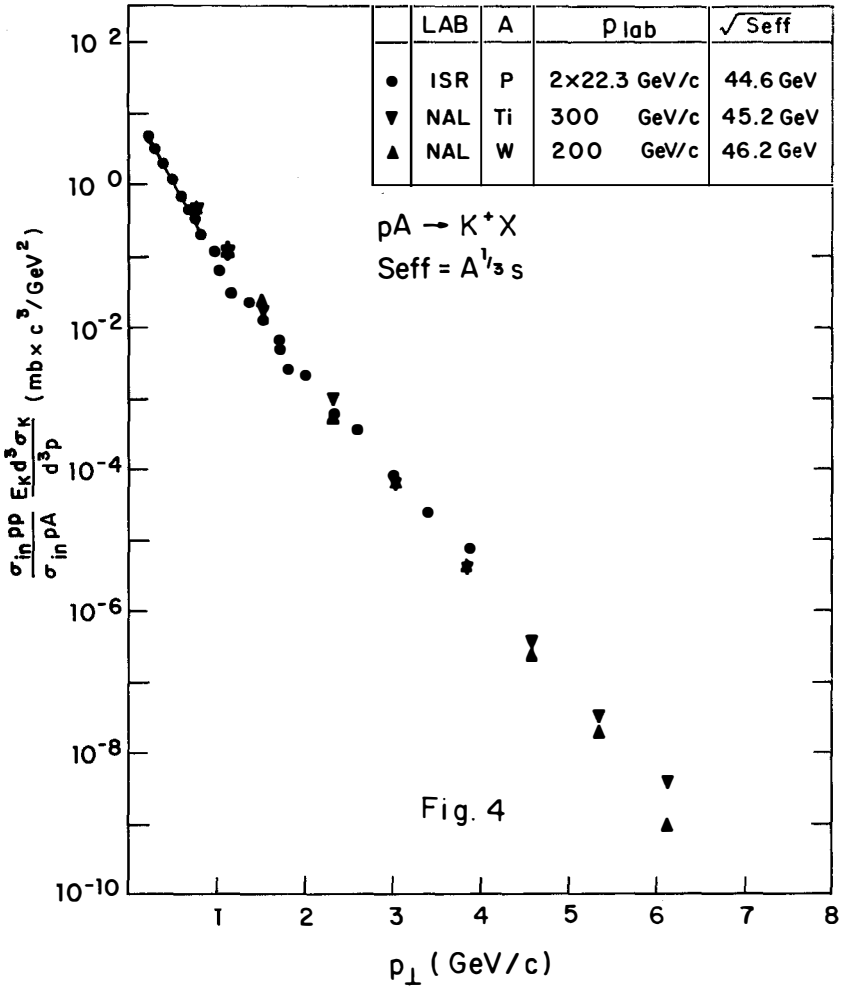
LAB
A
p lab
√Seff
ISR
P
2×22.3 GeV/c
44.6 GeV
NAL
Ti
300 GeV/c
45.2 GeV
NAL
W
200 GeV/c
46.2 GeV
pA → K⁺X
Seff = A^1/3 s
Fig. 4
$\frac{\sigma_{in}pp}{\sigma_{in}pA}\frac{E_K d^3\sigma_K}{d^3p}$ (mb × c³/GeV²)
p⊥ (GeV/c)

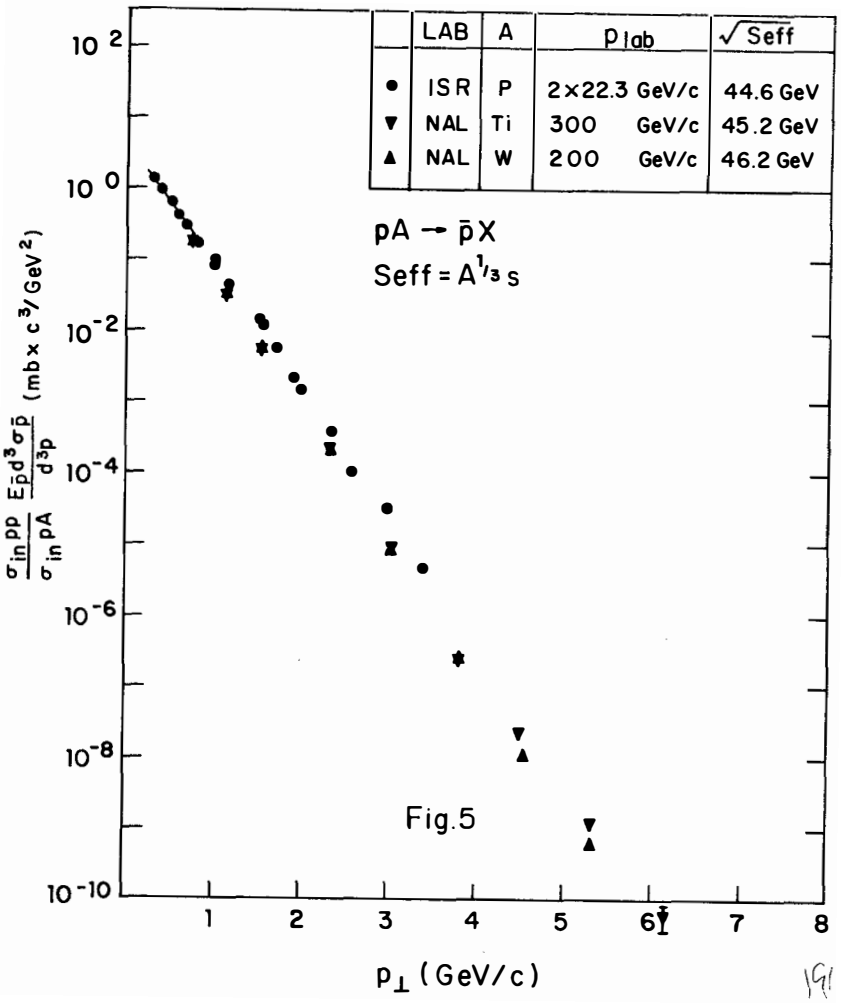
LAB
A
p lab
√Seff
ISR
P
2×22.3 GeV/c
44.6 GeV
NAL
Ti
300 GeV/c
45.2 GeV
NAL
W
200 GeV/c
46.2 GeV
pA → p̄X
Seff = A^1/3 s
Fig.5
$\frac{\sigma_{in\,pp}}{\sigma_{in\,pA}} \frac{E\bar{p}d^3\sigma\bar{p}}{d^3p}$ (mb x c³/GeV²)
p⊥ (GeV/c)
10 2
10 0
10-2
10-4
10-6
10-8
10-10
1
2
3
4
5
6
7
8

$$\frac{1}{\sigma_{in}^{pA}} \frac{d^3\sigma_c^{pA}}{d^2p_\perp dy}(s, y, p_\perp) = \frac{1}{\sigma_{in}^{pp}} \sum_{i=1}^{A} p(i, A) \frac{d^3\sigma_c^{pp}}{d^2p_\perp dy}(is, y + \frac{1}{2}\ell ni, p_\perp)$$

$$\simeq \frac{1}{\sigma_{in}^{pp}} \frac{d^3\sigma_c^{pp}}{d^2p_\perp dy}(A^{1/3} s, y + \frac{1}{6}\ell nA, p_\perp) \qquad (10)$$

Predictions [1-d] based on expression (10) for rapidity distributions in high energy particle-nucleus collisions are presented in Figs. (6) and (7). These predictions are in agreement with experimental observations [3].

b) Multiplicities [1-a] :

The coherent Tube Model yields the following prediction for the average charge multiplicity in particle-nucleus collisions :

$$\langle n(s)\rangle_A = \sum_{i=1}^{A} p(i, A) \langle n(is)\rangle_p \simeq \langle n(s_{eff})\rangle_p \qquad (11)$$

If one further assumes that the average charge multiplicity in particle-nucleon collision increases with s like a power law :

$$\langle n(s)\rangle_p \simeq \langle n(s_o)\rangle_p (s/s_o)^\alpha \qquad (12)$$

then the multiplicity ratio R_A, given by [1-a] :

$$R_A \equiv \frac{\langle n(s)\rangle_A}{\langle n(s)\rangle_p} = \sum_{i=1}^{A} p(i, A) i^\alpha \equiv \langle i^\alpha\rangle_A \qquad (13)$$

is energy independent. Prediction (13) is compared with experimental data [4] on p-nucleus and π-nucleus collisions in Figure (8). Good agreement between theory and experiment is obtained. For a nucleus of atomic number A and atomic charge z, the average charge multiplicity as function of N_p the number of fastly recoiling protons, is predicted by the model to be given by [1-a] :

$$\langle n(s)\rangle_{N_p} = \sum_{i=0}^{A-z} p(i+N_p, A) \langle n((N_p+i)s)\rangle_p \simeq \langle n(\frac{A}{z} N_p s)\rangle_p \qquad (14)$$

With the aid of assumption (12) the multiplicity ratio R_A as function of N_p is then given by [1-a] :

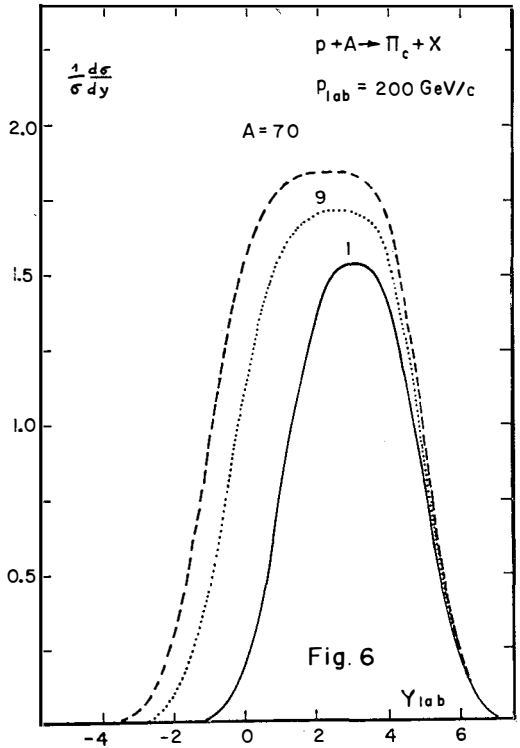

Rapidity distribution of pions produced in p-Be collisions and in p-Emulsion collisions at 200 GeV/c incident proton energy, as predicted by relation (10). The rapidity distributions for π production in high energy pp collisions were taken from ISR data. (Only the data at p_{LAB} = 200 GeV/c is shown here).

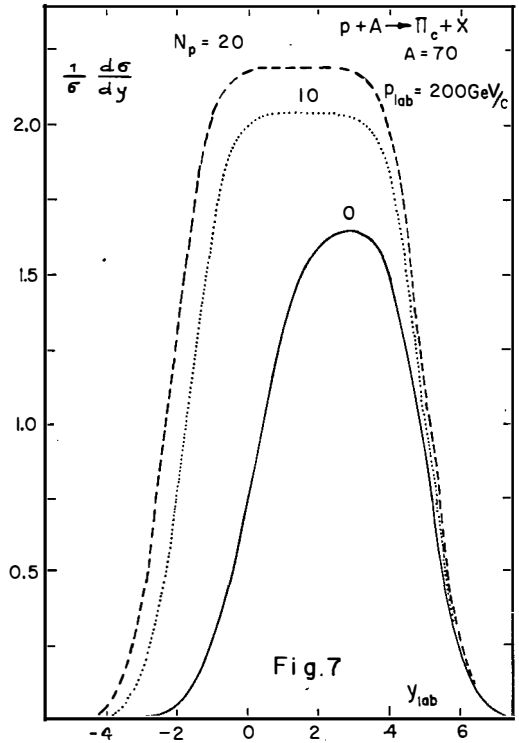

Rapidity distributions of pions produced in p-Emulsion collisions at 200 GeV/c incident proton energy as function of N_h, the number of heavy prongs, as predicted in reference [1-d] by the Coherent Tube Model.

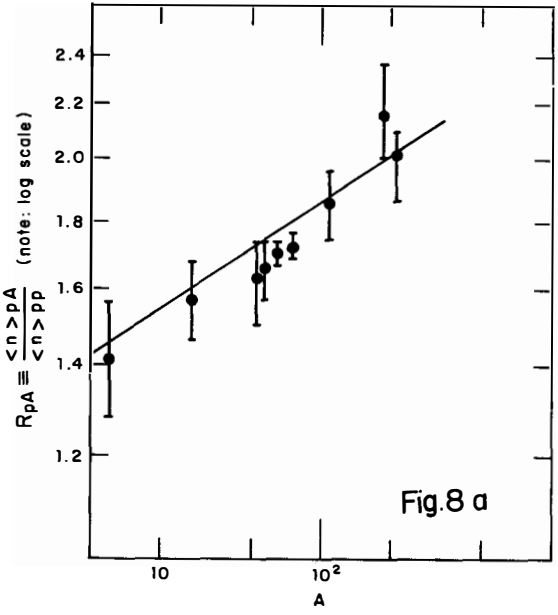

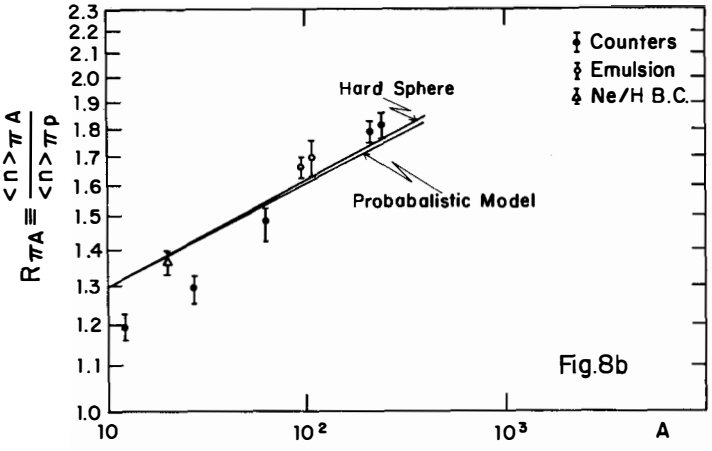

Comparison between experimental data compiled in references [1-a] and [4] on the multiplicity ratio R_A as function of A, and the prediction of the Coherent Tube Model given by eq. (13), for :

a) p-nucleus collisions

b) π-nucleus collisions

at high energies. In the calculation we used the "world average value" α = .285.

$$R_A(N_p) \equiv \frac{\langle n(s)\rangle_{N_p}}{\langle n(s)\rangle_p} \overset{\sim}{=} \left[\frac{A}{z} N_p\right]^{\alpha} \tag{15}$$

In Figures (9)-(10) prediction (15) is compared with experimental data on multiparticle production in π-Ne collisions [5] and in p-emulsion collisions [6] at high energies. Good agreement between theory and experiment is obtained. The multiplicity distribution in particle-nucleus collisions can be expressed in terms of the KNO scaling function [7] for particle-nucleon collisions :

$$\Psi_p(z) \equiv \langle n\rangle_p \frac{\sigma_n^p}{\sigma_{in}^p} , \quad \text{where} \quad z \equiv \frac{n}{\langle n\rangle_p} \tag{16}$$

The model predicts that Ψ_A for particle-nucleus collision is given by [1-a] :

$$\Psi_A(z) \equiv \langle n\rangle_A \frac{\sigma_n^A}{\sigma_{in}^A} = R_A \sum_{i=1}^{A} p(i, A) i^{-\alpha} \Psi_p(i^{-\alpha} R_A z) \overset{\sim}{=} \Psi_p(z) \tag{17}$$

where $z \equiv n/\langle n\rangle_A$ and consequently also :

$$D_A(s) \overset{\sim}{=} D_p(s_{eff}) \tag{18}$$

where :

$$D_i \equiv \sqrt{\langle n^2\rangle_i - \langle n\rangle_i^2} \tag{19}$$

In Figs. (11) and (12) predictions (17) and (18) are compared with experimental data on π-nucleus collisions at high energies [5], [8]. Good agreement between theory and experiment is obtained.

Figures (1) through (12), in our opinion, provide evidence that the average center of mass energy squared available for the production of particles in high energy particle-nucleus collisions is approximately given by $A^{1/3}$ s.

HIGH ENERGY NUCLEUS-NUCLEUS COLLISIONS.

The "coherent Tube Model" can be extended to describe also high energy nucleus-nucleus collisions [1-e]. Such collisions are described in terms of simultaneous collisions of the "nuclear tubes" of one nucleus with the opposing "nuclear tubes" of the second nucleus. These tube-tube collisions are assumed to resemble nucleon-nucleon collisions at the same c.m.

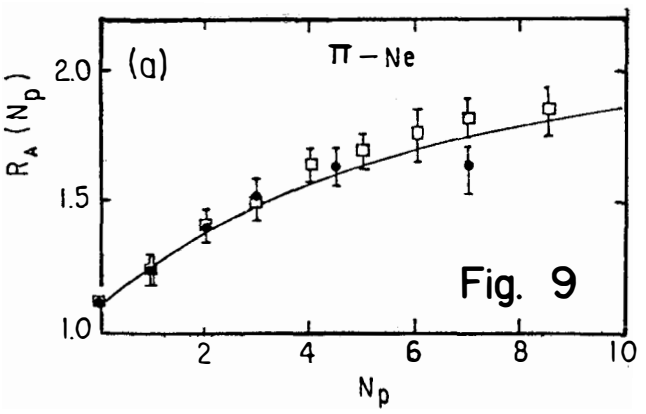

Comparison between experimental data [5] on the multiplicity ratio R_A as function of N_p, and the prediction of the Coherent Tube Model as given by eqs. (14) and (15).

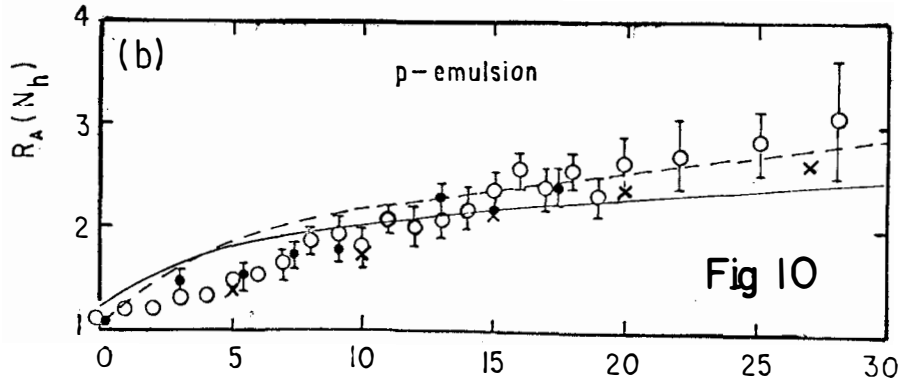

Comparison betwwen experimental data [6] on the multiplicity ratio R_A as function of N_h, the number of heavy prongs in p-Emulsion collisions at high energies, and the prediction of the Coherent Tube Model given by eqs. (14) and (15) and the "world average result" $N_p \cong 1.2\ N_h$.

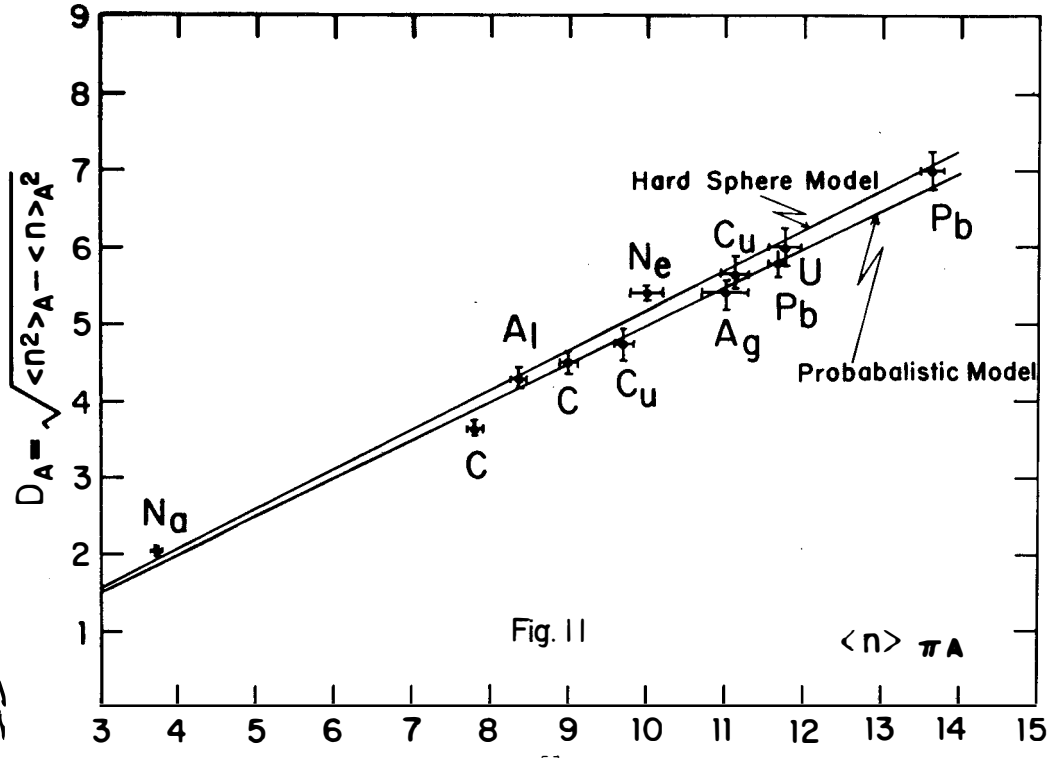

Comparison between experimental [8] on the dispersion D_A of the charged multiplicity as function of $\langle n \rangle_A$ in high energy π-nucleus collisions, and the prediction of the Coherent Tube Model given by eq. (17).

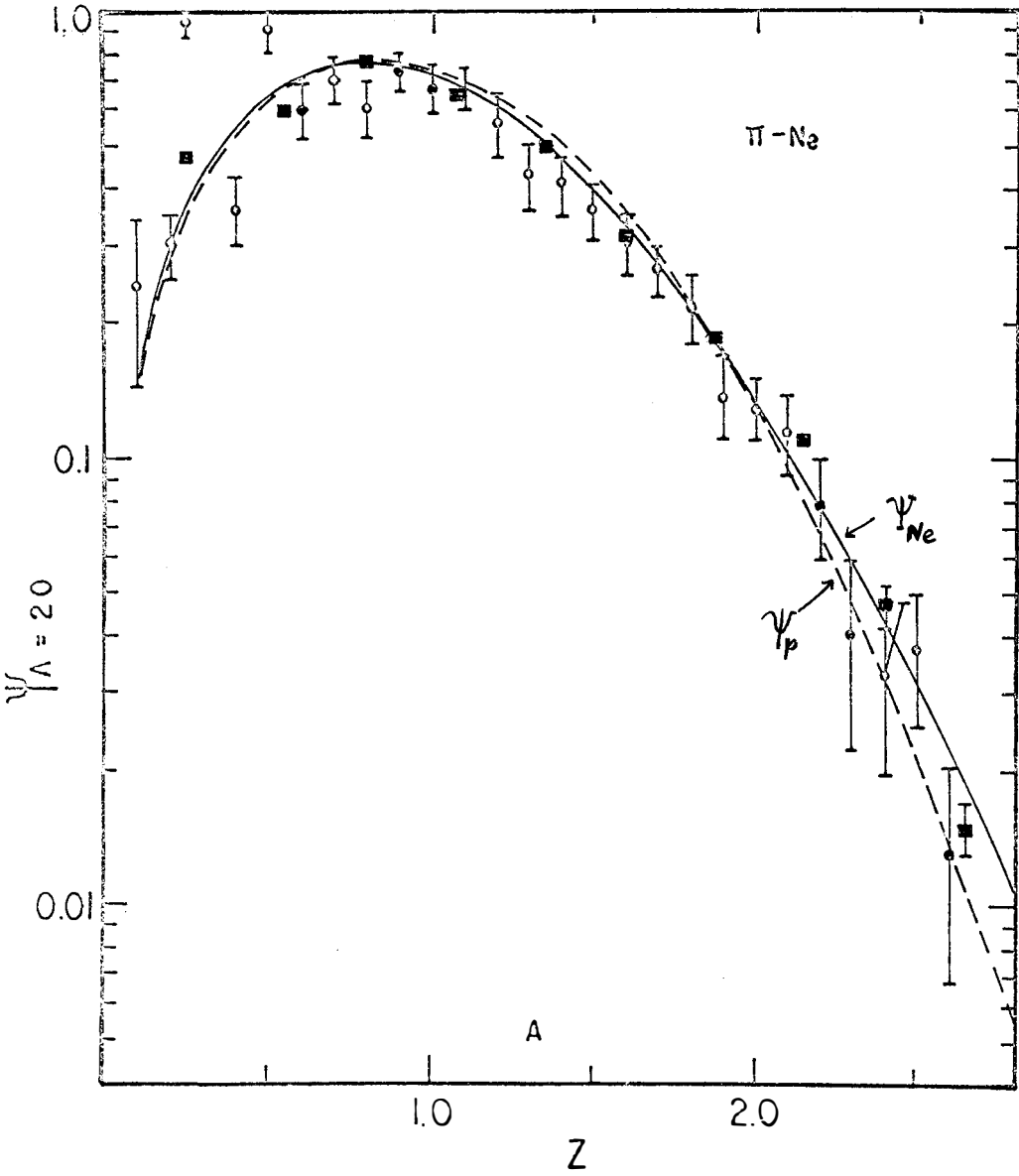

Fig. 12 Comparison between the measured [5] KNO scaling function Ψ_A for high energy π-Ne collisions and the prediction of the Coherent Tube Model given by eq. (17).

energy. Consequently nucleus-nucleus collisions can be calculated directly from nucleon-nucleon collisions. In particular, the inclusive cross section for $A_1 + A_2 \to c$ + anything is approximately given by [1-e] :

$$E \frac{d^3\sigma_c^{A_1A_2}}{dp^3}(s, E + p_{\parallel}, p_{\perp}) \simeq \frac{\sigma_{in}^{pA_1}}{\sigma_{in}^{pp}} \frac{\sigma_{in}^{pA_2}}{\sigma_{in}^{pp}} \sum_{i_1=1}^{A_1} \sum_{i_2=2}^{A_2} p(i_1, A_1)\, p(i_2, A_2) \frac{E\, d^3\sigma_c^{pp}}{dp^3}$$

$$(i_2 s, \sqrt{i_2}(E + p_{\parallel}), p_{\perp}) \simeq \frac{\sigma_{in}^{pA_1}}{\sigma_{in}^{pp}} \frac{\sigma_{in}^{pA_2}}{\sigma_{in}^{pp}} \frac{E\, d^3\sigma_c^{pp}}{dp^3}(s_{eff}, (A_2)^{1/6}(E + p_{\parallel}), p_{\perp}) \tag{20}$$

where A_1 is the atomic number of the incident nucleus, A_2 is the atomic number of the target, s is the c.m. energy squared for the collision of a single nucleon from the incident nucleus with a single nucleon of the target nucleus, and s_{eff} is given by formula (4). Expression (20) can be integrated in order to obtain the following prediction [1-e] for the average multiplicity in high energy nucleus-nucleus collisions :

$$R_{A_1A_2} \equiv \frac{\langle n(s)\rangle_{A_1A_2}}{\langle n(s)\rangle_{pp}} \simeq R_{A_1} R_{A_2} \frac{(\sigma_{in}^{pA_1}/\sigma_{in}^{pp})(\sigma_{in}^{pA_2}/\sigma_{in}^{pp})}{(\sigma_{in}^{A_1A_2}/\sigma_{in}^{pp})} \tag{21}$$

where R_{A_i} are given by expression (13).

Are predictions (20), (21) supported by experiments ? First generation experiments with relativistic nuclear beams at LBL [9] and Dubna [10] produced results which are consistent with the idea of accumulation of energy through cooperative behaviour of few nucleons : for instance, at Dubna, pions produced by 8 GeV/c deuterons (4 GeV/c per nucleon) were found to carry away up to 98 % of the deuteron kinetic energy. At LBL the energy spectrum of pions produced by various nuclear projectiles with fixed energy per nucleon increased with the atomic number of the projectile nucleus and extended up to energies few times the energy per nucleon in the incident nucleus (see Fig. 13). Unfortunately, the available experimental data on high energy nucleus-nucleus collisions is at energies too low for our model to be applicable. Moreover, at such energies also the fermi motion of the nucleons in the colliding nuclei may lead to increase in the available c.m. energies for particle production. (Note, however, that the fermi motion effect will depend only weakly on the atomic numbers of the colliding nuclei). More experiments with high energy nuclear beams at higher incident energies are required before a definite proof can be provided for the energy accumulation effect in high energy nucleus-nucleus collisions.

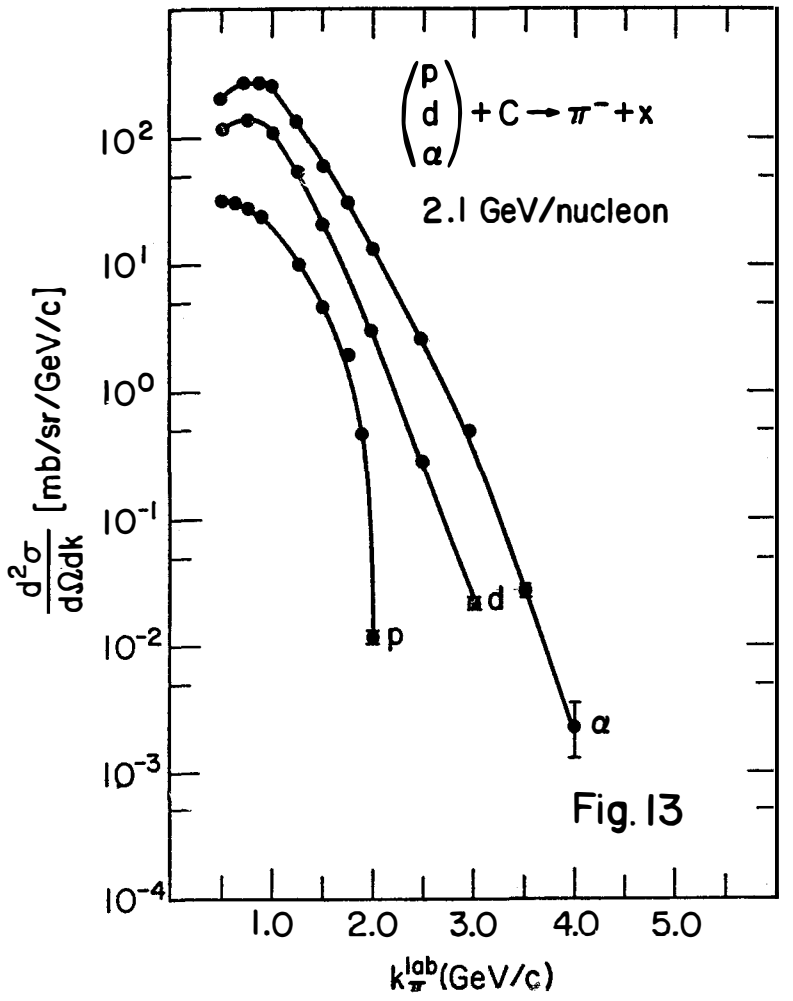

Energy spectrum of π^- at $\theta_{LAB} = 2.5°$ produced in pC, dC and αC collisions with 2.1 GeV per incident nucleon. (Neglecting fermi motion, an incident nucleon can not produce pions with momenta greater than its incident kinetic energy).

REFERENCES.

[1-a] G. BERLAD, A. DAR and G. EILAM, Phys. Rev. D13, 161 (1976).

[1-b] Y. AFEK, G. BERLAD, G. EILAM and A. DAR, "Scaling Laws for Inclusive Production of Hadrons in High Energy Particle-Nucleus Collisions", Technion Preprint PH-76-12, February 1976 (to be published in Phys. Rev. D).

[1-c] Y. AFEK, G. BERLAD, G. EILAM and A. DAR, "Cumulative Enhancement of J/ψ Production in Hadron-Nucleus Collisions", Technion Preprint PH-76-24, March 1976 (to be published).

[1-d] Y. AFEK, G. BERLAD, G. EILAM and A. DAR, "Rapidity Distributions in High Energy Particle-Nucleus Collisions" Technion Preprint, PH-76 March 1976 (to be published).

[1-e] Y. AFEK, G. BERLAD, G. EILAM and A. DAR, "Particle Production in High Energy Nucleus-Nucleus Collisions", Technion Preprint, PH-76 (to be published).
Similar models and ideas have been proposed also by :

[1-f] S.Z. BELENKIJ and L.D. LANDAU, Nuovo Cimento, Suppl. 3, 15 (1976).

[1-g] A.Z. PATASHINSKII, JETP Lett. 19, 654 (1974).
(Engl. Transl. 19, 338 (1974).

[1-h] A.M. BALDIN et al., Yad Fiz. 20, 1201 (1974).
(Sov. J. Nucl. Phys. 20, 629 (1975).

[1-i] A. DAR, Proceedings of the ICTP Topical Meeting on High Energy Reactions Involving Nuclei. Trieste, September 1974.

[1-j] S. FREDRIKSSON, Stockholm Royal Institute of Technology Preprint, December 1975.

[2] J.W. CRONIN et al., Phys. Rev. D11, 3105 (1975), B. ALPER et al., Nucl. Phys. B87, 19 (1975).

[3] Detailed list of references can be found for instance in W. BUSZA, Proceedings of the VI International Conference on High Energy Physics and Nuclear Structure, Santa fe, June 1975.

[4] Experimental data was taken from the list of references quoted in references [1-a] and [3].

[5] J.R. ELLIOT et al., Phys. Rev. Lett. 34, 607 (1975).

[6] P.L. JAIN et al., Phys. Rev. Lett. 33, 660 (1974).

[7] Z. KOBA, H.B. NIELSEN and P. OLESEN, Nucl. Phys. B40, 317 (1972).

[8] W. BUSZA et al., Phys. Rev. Lett. 34, 836 (1975).

[9] I. JAROS et al., Phys. Rev. Lett. 34, 601 (1975).
J. PAPP, (Ph.D. Thesis) LBL Publication n° 3633 (May 1975).

[10] A.M. BALDIN, Proceedings of the VI Inter. Conference on High Energy Physics and Nuclear Structure, Santa Fe, June 1975 and references therein.

MODIFIED ADLER SUM RULE AND VIOLATION OF CHARGE SYMMETRY*

C.A. DOMINGUEZ, H. MORENO AND A. ZEPEDA
Departamento de Física. Centro de
Investigación y de Estudios Avanzados
del I.P.N. MEXICO

Abstract: The consequences of a once subtracted dispersion relation in the derivation of the Adler Sum Rule are investigated.
It is shown that one can expect a breakdown of charge symmetry, of the isotriplet current hypothesis, and of scaling of the structure functions. These breakdowns are related to the possible presence of a non-zero subtraction function at asymptotic energies and arbitrary q^2.
We also comment about second class currents and PCAC relations.

*Presented by C.A. Dominguez. Work supported in part by CONACyT (México) under contract #540-A.

It is well known that the Adler Sum Rule[1] (ASR) provides one of the most direct tests of the Current Algebra hypothesis[2]. However in its derivation one introduces additional assumptions[3] such as the validity of the $\vec{p} \to \infty$ method or a no subtraction hypothesis in a dispersion relation approach. The lack of clear justification in this last case was expressed in the past by Gribov et al.[4] In this paper we discuss the consequences of a once subtracted dispersion relation leading to a modified ASR for the case $\Delta Y=0$. We show that the presence of a non-zero subtraction function can result in a breakdown of charge symmetry, and consequently of the isotriplet current hypothesis[5] (ICH). Moreover if the subtraction function is q^2-dependent it follows that the structure functions $\nu W_2^{\nu,\bar{\nu}}$ shall no longer scale. Finally we discuss the conditions under which charge symmetry and the ICH can be effectively restored at $q^2 = 0$.

Let us start by writing the amplitude for neutrino scattering off an unpolarized nucleon (proton or neutron) summing over final polarizations

$$T_{\mu\nu}^{(\nu)} = \frac{p_o V}{M} \frac{i}{\pi} \int d^4x\, e^{iq\cdot x} \langle N(p) | T^*(J_\mu^{(-)}(x) J_\nu^{(+)}(0)) | N(p) \rangle$$

$$= -g_{\mu\nu} T_1(\nu,Q^2) + \frac{p_\mu p_\nu}{M^2} T_2(\nu,Q^2) \qquad (1)$$

$$- \frac{i}{2M^2} \varepsilon_{\mu\nu\alpha\beta} p^\alpha q^\beta T_3(\nu,Q^2)$$

$$+ \frac{q_\mu q_\nu}{M^2} T_4(\nu,Q^2) + \frac{1}{2M^2} (p_\mu q_\nu + q_\mu p_\nu) T_5(\nu,Q^2)$$

The absorptive part of this amplitude is given by

$$W_{\mu\nu}^{(\nu)} = \frac{p_o V}{M} \frac{1}{2\pi} \int d^4x\, e^{iq\cdot x} \langle N(p) | \left[J_\mu^{(-)}(x), J_\nu^{(+)}(0) \right] | N(p) \rangle \qquad (2)$$

with a similar invariant decomposition. Considering $\Delta Y=0$ processes (Cabibbo angle set equal to zero) one obtains the following Ward-Takahashi identity

$$q^\mu T_{\mu\nu} = \frac{4}{\pi M} p_\nu \langle N | J^{(0)} | N \rangle + D_\nu \qquad (3)$$

where

$$D_\nu = -\frac{p_o V}{M} \frac{1}{\pi} \int d^4x\, e^{iq\cdot x} \langle N(p) | T^*(\partial^\mu J_\mu^{(-)}(x) J_\nu^{(+)}(0)) | N(p) \rangle \qquad (4)$$

$$= \frac{p_\nu}{M} D_1(\nu,Q^2) + \frac{q_\nu}{M} D_2(\nu,Q^2)$$

and $J_\nu^{(0)}$ is defined through the commutation relation

$$\delta(x_o) \left[J_\nu^{(+)}(0), J_o^{(-)}(x) \right] = 4\delta^3(x) J_\nu^{(0)}(0) \qquad (5)$$

and the currents are of the usual (V-A) type, the vector part being conserved. Assuming the ICH, $J^{(o)}$ is identified with I_3, the third component of isospin. However, we shall leave $J^{(o)}$ unspecified for the moment for reasons that will become clear later.

Substituting Eq. (1) and (4) in Eq. (3) it follows that

$$\nu T_2(\nu,Q^2) - \frac{Q^2}{2M} T_5(\nu,Q^2) - D_1(\nu,Q^2) = \frac{4}{\pi} \langle N|J^{(0)}|N\rangle \tag{6}$$

Defining

$$A(\nu,Q^2) = \frac{Q^2}{2M} T_5(\nu,Q^2) + D_1(\nu,Q^2) \tag{7}$$

and writing a dispersion relation for the separate amplitudes $A^{\nu p}$ and $A^{\nu n}$, a subtraction might be in order and we find

$$\begin{aligned} \mathrm{Re}A^{\nu N}(\nu_s,Q^2) &- \frac{\nu_s}{\pi} \int_{\nu_o}^{\infty} \frac{d\nu'}{\nu'^2-\nu_s^2} \nu' \left[W_2^{\nu N}(\nu',Q^2) + \right. \\ &\left. + W_2^{\bar{\nu}N}(\nu',Q^2) \right] \\ &- \frac{\nu_s^2}{\pi} \int_{\nu_o}^{\infty} \frac{d\nu'}{\nu'^2-\nu_s^2} \left[W_2^{\nu N}(\nu',Q^2) - W_2^{\bar{\nu}N}(\nu',Q^2) \right] \\ &= -\frac{4}{\pi} \langle N|J^{(0)}|N\rangle \end{aligned} \tag{8}$$

where ν_s is the subtraction point and N stands for either proton or neutron.

Taking the limit $\nu_s \to \infty$, Eq. (8) reduces to[6]

$$\begin{aligned} -\mathrm{Re}A^{\nu N}(\infty,Q^2) &+ \frac{1}{\pi} \int_{\nu_o}^{\infty} d\nu \left[W_2^{\bar{\nu}N}(\nu,Q^2) - W_2^{\nu N}(\nu,Q^2) \right] \\ &= \frac{4}{\pi} \langle N|J^{(0)}|N\rangle \end{aligned} \tag{9}$$

From crossing symmetry one has

$$\mathrm{Re}A^{\nu N}(\nu,Q^2) = -\mathrm{Re}A^{\bar{\nu}N}(-\nu,Q^2) \tag{10}$$

While from Eqs. (8) and (9) it follows that

$$\mathrm{Re}A^{\nu N}(\infty,Q^2) = \mathrm{Re}A^{\nu N}(-\infty,Q^2) \tag{11}$$

Thus,

$$\mathrm{Re}A^{\nu N}(\infty,Q^2) = -\mathrm{Re}A^{\bar{\nu}N}(\infty,Q^2) \tag{12}$$

Under the assumption of asymptotic dominance of Pomeron exchange, one also has

$$\left[A^{\nu N}(\infty,Q^2) - A^{\bar{\nu}N}(\infty,Q^2) \right]_{I=0} = 0 \tag{13}$$

Comparing Eqs. (12) and (13) one obtains

$$\mathrm{Re}\, A^{\nu N}(\infty,Q^2) = \mathrm{Re}\, A^{\bar{\nu}N}(\infty,Q^2) = 0 \tag{14}$$

The $\mathrm{Re}A^{\nu N}(\infty,Q^2)$ can be identified with the real part of the Pomeron in this amplitude and in turn is related to the real part of the Pomeron in νT_2 (note that the $J=1$ right signatured fixed pole in T_2 has a real and q^2-independent residue). Consequently, Eq. (9) can be reduced to the ordinary ASR (if J^o is identified with I_3) and the Pomeron is purely imaginary.

We remark that this result is independent of charge symmetry.

Let us now study the case in which $\mathrm{Re}A^{\nu N}(\infty,Q^2) \neq 0$. This would imply that

$$A^{\nu N}(\infty,Q^2) - A^{\bar{\nu}N}(\infty,Q^2) \neq 0. \tag{15}$$

This difference may only have I=1 or I=0 pieces in the t-channel. The first case leads to a modified ASR similar to the one conjectured by Harari[7] (although on different grounds) who suggested the presence of an I=J=1 fixed pole in the amplitude $A(\nu,Q^2)$. The second possibility (I=0) implies a violation of charge symmetry, as we shall immediately show. Assuming that the I=0 exchange is dominant at high energy (both for the individual amplitudes as well as for their difference) we have

$$A^{\nu p}(\infty,Q^2) = A^{\nu n}(\infty,Q^2) \tag{16}$$

Comparing Eq. (12) with Eq. (16) and using charge symmetry one concludes that $\mathrm{Re}A^{\nu p} = \mathrm{Re}A^{\nu n} = 0$. Hence, if this real part does not vanish it implies:

i) A violation of charge symmetry.

ii) $J_\mu^{(+)}, J_\mu^{(-)}$ and $J_\mu^{(0)}$ are no longer members of an isostriplet although the commutation relation, Eq. (5), still holds. $J_\mu^{(0)}$ is now in general no longer the isovector part of the electromagnetic current. As a matter of fact since the difference Eq. (15) in the t-channel is related to a current commutator one would expect that $J_\mu^{(0)}$ contains an isoscalar piece.

ii) Since charge symmetry is violated, this implies the presence of second class currents if time reversal invariance holds to lowest order in G.

iv) A breakdown of the scaling property of the structure functions.

Let us now turn our attention to $q^2=0$ and discuss how charge symmetry and the ICH can be effectively restored in this point.

Considering first the vector part of the ASR we have the following Born Term

$$W_2^{\nu n}{}_{BORN} = 2M\delta(Q^2-2M\nu)\left[F_1^2(Q^2) + \frac{Q^2}{4M^2}F_2^2(Q^2)\right] \tag{17}$$

where we have assumed that the vector part of the weak current is conserved (not necessarily implying the ICH) in order to have only two form factors. A similar expression holds for $W_2^{\nu p}{}_{BORN}$ although the form factors need not be the same as for $W_2^{\nu n}{}_{BORN}$ if charge symmetry does not hold. However we can safely assume

$$\begin{aligned} \langle p|J_\mu^{+}|n\rangle &= \langle p|I_\mu^{+}|n\rangle \\ \langle N|J_\mu^{(0)}|N\rangle &= \langle N|I_\mu^{3}|N\rangle \\ \langle n|J_\mu^{-}|p\rangle &= \langle n|I_\mu^{-}|p\rangle \end{aligned} \tag{18}$$

where I_μ is the isospin current. The above equations hold if the possible extra pieces in J_μ have vanishing matrix elements between nucleons which is the case if these have no new quantum numbers.

In other words, it is possible to restore charge symmetry in the restricted sense

$$\langle p|J_\mu^{(+)}(0)|n\rangle = \langle n|J_\mu^{(-)}(0)|p\rangle \tag{19}$$

Under these assumptions we obtain, after substituting the Born terms in Eq. (9), that

$$\begin{aligned} F_1^2(0) &= 1 - \pi\mathrm{Re}A^{\nu n}(\infty,0)_{VV} \\ &= 1 + \pi\mathrm{Re}\,A^{\nu p}(\infty,0)_{VV} \end{aligned} \tag{20}$$

or else,

$$\mathrm{Re}\, A^{\nu N}(\infty,0)_{VV} = 0 \qquad (21)$$

where we have used Eq. (16). Thus, $F_1^2(0) = 1$ and CVC[5] is restored in an effective way at $q^2=0$. It is important to remark however, that the assumptions made regarding the matrix elements of $J_\mu^{(\pm)}$ and $J_\mu^{(0)}$ do not hold beyond the Born approximation if the subtraction function is non zero for $q^2 \neq 0$.

Turning now to the axial part of the ASR and proceeding analogously as with the vector part, we obtain

$$G_1^2(0) = 1 + \int_\nu^\infty d\nu \left[\bar{W}_2^{\nu n}(\nu,0) - W_2^{\nu n}(\nu,0) \right]_{AA} - \mathrm{Re}A^{\nu n}(\infty,0)_{AA}$$

$$= 1 - \int_{\nu_0}^\infty d\nu \left[\bar{W}_2^{\nu p}(\nu,0) - W_2^{\nu p}(\nu,0) \right]_{AA} + \mathrm{Re}A^{\nu p}(\infty,0)_{AA} \qquad (22)$$

where G_1 is the axial form factor and the integrals are performed over the continuum. Although $\mathrm{Re}A^{\nu n}$ is equal to $\mathrm{Re}\, A^{\nu p}$ we can no longer conclude that they vanish because the two integrals in Eq. (22) are in principle different. Furthermore, the presence of a subtraction function which implies a violation of charge symmetry also implies in turn a breakdown of the PCAC relations

$$W_2^{\nu p}(\nu,Q^2) \to \frac{f_\pi^2}{\pi\nu}\, \sigma_{\pi+p}(\nu)$$

$$W_2^{\nu n}(\nu,Q^2) \to \frac{f_\pi^2}{\pi\nu}\, \sigma_{\pi-p}(\nu) \qquad (23)$$

$$\text{for } Q^2 \to 0,\ \nu \neq 0$$

However, the Goldberger-Treiman relation shall remain valid if Eq. (19) is assumed.

ACKNOWLEDGMENT

We are grateful to Dr. Jean Pestieau for an illuminating discussion.

REFERENCES AND FOOTNOTES

1) S.L. Adler, Phys. Rev. 143, B1144 (1966).
2) M. Gell-Mann, Physics 1, 63 (1964); S.L. Adler and R.F. Dashen, "Current Algebras" (W.A. Benjamin Inc., New York, Amsterdam 1968).
3) C.H. Llewellyn Smith, Phys. Reports 3C, 263 (1972)
4) V.N. Gribov, B.L. Ioffe and V.M. Shekhter, J. Nucl. Phys. (USSR) 5, 387 (1967), English translation Sov. J. of Nuclear Phys. 5, 272 (1967).
5) For convenience we shall make the distinction betweeen the conservation of the vector part of the weak current and the isotriplet current hypothesis (frequently referred to as CVC).
6) We remark that even though we are writing a dispersion relation for $A^{\nu p}$ and $A^{\nu n}$ separately, there appear two structure functions inside the integral due to crossing symmetry.
7) H. Harari: Phys. Rev. Lett. 22, 1078 (1969).

CP-VIOLATION, HEAVY FERMIONS AND ALL THAT

D.V. NANOPOULOS

Laboratoire de Physique Théorique, Ecole Normale Supérieure

24 rue Lhomond, 75231-Paris Cédex 05, France.

Abstract : We examine consequences of the possible existence of a heavy lepton, as indicated by recent experiments, in the framework of gauge theories. It appears that in the SU(2)xU(1) model one has to introduce more quarks beyond the usual four ones. In that case CP-violation emerges in a natural way and, as we show, an analysis of CP-violation phenomena along these lines gives encouraging results when confronted with experiment.

Résumé : Dans le cadre des théories de jauge, nous étudions les conséquences de l'éventuelle existence d'un lepton lourd tel que des expériences récentes l'ont signalé. Nous montrons que dans le modèle SU(2)xU(1) on doit introduire plus des quatre quarks habituels. Dans ce cas, la violation de CP apparaît naturellement et, comme nous le montrons, une analyse des phénomènes de la violation de CP en ce sens donne des résultats encourageants si on les compare à l'expérience.

INTRODUCTION

There was a time when three quarks along with the electron, the muon and their neutrinos could be considered as the fundamental blocks of matter. The discovery of new states, which do not fit in the conventional (pre-November 1974) picture, raises new questions and simultaneously a great hope that we are going to learn more about Nature's secrets.

Most of the new experimental information is consistent with the production of new hadronic degrees of freedom. At the same time there exists rather solid evidence that new leptonic states are produced. Needless to say that the simultaneous production of new hadrons and new leptons make the situation very difficult and leads sometimes to misinterpretation and wrong understanding of the data. (Remember the μ-π puzzle a few decades ago!) I am going to review tha available evidence for heavy lepton production, then discuss the consequences of the existence of heavy leptons in connection with the hadronic world, and finally concentrate on CP-violation phenomena.

I. HEAVY LEPTON PRODUCTION ?

The most positive piece of information concerning the existence of heavy leptons comes from the study at SPEAR[1] of the reaction :

$$e^+ e^- \to e^\pm \mu^\mp + \text{"missing energy"} \qquad (1)$$

where "missing energy" means energy not carried by charged particles, or γ-rays ; therefore, it should be energy carried by neutrals. The facts which make it possible for reaction (1) to actually go via

$$e^+ e^- \to L^+ L^- \qquad (2)$$

which subsequently decay, are :

i) the θ-coppl. and θ-collin. distributions show three-body decay characteristics.

ii) $< p_e > = < p_\mu > \simeq \frac{1}{4}$ of the total energy

iii) the (missing mass)^2 distribution (M_m^2) which shows that at least two particles are not detected.

These facts are more or less known for some time now. Very recently, some more information has become available from SPEAR :

iv) the $\# e^\pm e^\mp = \# \mu^\pm \mu^\mp = \# \frac{1}{2} e^\pm \mu^\mp$ events

v) limits of the form :

fraction of $e\mu$ events with $K_L^0 < 5\%$ at 90% C.L.

fraction of $e\mu$ events with $\pi^0 < 9\%$ at 90% C.L.

vi) upper bounds on the cross section for :

$e^+ e^- \to \mu^\pm + \gtrsim 2$ charged particles $+ n\pi^0$

which is ~ 370 pb for $p_\mu > 0.9$ GeV.

It is clear that all the above facts may easily be explained (without saying uniquely) by the production and subsequent decay of heavy leptons :

$$e^+ e^- \to L^+ L^- \qquad (3)$$
$$L^\pm \to \nu_L + \ell^\pm + \nu_\ell$$

Actually, analyses along these lines gave a quantitative agreement with data, with $M_{\text{heavy lepton}} \simeq 2$ GeV and B.R.($L \to \nu_L \ell \nu_\ell$) $\simeq$ 20%. This branching ratio is exactly what one naively expects by simple counting: 1e, 1μ, 3 q (3 for the colour) (Fig. 1)

$$\text{B.R.}(L \to \nu_L \ell \nu_\ell) \simeq \frac{1}{5} = 20\% \qquad (4)$$

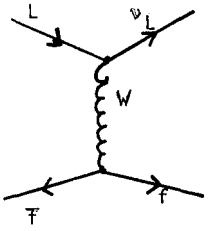

Fig.1

f : e, μ , q

$\bar{f}$: ν_e, ν_μ , $\bar{q}$

In addition, the fact that $\# e^\pm e^\mp = \# \mu^\pm \mu^\mp = \# \frac{1}{2} e^\pm \mu^\mp$ shows that it is a sequential heavy lepton i.e. it carries its own leptonic quantum number and has its own neutrino ν_L. This is very easy to see : Consider the case of an electronic heavy lepton (see Fig.2) ;

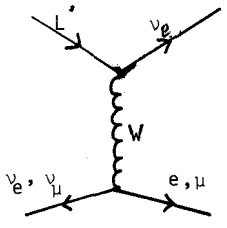

Fig.2

Then we have twice as many diagrams for the electron as for the muon (because of ν_e)

Possibilities

$(2e^+, 2e^-)$; $2e^+, \mu^-$

$2(\mu^+, e^-)$; μ^+, μ^-

Which, in turn, means :

$$\#e^+ e^- = \#e^\pm \mu^\mp = 4\#\mu^+ \mu^-$$

(In the case of muonic heavy lepton we would have :

$\#\mu^+ \mu^- = \#e^\pm \mu^\mp = 4 \#e^+ e^-$).

So, we have already solid evidence (and we are going to assume that this is the case) for the production and subsequent decay of sequential heavy (M ≃ 2 GeV.) leptons at SPEAR with B.R. $(L \to \nu_L \ell \nu_\ell) \simeq 20\%$. Then one has to look for the consequences of such a heavy lepton elsewhere. The new SPEAR limits (on K_L^o, π) evidently put constraints on the semileptonic decays of charmed particles. On the other hand, if one wants to explain the "di-muons" in neutrino-production as coming from charm, a quite substantial semileptonic branching ratio is needed. The situation seems a little cloudy. However, one may argue that because of the experimental cuts, one is missing μ,e coming from charmed mesons but not coming from heavy leptons. Clearly, most of the analysed data come from a sample at $E_{C.M.} = 4.8$ GeV., and if the leptons come from the decay of charmed particles then $p_{e,\mu} \lesssim \frac{E_{C.M}}{4}$ ≃ 1.2 GeV. Actually, $p_{e,\mu}$ may be away from the upper limit, because angular correlations indicate the possibility of a 3 body decay. Then if we take into account the fact that a cut has been made : $p_{e,\mu} > 0.65$ GeV., it becomes clear that it is very probable that the e,μ which come from charmed particles are not fully detected at SPEAR.

II. IMPLICATIONS OF THE EXISTENCE OF A HEAVY LEPTON

As I have mentioned in the introduction, the simultaneous existence of heavy leptons and of "heavy" hadrons makes life difficult. Of course with some effort, we may learn a lot about both species. On the other hand, the existence of heavy leptons may give some help for the "charm" business. It is well known by now that the conventional Glashow-Iliopoulos-Maiani (GIM) charm has the following difficulties :

i) $R \equiv \frac{\sigma(e^+ e^- \to \gamma \to \text{hadrons})}{\sigma\ (e^+ e^- \to \mu^+ \mu^-)}$ is 5.5. instead of $\frac{10}{3}$

ii) the $\frac{K}{\pi}$ (or the $\frac{\#\ K}{\text{event}}$) does not show any changes around 4 GeV where one expects the "charm" threshold and hence the $\frac{\#\ K}{\text{event}}$ must almost be doubled.

iii) the "μe" SPEAR events (see Eq. 1)

iv) absence of direct evidence of charmed particle-production at SPEAR.

The evidence for production of new hadrons in neutrino experiments perhaps means that the SPEAR searches were unlucky enough. The "μe" SPEAR events were our starting point to introduce heavy leptons, so it remains to be shown that we evade problems i) and ii). Actually, this is the case : the existence of a heavy lepton takes out from R one unit. ($\Delta R_{\text{heavy lep.}} \simeq 1$), so we are left with $R \simeq 4$ which is much more comfortable, comparing with $\frac{10}{3}$ of charm, than before. (A bit of asymptotic freedom, a bit of threshold effects and we are home !).

The problem of $\frac{\#\ K}{\text{event}}$ (or $\frac{K}{\pi}$ ratio) may have a satisfactory explanation : the decays of heavy leptons to hadrons give mainly ($\cos^2 \theta_c \simeq 0.95$) S = 0 hadrons and only a few percent ($\sin^2 \theta_c \simeq 0.05$) contain strange particles. So, above the threshold of "new physics" the heavy lepton decays mainly to S = 0 hadrons, the "charmed" particles decay mainly to S ≠ 0 hadrons,

and so they manage to keep the $\frac{\#\,K}{event}$ (or $\frac{K}{\pi}$ ratio) almost unchanged below or above threshold. Then it is crucial here that $M_{heavy\ lep.} \simeq M_{light\ charm.\ part.}$ (For those that worry about this coincidence, I remind them the almost degeneracy in mass of the muon and the pion ; history repeats itself ?)

I am aware of the difficulty to swallow the above argument, namely the need of a tremendous conspiracy of heavy lepton-charm in order to keep the $\frac{K}{\pi}$ ratio almost the same below and above threshold. It is clear that because of the different threshold behaviour for heavy lepton and charm, a fluctuation of the $\frac{K}{\pi}$ ratio should be observed. Maybe an experimental way to test such a combined picture is, for instance, to look at the $\#$ of K's as a function of the multiplicity : it is possible that low multiplicity events have almost no K's (heavy lepton case) and high multiplicity events have many K's (charm case).It seems that a heavy lepton helpds the "charm" situation. The next question to consider is of course the theoretical framework in which such a heavy lepton may find a natural place. It is too early to give a definite answer, but we have a picture of nature which, up to now, seems to work quite successfully :

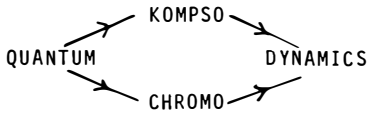

("kompsos" : Greek word meaning "elegant", "chroma" : Greek word meaning "colour")

Quantum Kompsodynamics (QKD) is the usual unified theory of weak and electromagnetic interactions, and quantum chromodynamics is the usual gauge theory of strong interactions, where we gauge the colour. The most popular and by now in good agreement with experiment is the Weinberg-Salam SU(2)xU(1) gauge model with four

flavour) quarks (u,d,s,c),(in order to avoid $\Delta S = 1$ neutral currents, à la Glashow-Iliopoulos-Maiani), with three colours ($SU(3)_{col.}$) (in order to have correct spin-statistics (Han-Nambu), $\pi^0 \to 2\gamma$ and R = 2, not $\frac{2}{3}$ in low energies (Gell-Mann) and to avoid Adler anomalies à la Bouchiat-Iliopoulos-Meyer (BIM)). Actually, results on neutral currents[2] from Gargamelle and the Caltech-Fermilab experiment indicate that not only the Weinberg Salam SU(2)xU(1) model is consistent with experiment, but also its minimal Higgs content seems to be correct. (One does a two parameter fit, where $b = M_W^2 / M_Z^2 \cos^2\theta_W$ and $\sin^2\theta_W$ are taken as independent parameters. Then one finds $b \simeq 1$ which means that the original-minimal Higgs content of Weinberg and Salam seems to work.)

Undoubtedly the most economical way to embed the heavy lepton with its neutrino in such a picture, is to put another doublet under $SU(2)_L$ weak. Then, if we do not want to spoil the renormalisation of the theory through Adler anomalies, we'd better put also a quark doublet (say t (with $Q_t = \frac{2}{3}$) and b (with $Q_b = -\frac{1}{3}$)), because then the usual relation $\sum_{\text{fermions}} Q_{\text{fermions}} = 0$ is satisfied and no anomaly exists any more.

The picture that emerges is :

$$\begin{pmatrix} \nu_e \\ e \end{pmatrix}_L \quad ; \quad \begin{pmatrix} \nu_\mu \\ \mu \end{pmatrix}_L \quad ; \quad \begin{pmatrix} \nu_L \\ L \end{pmatrix}_L \qquad (5)$$

$$\begin{pmatrix} u \\ d_c \end{pmatrix}_L \quad ; \quad \begin{pmatrix} c \\ s_c \end{pmatrix}_L \quad ; \quad \begin{pmatrix} t \\ b \end{pmatrix}_L \quad , \text{ everything else is SU(2) singlet.}$$

This is a very naive picture and we wrote it down just to indicate lepton-quark analogy. We will see soon that there are mixings between d_c, s_c and b.

It is clear from (5) that the nice quark-lepton analogy is restored (perhaps the Adler anomaly cancellation is the result of this deeper quark-lepton analogy). So, if we want to remain inside the conventional SU(2)xU(1)xcharm model, the existence of a heavy lepton forces us to introduce two more quarks (flavours).

Actually, this is what happened before : if we did not know anything about the muon, u and d quarks would be enough, no Adler anomalies, no strangeness, a renormalisable (≡ respectable) theory. Then the discovery of the muon (by means, say, of Adler anomalies) would force us to introduce two more quarks c, s (charm and strangeness), then again, no Adler anomalies, but strangeness, charm, a very good theory. BUT in this case, we have something more, automatically we do not have $\Delta S = 1$ neutral currents and we understand the smallness of the K_L-K_S mass difference, which is a real bonus in this picture.

In the case of a heavy lepton, we again introduce two more quarks (t, b) ; is there any extra bonus in that case ? Very fortunately the answer is affirmative and what comes out in a more or less "natural" way (maybe for the first time) is a reasonable explanation of CP violation. Before analysing the CP violation phenomenon in this framework, let me give a diagrammatic view of the situation that we have described above :

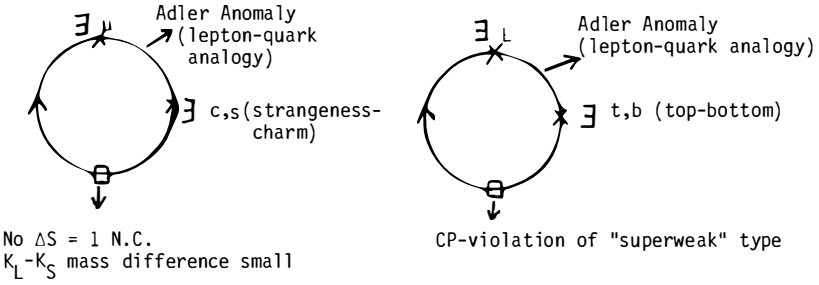

Fig. 3

The diagrams of Fig. 3 are meant to be circles (all the points are equivalent, there is no start nor end, or the snake which eats its tail, the famous ancient Greek fable of obvious meaning). It is obvious that in order to start, we need some independent argument, e.g. strangeness has to exist for purely cosmological reasons etc. We turn now to our main topic, CP violation.

III. CP-VIOLATION

Because there has been a long time (> 10 years) since Christenson, Cronin, Fitch and Turlay discovered the famous CP violation, I start by giving a flash review of the situation.

1° Present Status of CP Violation.

The phenomenon of CP-violation was first observed in the reaction $K_L^0 \to \pi^+ \pi^-$ which, of course, does not go if CP is conserved. The experimental information that we have at our disposal up to now is the following :

Define

$$n_{+-} \equiv \frac{<\pi^+ \pi^- | K_L^0>}{<\pi^+ \pi^- | K_S^0>}$$

$$n_{oo} \equiv \frac{<\pi^0 \pi^0 | K_L^0>}{<\pi^0 \pi^0 | K_S^0>} \qquad (6)$$

and

$$\delta_L \equiv \frac{\Gamma(K_L^0 \to \pi^- \ell^+ \nu) - \Gamma(K_L^0 \to \pi^+ \ell^- \nu)}{\Gamma(K_L^0 \to \pi^- \ell^+ \nu) + \Gamma(K_L^0 \to \pi^+ \ell^- \nu)}$$

where K_S^0, K_L^0 are the physical states of definite mass and lifetime, and they are related with the states of definite CP: K_1(CP = +1), K_2(CP = -1) in the usual way :

$$K_S^0 = \frac{K_1 + \varepsilon K_2}{\sqrt{1 + |\varepsilon|^2}} \quad ; \quad K_L^0 = \frac{K_2 + \varepsilon K_1}{\sqrt{1 + |\varepsilon|^2}} \qquad (7)$$

Then one has :

$$\begin{aligned} n_{+-} &= \varepsilon + \varepsilon' \\ n_{oo} &= \varepsilon - 2\varepsilon' \qquad (8) \\ \delta_L &\simeq 2\,\mathrm{Re}\,\varepsilon \quad \text{(we neglect } \Delta S = -\Delta Q \text{ effects)} \end{aligned}$$

ε' is a measure of the CP-violation in the decay transition. Physically, $\varepsilon \neq 0$ implies the existence of a CP-non-invariant term in the mass-matrix and $\varepsilon' \neq 0$ implies the existence of CP violation in the decay-transitions. Experimenters tell us now the following :

i) $n_{+-} = n_{oo}$ (in amplitude and phase), which implies $\varepsilon' \to 0$
(actually : $\left|\frac{\varepsilon'}{\varepsilon}\right| < 2.10^{-2}$) , and we may put $n_{+-} = n_{oo} = \varepsilon$

ii) $\left|\frac{\delta_L}{n_{+-}}\right| = 1.448 \pm 0.055$, which is consistent with i) because

$$\left|\frac{\delta_L}{n_{+-}}\right| = \frac{2\,\mathrm{Re}\varepsilon}{|\varepsilon|} = \frac{2\cos\phi\,|\varepsilon|}{|\varepsilon|} \simeq 2\cos\phi \simeq 1.443 \pm 0.005$$

Experimentally : $\phi_{+-} = (45 \pm 1.3)°$
$\phi_{oo} = (48.3 \pm 1.3)°$
so $\phi_{+-} \simeq \phi_{oo} \equiv \phi$

iii) CP or C violations have been searched for in strong-e.m. interactions and in weak decays not involving K^o mesons : NO EFFECT HAS BEEN FOUND YET.

So, it is clear that i), ii) and iii) are the obligations of a theory that tries to explain the CP-violation phenomenon. Since the early days it was known that a superweak theory has exactly the features i), ii) and iii). But at the same time it was clear that it was an ad-hoc addition of a strange $\Delta S = 2$ interaction just to explain this phenomenon.

Everybody was hoping since then that one might produce a reasonable milliweak-type theory which possesses the features of the superweak theory, but no ad-hoc terms, where the CP-violation emerges in a natural way. Very recently, there has been a revival of this problem with an observation made by some people[3-4-5], namely that if one has more than four quarks (flavours) it is possible to give a reasonable explanation of CP violation. I now turn my attention to such a fancy possibility.

2°. CP-Violation in a Model with Six Quarks and Left-handed Currents.

In the previous sections, I analysed the evidence (experimental) for heavy leptons and also a scheme where a heavy lepton may find a natural place. Let us assume that the Weinberg Salam SU(2)xU(1) model has something to do with reality, and suppose that we have n quarks with charge $\frac{2}{3}$ and n quarks with charge $-\frac{1}{3}$. Let us put

$$P = \begin{pmatrix} u \\ c \\ t \\ \vdots \end{pmatrix} \quad ; \quad N = \begin{pmatrix} d \\ \lambda \\ b \\ \vdots \end{pmatrix} \tag{9}$$

n quarks of charge $\frac{2}{3}$ n quarks of charge $-\frac{1}{3}$

Further, assume that the "left components" of the quarks are collected in doublets under SU(2) and everything else is SU(2) singlet. Then the V-A charged current has the form :

$$J_\mu^- = \bar{P}_L \gamma_\mu V N_L \tag{10}$$

where $P_L = \frac{1}{2}(1 - \gamma_5)P$ etc., and V is an n x n matrix. Then commuting J_μ^+ with J_μ^-, we take the neutral current, which is a mixture of $J_{electr.}$ and of

$$J_\mu^0 = \bar{P}_L \gamma_\mu V^+ V P_L + \bar{N}_L \gamma_\mu V^+ V N_L \tag{11}$$

We see, at once, that in order to avoid $\Delta S = 1$ neutral currents, J^0 must be diagonal in the quark fields, which in turn implies that $V^+ V = V V^+ = 1$; i.e. V has to be a unitary matrix (GIM mechanism).

In order to specify V, an nxn unitary matrix, we need n^2 parameters, one of which is an unobservable over-all phase, so that we are left with $n^2 - 1$ parameters. Fortunately, we can play with the phases of the quark fields and achieve further

reduction of the number of parameters needed to determine V. The easiest way to proceed is the following : we write down the mass matrix for the quarks :

$$M = \bar{P}_L \, M_p \, P_R + \bar{N}_L \, M_N \, N_R \qquad (12)$$

where M_p and M_N are assumed to be real and diagonal matrices ; we would like to keep them as such. Thus, the most general transformation that leaves (12) invariant is :

$$P_{L,R} \to e^{i \sum_{j=1}^{n-1} a_j \lambda_j^{\text{diagon.}}} P_{L,R}$$
$$N_{L,R} \to e^{i \sum_{j=1}^{n-1} b_j \lambda_j^{\text{diagon.}}} N_{L,R} \qquad (13)$$

where $\lambda_j^{\text{diagon.}}$ is the n-1 diagonal matrices of the SU(n) group. It is trivial to check that substitution of (13) to (12) leaves M invariant. We then have at our disposal (n-1) parameters (a_j) from P fields and (n-1) parameters (b_j) from N fields that can be transformed away.

Therefore the number of parameters needed for V now becomes $n^2 - 1 - 2(n-1) = (n-1)^2$. The number of real parameters that one needs to determine an n x n orthogonal matrix is $\frac{n(n-1)}{2}$. So, in the general case to determine V we will need

$$(n-1)^2 - \frac{n(n-1)}{2} = \frac{(n-1)(n-2)}{2} \text{ complex paremeters.}$$

In conclusion, the V matrix needs $(n-1)^2$ parameters, where $\frac{(n-1)(n-2)}{2}$ of them are complex.

In the case of GIM we have n = 2 ; therefore we do not have any complex parameter :

$$J_\mu^- = (\bar{u}, \bar{c})_L \, \gamma_\mu \underbrace{\begin{pmatrix} \cos\theta_c & \sin\theta_c \\ -\sin\theta_c & \cos\theta_c \end{pmatrix}}_{V(n=2)} \begin{pmatrix} d \\ s \end{pmatrix}_L \qquad (14)$$

BUT, if n > 2, then we have complex parameters which of course are going to introduce CP violating effects. Take for instance n = 3, then we have one complex parameter and the question is

whether we can obtain a reasonable explanation of CP-violation phenomenology in this case. As we shall see, this turns out to be the case.

Before giving an analysis of CP-violation in this framework, let me make a few comments :

i) the idea that a phase difference between different parts of the current may produce CP-violation is an old one[6]. But it was always introduced by hand, whereas here it emerges in a more natural way.

ii) The number of complex parameters ($\frac{(n-1)(n-2)}{2}$) increases as we increase the number of quarks (flavours) ; e.g. for n = 4 we have 3 complex parameters, etc. We do not want to imply that with more than one complex parameter we cannot take the correct form of CP-violation, but it is a temptation to observe that with six and only six flavours we have just one complex parameter and we can fit everything. Perhaps it is a coincidence, perhaps it is something deeper.

iii) It should be noticed that we arrived at the picture of six quarks (flavours) by the possible existence of the SPEAR heavy lepton. Here the situation is reversed with respect to the existence of muon and the absence of $\Delta S = 1$ neutral currents. If we had thought of the analogy before, the observation of CP-violation in nature, we would have been forced to go to six quarks and then of course to six leptons, i.e. the heavy lepton would have been predicted to be there.

In the following I shall concentrate on the case of six quarks (n = 3, which means one complex parameter). In this case, the charged current takes the form :

$$J_\mu^- = (\bar{u},\bar{c},\bar{t})_L\ \gamma_\mu \underbrace{\begin{pmatrix} c_1 & -s_1c_3 & -s_1s_3 \\ s_1c_2 & c_1c_2c_3-s_2s_3e^{i\delta} & c_1c_2s_3+s_2s_3e^{i\delta} \\ s_1s_2 & c_1s_2c_3+c_2s_3e^{i\delta} & c_1s_2s_3-c_2c_3e^{i\delta} \end{pmatrix}}_{V(n=3)} \begin{pmatrix} d \\ s \\ b \end{pmatrix}_L \qquad (15)$$

where $c_i(s_i) \equiv \cos\theta_i(\sin\theta_i)$, $i = 1,2,3$.

It is evident that the current (15), in the limit $\theta_1 \to \theta_{cabibbo}$; $s_{2,3} \to 0$; $\delta \to 0$, is nothing else but the conventional Cabibbo-Glashow-Iliopoulos-Maiani current (14). It is clear that the validity of the Cabibbo theory, which involves u,d and s quarks, would restrict possible values of the new angle parameters.

Actually, one finds, in order to agree with experiment, that

$$\theta_1 \simeq \theta_c \quad ; \quad s_1^2\, s_3^2 < 0.003 \qquad s_3^2 < 0.06 \qquad (16)$$

Up to now, we have no information about the validity of the GIM theory, but one can produce arguments showing that c_2 cannot be too small. By simple inspection of the form of the current (15) we get :

A *UNCHARMED PARTICLES*

1. Semileptonic processes.

These processes (for uncharmed hadrons) involve only u,d and s quarks,and the first row of V in (15) does not contain any CP-violation. So we do not expect any CP-violation in ordinary semileptonic processes.

2. Non-leptonic processes

We may have CP-violation in this case, arising from terms of the form : $(\bar{s}_L\ \gamma_\mu\ c_L)(\bar{c}_L\ \gamma_\mu\ d_L)$; $(\bar{s}_L\ \gamma_\mu\ t_L)(\bar{t}_L\ \gamma_\mu\ d_L)$ which enter in the current-current product with complex coefficients relative to the usual term $(\bar{s}_L\ \gamma_\mu\ u_L)(\bar{u}_L\ \gamma_\mu\ d_L)$. One may worry that we have a first order effect coming from the diagram :

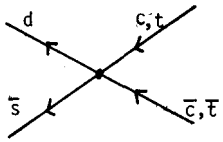

Fig. 4

But this diagram is strongly suppressed due to the Zweig rule (annihilation of the two heavy quarks to ordinary quarks). The only other additional first order effect may arise from the diagram

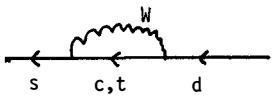

Fig. 5

But, in this case, an explicit calculation shows that in the limit $(\frac{m_q}{M_w})^2 \to 0$, this diagram vanishes because of the form of the current. Also both diagrams (Figs. 4, 5) vanish in the limit $m_c = m_t$. (This corresponds to the case in which we have no $\Delta S = 1$ neutral current effects to all orders if $m_c = m_u$).

Also, one may notice that the operators that create the CP-violation induce pure $\Delta I = \frac{1}{2}$ transitions. It is well known that a milliweak theory with the above properties reproduces for K-decays the same results as a superweak theory. Having shown the absence of first-order CP-violation effects, we are left with the explicit calculation of the ε-parameter in K-decay. This can be done by studying the neutral K-mass-matrix, which means that one has to calculate the diagram :

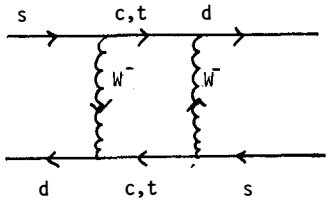

Fig. 6

One then finds :

$$\varepsilon \simeq \sqrt{2}\, s_2 s_3 \sin\delta \left[\cos 2\theta_2 \cdot \frac{m_t^2}{M_t^2 - m_c^2} \ln\left(\frac{m_t^2}{m_c^2}\right) + s_2^2 \left(\frac{m_t^2}{m_c^2}\right) - c_2^2\right] \tag{17}$$

We see that ε is a complicated function of the new angles and of the masses of the charmed and heavy quarks. We notice here that the factor $s_2 s_3 \sin\delta$ is a typical factor which always appears in the ratio $\frac{\text{(CP-violated) amplitude}}{\text{(CP-conserved) amplitude}}$ and so it can be determinded from a given process, and then we may use its value to study other processes. (Actually, one uses the experimental information on ε, determines the value of $s_2 s_3 \sin\delta$ and uses it, say, to determine the value of the electric dipole moment of the neutron (see below)) In order to see how well this kind of theory resembles the superweak, one has to study the ratio $\frac{\varepsilon'}{\varepsilon}$. Then one finds

$$\frac{|\varepsilon'|}{|\varepsilon|} \lesssim \frac{1}{450} \tag{18}$$

which is in excellent agreement with experiment, and practically we may put $\varepsilon' \simeq 0$ (superweak theory). Here I want to stress the following fact : contrary to some claims in the literature, relation (18) IS INDEPENDENT OF THE HEAVY QUARK MASSES and of the factor $s_2 s_3 \sin\delta$ which of course drops out from the ratio $\frac{|\varepsilon'|}{|\varepsilon|}$. That is to say this kind of CP-violation resembles the superweak theory whatever the value of m_t. We shall see later that the electric dipole moment of the neutron is very sensitive to the heavy quark quark masses. The observed magnitude of CP-violation effects in

the neutral K-mass-matrix clearly implies :

$$|s_2 \cdot s_3 \sin\delta| = O(10^{-3}) \qquad (19)$$

The "naturalness" of such a relation may create quite long arguments for and against it. Here I just want to make the following observation : we saw that the Cabibbo theory, with its great experimental success, puts severe limits on s_3 (see Eq. (16)). Then "accepting"such limits for s_2 too, we are not far from an almost "natural" explanation of Eq. (19). Therefore, in this framework the smallness of CP-violation has something to do with the validity of the Cabibbo theory. In other words, there appears an interelation between the Cabibbo angle and CP-violation.

In conclusion, we can reproduce all the known experimental information for CP-violation (concerning common K decays) in a satisfactory way which resembles very much a superweak theory ($\varepsilon' \to 0$, etc.) through a well-defined milliweak theory. It seems to me that an appropriate name for such a theory is MICROWEAK THEORY.

3. Rare K-decays.

Here one finds drastic departures from superweak theory, but I do not discuss them here, because even the CP-conserving rare decays are very difficult to detect experimentally, and so these departures are not going to appear in the near future.

B. *CHARMED PARTICLES*

Here the analogue of the K^o-$\bar{K}^o$ system is the D^o-$\bar{D}^o$ system. Then a systematic theoretical analysis[5] shows that no dramatic CP-violation effects appear, namely if ε_c is the charm analogue of ε, then $|\varepsilon_c| \simeq |\varepsilon|$. It is true that in the charmed particle decays, as in the rare K-decays, one is going to see deviations from the superweak theory, but it is premature to

discuss here the deviations from superseak theory in the decays of particles which have not been shown to exist as yet. For a detailed analysis of such effects in rare K-decays and charmed particle decays one may consult Ref.(5).

Finally a few words for the Electric dipole moment of the neutron : from the early days of the observation of the CP-violation, it was clear that the electric dipole moment of the neutron (EDM) was an independent delicate test of any ambitious theory of CP-violation. Namely, if one assumes the validity of CPT-invariance, then CP-violation means necessarily T-violation which combined with the P-violation creates the possibility of EDM for the neutron. In the framework which I have considered, one may calculate the neutron dipole moment in terms of the quark dipole moment. One finds[7] :

$$|\frac{D}{e}|_n = |\frac{D}{e}|_{u,d} = \begin{cases} (10^{-27} - 10^{-28})\text{cm}, & \text{for } m_{t,b} \sim m_W \\ (10^{-30} - 10^{-31})\text{cm}, & m_{t,b} \sim 5 \text{ GeV} \end{cases} \quad (20)$$

One notice here that we do not get very different results from superweak theory ($\sim 10^{-29}$cm) and in the context of this model, knowledge of m_t and m_b would enable a better prediction of the neutron electric dipole moment and vice versa.

The sophisticated reader may also notice that, unlike in the magnetic moment case, the additivity of the EDM of the constituents to give the EDM of the system is not obvious at all, and in atomic physics one may find examples in which additivity is a very bad assumption[8].

IV. CONCLUSIONS

I have tried to show that we may have a reasonable explanation for CP-violation with an almost trivial extension of the Weinberg-Salam-GIM model, which will be necessary if a heavy

lepton really exists. In such a case we found that :

i) superweak results for common K-decays are reproduced to high accuracy, whatever the masses of the top end bottom quarks.

ii) in rare K-decays, direct CP-violating effects in the amplitude may be comparable with superweak CP-violating effects, but these effects seem essentially unobservable.

iii) in principle, there may be observable deviations from superweak predictions for charmed particle decays.

iv) the neutron electric dipole moment is very sensitive to the masses of the top and bottom quarks.

This picture introduces CP-violation in a natural way, as a result of weak mixing between the quarks analogous to the Cabibbo angle in the GIM model. THUS TWO PUZZLES ARE REDUCED TO ONE. It is evident that one may worry that we had a theory with one angle (Cabibbo angle) and now we have a theory with three angles ($\theta_{1,2,3}$) and one phase (δ). But the interelation that starts to appear now gives the hope that one may understand all these phenomena at once.

Here I have concentrated on the possibility of six quarks and only left-handed currents. Actually, there is no fundamental reason for these two assumptions. I believe that more than six quarks (8,...) are not going to change the CP-violation analysis. As for the presence of right-handed currents, if they survive from experiments, they may help in understanding the interelation of Cabibbo angle, CP-violation and fermion masses in a natural way.

This moment, things are looking very promissing : phenomena completely unrelated up to now seem to have common roots (Cabibbo angle, CP-violation and, maybe, fermion masses). Let us hope that this is not again one of those dramatic coincidences that have happened many times in the past...

ACKNOWLEDGEMENTS

I would like to thank Claude Bouchiat and Nicos Papanicolaou for useful conversations and reading the mansucript. I would also like to thank my wife Myrto for reading the manuscript and for her encouragements.

REFERENCES

(1) See talks by M. Perl and G. Goggi in the Proceedings of the International Meeting on Storage Ring Physics, Flaine, France February 1976.

(2) See talks by V. Brisson (GGM) and A. Bodek (Caltech) in these Proceedings.

(3) M. Kobayashi and K. Maskawa. Prog. Theor. Phys. 49, 652, (1973).

(4) S. Pakvasa and H. Sugawara. Univ. of Hawai Preprint UH 511 204-75, (1975)
L. Maiani. Istituto Superiore di Sanità, Rome Preprint, (revised version) ISS P 75/10, (1975).

(5) J. Ellis, M.K. Gaillard and D.V. Nanopoulos, CERN Preprint, TH-2116, (1976).

(6) S.L. Glashow. Phys. Rev. Letters, 14, 35, (1965)
B. d'Espagnat and M.K. Gaillard. Proc. Coral Gables Conf. Freeman and Co., (1965), p. 380.

(7) See L. Maiani (Ref. 4) ; Ref. 5 ; and S.L. Glashow (unpublished).

(8) This observation is due to Claude Bouchiat.

LATEST RESULTS ON THE AXIAL VECTOR FORM FACTOR

A. GIAZOTTO
I.N.F.N., Sezione di Pisa

Abstract: The results of a recent π^+ threshold electroproduction experiment at $|K^2|$ = .45, .58, .88 $(GeV/c)^2$, together with all the available π^+ threshold electroproduction coincidence data, are used to evaluate the axial vector form factor of the nucleon $G_A(K^2)$. It is found that the dipole parametrization is favoured over the monopole. The value of M_A in the dipole parametrization is, using a 'weak PCAC' model, 0.96 $\pm$.03 GeV, in excellent agreement with the results obtained by the reaction $\nu+D \rightarrow P+P_s+\mu^-$.

Résumé: Le facteur de forme axial du nucléon, $G_A(K^2)$, a été calculé en utilizant les résultats d'une récente expérience d'électroproduction de π^+ au seuil à $|K^2|$ = .45, .58, .88 $(GeV/c)^2$, avec tous les autres resultats disponibles pour l'éléctroproduction de π^+ au seuil. Une dépendance dipolaire du facteur de forme reproduit les données expérimentales mieux qu'une dépendence monopolaire. D'après le modèle de "weak PCAC" on trouve M_A = .96 ± .03 GeV en très bon accord avec les résultats obtenus par la réaction $\nu+D \rightarrow P+P_s+\mu^-$.

The process e p → e' n π^+, assuming one photon exchange, can be represented by the diagram (Fig. 1).

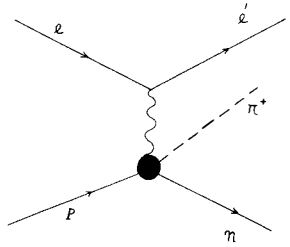

Fig. 1

We use the following notations

$\ell = (E, \vec{P}_e)$, $\ell' = (E', \vec{P}'_e)$ initial and final lepton fourmomentum

Θ_e = scattered electron L.S.angle

$K = \ell - \ell'$ virtual photon fourmomentum

$\tilde{q}$ = neutron momentum in π^+_- n C.M.S.

$q = (E_\pi, -\tilde{q})$ π^+ fourmomentum in the π^+_- n C.M.S.

$\tilde{\Theta}$, ϕ = polar and azimuthal neutron angles in the π^+n C.M.S. referred to the virtual photon direction.

$P_n = (E_n, \vec{P}_n)$ L.S. neutron fourmomentum

$K^2 = -2EE'(1-\cos\Theta_e)$ square mass of the virtual photon

$W = \sqrt{\tilde{q}^2 + M_n^2} + \sqrt{\tilde{q}^2 + M_\pi^2}$ invariant mass of the π^+_- n system

$\varepsilon = 1 / (1 - \frac{2|\vec{K}|^2}{K^2} \operatorname{tg}^2\Theta_e/2)$ polarization of the virtual photon

$\varepsilon_L = K^2/K_o^2\ \varepsilon$ longitudinal polarization

$K_L = (W^2 - M_p^2)/2M_p$ equivalent photon energy

The virtual photon polarization density matrix ρ shows that the electroproduction cross section takes contributions from the incoherent sum of the two pure virtual photon states:

$$\rho = \begin{bmatrix} \frac{1}{2}(1+\varepsilon) & 0 & -\left|\frac{1}{2}\varepsilon L(1+\varepsilon)\right|^{1/2} \\ 0 & \frac{1}{2}(1-\varepsilon) & 0 \\ -\left|\frac{1}{2}\varepsilon_L(1+\varepsilon)\right|^{1/2} & 0 & \varepsilon_L \end{bmatrix}$$

$$V_1 = \left(\left[\tfrac{1}{2}(1+\varepsilon)\right]^{1/2},\ 0,\ -\varepsilon_L^{1/2}\right), \qquad V_2 = \left(0,\ \left[\tfrac{1}{2}(1-\varepsilon)\right]^{1/2},\ 0\right)$$

The differential cross section is:

$$\frac{d\sigma}{dE'd\Omega_e d\Omega_\pi} = \Gamma_t\{\sigma_u + \varepsilon\sigma_L + \sqrt{\frac{\varepsilon(\varepsilon+1)}{2}}\cos\phi\sigma_I + \varepsilon\cos 2\phi\sigma_p\} = \Gamma_t\sigma$$

where

$$\Gamma_t = \frac{\alpha}{2\pi^2}\,\frac{E'}{E}\,\frac{K_L}{|K^2|}\,\frac{1}{1-\varepsilon}$$

is the flux of the virtual photons and σ is the virtual photoproduction cross section.

σ_u arises from the transversal component of the virtual photon and σ_L from the longitudinal one. σ_I and σ_P arise from the transversal-transversal and transversal-longitudinal interference respectively. A simple picture can be useful to understand how $G_A(K^2)$ is connected with π^+ electroproduction. The transition matrix element for electroproduction can be written with standard notations

$$<\pi^+(q),n(P_n)|J_\mu(0)|P(p)>\frac{1}{K^2}\bar{u}(\ell')\gamma_\mu u(\ell) = \frac{M_\mu j_\mu^{\text{lepton}}}{K^2}$$

Contracting the π^+ we obtain, for off shell pions

$$M_\mu = i(M_\pi^2 - q^2)\int dx^4\, e^{iqx} < n|T[\phi_\pi(x),\, J_\mu(0)]|P>$$

where

$$T[\phi_\pi(x),\, J_\mu(0)] = \Theta(x_o)[\phi_\pi(x),\, J_\mu(0)]$$

Making use of PCAC

$$\phi_\pi(x) = \partial_\mu A_\mu(x)\,/(M_\pi^2 f)$$

we have

$$M_\mu = \frac{M_\pi^2 - q^2}{M_\pi^2 f}\,\{q_\nu \int dx^4\, e^{iqx}<n/T[A_\nu(x),\, J_\mu(0)]|P> -$$

$$- i\int dx^3\, e^{-i\vec{q}\vec{x}}<n|[A_o(0,x),\, J_\mu(0)]|P>$$

In the limit $q \to 0$ the first integral contributes with the two Born terms, which are $O(1/q)$; hence it gives a finite result when multiplied by q_ν. The second integral, in the same limit $q \to 0$, can be evaluated using E.T.C.:

$$\lim_{q\to 0} \int d^3x\, e^{-i\vec{q}\vec{x}} \langle n|\,[A_o(0,x),\, J_\mu(0)]\,|P\rangle \;=\; -\langle n|\,[A_\mu(0)]\,|P\rangle \;=$$

$$= G_A(K^2)\;\bar{u}(P_n)\gamma_5\gamma_\mu u(P) + h_A(K^2)\;\bar{u}(P_n)\gamma_5 u(P)\;K_\mu$$

After a straighforward calculation one obtains the q→0 gauge invariant result:

$$\lim_{\tilde{q}\to 0} \frac{K_L}{\tilde{q}}\sigma = \{\sqrt{1 - \frac{K^2}{M_p^2}}\; g_{\pi nn}\; (\frac{G_A(K^2)}{G_A(0)} - \frac{K^2}{2M^2 - K^2}\; G_M^n(K^2))\}^2 + \varepsilon\,|\frac{L_{o+}}{K_o}|^2\;(-K^2)$$

where L_{o+} is the longitudinal s-wave multipole, proportional to $G_E^n(K^2)$ in the soft pion limit. For on mass shell pions two models evaluate finite mass corrections in a rather wide range of K^2. The first model, due to Furlan, Paver and Verzagnassi (5) has a validity up to $|K^2| \simeq .3$ $(GeV/c)^2$. The other one, due to Benfatto, Nicolò and Rossi (BNR) (6), uses "weak PCAC" and can be used up to $|K^2| \simeq 1$ $(GeV/c)^2$. Both these models use the soft pion results as a subtraction constant for the dispersive representation of the on mass shell amplitudes and give $\lim_{\tilde{q}\to 0} K_L\sigma/\tilde{q}$ as a function of $G_A(K^2)$. For this reason we have expanded the cross section in powers of $\tilde{q}$ around threshold ($\tilde{q}$=0):

$$\sigma = \frac{1}{2\pi}\,\frac{\tilde{q}}{K_L}\,[A_1 + B\tilde{q}^2 + C\tilde{q}^4 + \frac{\pi}{4}\,A_4\tilde{q}\,\cos\phi + \frac{2}{3}\,A_5\tilde{q}^2\,\cos 2\phi] \qquad (1)$$

where, $A_1 = \lim_{\tilde{q}\to 0}(K_L\sigma)/\tilde{q}$ contains $G_A(K^2)$; B and C account for the variation of σ above threshold and are necessary to obtain a correct value of A_1. A_4 and A_5 give σ_I and σ_P at threshold.

The experiment:

this experiment has been performed at the NINA Synchrotron by the Daresbury-Frascati-Pisa collaboration.
The following physicists were involved in the experiment:
D.R. Botterill, H.E. Montgomery, P.R. Norton (Daresbury), G. Matone (Frascati), A. Del Guerra, A.Giazotto, M.A. Giorgi, A. Stefanini (Pisa).
In this experiment the neutron was detected in coincidence with the scattered electron. We detected the neutron since, unlike the π^+, it was going in a narrow cone around the virtual photon direction, even for large W.
In this experiment the maximum W was chosen to have the neutron cone always

well inside the neutron detector; in this way we avoided geometry corrections. Table I contains the values of the relevant kinematical variables and the experimental settings.

Table I

$-K^2$ (GeV/c)^2	.45	.58	.88
E (GeV)	3.198	3.198	3.511
E' (GeV)	2.754	2.685	2.839
θ_e	13.0°	15.0°	17.1°
W_{max} (GeV)	1.132	1.144	1.132
ε	.96	.95	.94
θ_{nc}	53.0°	50.5°	46.5°
T_n (MeV)	130-330	175-400	270-540

Fig. 2 shows the experimental layout; the target was a cell containing 10 cm liquid H_2, with an identical empty cell underneath for BKG subtraction.

The electron spectrometer

was composed by two half quadrupoles and a vertical deflecting bending magnet. It includes a CO_2 $\check{C}$ counter and a shower counter. The resolutions were $\Delta P/P = \pm.25\%$ and $\Delta\theta_e = \pm.05^o$; the acceptances $\Delta P = 8\%$ and $\Delta\Omega_e = .6$ msr.

The neutron counter

was composed by an array of 145 blocks of plastic scintillator, each 15 x 15 x 27 cm^3; each block was seen by a RCA 8575 phototube; the neutron kinetic energy was measured by time of flight (TOF) ($\Delta\tau = \pm 1$ ns). A system of 26 veto counters pairs, with TOF facility, allowed to off-line coincide or anti-coincide the charged yield. The whole system was encased in a 40 tons Pb-Fe case with a front window of 5 cm Pb (see Fig. 3). An additional telescope (WAB counter) provided a signature for the protons from the process $ep \to ep\gamma$. The efficiency of the neutron detector was carefully measured both for true neutrons ($\eta_{nn} \simeq 20\%$), and for protons converted to neutrons in the front shielding ($\eta_{pn} \simeq 3\%$).

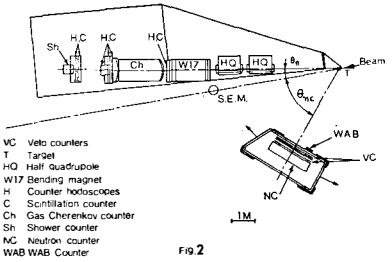

Fig. 2

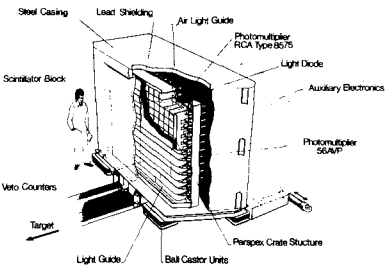

Fig. 3

Data analysis:

the data were binned in 45 W bins in the range .98 < W < 1.16 GeV and in 6 ϕ bins between 0 and 180°. Since we measure the L.S. kinetic energy and the angles of the neutron we could reconstruct the pion missing mass in each of the 45 x 6 bins. The pion mass peak was sitting on the random BKG and the S/N ratio was always > 3.

π^op subtraction and results:

to subtract the signal from the process $ep \to e'p\pi^o$ we had to know the expansion coefficients (see eq. (1)) for this reaction. For $|K^2|$ = .45 and .6 $(GeV/c)^2$ we used model dependent coefficients while at $|K^2|$ = .88 $(GeV/c)^2$ we directly measured this reaction using the neutron counter as a proton detector. The M.Carlo-simulated neutron yield in every W and ϕ bin was given by

$$G(W,\phi) = \int\int\int_{\text{accept.}} \{K^+(W,\phi|\tilde{q},\phi') \cdot \eta_{nn} \cdot [A_1 + B\tilde{q}^2 + C\tilde{q}^4 + \frac{\pi}{4}A_4\tilde{q}\cos\phi' + \frac{2}{3}A_5\tilde{q}^2\cos 2\phi'] +$$

$$+ K^o(W,\phi|\tilde{q},\phi') \cdot \eta_{pn} \cdot [A_1^o + B^o\tilde{q}^2 + C^o\tilde{q}^4 + \frac{\pi}{4}A_4^o\tilde{q}\cos\phi' + \frac{2}{3}A_5^o\tilde{q}^2\cos 2\phi']\}$$

where A_1, B, C, ... are the unknown $\pi^+ - n$ coefficients; A_1^o, B^o, C^o... are the known $\pi^o p$ coefficients. K^+ and K^o are the functions, evaluated by M.Carlo method, which measured the distortion on the data produced by the finite resolution of the apparatus; they include $\Gamma_t\tilde{q}/K_L$ and the radiative corrections. The final step of the analysis was to minimize with respect to A_1, B, C, A_4,

A_5 the χ^2 between the neutron yield and $G(W, \phi)$. The contributions of the $\pi^o p$ BKG to the $\pi^+ n$ yield was 5.5%, 10%, 15% at $|K^2|$ = .45, .6, .88 $(GeV/c)^2$ respectively. We estimate an overall 2% uncertainty due to this BKG subtraction.

In Fig. 4 the coefficient A_1 is plotted together with the results of our previous experiment (1) and the Desy results (4). The continuous line is the prediction of Devenish and Lyth dispersive model (8). To evaluate $G_A(K^2)$ we used the BNR (6) model, parametrizing:

$$\frac{G_A(K^2)}{G_A(0)} = 1 \;/\; (1 + \frac{|K^2|}{M_A^2})^n \quad \text{with } n=1,\ 2;$$

the best fit was done using the world's coincidence data (1,2,3,4) and the results of this experiment. See Fig. 5. The fit favoured the dipole representation (n=2) and gave a mass parameter M_A = .96 ± .03 GeV. One can see from the curves (a) and (b) of Fig. 5, that it is the point at $|K^2|$ = .88 $(GeV/c)^2$ which allowed to discriminate between dipole and monopole.

To further investigate the functional character of $G_A(K^2)$ we used the parametrization

$$\frac{G_A(K^2)}{G_A(0)} = 1 \;/\; (1+2C_A^2|K^2|+C_B^4|K^2|^2)$$

which reduces to the monopole for C_B=0 and to the dipole for C_A=C_B. Using the same data points and the BNR model we minimized the χ^2 with respect to C_A and C_B (see Fig. 6). The minimum is on the dipole line and there is evidence of dipole shape up to $\sqrt{2}$ ST.

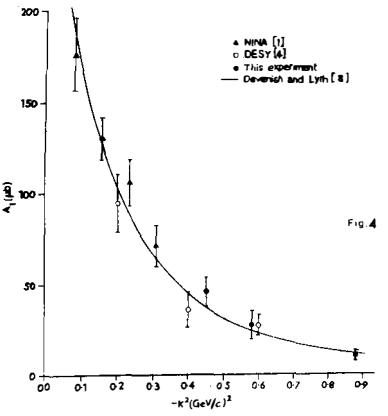

Fig. 4

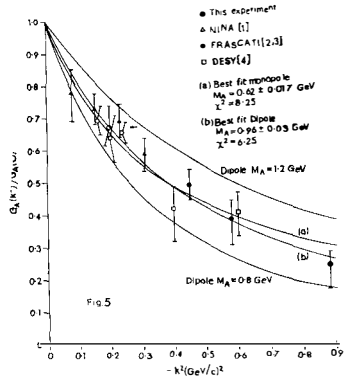

Fig. 5

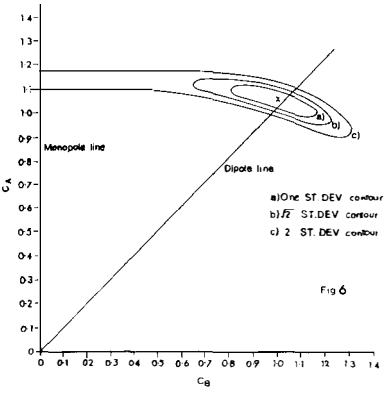

Fig. 6

DEV. A check on the finite pion mass corrections was done and it was found to be 8%, 13%, 20% at $|K^2|$ = .45, .6, .88 $(GeV/c)^2$ respectively. Electroproduction looks a very sensitive tool to measure $G_A(K^2)$: using BNR we obtained for the quantity

$$\delta_A(K^2) = \frac{\sigma(K^2, M_A = 1.1) - \sigma(K^2, M_A = 1.0)}{\sigma(K^2, M_A = 1.0)}$$

which is the relative variation of σ for 100 MeV M_A variation, the values 24%, 29%, 37% at $|K^2|$ = .45, .6, .88 $(GeV/c)^2$ respectively.

For the reaction $\nu + D \rightarrow P + P_s + \mu^-$, using a dipole representation for $G_A(K^2)$, Barish et al (7) quoted M_A = .84 ± .11 GeV from the differential cross section and M_A = .98 ± .13 GeV from the total cross section. This result is pictorially shown in Fig. 7 together with the value obtained in electroproduction using the BNR model. It is evident that there is full agreement between the neutrino and the electroproduction measurements of $G_A(K^2)$.

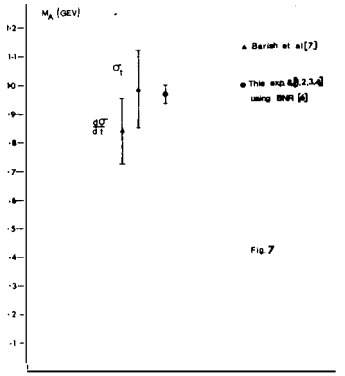

Fig. 7

References

(1) A.Del Guerra et al., Nucl. Phys. B99 (1975) 253.

(2) E. Amaldi et al., Nuovo Cimento 65A (1970) 377.

(3) E. Amaldi et al., Phys. Letters 41B (1972 (216).

(4) P. Brauel et al., Phys. Letters 45B (1973) 389 and Phys. Letters 50B (1974) 507.

(5) G. Furlan et al., Nuovo Cimento 62A (1969) 519.

(6) G. Benfatto et al., Nucl. Phys. B50 (1972) 205.

(7) S.J. Barish et al., quoted by D.H. Perkins, Invited talk, 7th Int. Symp. on Lepton and Photon Interactions, Stanford 1975.

(8) R.C.E. Devenish et al., Phys. Rev. D5 (1972) 47 and Nucl. Phys. B93 (1975) 109.

MORE THAN FOUR QUARK FLAVORS AND VECTOR-LIKE MODELS

F. HAYOT

DPh-T. C.E.N. Saclay

Abstract : This report gives a brief description of vector-like models, with emphasis - for experimentalist's sake - on the vector caracter at all energies of the weak neutral current in these models.

Résumé : Dans ce rapport on décrit brièvement les modèles dits "vectoriels", en insistant sur le caractère vectoriel à toute énergie du courant faible neutre dans ces modèles.

Many models with more than the usual four quark flavors have by now appeared in the literature. In this report we will limit ourselves to a description of vector-like models based on the weak gauge group $SU(2) \times U(1)$ of Weinberg and Salam[1]. These models appear to be the must compelling from a theoretical and esthetical point of view. Moreover, independently of the arrangement of additional quarks, they make some definite prediction about the nature of the weak current which can be tested at present energies.

As an introduction we recall that in the standard quark model, with flavors c, u, d and s, quarks are arranged, with respect to $SU(2) \times U(1)$, in two left-handed doublets

$$\begin{pmatrix} u \\ d_\theta \end{pmatrix}_L \qquad \begin{pmatrix} c \\ s_\theta \end{pmatrix}_L \tag{1}$$

and a number of right-handed singlets. Here

$$d_\theta = d \cos\theta + s \sin\theta$$

and $$s_\theta = -d \sin\theta + s \cos\theta,$$

where θ is the Cabibbo angle.
The leptons appear in the left-handed doublets

$$\begin{pmatrix} \nu_e \\ e^- \end{pmatrix}_L \qquad \begin{pmatrix} \nu_\mu \\ \mu^- \end{pmatrix}_L \tag{2}$$

and the right-handed singlets e_R and μ_R.
Left-handed here means that the couplings of the pairs (ν_e, e^-) and (u, d_θ), for example, to the intermediate vector boson are of V-A type.
There are two features of the arrangements (1) and (2) which we would like to point out. The first one is the existence of a lepton-hadron symmetry in the sense that four leptons have as a counterpart four quark flavors. The other one is the absence of the so-called triangular anomalies[2]. These anomalies, which occur in field theories with vector and axial vector currents, prevent renormalization and therefore have to be eliminated. In the above case these anomalies cancel because the sum of the charges of all leptons and quarks appearing in doublets is zero. (We always assume that each quark flavor appears in three colors). The most natural and elegant way to eliminate these anomalies is obviously to have no axial current at all. To obtain this result within the present framework, one has to introduce additional quarks of charges 2/3 and -1/3, and to arrange all available quarks in right-handed and left-handed doublets, in such a way that each single quark occurs in one

right-handed and one left-handed doublet. This is what happens in vector-like models, where above threshold for the production of any quark the theory becomes pure vector. Correspondingly, in the leptonic sector, which now is no longer linked to the hadronic one in order for the anomalies to cancel together, the introduction of new heavy leptons and right-handed doublets is required.

Phenomenologically, the four quark model, with the charmed quark, has been quite successful. The BNL event[3], the dimuon events of the HPWF collaboration[4], the μe events observed at Gargamelle and FNAL (discussed by M.Jaffre and D.Cundy at this Meeting), are interpreted in terms of the production and decay of charmed particles. Moreover, the "charmonium" spectroscopy explains the recently found new particle states. There are nevertheless indications that one will have to go beyond the four quark model : the apparent rich structure observed around 4 GeV/c in electron-positron annihilation, the value of 5.5 reached by R above 5 GeV/c in e^+e^- annihilation (whereas R = 3 1/3 in the four quark model and 4 1/3 if in addition a heavy lepton contributes to the hadronic state), the rise with energy of the ratio of the total antineutrino and neutrino cross-sections in deep inelastic $\nu(\bar{\nu})$ hadron $\rightarrow \mu^-(\mu^+)X$ scattering. (Preliminary results reported by C.Rubbia at this Meeting).

Among the many models with more than four quarks we will now describe the vector-like models, which we have introduced above, and whose theoretical justification appears the most compelling. To build a vector-like model, one has to add at least one new left-handed doublet to the two standard doublets given in (1). One then has for the left-handed doublets :

$$\begin{pmatrix} u \\ d_\theta \end{pmatrix}_L \qquad \begin{pmatrix} c \\ s_\theta \end{pmatrix}_L \qquad \begin{pmatrix} u' \\ d' \end{pmatrix}_L \quad , \tag{3}$$

where the only parameter retained is the Cabibbo angle. As mentioned above, each of the quarks in (3) has to appear also in a right-handed doublet. If one requires that ordinary $\Delta S = 0, 1$ decays are pure V-A, one is left with essentially two possibilities. These are

$$\begin{pmatrix} u \\ d' \end{pmatrix}_R \qquad \begin{pmatrix} c \\ d \end{pmatrix}_R \qquad \begin{pmatrix} u' \\ s \end{pmatrix}_R \tag{4}$$

or

$$\begin{pmatrix} u \\ d' \end{pmatrix}_R \qquad \begin{pmatrix} c \\ s \end{pmatrix}_R \qquad \begin{pmatrix} u' \\ d \end{pmatrix}_R \tag{5}$$

The set (3) + (4) (model I) is the model proposed by De Rujula, Georgi and Glashow[5], and (3) + (5) (model II) has been considered by many people[6]. There are constraints on all these models imposed by the $K_L - K_S$ mass difference, and by the relative sign of the I = 1/2 and I = 3/2 contribution in $K \to 2\pi$ and $K \to 3\pi$ decays[7]. The effects of these constraints are hard to evaluate and we will not discuss them here (for a short review see ref.8). Models (I) or (II) are the simplest vector-like models one can consider, with six quark flavors and as sole parameter the Cabibbo angle. They will serve to illustrate the general behavior of the weak charged hadronic current in vector-like models. First, the is a series of thresholds associated with the energies necessary to create the heavy quarks. Above all thresholds the theory is vector and thus, in this region, the differential cross-sections in inelastic neutrino-hadron and antineutrino-hadron scattering become equal. In particular the ratio

$$R = \frac{\sigma(\bar{\nu}p \to \mu^+ X) + \sigma(\bar{\nu}n \to \mu^+ X)}{\sigma(\nu p \to \mu^- X) + \sigma(\nu n \to \mu^- X)} \qquad (6)$$

goes to 1, and this holds in any model.

In model I it is assumed that the u' and d' quark are much heavier than the charmed quark. Relative to the four quark model (3), the new contribution above charm thershold will come from the right-handed doublet $\begin{pmatrix} c \\ d \end{pmatrix}_R$.

This term acts on the valence quarks in neutrino scattering only, thus destroying charge symmetry (as measured for instance by the Adler sum rule) between ν and $\bar{\nu}$ scattering on an isoscalar target. Moreover while the $\begin{pmatrix} c \\ d \sin\theta \end{pmatrix}_L$ doublet contributes to the inelastic differential ν-hadron cross-section a term independent of the standard variable y, the right-handed $\begin{pmatrix} c \\ d \end{pmatrix}_R$ contributes a $(1-y)^2$ dependent term. This is a general feature, namely in a given scattering process the y dependence of a right-handed doublet is 1 (respectively $(1-y)^2$) if the y dependence of the corresponding left-handed doublet is $(1-y)^2$ (respectively 1). In the present case the ratio R (6), above c threshold(below u', d') decreases to 1/4 from the 1/3 of the valence quark contributions below it, while it will ultimately increase to 1, as mentioned above.

In model II, the c quark is not excited from the valence quarks (when $\theta = 0$), and therefore we assume that at present energies the u', d' quarks are excited. As a possibility, we consider the masses of the c, u', d' quarks to be degenerate. Then one obtains a valence quark contribution in inelastic ν and $\bar{\nu}$ scattering from the right-handed doublets $\begin{pmatrix} u' \\ d \end{pmatrix}_R$ and $\begin{pmatrix} u \\ d' \end{pmatrix}_R$ respectively. While the average $\langle y \rangle_{\bar{\nu}}$ in $\bar{\nu}$ scattering below c, u', d' is 1/4 for the valence

quark distribution at low energies, it remains at this value (above c and below u', d') in model I, but reaches the value of 7/16 in II (above u', d'). However in II, above this same threshold, R reaches the value of 1. These and other results are summarized in the Table for the valence quark contributions (and $\theta = 0$) in deep inelastic ν and $\bar{\nu}$ scattering. The numbers given here correspond to phenomena well above threshold, and it clearly remains an important question at what pace these numbers are approached.

Table

For models I and II, valence quark contributions (for zero Cabibbo angle) in deep inelastic neutrino- and antineutrino- scattering on an isoscalar target. For differential and total cross-sections, only the y dependence is given. The average values of y and the ratio R are of course independent of the x distributions.

Quark doublet contributions	$\begin{pmatrix} u \\ d \end{pmatrix}_L$	Model I (above c threshold below u', d') $\begin{pmatrix} u \\ d \end{pmatrix}_L + \begin{pmatrix} c \\ d \end{pmatrix}_R$	Model II $\begin{pmatrix} u \\ d \end{pmatrix}_L + \begin{pmatrix} u \\ d' \end{pmatrix}_R$ or $\begin{pmatrix} u' \\ d \end{pmatrix}_R$
$\frac{d\sigma^\nu}{dxdy} \equiv d\sigma^\nu$	1	$1 + (1-y)^2$	$1 + (1-y)^2$
σ^ν	1	$\frac{4}{3}$	$\frac{4}{3}$
$\langle y \rangle_\nu$	$\frac{1}{2}$	$\frac{7}{16}$	$\frac{7}{16}$
$d\sigma^{\bar{\nu}}$	$(1-y)^2$	$(1-y)^2$	$(1-y)^2 + 1$
$\sigma^{\bar{\nu}}$	$\frac{1}{3}$	$\frac{1}{3}$	$\frac{4}{3}$
$\langle y \rangle_{\bar{\nu}}$	$\frac{1}{4}$	$\frac{1}{4}$	$\frac{7}{16}$
$R = \frac{\sigma^{\bar{\nu}}}{\sigma^\nu}$	$\frac{1}{3}$	$\frac{1}{4}$	1

Vector-like models with more than six quarks are of course possible. Actually, eight quarks are required if one wants to have complete lepton-hadron symmetry, in the sense that in the leptonic vector also, the right-handed doublets contain the same leptons as the left-handed ones. One is then lead to a model with at least eight leptons, in order to avoid the occurrence of a right-handed $\begin{pmatrix} \nu_\mu \\ \mu^- \end{pmatrix}_R$ or $\begin{pmatrix} \nu_e \\ e^- \end{pmatrix}_R$, incompatible with the data. Right-handed partners of the ν_e and ν_μ nevertheless appear, but only in association with some heavy charged lepton. By symmetry between leptons and hadrons, this consideration leads to eight quark flavors in the hadronic vector. Here of course many combinations are possible. In some models, moreover, of different type, one introduces massive Majorana spinors in the leptonic sector as

in $\begin{pmatrix} M \\ \mu^- \end{pmatrix}_R$ which leads to neutrinoless double μ decays.

It is clear from the preceding description and discussion that as far as the structure of the weak charged current is concerned, it will not be easy to pinpoint its features, in particular its quark content, from the data, and even to establish the relevance of vector like models. Fortunately there is one aspect of these models that can be put to exprimental test : in all of them the weak neutral hadronic current in pure vector, and so are the electron and muon couplings, and this holds at all energies. A number of important consequences follow :

a) there are no parity violating effects in atomic physics in lowest order of G.

b) the differential cross-sections

$$\nu + A \rightarrow \nu + B$$

$$\bar{\nu} + A \rightarrow \bar{\nu} + B$$

where A, B are any hadronic states, are equal.

In particular

(i) in elastic $\nu_\mu(\bar{\nu}_\mu)\, e^-$ scattering the quantity $g_A = 0$ whereas, for comparison, in the Weinberg-Salam model $g_A = -1/2$.

(ii) in inelastic $\nu(\bar{\nu})$ hadron $\rightarrow \nu(\bar{\nu})X$ scattering, the differential cross-sections for ν and $\bar{\nu}$ are equal (at all x and y).

The relevant couplings to the u and d quarks are given by the Lagrangian

$$\mathcal{L}_{\text{neutral}} = \frac{G}{\sqrt{2}} \bar{\nu}\, \gamma^\mu (1-\gamma_5)\nu \left\{ \bar{u}\, \gamma_\mu \left[\alpha(1-\gamma_5) + \beta(1+\gamma_5)\right] u + \bar{d}\, \gamma_\mu \left[\gamma(1-\gamma_5) + \delta(1+\gamma_5)\right] d \right\} \qquad (7)$$

In vector-like models one has

$$\alpha = \beta = 1/2\left(4/3 \sin^2 \theta_W - 1\right)$$

$$\gamma = \delta = 1/2(1 - 2/3 \sin^2 \theta_W)$$

where θ_W is the Weinberg angle. Except for a factor of α in the u quark coupling and a factor γ in the d coupling, the expression is identical to the

hadronic coupling in deep inelastic electron scattering, where the y dependence is given by $1 + (1-y)^2$.

Evidently in the Weinberg-Salam model $\alpha \neq \beta$ and $\gamma \neq \delta$, since there the weak neutral current has a V-A piece.

Consider in particular the ratios

$$R_{\bar{\nu}} = \frac{\sigma(\bar{\nu}p \to \bar{\nu}X + \bar{\nu}n \to \bar{\nu}X)}{\sigma(\bar{\nu}p \to \mu^+ X + \bar{\nu}n \to \mu^+ X)}$$

and similarly for R_ν.

For vector-like models one has a linear relationship between R_ν and $R_{\bar{\nu}}$, given by

$$R_\nu = \frac{\sigma(\bar{\nu}p \to \mu^+ X + \bar{\nu}n \to \mu^+ X)}{\sigma(\nu p \to \mu^- X + \nu n \to \mu^- X)} R_{\bar{\nu}}$$

where, as indicated above,

$$R_\nu = (\alpha^2+\gamma^2) \frac{\int dE \phi_\nu(E) \int_{E_o/E}^{1} \left[1+(1-y)^2\right] dy}{\int dE\, \phi_\nu(E) \int_{E_o/E}^{1} dy} .$$

Here $\phi_\nu(E)$ describes the incoming neutrino spectrum and we have assumed that there is a lower bound E_o on the observed hadronic energy. We have also used a ratio equal to 1 for the mass of the neutral weak boson to the corresponding mass as given in the Weinberg-Salam model. Comparison with experiment shows that this is reasonable[9].

Clearly, from the experimental point of view, it is the vector nature of the neutral current which provides the crucial tests for the relevance of vector-like models. The nature of the neutral current has been investigated both by the Gargamelle group (report by V.Brisson at this Meeting) and by the Caltech group (report by H.Bodeck at this Meeting) in inelastic ν and $\bar{\nu}$ scattering.

The results reported by the Gargamelle group are such as to exclude a pure vector neutral current (four standard deviation effect) while the results of the Caltech group are best fitted by a V-A current with V admixture, as in the Weinberg-Salam model, without however excluding a pure V current (one standard deviation effect). Further tests about the V and A components of the neutral current are required and will soon tell whether the elegance of the way of eliminating field theoretical triangular anomalies, used in vector-like models, is supported by the physics of neutral currents.

Acknowledgments :

I am very thankful to J. Zinn-Justin for his help and for very instructive discussions.

References

(1) For a review, see E.S.Abers and B.W.Lee, Physics Reports 9C, 1 (1973)

(2) S.L.Adler in Lectures on Elementary Particles and Quantum Field Theory, edited by S.Deser, M.Grisaru and H.Pendelton (MIT Press, Cambridge, Mass. 1970)

(3) N.P.Samios, in Proceedings of the 1975 International Symposium on Lepton and Photon Interactions at High Energies, edited by W.T.Kirk, SLAC (1975)

(4) C.Rubbia, in Proceedings of the 1975 International Symposium in Lepton and Photon Interactions at High Energies, edited by W.T.Kirk, SLAC (1975)

(5) A.de Rujula, H.Georgi, and S.L.Glashow, Phys.Rev.Letters 35, 69 (1975)

(6) For a review and references see R.M.Barnett,Fermilab-Conf-75/71-THY preprint (September 1975)

(7) E.Golowich and B.R.Holstein, Phys.Rev.Letters 35, 831 (1975)

(8) B.W.Lee, Fermilab -Conf-76/20-THY/EXP preprint (February 1976)

(9) A.de Rujula, H.Georgi and S.L.Glashow, Harward preprint (1975).

o o
o

Five-Quark Model with Flavour-Changing Neutral Current and Dimuon Events*

J. E. Kim and Kyungsik Kang

Department of Physics
Brown University
Providence, R.I. 02912, U.S.A.

ABSTRACT

The recent dimuon data seem to suggest either the necessity of flavour-changing hadronic neutral current or proliferation of quarks beyond charm or both. We show here how a five-quark model based on simple gauge group SU(2) x U(1) x U(1)' can generate the flavour-changing, in particular the needed charm-changing, neutral current in a natural fashion. A substantial D^o-$\bar{D}^o$ mixing can be obtained to account for the "wrong-sign" dimuons observed in ν_μ-induced reactions. Because of the role of the extra neutral boson in this model, the flavour-changing neutral current is decoupled from leptonic sectors, thus suppressing the trimuon events as experiments indicate thus far.

1. Recent Developments

The four-quark scheme[1] of Glashow, Iliopoulous, and Maiani (GIM) coupled with the minimal gauge group[2] SU(2) x U(1) has been quite successful in leptonic and semileptonic phenomenology; it has the symmetry between leptons and hadrons, suppresses the strangeness-changing neutral current processes and can explain the narrow ψ-particles as bound states of the fourth charmed quark-antiquark pair ($c\bar{c}$). Despite its success, recent efforts suggest further proliferation of quarks beyond c and/or going beyond the minimal gauge group of Weinberg and Salam (WS). Namely,

A. The ratio R of cross sections for $e^+e^- \to$ hadrons and $e^+e^- \to \mu^+\mu^-$ is approximately constant about 5 at high energies[3],

B. The neutrino experiments[4] by HPWF collaboration have observed dimuons in abundance, i.e., $\sigma_\nu(\mu^-\mu^+)/\sigma_\nu(\mu^-) \simeq 10^{-2}$, $\sigma_{\bar{\nu}}(\mu^+\mu^-)/\sigma_\nu(\mu^-\mu^+) \simeq 0.8 \pm 0.6$. Furthermore, the wrong-sign dimuons have been observed both for ν_μ and $\bar{\nu}_\mu$ interactions, i.e., $\sigma_\nu(\mu^-\mu^-)/\sigma_\nu(\mu^-\mu^+) \simeq 10^{-1}$, while no trimuon events are seen yet.

C. Efforts[5] to construct the anomaly-free vectorlike theory have to introduce at least two more quarks beyond c in order to be consistent with the known experimental constraints.

The point A has been the basis[6] of speculating more quarks, such as t and b, with the usual color tripling so that R becomes 15/3. In vectorlike theory with the minimal gauge group, these are assigned to a doublet along with the two doublets of GIM. From lepton-hadron symmetry, such theory then requires one more charged heavy lepton plus a few neutrals. However, we notice from the point B that the standard model, i.e., the four-quark model of GIM based on the WS gauge group, may have to be modified either through proliferation of heavy quarks or through enlargement of the gauge group or perhaps both. Namely, the standard model says;

(1) Since c is produced through the charged current from d-quark and because of rarity of sea partons in the nucleons, one gets $\sigma_\nu(\Delta C=1)/\sigma_\nu(\Delta C=0) \simeq \sin^2\theta_c \simeq 4\%$. On the other hand, from experi-

ments, the leptonic and semileptonic $\Delta C=1$ cross section is about 1%, which puts a lower bound of the branching ratio, $B>20\%$. This number for B is somewhat uncomfortably larger than the usual estimate based on the stadard model.[7]

(2) Because of no valence quark contribution, $\sigma_{\bar{\nu}}(\Delta C=-1)$ in $\bar{\nu}$-induced reactions is expected to be suppressed but the experiments, though the data is meager at the moment, show that dimuons are produced in $\bar{\nu}$-reactions at a comparable rate as in ν-reactions. Clearly, any modification of the standard model to enhance $\sigma_{\nu}(\Delta C=1)$ must also do the same for $\sigma_{\bar{\nu}}(\Delta C=-1)$.

(3) The standard model can give at the most 0.1% instead of 10% for $\sigma_{\nu}(\mu^{-}\mu^{-})/\sigma_{\nu}(\mu^{-}\mu^{+})$. Thus one is needed to have a substantial $D^{o}(c\bar{u})$-$\bar{D}^{o}(\bar{c}u)$ mixing[8] analogous to K^{o}-$\bar{K}^{o}$ mixing and this can be done through proliferation of more heavy quarks or the charm-changing neutral current. However, a model with charm-changing neutral current based on the gauge group SU(2) x U(1) is expected to give trilepton events through Z_{μ} decay into a $\mu^{+}\mu^{-}$ pair, though it is possible to make the charm-changing neutral current small while maintaining the maximal D^{o}-$\bar{D}^{o}$ mixing.

(4) If the associated production of charmed hadron and its antiparticle pairs in $\Delta C=0$ charged current reactions is the source of the wrong-sign dimuons, one should occasionally see trimuon events at a comparable rate.

Thus we may say that if the present data on the dimuon events is born out by further experiments, one has to modify the standard model by going beyond the minimal gauge group SU(2) x U(1) and perhaps with more heavy quarks. We note in addition that no flavour-changing neutral current exists in a scheme where all of the left-handed (or right-handed) quarks are assigned to the equal dimensional representation of the weak SU(2) group as in the vectorlike models.

2. SU(2) x U(1) x U(1)' Gauge Group

The standard model is known to account for only about 25% of the

needed $\Delta I = \frac{1}{2}$ enhancement in nonleptonic weak decays. To salvage this, an additional charm-changing right-handed charged current $\bar{c}\gamma_\mu(1-\gamma_5)d$ has been suggested.[9] But this current makes the K_L-K_S mass difference too big when evaluated by keeping the vacuum intermediate state.[8] Though it may be still possible to give desirably small mass difference as the CP odd states contribute negatively,[10] this right-handed current does not agree with the requirement of PCAC and current algebra for $K \to 2\pi$ and 3π decays, which is supported by experiments.[11] We have originally proposed[12] the gauge group SU(2) x U(1) x U(1)' with the GIM quarks to explain the $\Delta I = \frac{1}{2}$ rule and suppression of $\Delta S=2$ transition simultaneously. As we have discussed in Ref. 12 the extra gauge group U(1)' may be a subgroup of $SU(3)_{color}$ x · · · · or manifestation of octet gluons in a picture where the strong interactions are exactly gauge invariant under color-tripling of quarks, and octet color gluons etc.

In this group, a triplet gauge field $A_\mu^\alpha(\alpha=1,2,3)$ and two singlets B_μ and C_μ are coupled to the weak isospin, hypercharge and charm groups $\vec{I}$, Y and C respectively. In addition there are a scalar doublet $\begin{pmatrix}\phi^+\\ \phi^o\end{pmatrix}$ and a neutral singlet ϕ' to give rise the spontaneous symmetry breaking. Since the charge assignment in a multiplet is dictated by $Q=I_3+(Y+C)/2$, one has freedom to choose Y or C and fix the other from this relation, thus introducing one more parameter for every multiplet than in SU(2) x U(1). However this freedom can be severely restricted by requiring that the additional neutral vector boson X_μ, which is obtained along with the usual Z_μ and the photon field A_μ through the three orthogonal combinations of A_μ^3, B_μ and C_μ, does <u>not</u> couple to leptons. In this way, the successful aspect of the standard model concerning the leptonic and semileptonic phenomenology is kept intact. To have the correct EM interactions of electrons, the three coupling constants in the model are related by $-e = g\sin\theta_w = g'\cos\theta_w\sin\zeta = g''\cos\theta_w\cos\zeta$ and $e^{-2} = g^{-2}+g'^{-2}+g''^{-2}$. The masses of the gauge bosons are $M_w^2 = g^2/4\sqrt{2}G_F$, $M_Z = M_w\sec\theta_w$, $M_A = 0$ and $M_X = Gv'/2$ where $v' = \sqrt{2}\langle\phi'\rangle_o$ and $G = (g'^2+g''^2)^{\frac{1}{2}}$. Note that M_X is independent from M_w or M_Z.

3. Flavour-Changing Neutral Currents With Five Quarks

The experimental constraints elaborated in Section 1 can easily be satisfied[13] by the tricolored five quarks u, d, s, c, and f with the gauge group SU(2) x U(1) x U(1)' where f is the heaviest quark with charge 2/3 carrying fancy quantum number. If we arrange the gauge parameters so that X_μ couples to hadronic charm-changing neutral current only, the observed dimuon parameters and absence of trimuons can be explained naturally in this model. Namely, focusing on the $D^o(c\bar{u})$ formation in ν_μ-induced reactions, the right-sign dimuons are produced through its semileptonic decay to $K^-\mu^+\nu_\mu$ and the wrong-sign dimuons through switching to $\bar{D}^o(\bar{c}u)$ and its subsequent decay to $K^+\mu^-\bar{\nu}_\mu$. Since X_μ does not couple to leptons, no trimuons are expected in this model.

In this five quark scheme, we must have two left-handed doublets to suppress the strageness-changing neutral current and therefore a left-handed singlet is left, which is responsible for charm-changing or fancy-changing neutral current. We take them as

$$L_1 = \begin{pmatrix} u' \\ d' \end{pmatrix}_L \quad , \quad L_2 = \begin{pmatrix} c' \\ s' \end{pmatrix}_L \quad , \quad f'_L \tag{1}$$

where

$$\begin{pmatrix} u' \\ c' \\ f' \end{pmatrix} = \begin{pmatrix} \cos\theta_c & -\sin\theta_c\cos\alpha & -\sin\theta_c\sin\alpha \\ \sin\theta_c & \cos\theta_c\cos\alpha & \cos\theta_c\sin\alpha \\ 0 & -\sin\alpha & \cos\alpha \end{pmatrix} \begin{pmatrix} u \\ c \\ f \end{pmatrix} \tag{2}$$

The 3 x 3 orthogonal transformation (2) warrants not only the correct Cabibbo charged current but also the decoupling (coupling) of the flavour-changing current from (to) $Z_\mu(X_\mu)$. The neutral interaction is given by

$$\mathcal{L}^o_{int} = -eV^{em}_\mu A_\mu - \frac{g}{2}\sec\theta_w J^Z_\mu Z_\mu - \frac{G}{2} J^X_\mu X_\mu \tag{3}$$

where V^{em}_μ and J^Z_μ for $\alpha=0$ have exactly the same structure as in the standard model and J^X_μ contains charm or fancy changing neutral currents,

$$J^X_\mu \sim -i\sin 2\theta_c\{\cos\alpha(\bar{u}_L\gamma_\mu c_L+\bar{c}_L\gamma_\mu u_L)+\sin\alpha(\bar{u}_L\gamma_\mu f_L+\bar{f}_L\gamma_\mu u_L)\} \tag{4}$$

of which the first term is responsible for the D^o-$\bar{D}^o$ mixing discussed above.

Finally we mention that a vectorlike model can be constructed in this five quark scheme by considering (1) and

$$R_1 = \begin{pmatrix} c \\ s \end{pmatrix}_R \quad , \quad R_2 = \begin{pmatrix} f \\ d \end{pmatrix}_R \quad , \quad u_R \tag{5}$$

From lepton-hadron symmetry, one heavy charged lepton is needed;

$$\begin{pmatrix} \nu_e \\ e^- \end{pmatrix}_L \quad , \quad \begin{pmatrix} \nu_\mu \\ \mu^- \end{pmatrix}_L \quad , \quad L^-_L \quad , \quad \begin{pmatrix} \nu_e \\ L^- \end{pmatrix}_R \quad , \quad \begin{pmatrix} N_\mu \\ \mu^- \end{pmatrix}_R \quad , \quad e^-_R \tag{6}$$

Here, N_μ is the Majorana spinor composed of right-handed muon neutrino and its antiparticle. Note that in this model the neutral currents are not of pure V-type due to the presence of singlets. The ratio R_C of cross sections of $\bar{\nu}_\mu + N \to \mu^+ \cdots$ and $\nu_\mu + N \to \mu^+ + \cdots$ is $\frac{1}{4}$ above the fancy threshold. It is interesting to observe that the heavy lepton L^- should decay right-handedly, which leads to speculation that the recently discovered U particle[14] is a possible candidate.[15]

Footnote and References

1. S. L. Glashow, J. Iliopoulos and L. Maiani, Phys. Rev. D2, 1285 (1970).
2. S. Weinberg, Phys. Rev. Lett. 19, 1264 (1967); 27, 1688 (1972); A. Salam, in Elementary Particle Theory: Relativistic Groups and Analyticity (Nobel Symposium No. 8), edited by N. Svartholm (Almquist and Wiksells, Stockholm, 1968), p. 367.
3. R. Schwitters, in International Symposium on Lepton and Photon Interaction at High Energies, (Stanford University, 1975).
4. A. Benvenuti et al., Phys. Rev. Lett. 34, 419 (1975); 35, 1199; 1203; 1249 (1975).
5. H. Georgi and S. L. Glashow, Phys. Rev. D6, 429 (1972); A. DeRujula, H. Georgi and S. L. Glashow, Phys. Rev. D12, 3589 (1975); H. Fritzch, M. Gell-Mann and P. Minkowski, Phys. Lett. 59B, 256 (1975).
6. H. Harari, SLAC preprint, SLAC-PUB-1568 (1975).
7. M. K. Gaillard, in Proceedings of the Xth Rencontre de Moriond, (Méribel-lès-Allues, France, 1975), edited by J. Tran Thanh Van; A. Pais and S. B. Treiman, Phys. Rev. Lett. 35, 1556 (1975).
8. R. L. Kinglsey, S. B. Treiman, F. Wilczek, and A. Zee, Phys. Rev. D11, 1919 (1975); F. A. Wilczek, A. Zee, R. L. Kingsley and S. B. Treiman, Phys. Rev. D12, 2768 (1975).
9. A. DeRujula, H. Georgi and S. L. Glashow, Phys. Rev. Lett. 35, 69 (1975).
10. G. Branco, R. N. Mohapatra and T. Hagiwara, CCNY Preprint COO-2232B-84 (1975); See also the second reference of Ref. 5.
11. E. Golowich and B. R. Holstein, Phys. Rev. Lett. 35, 831 (1975).
12. K. Kang and J. E. Kim, Brown University preprints COO-3130TA-325; COO-3130TA-327, in which the details of the SU(2) x U(1) x U(1)' gauge model can be found.
13. Further details of the analysis can be found in K. Kang and J. E. Kim, Brown University Preprint COO-3130TA-330.
14. M. L. Perl et al., Phys. Rev. Lett. 35, 1489 (1975).
15. See for example the analysis of S. Y. Park and A. Yildiz, Harvard University preprint.

NEUTRAL CURRENTS

IN GARGAMELLE

Violette BRISSON
Ecole Polytechnique, Palaiseau, France

Abstract : We present here all the new results on neutral currents which have appeared since about a year in the Gargamelle experiment. Three channels have been investigated : purely leptonic reactions, and in hadronic reactions, inclusive and one pion channels.

Résumé : Ici sont présentés tous les résultats nouveaux sur les courants neutres qui ont été extraits de l'expérience Gargamelle depuis environ un an. Les courants neutres ont été recherchés de trois manières différentes : dans les réactions purement leptoniques, et en ce qui concerne les hadroniques, dans les réactions inclusives et dans les canaux à un pion.

In this report, I will concentrate on what new results have been obtained in the different channels in which we have looked for neutral currents since about a year.

The chamber used was Gargamelle filled with heavy freon CF_3Br. The energy spectrum of the neutrino and antineutrino beams is peaked around 2 GeV.

Three different ways of investigating neutral currents have been chosen, and will be successively described :

- Purely leptonic neutral currents
- Hadronic neutral currents :
  - . one pion channels
  - . inclusive reactions

I. PURELY LEPTONIC NEUTRAL CURRENTS

The reaction

$$\bar{\nu}_\mu + e^- \rightarrow \bar{\nu}_\mu + e^-$$

has been studied in 1.400.000 pictures taken partly with booster, corresponding to a total number of $4.7\ 10^{18}$ protons on the target. The useful volume in Gargamelle was $6.3\ m^3$.

The analysis is now completely finished. Events looked for were e^-, e^+ and $e^\pm$ candidates, and isolated e^+e^- pairs, in the following cuts : $0.3 < E_e < 2$ GeV, and $\theta_{(e,beam)} < 5°$.

We have found $3e^-$, $6e^+e^-$ pairs, and one event ambiguous e^-/e^+e^- pair.

A. *Background*

1. Isolated γ's without wisible e^+

The probability for a γ to appear like an e^- has been found to be $(3.4 \pm .7)\%$. The 6 pairs inside the cuts and the e^-/γ ambiguous event lead to a background of $7 \times .034 = .24 \pm .11$ event.

Remark : The number of pairs is consistent with expectation from $1\pi°$ NC with only 1γ detected.

2. $\nu_e + n \rightarrow e^- + p$ with an e^- inside the cuts and a proton not seen.

The estimation comes from the reaction $\nu_\mu + n \rightarrow \mu^- + p$ with $\theta_\mu < 5°$ and a proton not seen, which has been determined experimentally as (1.4 ± .5)% of $\nu_\mu + n \rightarrow \mu^- + mp$. Among those events, only 1 out of 15 satisfy the $E_e < 2$ GeV cut. The total number of $\nu_e + n \rightarrow e^- + mp$ events is 70, leading to a background of 0.07 ± 0.04 event.

3. $\nu_e(\bar{\nu}_e) + e^- \rightarrow \nu_e(\bar{\nu}_e) + e^-$

These reactions occur through both CC and NC : the cross section for charged currents, computed in supposing V-A coupling lead to a background of 0.03 ± 0.02 ev. for ν_e and 0.08 ± 0.06 ev. for $\bar{\nu}_e$.

The total background is .42 event. The probability that the three events are due to background is 1%.

B. *Signal losses*

Events can be lost for three reasons :

1. Scanning losses : the scan efficiency has been measured to be 92%.

2. Identification ambiguities

The probability that an e^- looks like a γ has been determined experimentally and varies from 8% to 20% inside the cuts.

The impossibility to determine the charge of electrons varies from 5% to 13% inside the cuts. The corrections for these losses depend on the electron energy spectrum and are model dependent.

3. Kinematical losses due to the cuts depend on the model.

For Weinberg model, the overall efficiency is about 50%, whatever the value of $\sin^2\theta_w$.

C. *Interpretation*

The observed cross section uncorrected for losses depending on the model is

$$\sigma_{obs} = .05\ 10^{-41}\ E_{\bar{\nu}}\ cm^2/e$$

The 90% C.L. limits are :

$$.01\ 10^{-41}\ E_{\bar{\nu}} < \sigma_{obs} < .12\ 10^{-41}\ E_{\bar{\nu}}\ cm^2/e$$

Our data can be compared to theoretical predictions, after correction for signal losses. Assuming that the neutral leptonic current is a linear combination of V and A,

$$l_\mu = \bar{\nu}_\mu\ \gamma_\mu\ (1 + \gamma_5)\nu_\mu\ \bar{e}\gamma_\mu(G_V + G_A\ \gamma_5)e$$

the differential cross section can be expressed as :

$$\frac{d\sigma}{dy} = \frac{2G^2 m E_{\bar{\nu}}}{\pi}\left[\left(\frac{G_V + G_A}{2}\right)^2 (1 - y)^2 + \left(\frac{G_V - G_A}{2}\right)^2\right], \text{ with } y = E_e - / E_{\bar{\nu}}$$

Integration over the electron energy (taking account of identification probability) and on the $\bar{\nu}_\mu$ spectrum, and correction for scan efficiency lead to a predicted number of events $n = f(G_V, G_A)$. We can compute a likelihood function $(G_V, G_A) = \frac{m^3 e^{-m}}{6}$ where m = n + background. The most probable countour and the 90% confidence area are shown in fig. 1.

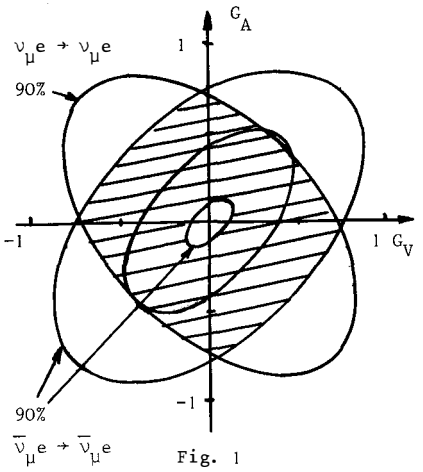

Fig. 1

The shaded area is the zone for G_A and G_V allowed by both results from ν and $\bar{\nu}$ (1).

In the frame of Weinberg model, the only parameter is θ_w, such as

$$G_V = -\frac{1}{2} + 2\sin^2\theta_W\ ,\quad G_A = -\frac{1}{2}$$

A one parameter likelihood function leads to $\sin^2\theta_W < .4$, with 90% confidence. Combining this result with our previous results on $\nu_\mu e^- \to \nu_\mu e^-$ we get

$$0.1 < \sin^2\theta_W < 0.4$$

Remark.- A new run of 250.000 pictures in a ν_μ beam has allowed the observation of one candidate for the reaction $\nu_\mu e^- \to \nu_\mu e^-$. The analysis is being performed.

II. ONE PION NEUTRAL CURRENTS

All the details about the determination of the ratios

$$R_{\nu(\bar{\nu})} = \frac{\sigma(\nu_\mu(\bar{\nu}_\mu) + N \to \nu_\mu(\bar{\nu}_\mu) + N' + \pi^\circ)}{2\sigma(\nu_\mu(\bar{\nu}_\mu) + N \to \mu^- (\mu^+) + N' + \pi^\circ)}$$

have been published in 1975[2]. Here only the results are recalled to introduce the study on isospin properties of neutral current which has been performed recently. The analysis has been done on 120.000 ν pictures and 120.000 $\bar{\nu}$ pictures (partly with booster). NC candidates were defined as events with 1 or 2γ's and protons, or 2γ's without protons. Because most of the events were not very energetic, no hadronic energy cut could be made, which lead to difficulties for evaluating the background : it is probable that we have a contamination from low energy neutrons coming from beams. Two evaluations of the background have been given :

- a minimum background has been computed, which accounts only for neutrino induced neutrons.

- a maximum background has been estimated from the very pessimistic assumption that all NC candidates with a single π^- (+ protons eventually) are due to neutron interactions.

The final numbers are given in Table 1.

	CC	NC				
	π° events	π°events	π^- events	π°/π^-	Max BG	Min BG
ν	338±27	146±13	60	2.4±.5	60±19	22 ±8
$\bar{\nu}$	199±15	176±14	42	4.2±.7	42±11	9 ± 4
AS		39 (28 in ν, 11 in $\bar{\nu}$)	40	.97±.23		

with maximum background, we get

$$R_{\nu}^{max} = .18 \pm .02 \qquad R_{\bar{\nu}}^{max} = .40 \pm .04$$

with minimum background :

$$R_{\nu}^{min} = .13 \pm .03 \qquad R_{\bar{\nu}}^{min} = .32 \pm .06$$

with 68% probability : $0.10 < R_{\nu} < 0.20$

$$0.26 < R_{\bar{\nu}} < 0.44$$

Interpretation

A tentative interpretation has been made in the frame of Weinberg-Salam model. We need a model for estimating the effects of nuclear rescattering. An early attempt was made by Albright et al[3], who give a lower bound for R_{ν}, related to the cross section for the reaction $e^{-}N \rightarrow e^{-}\pi^{\circ}N'$, and to the ratio of charged pions over neutral pions in the charged currents, which has been measured in our experiment as 2.06 ± .13. Another prediction has been made by Adler[4], who has evaluated the nuclear corrections for an Al target (for CF_3Br, corrections differ by about 5%). Both predictions are shown in fig.2 as a function of $\sin^2\theta_W$.

From Albright et al, we get $\sin^2\theta_W > 0.07$
From Adler, we get $\sin^2\theta_W > 0.35$

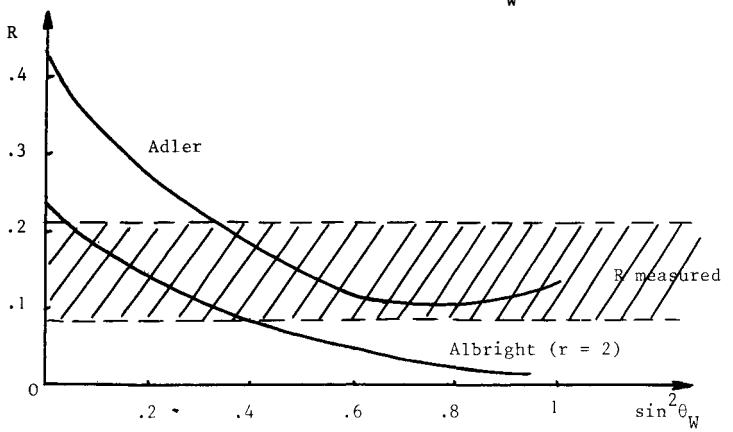

Fig. 2

Isospin properties of neutral current

The preceding results have been used to try to get informations about the isospin properties of neutral current, i.e. to determine whether the reaction

$$\nu(\bar{\nu}) + N \rightarrow \nu(\bar{\nu}) + \pi + N'$$

occurs via a $\Delta I = 0$ or $\Delta I = 1$ transition.

1. Hypothesis : only $\Delta I = 0$ is present

The relative rates of the possible reactions are :

for $\nu(\bar{\nu}) + p \rightarrow \nu(\bar{\nu}) + p + \pi^\circ$, rate = 1/3
for $\nu(\bar{\nu}) + p \rightarrow \nu(\bar{\nu}) + n + \pi^+$, rate = 2/3
for $\nu(\bar{\nu}) + n \rightarrow \nu(\bar{\nu}) + p + \pi^-$, rate = 2/3
for $\nu(\bar{\nu}) + n \rightarrow \nu(\bar{\nu}) + n + \pi^\circ$, rate = 1/3

and the different pions are created with the relative frequencies $\pi^+/\pi^\circ/\pi^- = 1/1/1$, for an isoscalar target.

The final states are perturbated by reinteractions inside the nucleus. The possible reactions are :

(a) $\pi^\circ p \rightarrow \pi^+ n$ (c) $\pi^+ n \rightarrow \pi^\circ p$
(b) $\pi^\circ n \rightarrow \pi^- p$ (d) $\pi^- p \rightarrow \pi^\circ n$

Because they are reverse reactions, we have : (a) = (c) and (b) = (d). From charge symmetry, we get (a) = (b) and (c) = (d). So, after reinteractions, for a I = 1/2 final state, we still have :

$$\pi^+/\pi^\circ/\pi^- = 1/1/1$$

An experimental determination of theses frequencies can allow to check this prediction. We have seen that in the preceding analysis we have determined the raw ratio π°/π^-. To compare to the prediction, we have to correct the ratio for the different detection efficiencies, and to correct slightly the prediction to take into account some second order effects, essentially due to the fact that the target is not isoscalar, which reduces the prediction for π°/π^- ratio to .9.

The detection efficiencies for events with π° and events with π^- have been determined experimentally, as 86 ± 7% for π°'s and 49 ± 6% for π^-'s. The results are given in table 2 :

	π°			π^-			
	NC	eff.	Background min	NC	eff.	Background min	π°/π^- (no background)
ν	142	86±7%	22	60	49±6%	22	1.4 ± .2
$\bar{\nu}$	152	"	9	42	"	9	2.1 ± .4

Without taking account of the background, the two values gotten for π°/π^- ratio are not compatible with 1, at least for $\bar{\nu}$. If we substract the minimum background, the ratios increase, since the relative background is larger in π^- events ; in that case the values are 1.9 ± .35 for ν and 2.5 ± .6 for $\bar{\nu}$. And if we do the crazy assumption that the background is maximum for π° and minimum for π^-, which gives the lower limit obtainable for π°/π^- ratio, we get 1.25 ± .4 for ν and 1.95 ± .5 for $\bar{\nu}$.

We can conclude that the experimental results are incompatible with the predicted value of .9, and that a pure $\Delta I = 0$ transition is ruled out.

2 . Hypothesis : both $\Delta I = 0$ and $\Delta I = 1$ transitions are present

In that case, if A_1 is the amplitude for $\Delta I = 0$ and A_3 the amplitude for $\Delta I = 1$, it is easy to compute that :

$$R = \frac{\pi^\circ \text{ events}}{\pi^+ \text{ events} + \pi^- \text{ events}} = \frac{2 + (|A_1|/|A_3|)^2}{1 + 2\,(|A_1|/|A_3|)^2}$$

For a pure $\Delta I = 0$ transition, $A_3 = 0$ and $R = 1/2$

For a pure $\Delta I = 1$ transition, $A_1 = 0$ and $R = 2$

A measurement of the ratio R leads to the determination of the proportions of $\Delta I = 0$ and $\Delta I = 1$ amplitudes. In spite of some experimental problems (ambiguity in the identification of the positively charged tracks, and reinteractions in the nucleus) there is some hope to get a result in a near future.

III. INCLUSIVE NEUTRAL CURRENTS

During this last year, the statistics for inclusive channels has been multiplied by 3 in $\bar{\nu}$, and attempts have been made for interpreting the results in the frame of some theoretical models. What we measure essentially is the ratio

$$R^{obs}_{\nu(\bar{\nu})} = \frac{\nu\ (\bar{\nu}) + N \to \nu(\bar{\nu}) + (\text{identified hadrons, at least one } \pi)\ E_H > 1\text{GeV}}{\nu\ (\bar{\nu}) + N \to \mu^-(\mu^+) + (\text{identified hadrons, at least one } \pi)\ E_H > 1\text{GeV}}$$

We do not measure absolute values of cross sections for neutral currents. In principle, this should be feasible, but we should have to correct for different efficiencies, not always well known, and which disappear when we measure only ratios. The final numbers appear in table 3 :

	pictures		rough #	Neutron BG	False CC	ν contamination	Corrected #
ν	150 K	NC	183	20			163
		CC	783		27		756
$\bar{\nu}$	325 K	NC	172	14		10	148
		CC	292		25		267

The ratios obtained from these numbers are R_{ν}^{obs} = ,22 ± ,03 and $R_{\bar{\nu}}^{obs}$ = .55 ± .07. Thev still have to be corrected for the identification ambiguities in positive interacting tracks. Up to this point every interacting track has been taken as a π^- in fact the probability for being a π^+ or a proton varies with the energy. This correction has the effect of removing events both in NC and CC samples, either because the hadronic energy becomes less than 1 GeV, or because the event has no more pions and do not answer anymore the selection criteria. The study is being made now and we have only preliminary results, which will be used for comparison with theory, but may still change.

These results are :

$$R_{\nu}^{obs} = .27 \pm .04$$

$$R_{\bar{\nu}}^{obs} = .50 \pm .08$$

caution : preliminary results

All numbers derived farther from these ratios are of course also preliminary.

Comparison with theory

The main feature of our observed ratios is the 1 GeV hadronic energy cut, large compared to the mean energy of the beam (about 2 GeV) ; important corrections are expected when comparing to theory, especially for $\bar{\nu}$.

Starting with theoretically predicted y distributions ($y = E_H/E_\nu$), we have to compute ratios :

$$R_{\nu}^{obs} = \frac{\int \phi(E) \left[\int_{y\ min}^{1} d\sigma^{NC}(E,y)/dy \; dy \right] dE}{\int \phi(E) \left[\int_{y\ min}^{1} d\sigma^{CC}(E,y)/dy \; dy \right] dE}$$

where $\phi(E)$ is the beam energy spectrum,

$d\sigma^{NC}(E,y)/dy$ = theoretically predicted y distribution for NC

$d\sigma^{CC}(E,y)dy$ = same for CC

$$y_{min} = \frac{E_{H\ min}}{E} = \frac{I}{E}$$

In all what follows, we will make the following general assumptions :

- scaling is valid
- charged currents are V - A
- neutral currents are a mixing of only V and A
- we have point like spin 1/2 quarks

We have to define parameters for charged and neutral currents :

1. Parameters for CC

The y-distribution can be written as :

$$\frac{d\sigma_{\nu}^{CC}}{dy} = \frac{G^2 M\ E}{\pi}\left[a_1 + a_2\ (1-y)^2\right] \quad , \quad \frac{d\sigma_{\bar{\nu}}^{CC}}{dy} = \frac{G^2 M\ E}{\pi}\left[a_1\ (1-y)^2 + a_2\right]$$

where a_1 is related to the contribution of quarks and a_2 is related to the contribution of antiquarks. a_1 and a_2 are obtained from measured slopes of σ's :

$$\sigma_{\nu}^{CC} = \frac{G^2 M\ E}{\pi}\ (a_1 + a_{2/3}) = (.76 \pm .08)E\ 10^{-38} cm^2$$

$$\sigma_{\bar{\nu}}^{CC} = \frac{G^2 M\ E}{\pi}\ (a_{1/3} + a_2) = (.28 \pm .03)E\ 10^{-38} cm^2$$

We get :

$$a_1 = .48 \pm .05 \qquad a_2 = .02 \pm \begin{matrix} 0.04 \\ 0.02 \end{matrix}$$

$\varepsilon = a_2/a_1$ can be evaluated more accurately from $r = \sigma_{\bar{\nu}}^{CC}/\sigma_{\nu}^{CC} = .38 \pm .02$:

$$\varepsilon = .053 \pm .023$$

2, Parameters for NC

If only V and A are present

$$\frac{d\sigma_{\nu}^{NC}}{dy} = \frac{G^2 M E}{\pi}\left[A_L + A_R(1-y)^2\right] \quad , \quad \frac{d\sigma_{\bar{\nu}}^{NC}}{dy} = \frac{G^2 M E}{\pi}\left[A_L(1-y)^2 + A_R\right]$$

If there is no $q\bar{q}$ sea, A_L is related to the V-A contribution and A_R to the V + A contribution. In fact, we have seen that ε is not zero, and the $q\bar{q}$ sea contributes.

The ratios of neutral to charged currents can be written as :

$$R^{obs}_{\left\{\begin{matrix}\nu\\ \bar{\nu}\end{matrix}\right.} = \frac{\int E\,\phi(E)\,dE\left[\int_{y\,min}^{1}\left(\left\{\begin{matrix}A_L\\ A_R\end{matrix}\right. + \left\{\begin{matrix}A_R\\ A_L\end{matrix}\right.(1-y)^2\right)dy\right]}{\int E\,\phi(E)\,dE\left[\int_{y\,min}^{1} a_1\left(\left\{\begin{matrix}1\\ \varepsilon\end{matrix}\right. + \left\{\begin{matrix}\varepsilon\\ 1\end{matrix}\right.(1-y)^2\right)dy\right]}$$

We have :

$$R_{\nu}^{obs} = .27 \pm .04 = (.99\ A_L + 15\ A_R)/\ a_1$$

$$R_{\bar{\nu}}^{obs} = .50 \pm .08 = (.71\ A_L + 5.42\ A_R)/\ a_1$$

which gives $A_R = .03 \pm .01$ $\qquad$ $A_L = .13 \pm .02$

The determination of A_R/A_L and ε allows to correct $R^{obs}_{\nu,\bar{\nu}}$ for the 1 GeV cut, independently of any V and A mixing model.

We get :

$$R_{\nu}^{corr} = 1.05 \times R_{\nu}^{obs} = .28 \pm .04 \quad , \quad R_{\bar{\nu}}^{corr} = .76 \times R_{\bar{\nu}}^{obs} = .38 \pm .06$$

3. Comparison with some models

a) Parity conserving models

All models which predict pure V or pure A neutral currents lead to $A_R = A_L$ and $\sigma_{NC}(\nu) = \sigma_{NC}(\bar{\nu})$. With $\sigma_{CC}(\bar{\nu})/\sigma_{CC}(\nu) = .38$, $R_{\bar{\nu}}$ must be $2.6\ R_{\nu}$.

We get :

$$A_L - A_R = .10 \pm .022 \quad , \quad 2.6\, R_\nu - R_{\bar{\nu}} = .32 \pm .08$$

which is about 4 standard deviations from the prediction, and we can deduce that our results are incompatible with these models.

b) Weinberg - Salam model

A_R and A_L can be expressed as functions of $\sin^2\theta_W$,

If there is no sea :

$$A_L = a_1 \left[\frac{1}{2} - \sin^2\theta_W + 5/9 \sin^4\theta_W \right]$$

$$A_R = a_1 \cdot \frac{5}{9} \sin^4 \theta_W$$

To include the contribution of $q\bar{q}$ sea required by the value $\varepsilon = 0.053 \pm .023$, we have used the assumption (Ref.5) that all quarks of the sea contribute by the same structure function. A_R and A_L become functions of $\sin^2\theta_W$ and ε, and their variations are shown in fig.3, which shows also our experimental point. The value found for $\sin^2 \theta_W$ is

$$\sin^2\theta_W = .28 \pm .05$$

In fig. 4 are shown the variations of R_ν^{obs} and $R_{\bar{\nu}}^{obs}$ (taking into account the 1 GeV cut) as a function of $\sin^2 \theta_W$.

The two values found for $\sin^2\theta_W$ are in very good agreement.

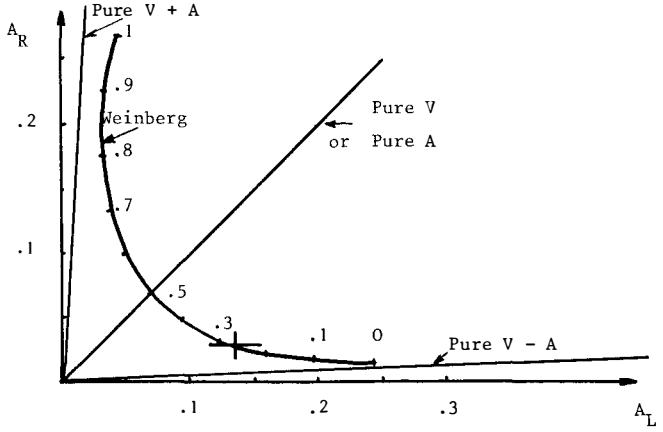

Fig. 3

In fig. 5, the values of R_ν and $R_{\bar\nu}$, for given values of $\sin^2\theta_W$, are presented : curve (a) represents the theoretical variation corrected for the 1 GeV cut, and the corresponding experimental points are R_ν^{obs} and $R_{\bar\nu}^{obs}$. Curve (b) represents the theoretical variation without the 1 GeV cut, the corresponding experimental points being corrected for this cut (R_ν^{corr} and $R_{\bar\nu}^{corr}$). For comparison with other experiments, this last curve (b) has to be used.

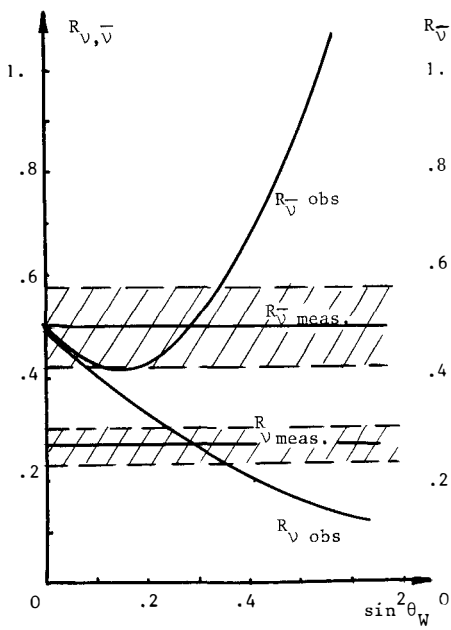

Fig. 4

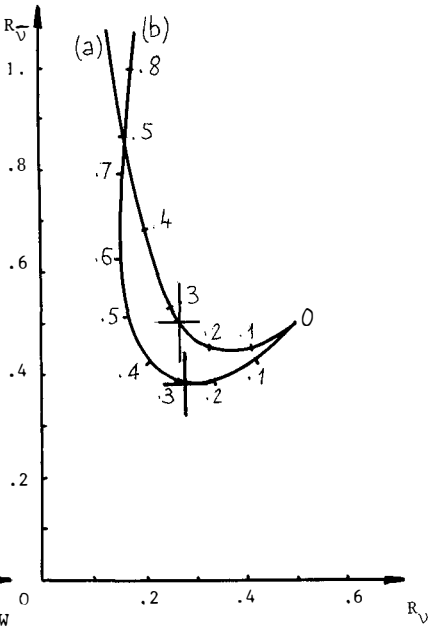

Fig.5

As a conclusion, I like to remark that in the three different studies of neutral currents, the results are in good agreement with the Weinberg-Salam model, with a value of $\sin^2\theta_W$ between .3 and .4.

REFERENCES

1. Hasert et al, Gargamelle Collaboration, PL 46B, 121.
2. Hasert et al, Gargamelle Collaboration, PL 59B, 485.
3. Albright, Lee, Paschos and Wolfenstein, PR D7, 2220 (1973).
4. S.L. Adler, COO 2220-44.
5. L.M. Sehgal, Nucl. Physics B65, 141 (1973).

EXPERIMENTAL STUDIES OF NEUTRAL CURRENTS WITH THE FERMILAB NARROW BAND NEUTRINO BEAM

ARIE BODEK

California Institute of Technology,
Pasadena, California 91125 (USA)

Abstract : The structure of the neutral current coupling was investigated using the Fermilab narrow band neutrino beam. The final state hadron energy distributions of neutral current events were measured with incident neutrino and antineutrino beams. The best fit to the shapes and relative normalizations of the neutrino and antineutrino distributions yields both negative and positive helicity contributions. The results are in agreement with gauge theory models.

Résumé : Nous étudions la structure du couplage du courant neutre à l'aide du faisceau neutrino à bande étroite de Fermilab. Nous mesurons les distributions en energie hadronique de l'état final pour les événements à courant neutre, avec les faisceaux neutrino et antineutrino.Le fit des données neutrino et antineutrino, formes et normalisations, donne les deux contributions d'hélicité négative et positive. Les résultats sont en accord avec les modèles de théorie de jauge.

Neutrino events without a visible muon in the final state were first observed in the CERN-GARGAMELLE bubble chamber experiment[1]. The incident neutrino beam used in that experiment was a low energy ($E_\nu \sim 1$ to 5 GeV) wide band beam. Subsequently such events were observed by other groups[2] and by the Caltech-Fermilab neutrino experiment[3]. The experiment used a narrow band high energy neutrino beam[4] ($E_\nu \sim 50$ GeV). The known peaked energy spectrum of the incident narrow band beam was used to establish experimentally that there was missing energy in the muonless events. This missing energy was carried out of the steel apparatus without interaction thus indicating that there was a neutrino like object in the final state. The present favored explanation for those events is that they proceed via a neutral current (NC) interaction of the type

$$\nu\,(\bar{\nu}) + N \longrightarrow \nu\,(\bar{\nu}) + \text{hadrons} \qquad (1)$$

which occurs in addition to the charged current (CC) interaction

$$\nu\,(\bar{\nu}) + N \longrightarrow \mu^-(\mu^+) + \text{Hadrons} \qquad (2)$$

The neutral current reaction is expected to be mediated by a heavy neutral boson (Z_0) in analogy to the charged W bosons mediating the charged current reaction.

The kinematic definitions in the CC and NC reactions are almost the same except that the final state lepton is different. The exchanged boson carries 4-momentum $\tilde{q}$. The energy transfer to the nucleon in the laboratory is $q_o = \nu = E_h$. The usual Bjorken scaling variable is $x = q^2/2M\nu$ where M is the nucleon mass. The quantity $y = E_h/E_\nu$ is the inelasticity where E_ν is the incident neutrino energy.

The narrow band beam which is sign selected (neutrinos or antineutrinos) and has a peaked and well understood neutrino energy spectrum is almost essential for the investigation of neutral current phenomena as the final state lepton is not observed. In this kind of beam the measured E_h distributions are directly related to the y distributions of the events. Also, neutrino and antineutrino cross sections can be measured separately. The narrow band beam was produced as follows. Secondaries produced near 0 mrad by 300 GeV protons were charge and momentum selected and focused into a parallel beam of 170 GeV central momentum. The momentum spread of the beam was $\pm 18\%$ (HWHM). The secondary beam was directed down a 345 m evacuated

decay pipe in which pion and kaon two body decays ($\mu\nu$) produced a neutrino spectrum in the forward direction that contained two bands. The high energy band was centered about 150 GeV (these neutrinos originated from kaon decays), and the low energy band was centered about 50 GeV (these neutrinos resulted from pion decays).

The Caltech-Fermilab neutrino target detector is located downstream of the decay pipe behind 500 meters of dirt and steel shielding. The target-detector consists of 143 tons of steel in the form of seventy slabs, each 1.5m x1.5m in area and 10 cm in thickness. Seventy scintillation counters (one after every 10 cm of steel) are used to signal the passage of charged particles and to measure the hadron energy using calorimetry techniques. The hadron energy resolution[5] is $\pm$ 33% (rms) at 10 GeV and $\pm$ 9% at 150 GeV (it varies like $1.1/\sqrt{E_h}$). Thirty five magnetorestrictive readout wire spark chambers (one every 20 cm of steel) monitor the final state muon trajectory in the detector. A 1.5m diameter solid steel toroidal magnet is located immediately downstream of the target-detector. It is in turn followed by a large array of spark chambers and several trigger counters. For muons traversing the magnet, the charges and momenta are determined from the direction and magnitude of the bend in the magnet. The muon energy is determined to $\pm$ 20% (rms) by adding the dE/dx energy loss in the target to the energy measured by the deflection in the magnet. The apparatus is triggered by either a muon traversing the magnet or by a significant energy deposition in the target ($E_h > 12$ GeV). The efficiency for triggering on hadron energy as a function of E_h is shown in figure 1. It was determined by investigating charged current events which had also been triggered on by a muon traversing the magnet.

For charged current events the incident energy of the interacting neutrino is determined by summing the measured muon and hadron energies. The measured energy distributions for charged current events where the muon traversed the magnet are shown in figure 2. The characteristic two band structure of the dichromatic beam (broadened by the experimental resolution) is clearly evident. For antineutrinos there is essentially only one band because the kaon neutrino peak is very low. This is due to the low cross section for the production of negative K's.

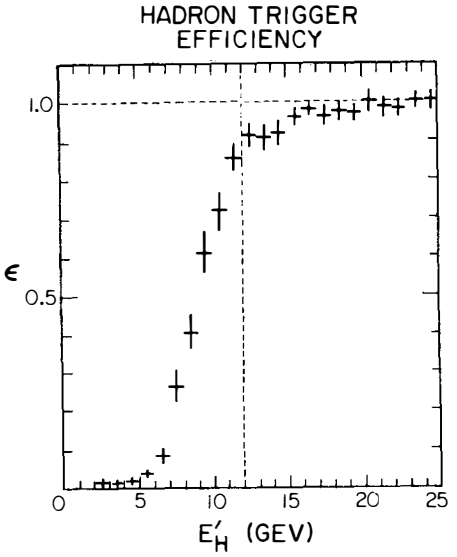

Figure 1: The detection efficiency for triggering on hadron energy deposition in the apparatus versus the energy of the hadrons.

Figure 2:
The measured E_ν energy ($= E_\mu + E_h$) distribution for charged current events.

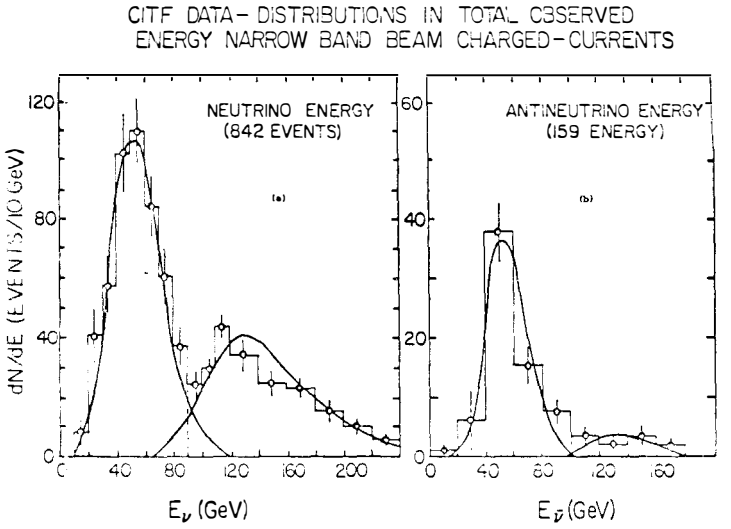

Charged current events are characterized by the presense of a very penetrating particle in the final state. The muon either traverses the magnet or exits the apparatus out the side. Neutral current events are characterized by low penetration particles with a penetration of about 1 meter of steel. An example of a neutral current event candidate is shown in figure 3.

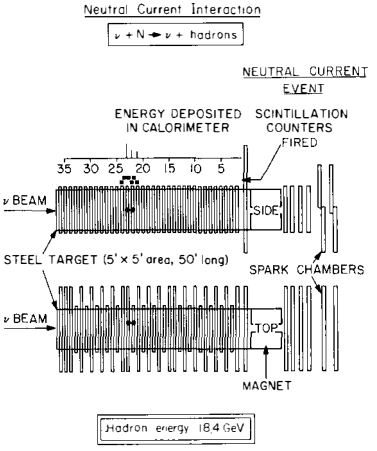

Figure 3: A neutral current event candidate in the Caltech-Fermilab apparatus. A neutrino enters from the left, interacts well within the steel target. There is no indication of a muon in the final state, and there is 18.4 GeV of hadron energy deposition.

The neutral current event sample is taken to be all events where the longitudinal penetration of the longest track particle (as determined by the last scintillation counter firing) is less than 1.5 meters of steel. Charged current events are taken to be events with penetrations greater than 1.5 m of steel. The final state hadron energy distributions are accumulated for both types of events. Subsequently, various corrections are made and hadron energy distributions from various background sources are subtracted from the accumulated distributions.

An important subtraction is that of the wide band contribut-ion. The narrow band beam contains a small wide band component that originates from decays occuring before the final sign and momentum selection. Since the wide band component contains low energy neutrinos, a larger fraction of the wide band charged current interactions tend to mimic low penetration NC events as the final state muons are at lower energy and larger angles. Also, the wide band component contains both neutrinos and anti-neutrinos. Therefore, neutral current events induced by this

component must be subtracted if neutrino and antineutrino NC cross-sections are to be separately measured. This wide band contribution is measured by running with the momentum slit at the entrance of the decay pipe closed, and thus eliminating the normal high energy narrow band beam.

There are also some small corrections of opposing signs that tend to cancell each other. These include: (1) cosmic ray events measured in a separate off-beam cosmic ray gate. The number of cosmic ray events was small because of the fast spill (2 msec) accelerator beam extraction mode that was used. (2) electron neutrino contamination in the beam. It was calculated from the known decay modes containing electron neutrinos in the final state. (3)long penetration hadron shower events, vertex inefficiency and back scattering hadrons. The sum total of these corrections was 1.9% of the final neutrino NC signal and 9.6% of the final antineutrino NC signal.

The last remaining background comes from regular high energy charged current events with a muon at such a large angle or of low energy that it traverses less that 1.5 meters of steel before it exits the target or ranges out. These events mimic the low penetration NC events. The background was calculated by fitting the observed distribution of identified long penetration charged current events and extrapolating to get the number and energy distribution of events with a muon of large angle and/or low energy in the final state. As will be discussed below three radically different models were used to fit the charged current data and all yield similar results. The final corrected hadron energy distributions for CC and NC events for the neutrino and antineutrino running are shown in figure 4.

We now digress to discuss the models that were used to fit the charged current data. There are basically two quantities to be extracted from the charged current data for use in the NC analysis. The first is η the ratio of short penetration CC events (mimicing NC events) to that of identified long penetration CC events. The second is the ratio of the total neutrino flux run during the neutrino running to that of the antineutrino flux run during the antineutrino running. The charged current events must be used as a monitor of the flux because the normal flux monitors which monitor the hadron beam in the decay pipe could not handle the high rate of fast spill extraction. Fast

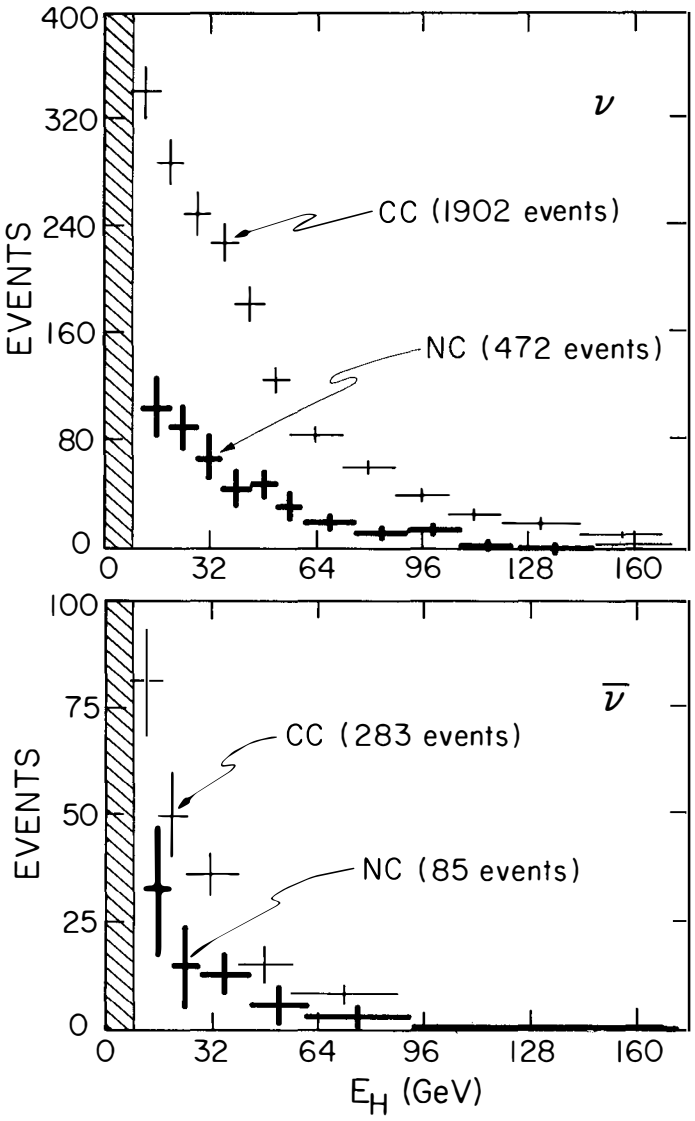

Figure 4: Charged and neutral current final state hadron energy distributions (E_h) for neutrinos and antineutrinos with $E_k > 12$ GeV.

spill is necessary in a neutral current experiment in order to minimize the cosmic ray background.

A general expression for the charged current cross section for a target containing equal number of protons and neutrons is

$$\left(\frac{d^2\sigma}{dxdy}\right)^{\nu}_{Cc} = \frac{G^2 M E_\nu}{\pi(1+q^2/M_w^2)^2} F_2^{\nu}(x,q^2)\left[n^{\nu}(x,q^2) + p^{\nu}(x,q^2)(1-y)^2 + f^{\nu}(x,q^2)y^2\right] \quad (3)$$

$$\left(\frac{d^2\sigma}{dxdy}\right)^{\bar{\nu}}_{Cc} = \frac{G^2 M E_{\bar{\nu}}}{\pi(1+q^2/M_w^2)^2} F_2^{\bar{\nu}}(x,q^2)\left[p^{\bar{\nu}}(x,q^2) + n^{\bar{\nu}}(x,q^2)(1-y)^2 + f^{\bar{\nu}}(x,q^2)y^2\right] \quad (4)$$

The mass M_w is assumed to be large and q^2/M_w^2 is neglected.

Model 1 : A scaling quark parton model with antiquarks and no new particle production. This model is charge symmetric i.e. $F_2^{\nu} = F_2^{\bar{\nu}} = F_2(x)$, $n^{\nu} = n^{\bar{\nu}} = n(x)$ and $p^{\nu} = p^{\bar{\nu}} = p(x)$. Also, as indicated in e-p experiments[6] there are few non spin 1/2 partons in the nucleon. We therefore set $f^{\nu} = f^{\bar{\nu}} = f(x) = 0$. We assume the following functional forms for the distributions of quarks ($q(x)$) and antiquarks ($\bar{q}(x)$) in the nucleon

$$q(x) + \bar{q}(x) = F_2(x)^{ed} \quad (5)$$

$$\bar{q}(x) = 0.5\, F_2(x)^{ed}\, e^{-\lambda x} \quad (6)$$

where $F_2(x)^{ed}$ is from electron deuteron scattering. Since there is no new particle production in model 1 $F_2(x) = F_2(x)^{ed}$ and $n(x) + p(x) = 1$. Here $F_2(x)n(x) = q(x)$ and $F_2(x)p(x) = \bar{q}(x)$. We fit to one unknown parameter of ignorance λ or equivalently the fraction of antiquarks α where

$$\alpha = \int \bar{q}(x)dx \Big/ \int (q(x)+\bar{q}(x))dx \ , \qquad 0.0 \leq \alpha \leq 0.5 \ .$$

Most of the sensitivity to α comes from the antineutrino data. Note that the interpertation of α as an antiquark fraction should be taken with caution as the result for α will somewhat depend on the assumed functional form for $\bar{q}(x)$. The best fit to the charged current data yields a surprisingly large α with $\alpha = 0.27^{-0.13}_{+0.08}$. There is indication in that data that α may be energy dependent (i.e. a violation of scaling), and in model 2 we let α be a function of energy.

Model 2: A quark parton model as is model 1, but it is non-scaling as the fraction of antiquarks α is allowed to vary with energy. The 50 GeV band and the 150 GeV band are fitted separately.

At 50 GeV the best fit is $\alpha_1 = 0.17^{-0.11}_{+0.13}$. And the few antineutrino events at 150 GeV yield the value $\alpha_2 = 0.32^{-0.15}_{+0.18}$.

Model 3: Barnett's[8] quark parton model which includes new particle production. In this model a new quark doublet $\binom{T}{B}$ is coupled to the normal $\binom{u}{d}$ quarks via a V+A current. The fraction of antiquarks α is fixed at 0.06 (to fit low energy electroproduction data and low energy neutrino data) and the flattening of the y distribution for antinuetrinos at high energies is due to a $u \longrightarrow B$ V+A current which occurs in addition to the usual $u \longrightarrow d$ V-A current. At high, but not too high, energies there is a violation of charge symmetry as the mass of the T quark is taken to be higher than the mass of the B quark. There is a threshold turnon due to the high mass of the B quark. We have taken the mass of the T quark to be so high such that it can be neglected. In that case, the structure functions for neutrino scattering are the same as in model 1 (but with $\alpha = 0.06$). For antineutrino scattering we now have an increase of the cross section due to the turnon of a new threshold. This violation of charge symmetery occurs only at large y and small x because the mass of the B quark introduces a modification to the scaling variable x. In this model

$$F_2^{\bar{\nu}}(x,q^2)p^{\bar{\nu}}(x,q^2) = \bar{q}(x) + q(x + M_B^2/(2ME_\nu y))$$

$$F_2^{\bar{\nu}}(x,q^2)n^{\bar{\nu}}(x,q^2) = q(x)$$

where $\bar{q}(x)$ is defined with $\alpha = 0.06$. The data is fit to one unknown parameter which is the mass of the B quark (M_B). The best fit to the data is $M_B = 5 \pm 1.5$ GeV.

It turns out that the three models (with the parameters that fit the data) give the same number for η (the fraction of CC events mimicking a NC signal). For antineutrinos the value of η is 12.5% . For neutrinos η is 26% .

For the flux normalizations we use all identified CC events in conjunction with the cross sections predicted by the three different models. For the 50 GeV band the models yield very similar cross sections and hence very similar fluxes. They vary substantially for the 150 GeV $\bar{\nu}$ events is small, the variation is not important. It is included in the systematic errors (see table 2)

We now proceed to fit the corrected and normalized E_h final state hadron energy distributions for ν and $\bar{\nu}$ neutral current events (see figure 4). A general expression for the NC cross sections which relies only on hermeticity is

$$\left(\frac{d^2\sigma}{dxdy}\right)^{\nu}_{Nc} = \frac{G^2 M E_\nu}{\pi(1+q^2/M_z^2)^2} F_2(x,q^2)\left[gN(x,q^2) + gP(x,q^2)(1-y)^2 + gF(x,q^2)\right]$$

$$\left(\frac{d^2\sigma}{dxdy}\right)^{\bar{\nu}}_{Nc} = \frac{G^2 M E_{\bar{\nu}}}{\pi(1+q^2/M_z^2)^2} F_2(x,q^2)\left[gP(x,q^2) + gN(x,q^2)(1-y)^2 + gF(x,q^2)\right]$$

Here g is the neutral current coupling constant (in units of G^2). The assumptions made in the analysis are the following: M_z is very large such that q^2/M_z^2 can be neglected; scaling; and $F_2(x) = F_2(x)^{ed}$. Also, since the final state neutrino is not observed, the measured cross sections are integrated over all x. Therefore define

$$Q = \int F_2(x)dx \quad , \quad N = \int N(x)dx \quad , \quad P = \int P(x)dx, \quad F = \int F(x)dx$$

then

$$\left(\frac{d\sigma}{dy}\right)^{\nu}_{Nc} = \frac{G^2 M E_\nu}{\pi} Q\left[gN + gP(1-y)^2 + Fy^2\right]$$

$$\left(\frac{d\sigma}{dy}\right)^{\bar{\nu}}_{Nc} = \frac{G^2 M E_{\bar{\nu}}}{\pi} Q\left[gP + gN(1-y)^2 + Fy^2\right]$$

where N is the negative helicity contribution, P is the positive helicity contribution and F is the helicity flip contribution[9]. The table below shows how various helicity terms in the y distribution can arise from various space time structures of the neutral current coupling. Note that the V-A and V+A currents yield different y distributions for scattering from quarks versus scattering from antiquarks, while the scalar (S), pseudoscalar (P) and tensor (T) couplings do not differentiate between quarks and antiquarks. In a scaling model a y^2 term can come only if there are S, P or T contributions. On the other hand, the confusion theorem states the S, P and T couplings can interfere and conspire to mimic any V,A y distributions. The present data rules out any pure y^2 distribution. How much F contribution can exist in addition to dominant P and N contributions is still being investigated. For the present analysis we set F=0 and do a two parameter fit that only includes P and N terms. The results

Reaction	Current				
	V-A	V+A	V,A	S,P	T
ν - q	flat	$(1-y)^2$	$1+(1-y)^2$	y^2	$(2-y)^2$
ν - $\bar{q}$	$(1-y)^2$	flat	$1+(1-y)^2$	y^2	$(2-y)^2$
$\bar{\nu}$ - q	$(1-y)^2$	flat	$1+(1-y)^2$	y^2	$(2-y)^2$
$\bar{\nu}$ - $\bar{q}$	flat	$(1-y)^2$	$1+(1-y)^2$	y^2	$(2-y)^2$

Table 1.

of the fit are shown in figure 5.

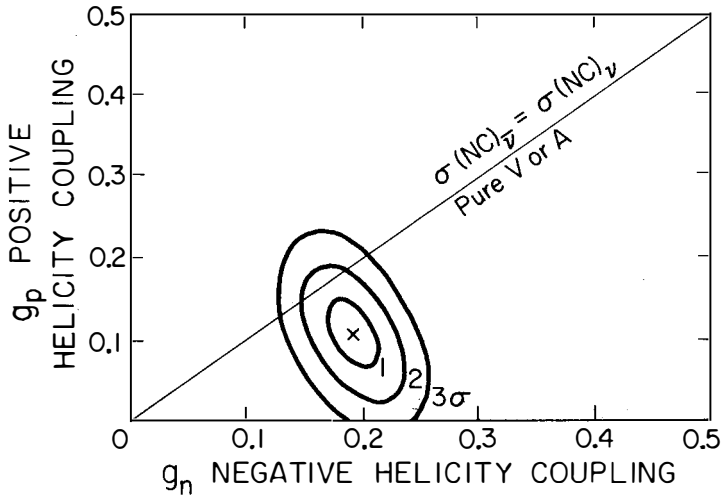

Figure 5: Two parameter contours for the best fit for the negative and positive helicity neutral current couplings.

The results are (including systematic errors in parenthesis)

$g_P = 0.11 \pm 0.04$ ($\pm$ 0.02)

$g_N = 0.19 \pm 0.02$ ($\pm$ 0.02)

or defining P+N = 1 we get

$g = 0.30 \pm 0.04$ ($\pm$ 0.02) and $P = 0.36 \pm 0.09$ ($\pm$0.04)

The systematic errors include the variations obtained when the three models for the charged current data were used to get the short penetration CC background in the NC signal and the flux

normalizations. These variations are shown in the table below.

CC model	Ignorance Parameter	χ^2	Extracted NC results	
			g	p
I Scaling	$\alpha = 0.27^{-0.13}_{+0.08}$	18.6	0.30 ± 0.03	0.36 ± 0.09
II Non-Scaling	$\alpha_1 = 0.17^{-0.11}_{+0.13}$ $\alpha_2 = 0.32^{-0.15}_{+0.18}$	15.8	0.30 ± 0.03	0.39 ± 0.09
III B-quark α=0.06	$M_B = 5 \pm 1.5$ GeV	20	0.32 ± 0.04	0.33 ± 0.09

Table 2.

The data favor both positive and negative helicity terms. The results give the strength and fraction of positive and negative helcity in the neutral current data. For example, a vector-like (or axial vector) theory predicts equal amount of positive and negative helicity contributions. The data is within 1.5 standard deviations of a vector-like theory line.

In a V,A theory a positive helicity term can come from a V-A current on antiquarks as well as a V+A current on quarks. In particular, if g_- and g_+ are the V-A and V+A couplings and the antiquark fraction is α then

$$gN = g_-(1-\alpha) + g_+\alpha$$
$$gP = g_-\alpha + g_+(1-\alpha)$$

Note that the neutral current is diagonal, so no new quarks can be produced. Therefore, only antiquarks can affect the y distributions, but an existence of a B quark has no effect. Figure 6 shows the g_- and g_+ values that are obtained with the two assumptions $\alpha = 0.06$ and $\alpha = 0.17$.

In the single parameter Weinberg model[10] g_+ and g_- are described in terms of a single angle θ_W where

$$g_- = (1/2)\sin^2\theta_W + (5/9)\sin^4\theta_W$$
$$g_+ = (5/9)\sin^4\theta_W$$

As can be seen in figure 6, the data are in agreement with the predictions of the single parameter model with $\sin^2\theta_W \sim 0.35$.

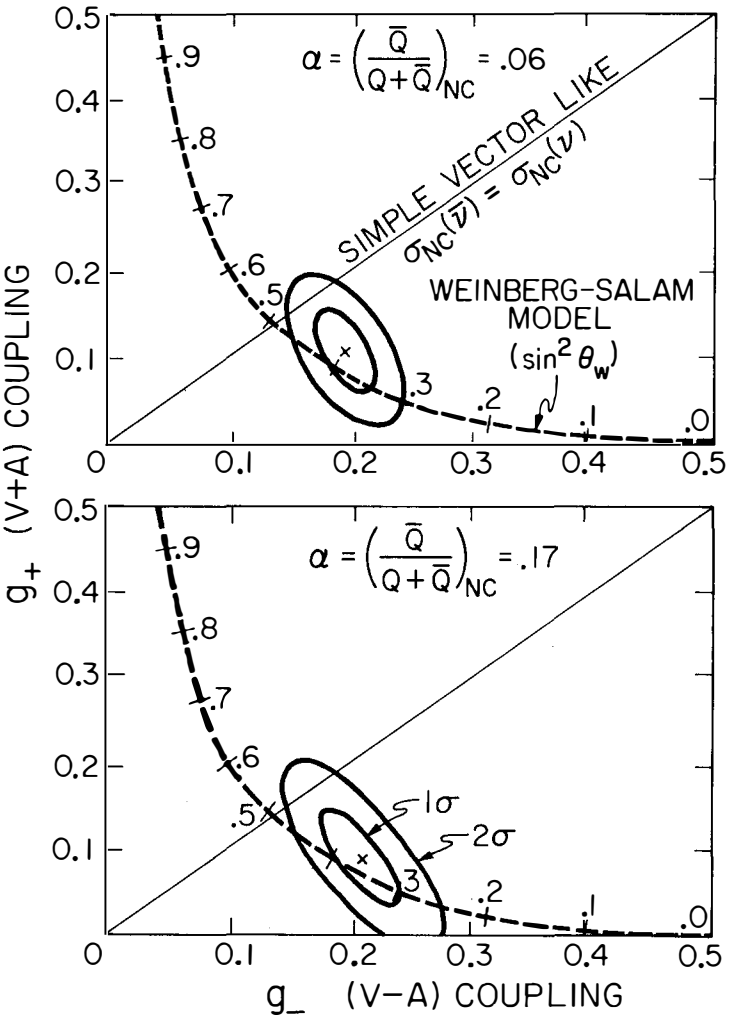

Figure 6: The g_- and g_+ (V-A and V+A) neutral current coupling strengths obtained with two assumptions for the fraction of antiquarks. Predictions of the Weinberg-Salam model and simple vector-like theories are shown for comparison.

In conclusion, the best fit to the neutral current data lies between V-A and V. The best fit is within 1.5 standard deviations of pure V (or pure A) and is also about 1.5 standard deviations from V-A (this last number is somewhat dependent on the amount of antiquarks in the nucleon). The results for the V-A and V+A coupling strengths g_- and g_+ are reasonably insensitive to the fraction of antiquarks (see figure 6) and are well described by the single parameter Weinberg-Salam model both in magnitude and in the V-A and V+A mixing parameter with $\sin^2\theta_w \sim 0.3 - 0.4$. The best results for θ_w are still being determined.

Further analysis and more data will yield information on possible S, P or T contributions and on whether the neutral current cross sections rise lineraly with the incident neutrino energy. The latter can be studied by varying the relative flux in the high energy band (ν_K neutrinos) versus the flux in the low energy band (ν_π neutrinos). This can be accomplished by steering the beam and thus varying the decay angle that is viewed by the neutrino detector. Also, improvements in the event detection such as determining the angle of the hadron shower are also under development.

References

* Work supported by the U.S. Energy Research and Development Administraction. Prepared under Contract E(11-1)-68 for the San Francisco Operations Office.

1. J. F. Hasert, et.al., Phys. Lett. 46B, 138 (1973).

2. A. Benveneuti, et.al., Phys, Rev. Lett. 32, 800(1974); B. Aubert, et.al., Phys. Rev. Lett. 32, 1456 and 1457(1974); S. J. Barish, et.al., Phys. Rev. Lett. 33, 448 (1974).

3. The Caltech-Fermilab group for this neutral current measurement consisted of F. Merritt, B. Barish, A. Bodek, D. Buchholz,L. Stutte, E. Fisk, G. Krafczyk, F. Jacquet, H. Suter and F. Sciulli.

   B. C. Barish et.al., Phys. Rev. Lett. 34, 538(1975); also Proceedings of La Physique du Neutrino a Haute Energie, Ecole Polytechnique, Paris, France (1975) (pg.291 presented by F. Merritt).

4. B. C. Barish et.al., Fermilab proposal no. 21(1970); P. Limon et.al., Nucl.Inst.&Meth. 116, 317(1974).

5. B. C. Barish,et.al. Nucl. Inst.&Meth. 130, 49(1975).

6. E. M. Riordan, et.al. Phys. Rev. Lett. 33, 561 (1974).

7. A. Bodek, Ph.D. Thesis, Massachusetts Institute of Technology (1972), available as LNS-COO-3069-116 (1972). The functional form for $F_2(x)^{ed}$ is $F_2(x) = \sum_{n=3}^{7} a_n(1-x)^n$ with $a_3 = 3.276$, $a_4 = -7.168$, $a_5 = 31.22$, $a_6 = -44.56$ and $a_7 = 18.384$.

8. R. Michael Barnett, Harvard preprint (Jan. 1976) Evidence in neutrino scattering for right handed currents associated with heavy quarks.

9. We name it helicity flip because a y^2 term can only occur (in a scaling model) if there are S, P, or T contributions. Such contributions change the helicity of the neutrino and predict that the final state neutrino in neutral current reactions is of the wrong helicity. This can be understood by the folowing example. The scalar coupling involves the exchange of a spin 0 boson (unlike the spin 1 Z_0), and the $\nu\bar{\nu}$ decay of that boson means that the final state neutrino has the wrong helicity.

10. S. Weinberg, Phys.Rev.Lett. 19, 1264(1967) and 27,1683(1972); A. Salam and J. C. Ward, Phys. Lett. 13, 168 (1964).

EXPERIMENTAL STUDY OF EXCLUSIVE NEUTRAL CURRENT REACTIONS AND SEARCH FOR μe-PAIRS AT BNL*

K. GOULIANOS+
The Rockefeller University
New York, N. Y. 10021 (USA)

Abstract : We describe briefly the Columbia-Illinois-Rockefeller neutrino experiment being performed at the AGS of Brookhaven National Laboratory, and we present results on single π^0 production by charged and neutral currents, on neutrino-proton elastic scattering, and on muon-electron pair production by muon neutrinos.

We report on an experimental study of the following neutrino-induced reactions:

a) Single π^0 production by charged and neutral currents,

$$\nu_\mu + N \rightarrow \nu_\mu(\mu^-) + N' + \pi^0 \quad (1)$$

b) Neutrino-proton elastic scattering,

$$\nu_\mu + p \rightarrow \nu_\mu + p \quad (2)$$

c) Muon-electron pair production,

$$\nu_\mu + N \rightarrow \mu + e + \text{anything} \quad (3)$$

The study was conducted at the Brookhaven AGS using a 26-ton spark-chamber/scintillation-counter detector, Figure 1, placed in a neutrino beam as shown schematically in Figure 2. The AGS was operated in the fast extraction mode so that each pulse consisted of 12 rf bunches separated by 220 nsec. The time of arrival of fast muons at the detector is shown in Figure 3. The width of the rf bunches is 2σ = 24 nsec. The time structure of the pulse was used to separate out neutron-induced events.

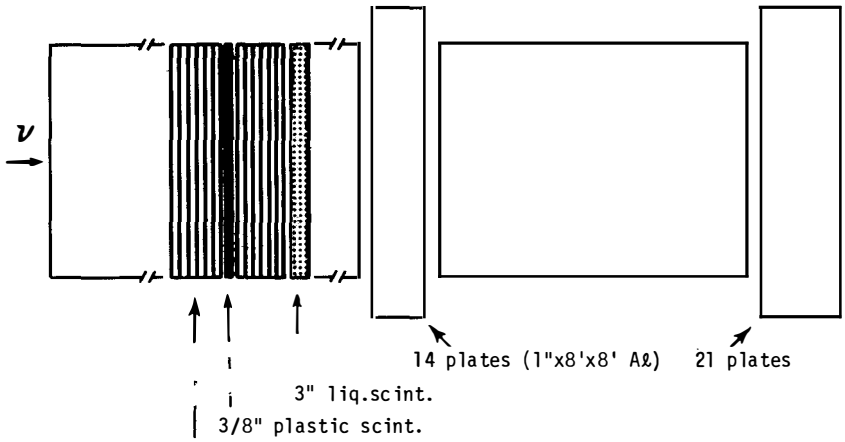

FIG. 1 - Schematic Diagram of Neutrino Detector

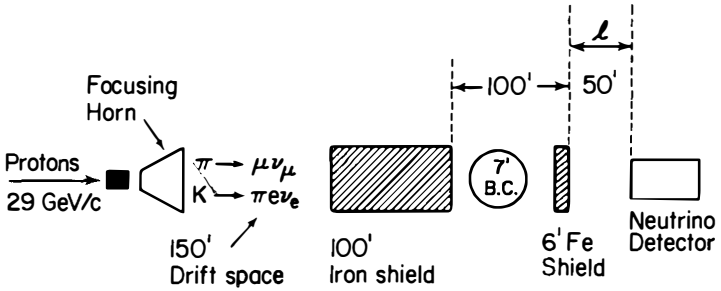

To reduce neutron background:

(i) No materials near the detector
(ii) ℓ large
(iii) Time-of-flight measurement

FIG. 2 - Beam-line Arrangement (not to scale)

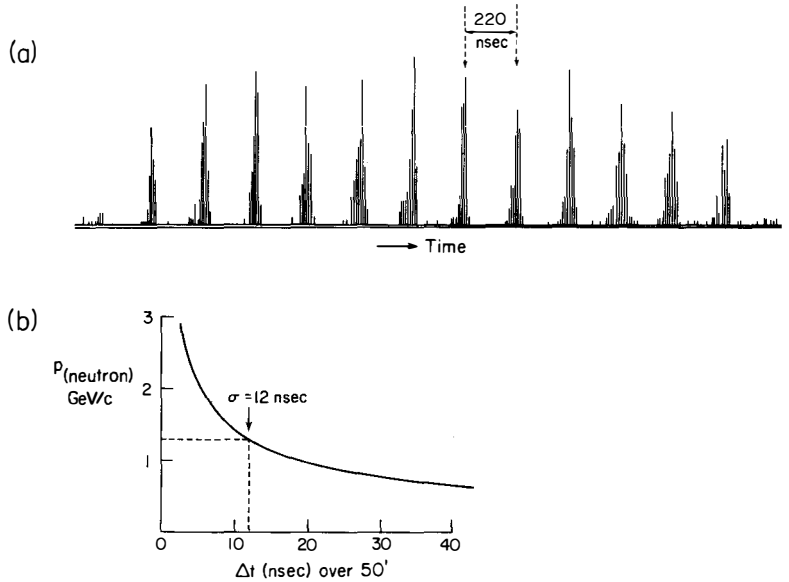

FIG. 3 - (a) Time structure of the beam (b) Time of arrival of neutrons originating in the shield 50' upstream of the detector.

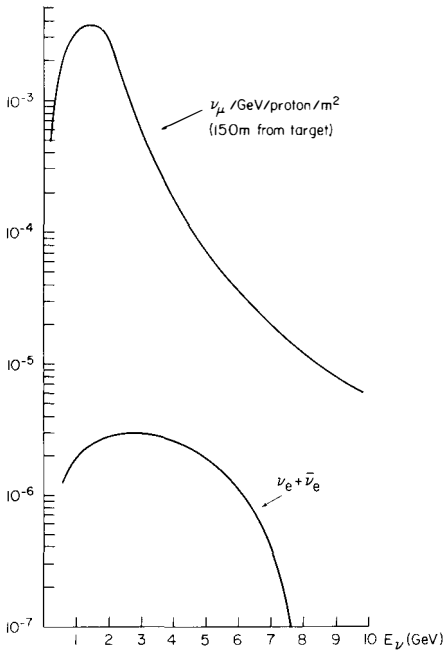

FIG. 4 - Neutrino energy spectrum at the detector (approximate)

Approximately 750,000 ν and 550,000 $\bar{\nu}$ pictures were taken. This report deals only with the neutrino pictures. The neutrino energy spectrum at the detector is shown in Figure 4. At an average beam intensity of 3×10^{12} protons/pulse and for six tons of 4' × 4' fiducial detector mass, the expected number of charged-current events is as follows (before corrections for detection efficiency):

Reaction	Cross-section ($\sigma \times 10^{38}$ cm^2)	Number of events (expected)
$\nu_\mu + N \rightarrow \mu^- X$	$0.8 \times E_\nu$(GeV)	22.5K (1.7K for $E_\nu > 4$ GeV)
$\nu_\mu + n \rightarrow \mu^- p$	0.8	6.5K (75% for $0.5 < E_\nu < 2.5$ GeV)
$\nu_\mu + n \rightarrow \mu^- p \pi^0$	0.2	1.6K
$\nu_e(\bar{\nu}_e) + N \rightarrow e^-(e^+) X$		60 (~0.3% of ν_μ events)

The results presented in this report for reactions (1), (2), and (3) are based on about 65%, 15% and 50% of the data, respectively.

I. Single π^0 production by charged and neutral currents.

The study of single π^0 production by neutrinos, reaction (1), is motivated by the interest in probing the isospin structure of the neutral current (N.C.) interaction. The isospin of the $N\pi^0$ final state may have the value of 1/2 or 3/2, while the initial nucleon has I = 1/2. Thus, the change in isospin is ΔI = 0, 1, or 2 corresponding to isoscalar, isovector, or isotensor interaction. For charged currents (C.C.), ΔI = 0 is forbidden since $|\Delta I_3|$ = 1. Recent results of the Argonne-Perdue collaboration[1] are consistent with a pure isovector transition, ΔI = 1. These results show that the $N\pi^0$ final state is dominated by $\Delta(1232)$ production, I = 3/2. Specifically, it is found that

$$|A_1/A_3| = 0.78^{+0.13}_{-0.17} \text{ for C.C.} \tag{4}$$

where $A_{1,3}$ are the amplitudes of the I = 1/2, 3/2 final state. Thus, about 2/3 of the $p\pi^0$ events in the C.C. case belong to the $\Delta(1232)$ resonance.

In the N.C. case, the questions of interest are:

a) Is there $\Delta(1232)$ excitation?

b) If "yes", what is the value of the ratio

$$R_0 = \frac{\sigma(\nu n \to n\pi^0) + \sigma(\nu p \to p\pi^0)}{2\,\sigma(\nu n \to \mu^- p\pi^0)} \tag{5}$$

evaluated for masses of the $N\pi^0$ system in the vicinity of the $\Delta(1232)$ resonance?

Observation of a $\Delta(1232)$ peak would establish the presence of an isovector piece in the neutral current interaction. The value of R_0 could then be used to test specific gauge models, e.g., the Weinberg-Salam model.

Detailed theoretical predictions of weak soft pion production have been reviewed recently by S. Adler[2]. These predictions include the effects of pion charge exchange inside the Aℓ or C nucleus which alter severely the value of R_0. Preliminary results of this experiment on the value of R_0' (value of R_0 in our aluminum-carbon detector) were reported at the 1975 Paris Conference[3].

From ~65% of the data, we now have obtained 536 C.C. and 170 N.C. events, yielding the value

$$R_0' = \frac{(NC) - (0.095 \pm 0.02)\ (CC)}{(1.2 \pm 0.1)\ \ [1.095\ (CC)]} = 0.17 \pm 0.03 \qquad (6)$$

The evaluation of R_0' takes into account two major corrections to the raw data:

(i) In 9.5 ± 2% of the C.C. events the muon is at a wide angle and is not seen in the spark chambers. These events are included in the raw N.C. count and must be subtracted.

(ii) The detection efficiency for $n\pi^0$ events is 0.4 ± 0.1 and for N.C. $p\pi^0$ events (no muon!) is 0.8. Therefore, the factor 2 in the denominator of eq. (5) is replaced by 1.2 ± 0.1 in eq. (6).

Figure 5 shows our result for R_0' plotted against the prediction[2] of the Weinberg-Salam model for an aluminum-carbon target. In evaluating the charge exchange effects, we have taken the π^+/π^0 ratio in the C.C. case to be equal to 3.9, as calculated from the Argonne-Perdue result given in eq.(4).

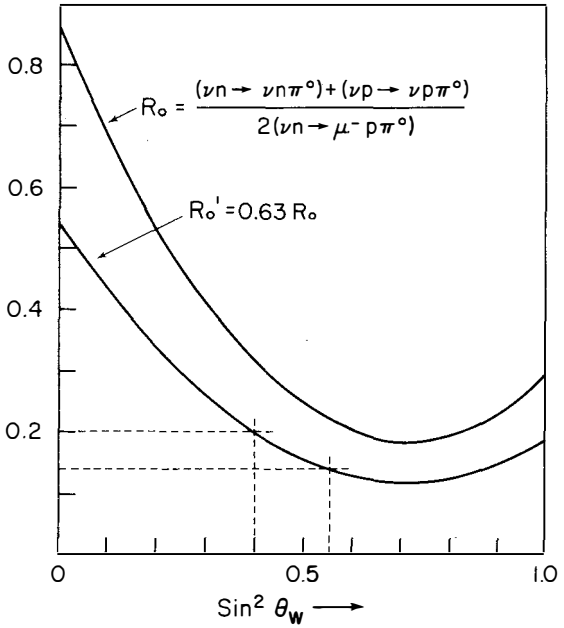

FIG. 5 - Values of R_0 and R_0' (for Aℓ + C) versus the Weinberg-Salam angle. The dotted lines correspond to our experimental result for R_0' .

From Figure 5 we obtain

$$\sin^2\theta_W = 0.48 \pm 0.08 \qquad (7)$$

This result, however, is meaningful only if the mass distribution of the $N\pi^0$ system is that predicted by the model. Figure 6 shows the charged and neutral current $p\pi^0$ mass distributions for a selected sample of events within the following cuts: $\theta_p < 70^0$, $p_p > 550$ MeV/c , $250 < p_{\pi^0} < 800$ MeV/c . This selection is necessary in order to insure high detection efficiency and minimize the effects of Fermi motion. A pure $\Delta(1232)$ distribution is also shown for comparison. Both charged and neutral current distributions show an enhancement in the $\Delta(1232)$ region and, within statistics, they are not different from each other. We conclude that our present experimental result does not exclude the existence of an isovector piece in the N.C. interaction, in general, and is not incompatible with the Weinberg-Salam model, in particular.

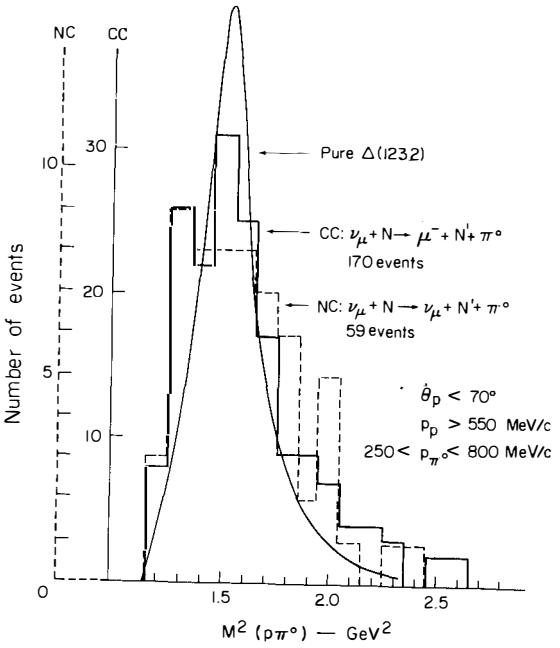

FIG. 6 - Mass spectrum of the $p\pi^0$ final state for charged and neutral currents.

II. Neutrino-proton elastic scattering.

We have scanned about 120,000 pictures for quasi-elastic events,

$$\nu_\mu + n \rightarrow \mu^- + p \qquad (8)$$

and for neutrino-proton elastic scattering events, reaction (2). Our scanning definitions for "muon" and "proton" were:

muon : straight track > 2 collision lengths
OR exiting straight track
OR stopping track with visible multiple scattering

proton: stopping straight track with range between 2" and 20" of Aℓ.

The time of flight of the events found is shown in Figure 7. The quasi-elastic events are all concentrated around t = 0 ± 12 nsec while the "elastic" ones contain a large number of flat off-time background above which a prompt peak is clearly visible. We believe that the flat background is caused by neutrons which yield protons by charge exchange. In fact, most of the off-time events are low energy protons entering from the top of the apparatus (neutron "sky-shine"). By removing events which originate at the top half or within 1.5 feet from the right or left edge of the chambers and point down, and by requiring p_p > 550 MeV/c (range > 3" Aℓ) and $25^0 < \theta_p < 70^0$ (most of the neutrino events are at angles larger than 25^0) we obtain the hatched histograms of Figure 7. The off-time events have been reduced uniformly by about a factor of 10 while only about 60% of the "signal" was lost. There are 39 prompt events within the time bin indicated by the markers in Figure 7a. After making a "flat" background subtraction we are left with 25 ± 6 candidates for the elastic $\nu_\mu p$ scattering process to be compared with 69 ± 8 candidates for the quasi-elastic process, reaction (8).

These numbers must be corrected for contamination from partially visible final states of neutrino induced reactions which simulate elastic or quasi-elastic scattering. The largest correction comes from our estimate that in about 8 ± 2% of the quasi-elastic events the muon is at such a wide angle ($90^0 \pm 15^0$) that it is not visible in the apparatus. Thus, about 6 ± 1.5 events must be added to the quasi-elastic ones and the same number must be

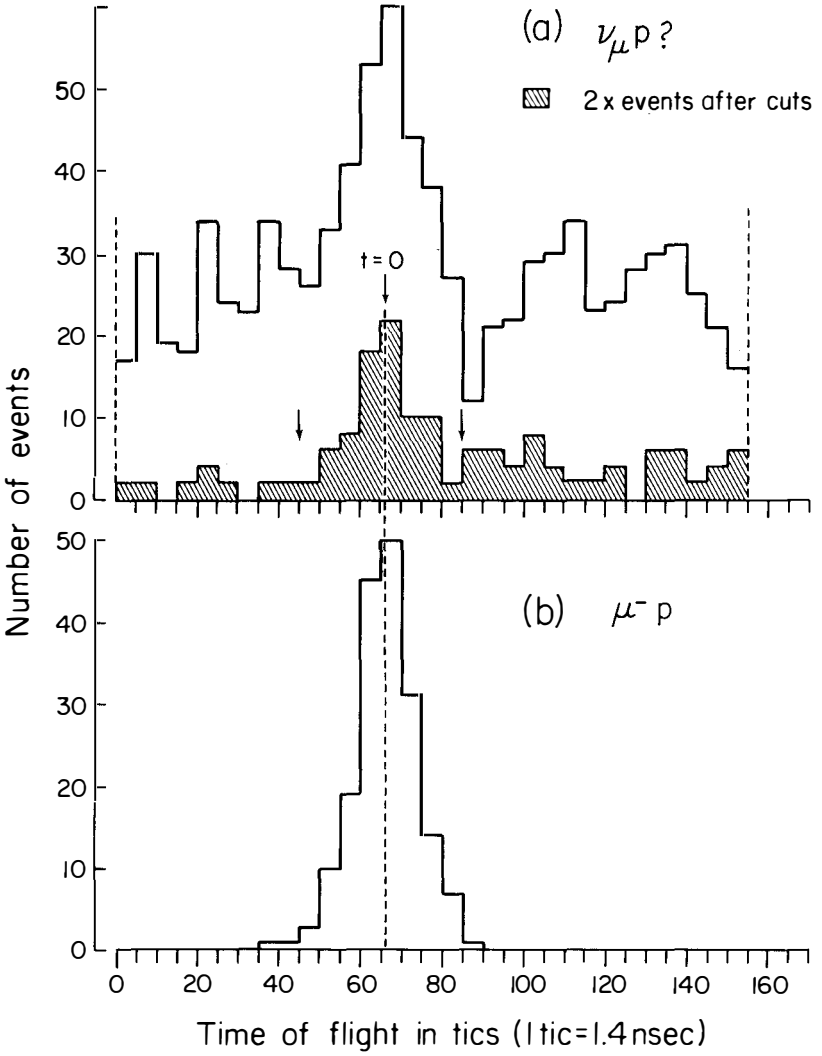

FIG. 7 - Time of flight distributions for (a) elastic (?) and (b) quasi-elastic neutrino events. The hatched histogram represents events surviving the following cuts:
(i) neutron "sky-shine" cut, as explained in text
(ii) tracks with polar angle $< 25^0$ or range < 3" Aℓ rejected.

subtracted from the elastic. These events are induced by low energy neutrinos, $0.5 < E_\nu < 1$ GeV, and the error is mainly due to the uncertainty in the low energy neutrino spectrum. In addition to the wide-angle muon correction, there are several inelastic neutrino reactions that contribute to the prompt signal. These are listed in Table I along with the estimated number of events they contribute to our sample.

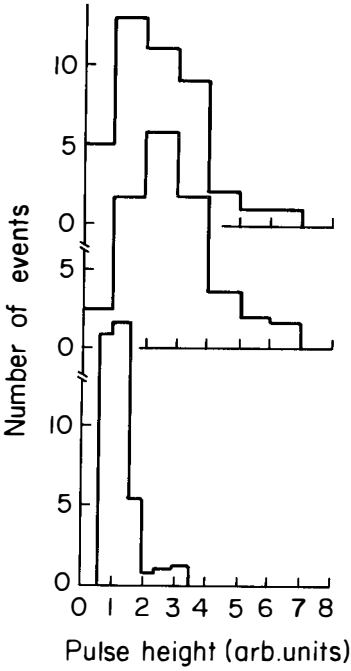

Fig.8 Pulse height distributions

TABLE I - Estimated number of events from neutrino induced inelastic reactions simulating $\mu^- p$ and $\nu_\mu p$ final states.

"$\mu^- p$"	No. of events	"$\nu_\mu p$"	No. of events I=1/2	I=3/2
$\mu^- p(\pi^0)$	2.7	$p(\pi^0)$	0.5	0.5
$\mu^- \pi^+(n)$	5.7	$\pi^+(n)$	3.0	0.7
$\mu^- \pi^+(p)$	4.5	$\pi^-(p)$	1.0	0.2
Total no.	12.9	Total number	4.5	1.4

In estimating these numbers we start from our measured rates for $\nu_\mu n \to \mu^- p\pi^0$ and $\nu_\mu p \to p\pi^0$, and calculate the $\pi^\pm$ production rates using

isotopic spin symmetry. In the case of charged currents we make use of Eq. 4, while for N.C. we consider the two extreme possibilities of I = 1/2 and I = 3/2 πN final states. In order for the inelastic reaction to simulate the (quasi) elastic one, the particle in parenthesis must not be seen in the apparatus while the additional hadron must meet the criteria of a "proton" as defined previously. We estimate the probabilities of occurrence of this combination using our knowledge of the distributions for the μ^-(or ν_μ)pπ^0 final states, of the distributions for the C.C. reactions[1], and of the interaction properties of pions in aluminum and carbon. The pulse height spectra shown in Figure 8 are consistent with the small number of pion background given in Table I and incompatible with a much larger pion contamination. By subtracting the "background" given in Table I from the corresponding C.C. and N.C. events obtained from Figure 7, and by making the wide angle muon correction mentioned above, we obtain $14 \pm 6 \leq N_{e\ell} \leq 17 \pm 6$ and 62 ± 9 events for the elastic and quasi-elastic channels, respectively. We conclude that we have observed elastic ν_μp scattering at the rate of

$$0.22 \pm 0.1 \leq R_{e\ell} = \frac{\sigma(\nu_\mu p \rightarrow \nu_\mu p)}{\sigma(\nu_\mu n \rightarrow \mu^- p)} \leq 0.27 \pm 0.1 \qquad (9)$$

in the q^2 range of $0.3 < q^2 < 1$ (GeV/c)^2.

III. Muon-electron pair production.

We have made a systematic study of all events containing a shower, searching for muon-electron pair candidates. Such events have been reported by the Gargamelle collaboration and by two experiments using the Fermilab 15' bubble chamber (talks given at this conference). Currently there is great interest in this type of events because the electron may be associated with the decay of a charmed particle produced in neutrino interactions. But aside from this possibility, μe-pairs, like the dimuon events observed at Fermilab, signal new particle production.

A μe - candidate, found among a sample of our neutrino events in 1975, is shown in Figure 9.

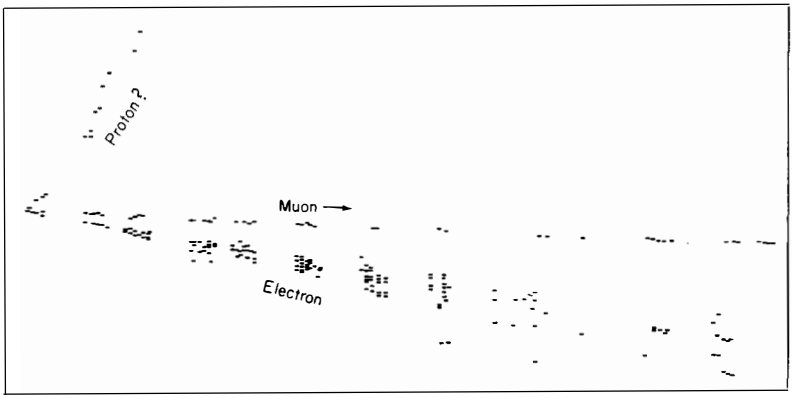

FIG. 9 - Muon-electron pair candidate.

The "muon" traverses about 3.5 collision lengths of material without visible interaction before exiting, while the "electron" shower is contained in the apparatus and has an estimated energy of about 1.7 GeV. Such an event, if not a genuine μe-pair, could be produced by the following two "normal" reactions:

$$\begin{aligned} &(a)\ \nu_\mu + N \to \mu^- + \pi^0 \quad (\to \text{"electron" shower}) + \ldots. \\ &(b)\ \nu_e(\bar{\nu}_e) + N \to e + \pi^\pm \quad (\to \mu^\pm) + \ldots. \end{aligned} \tag{10}$$

In about one-half of our pictures, corresponding to ~14,500 neutrino events, we observed ~ 400 showers with energy ≥ 200 MeV. In order to enrich this sample in "electrons" of the type shown in Figure 9, we made the following selection on the basis of the characteristics of the shower:

(i) Energy of shower ≥ 500 MeV (50 sparks)

(ii) Shower should have at least three single sparks in a straight line (~0.2 rad lengths) before multiple sparking occurs.

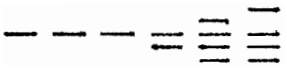

"e-type" shower

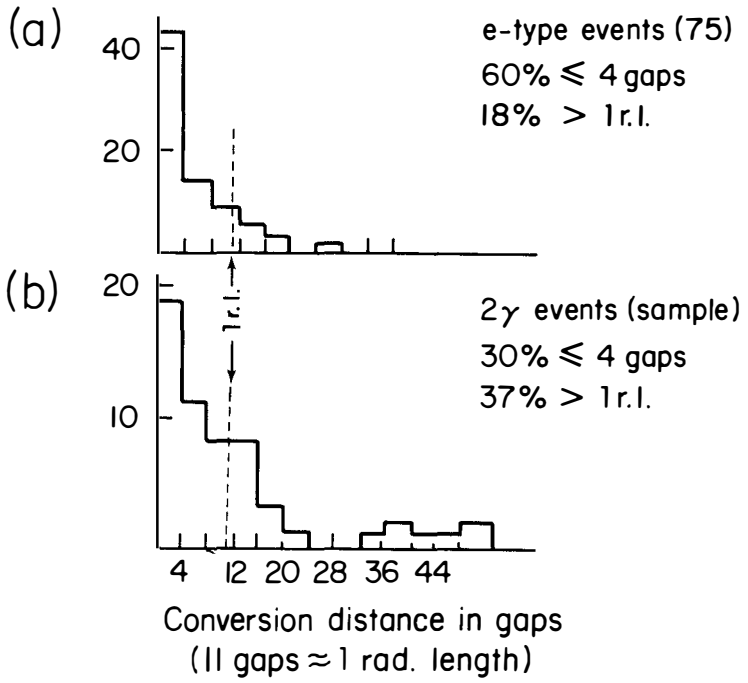

FIG. 10 - Conversion distance (origin of shower from vertex) distribution for (a) e-type events and (b) true γ-shower events.

The selected events are plotted in Figure 10a as a function of the conversion distance, i.e., the number of gaps from the vertex to the beginning of the shower. Figure 10b shows the conversion distance of true γ-showers obtained from a sample of events with two γ's. It is evident that the selected e-type events convert closer to the vertex as expected of a sample enriched in electrons. In particular, we estimate that the first bin ($\leq$4 gaps) contains ~ 65% of electrons.

In Figure 11a we plot the energy of the shower in number of sparks (~ 10 MeV/spark) versus the collision lengths traversed by the "muon" for the e-type events converting within the first three gaps from the vertex. We estimate that among the 37 events shown here there are ~ 10 γ-showers, the remaining 27 being genuine electrons. This number is consistent with the expected number of inelastic events induced by $\nu_e(\bar{\nu}_e)$. A similar plot is

shown in Figure 11b for non e-type 1γ events.

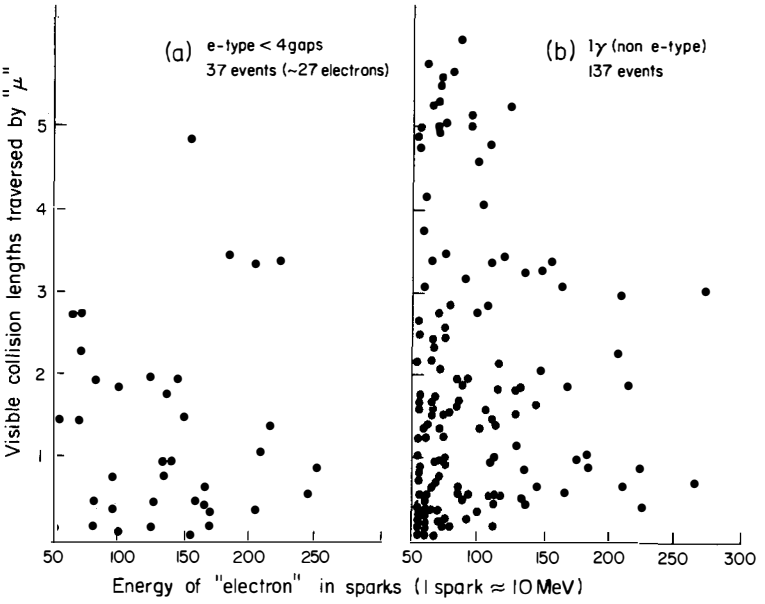

FIG. 11 - Energy of "electron" versus visible collision lengths traversed by "muon" (a) for e-type events converting within the first 3 gaps and (b) for non e-type one shower events.

From 137 events plotted here, only two are in the region

$$E_e \text{ (energy of electron)} > 150 \text{ sparks } (\sim 1.5 \text{ GeV})$$
$$R_\mu \text{ (range of muon)} > 3 \text{ C.L. (collision lengths)} \qquad (11)$$

as compared to four events in Figure 11a out of an estimated 10 γ-showers. Thus, the number of events in region (11) of Figure 11a due to γ-showers attributed to reaction 10a is ~0.15. From the 15 e-type events with energy greater than 150 sparks in Figure 11a, we estimate that ~0.35 may be due to reaction 10b with the pion either decaying early or punching through three collision lengths. Thus, the total number of background events due to processes 10a,b in region (11) of Figure 11a is expected to be at most 0.5 and the number of events found in this region is four. It is unlikely, then, that these 4 events are produced by reactions 10a,b and hence they could be genuine μe- pairs signaling the production of a new particle(s) in neutrino

interactions. If this preliminary conclusion is substantiated by the analysis of the rest of our pictures, it will be of interest that the μe^- pairs selected by our $E_e > 500$ MeV cut are not associated with V's which would signal the simultaneous production of strange particles as is the case with the Gargamelle events.

REFERENCES

* Work supported in part by the U.S. Energy Research and Development Administration under Contract E(11-1)-2232A.

+ This report is based on the work of: W. Lee, E. Maddry, W. Sippach, P. Sokolsky and L. Teig, Columbia University, New York, N. Y.; A. Bross, T. Chapin (presently at Rockefeller University), L. Nodulman (presently at UCLA), T. O'Halloran and C.Y. Pang, University of Illinois, Urbana, Ill.; K. Goulianos and L. Litt (presently at Michigan State University), Rockefeller University, New York, N.Y.

1. Barish, S.J. et al., Phys. Rev. Letters 36, 179 (1976).
2. Adler, S., VIth Hawaii Topical Conference in Particle Physics (August 1975 (to be published).
3. Lee, W. et al., La Physique du Neutrino a Haute Energie (Paris, 1975).

EIGHT QUESTIONS YOU MAY ASK ON NEUTRAL CURRENTS

J.J. SAKURAI*
CERN, Geneva

Abstract : The properties of weak neutral currents are reviewed from a phenomenological point of view. Some crucial experiments are suggested.

Résumé : Les propriétés des courants neutres sont revues d'un point de vue phénoménologique. Quelques expériences cruciales sont suggérées.

* John Simon Guggenheim Memorial Foundation Fellow on leave from the University of California, Los Angeles.

Nearly six months ago, I gave a series of lectures at the DESY Summer Institute entitled "Neutral Currents without Gauge Theory Prejudices", the written version of which has been available as a CERN preprint (TH-2099) for some time and will eventually be published in the Proceedings of the Summer Institute. When I decided to participate in the Rencontre, I was hoping that there would be much progress in the subject between September 1975 and March 1976, but unfortunately it turns out that there has not been too much new since my DESY talk. (Experimentally there are a few new results but they will be presented by the experimental speakers). Since the experts can study my DESY paper, I have decided to give a talk here which is even more pedagogical and elementary than my DESY talk. With apologies to those who made original contributions to this subject, I omit the names and references since a fairly complete bibliography can be found in my DESY Summer Institute paper.

In a conference dominated by the superstars of experimental neutrino physics the most sensible thing a theorist or a phenomenologist can do appears to be to ask a lot of questions. To this end I prepared eight questions related to neutral currents.

QUESTION 1 : WHY ARE NEUTRAL CURRENTS INTERESTING ?

To most theorists neutral currents are interesting because their discovery provided the first indication that the heroic efforts of some theorists to construct a renormalizable theory of weak interactions may actually be on the right track. Indeed, many theoretical talks - and even some experimental talks - on neutral currents start by pointing out that neutral currents are needed because otherwise the cross section for :

$$\nu + \bar{\nu} \to W^+ + W^- \tag{1.1}$$

would go like s. To me, however, neutral currents are interesting because they represent genuinely new phenomena. Until 1973, much of weak interaction physics could be visualized as being based on Fermi's 1933 Lagrangian with only minor modifications :

(i) Change V to V-A.

(ii) Change p and n to u and d_c ($\equiv d \cos\theta_c + s \sin\theta_c$).

(iii) Double the number of leptons :

$e \rightarrow e, \mu$

$\nu \rightarrow \nu_e, \nu_\mu$

With the advent of neutral currents some major modifications are needed ! After 40 years of physics with neutrinos, something qualitatively new is finally happening. Whenever we have genuinely new phenomena, it is profitable to study them in their own right, without recourse to any particular theoretical framework. We may also keep in mind the possibility that renormalizable gauge theories of weak interactions look attractive now only because we don't know anything better at this present moment.

Even if the general philosophy of gauge models is to triumph ultimately, there are now many gauge models that make very different predictions on neutral currents ; for example, so-called vector models are very different from the Weinberg-Salam model, which, with the currently accepted value of $\sin^2 \theta_W$ is mostly axial vector. Once a phenomenological framework is given, it becomes easier to compare your favorite model with your competitor 's in an objective manner.

QUESTION 2 : ARE ORDINARY NEUTRINOS INVOLVED IN NEUTRAL CURRENT PROCESSES ?

The original publication on the Gargamelle discovery of neutral currents is entitled, "Observation of neutrino-like interactions without muon or electron in the Gargamelle neutrino experiment". This is appropriate because the reaction under consideration is :

"invisible particle" + N → "invisible particle" + hadrons (2.1)

It is now almost certain that the initial invisible particle is ν from π or K decay. Any other possibility is rather remote if we realize that the neutral-to-charged current ratio is more or less independent of the manners in which the incident neutrino beams are produced - horn focused, unfor -cused ; narrow band, wide band, etc ... The outgoing invisible particle is also likely to be a massless or a very low mass object because the neutral current processes do not seem to exhibit any threshold effect. Neutral current events were induced by the ANL neutrino beam which peaks at about 500 MeV. It is not excluded, however, that the neutral current sample at high energies may contain some contamination from exotic particle production, e.g. production of charged or neutral heavy leptons that decay as :

$$L^+ \to \nu + \text{hadrons}$$
$$L^\circ \to \nu + \bar{\nu} + \nu \qquad (2.2)$$

Conversely, it is amusing to speculate that the production of charmed meson pairs by $\Delta C = 0$ neutral-current interaction :

$$\nu + N \to \nu + D^\circ + \bar{D}^\circ + \text{other hadrons}$$
$$\bar{D}^\circ \to K^- + \pi^+$$
$$D^\circ \to \bar{\nu} + \mu^- + K^+ \qquad (2.3)$$

may contaminate the charged current sample.

Even if the final "invisible" particle turns out to be a massless neutrino, it is still worth examining whether the final neutrino is of the same kind as the initial neutrino. This question of neutrino identity can, in principle, be settled by performing :

$$\bar{\nu}_e + e^- \to \bar{\nu}' + e^- \qquad (2.4)$$

at low (reactor) energies. First, note that this reaction occurs with $\bar{\nu}' = \bar{\nu}_e$ even in the old V-A charged-current theory since the charged-current can propagate in the s channel. The presence of neutral current interactions adds a diagram in which the current propagates in the t channel. The question of neutrino identity can be checked by studying whether the two diagrams interfere. Quite generally, if the neutral current interaction is of the V,A type, the energy distribution of the final electron is given by :

$$\frac{d\sigma}{dE_e} = (2G^2 m_e/\pi)\left[A + B(1 - E/E_\nu)^2 - C m_e E/E_\nu\right] \qquad (2.5)$$

To test neutrino identity we examine how A, B and C are related :

$$C^2 = A\,B \quad \text{if} \quad \bar{\nu}' = \bar{\nu}_e$$
$$C^2 = A(B-1) \quad \text{if} \quad \bar{\nu}' \neq \bar{\nu}_e \qquad (2.6)$$

As for semileptonic reactions, we may test the identity or nonidentity of the initial and final neutrinos in the following way. Suppose the initial and final neutrinos are the same. Then the space and time components of the hadronic neutral current must necessarily be Hermitian, i.e. if we write the interaction as :

$$\mathcal{L} \propto i \bar{\nu} \gamma_\lambda (1+\gamma_5) \nu J_\lambda \tag{2.7}$$

we must have :

$$J_k^+ = J_k \ , \quad J_o^+ = J_o \tag{2.8}$$

On the other hand, if the initial and final neutrinos are different, the current need not be Hermitian. An immediate consequence of the Hermiticity requirement is that :

$$\nu + I \to \nu + F \tag{2.9.a}$$

$$\bar{\nu} + I \to \bar{\nu} + F \tag{2.9.b}$$

are characterized by the same current matrix element $< F|J_\lambda|I >$. This does not necessarily mean that the two cross sections are equal because of VA interference which changes sign as we go from ν to $\bar{\nu}$. We can, however, specialize to the configurations in which VA interference must vanish just by kinematics :

(a) $q^2 \to 0$ with W (final hadronic mass) fixed (exclusive reaction)

(b) $E_\nu \to \infty$ with W fixed (exclusive reaction)

(c) $\nu \equiv q^2/2mE_\nu \to 0$ or $y \equiv 1-E_\nu'/E_\nu \to 0$ (inclusive reactions)

For these special configurations the cross sections for (2.9.a) and (2.9.b) must be equal. If not, we can conclude that the current is not Hermitian, which, short of a violation of the CPT theorem, is possible only if the final neutrino is different from the initial neutrino.

Another speculation that has been made is that the observed neutral current processes are actually electromagnetic one-photon-exchange processes where the neutrino that undergoes scattering is postulated to have an unusually large electromagnetic radius. Because the electric charge of the neutrino is strictly zero, the Dirac form factor of the neutrino must start as q^2, which just cancels the $1/q^2$ dependence arising from the photon propagator ; as a result, the net effect is just what one expects from a current-current interaction. This proposal makes the following specific predictions.

(i) Neutral current processes are parity conserving (pure V).

(ii) Apart from the absence of the $1/q^4$ factor in the cross section, the final states in the neutral current processes are the same as in electroproduction.

(iii) There is no neutral current effect observable in processes not involving neutrinos, e.g. $e^+ + e^- \to \mu^+ + \mu^-$, $\mu^- + p \to \mu^- +$ hadrons.

The main difficulty which this proposal is that the neutrino charge radius expected from conventional mechanisms, e.g. a model based on muon pair intermediate states in the photon channel, is too small to account for the observed neutral current cross section by a factor of :

$$\sim \left[\alpha \ln(\Lambda/m_\mu^2)\right]^2$$

QUESTION 3 : IS SPT RULED OUT ?

If we approach the subject of neutral currents without theoretical prejudices, we should not discard the possibility that covariants other than V and A are involved in neutral current processes. Actually, when we say "neutral currents", we are already prejudiced in favor of V and/or A. We should really say, "neutral density".

As is well known, the covariants $\bar{\nu}\nu$, $\bar{\nu}\gamma_5\nu$ and $\bar{\nu}\sigma_{\lambda\tau}\nu$ connect states of opposite helicity. The neutrinos used in accelerator neutrino experiments are left-handed because they come from π^+ and K^+ decay. With SPT, we have left-handed neutrinos in and right-handed neutrinos out. You may say that this violates the two-component neutrino condition, but so what ? The two-component condition may be just a property of the charged-current interaction, not an intrinsic property of the neutrino.

For orientation purposes let us start with the very simple case of $\nu_\mu e$ and $\bar{\nu}_\mu e$ scattering. If we have the most general combination of V and A, the y distribution can be written as :

$$\text{V and/or A} \quad : \quad C_L + C_R(1-y)^2, \quad C_L \geq 0, \quad C_R \geq 0 \tag{3.1}$$

The main point is that we always have a distribution that does not rise with increasing y. The situation is very different with SPT. When we have S and/or P, we get a y distribution that rises quadratically :

$$\text{S and/or P} \quad : \quad y^2 \tag{3.2}$$

Therefore, if we have a rising y distribution, we have unambiguous evidence in favor of S and/or P. On the other hand, with a tensor interaction, we again have a falling distribution :

$$T \; : \; 1-y + y^2/2 \tag{3.3}$$

and ST or PT interference that changes sign as we go from ν to $\bar{\nu}$ goes like :

$$\text{ST or PT interference} \; : \; y(2-y) \tag{3.4}$$

exactly the same as the y dependence of VA interference.

If we now turn to semileptonic inclusive reactions :

$$\overset{(-)}{\nu} + N \rightarrow \overset{(-)}{\nu} + \text{any} \tag{3.5}$$

the number of independent structure functions increases - e.g. there are three kinds of T structure functions - but the main features deduced by looking at $\nu_\mu e$ and $\bar{\nu}_\mu e$ scattering can be shown to survive. In particular, we have what is known as the "Confusion Theorem" :

> "For any admixture of V and A interactions there is a corresponding admixture of S, P and T interactions, which yields the same ν and the same $\bar{\nu}$ cross section".

Experimentally one does not directly measure the y distribution (recall y is defined as $y = \nu/E \simeq E_{had}/E$) but knowing the neutrino flux it is possible to predict what kind of E_{had} distributions are expected. By studying the E_{had} distributions both the Harward-Pennsylvania-Wisconsin group and the Caltech group have found that a y distribution that goes like y^2 is ruled out. (c.f. Bodek's talk at this meeting).

Even though the data rule out pure S and/or P, it is evident from the Confusion Theorem that we cannot rule out an STP combination by looking at the inclusive data. Recently, an astrophysical argument has been advanced against a sizable tensor interaction in neutral currents by Ruderman and collaborators. Their reasoning goes as follows. Suppose we have a tensor-type interaction. We then expect a finite magnetic moment for a neutrino due to Figure 1, which gives :

$$\mu_\nu = \frac{2}{\pi^2} \frac{2G_T}{\sqrt{2}} m_\ell \ln\left(\frac{\Lambda}{m_\ell}\right) \tag{3.6}$$

where G_T is the tensor-type coupling constant defined by :

$$\frac{2G_T}{\sqrt{2}} (\bar{\nu} \sigma_{\lambda\tau} \nu)(\bar{\ell} \sigma_{\lambda\tau} \ell) \tag{3.7}$$

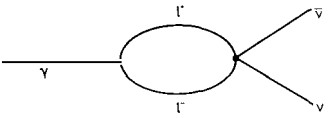

FIGURE I

Note that ℓ can also be a "quark". Now a photon in astrophysical plasma can be visualized as having a small effective mass :

$$m_{eff}\, c^2 = \hbar\, \omega_p \tag{3.8}$$

where ω_p is the plasma frequency. With a finite magnetic moment for ν, a plasma photon can decay into a $\nu\bar{\nu}$ pair. This mechanism may be relevant in stellar evolution where a transition from the high luminosity stage to the white dwarf stage takes place. Too high a ν production rate due to :

$$\gamma_{\text{plasma photon}} \rightarrow \nu + \bar{\nu} \tag{3.9}$$

implies that the cooling of a white dwarf would be too rapid, resulting in a marked deficiency in the distribution of white dwarfs. For quantitative estimates everything depends on what one uses for $\ell^{\pm}$ and the cut off Λ, but knowing that there are "quarks" at $\sim$ 300 MeV, heavy leptons at 1.8 GeV, etc ..., we may conservatively set :

$$(m_\ell/m_\mu)\ \ell n\ (\Lambda/m_\mu) \gtrsim 6 \tag{3.10}$$

Then the astrophysical cooling time inferred from the distribution of white dwarfs implies :

$$G_T/G \lesssim 1/15 \tag{3.11}$$

which is too small to account for the observed neutral current interactions. Since pure SP was already ruled out by the E_{had} distributions of the Caltech group, the situation does not look too promising for SPT enthusiasts.

QUESTION 4 : ARE THE NEUTRAL CURRENT INTERACTIONS PURE V, V-A OR IN BETWEEN ?

Having disposed of the "SPT heresy", I now proceed to discuss the space-time structure of neutral currents under the more orthodox assumption that only V and A are involved.

To start with let us review what we expect on the basis of the most naive version of quark parton models. When the antiquark content within the nucleon is ignored, we have the following well-known predictions for the y distribution in deep inelastic reactions.

$$\begin{aligned} &\text{V-A} && : \ 1 \text{ for } \nu, \ (1-y)^2 \text{ for } \bar{\nu} \\ &\text{V+A} && : \ (1-y)^2 \text{ for } \nu, \ 1 \text{ for } \bar{\nu} \\ &\text{pure V/pure A} && : \ \tfrac{1}{2}\left[1 + (1-y)^2\right] \text{ for both} \end{aligned} \tag{4.1}$$

The famous 1-to-3 ratio for $\sigma(\nu \to \mu^-)/\sigma(\bar{\nu} \to \mu^+)$ readily follows upon integration :

$$\frac{\int_0^1 (1-y)^2 \, dy}{\int_0^1 dy} = \frac{1}{3} \tag{4.2}$$

The neutral-to-charged current ratio usually quoted in the literature refers to :

$$R_{\overset{(-)}{\nu}} \equiv \frac{\sigma(\overset{(-)}{\nu} + N \to \overset{(-)}{\nu} + \text{hadrons})}{\sigma(\overset{(-)}{\nu} + N \to \mu^{-(+)} + \text{hadrons})} \tag{4.3}$$

where N stands for the average of proton and neutron. In terms of these ratios, we have :

$$\begin{aligned} &\text{V-A} && : \ R_\nu = R_{\bar{\nu}} \\ &\text{pure V/pure A} && : \ R_\nu = \tfrac{1}{3} R_{\bar{\nu}} \end{aligned} \tag{4.4}$$

Having stated what we expect on the basis of the naive quark parton model, I now would like to make a few cautionary remarks. At Gargamelle energies, a substantial fraction of events is eliminated by energy cuts ; when the experimentalists accept only events with $E_{had} > 1$ GeV, the $\bar{\nu}$-to-ν ratio for the charged-current case is no longer 1/3 but more like 0.25, which means

that the pure V/pure A prediction should be more like $R_\nu \simeq (1/4)R_{\bar{\nu}}$. At Fermilab energies, we must take account of the famous y distribution anomaly and the $\bar{\nu}$-to-ν ratio anomaly in the charged-current data reported by the HPW collaboration.

To be specific, let us suppose that the y distribution for the neutral-current ν data is not flat but has a nonvanishing $(1-y)^2$ component. This can be due to two reasons.

(i) The basic current is still V-A but the antiquark content in the quark model language is nonnegligible.

(ii) We have a genuine V+A current as well as V-A.

To disentangle the two effects a careful analysis of the charged-current data is needed ; for example, it is important to examine whether the deviations from the canonical expectations seen in the charged-current data are due to new particle production via V+A or to q^2 dependent scaling violations.

With these cautionary remarks in mind, you are invited to look at the latest experimental data reported by Mme Brisson (Gargamelle) and Bodek (Caltech). As far as I can see, both groups find that the best fit is somewhere between pure V/pure A and V-A. The Gargamelle Collaboration is closer to V-A than to pure V/pure A while the Caltech group is closer to pure V/pure A than to V-A. It is probably fair to say that neither pure V/pure A nor pure V-A is conclusively ruled out.

A question often asked is : how much of what one usually does with the neutral-to-charged current ratio etc ... is independent of the validity of the quark parton model ? In a model in which the neutral and charged currents are related simply via isospin rotations, we can derive clean relations just based on isospin invariance. Suppose the hadronic part of neutral currents is pure isovector and is related to the charged current via simple isospin rotations. The relevant interaction is given by :

$$\mathcal{L} = (G/\sqrt{2}) \left\{ \left[i\bar{\mu}\gamma_\lambda (1+\gamma_5)\, \nu\, (j_\lambda^{1+i2} + j_{5\lambda}^{1-i2}) + \text{H.C.} \right] \right.$$
$$\left. + i\bar{\nu}\gamma_\lambda (1+\gamma_5)\, \nu\, (v_3\, j_\lambda^3 + a_3\, j_{5\lambda}^3) \right\} \qquad (4.5)$$

where v_3 and a_3 are the vector and axial vector coupling constants. In such a model, with the additional "chiral symmetry" assumption that the vector and axial vector contributions to the charged-current reactions are equal,

we can readily derive :

$$\frac{1}{4}\,(v_3^2 + a_3^2) = \frac{\sigma(\nu\to\nu) + \sigma(\bar{\nu}\to\bar{\nu})}{\sigma(\nu\to\mu^-) + \sigma(\bar{\nu}\to\mu^+)} \tag{4.6.a}$$

$$\frac{1}{2}\,v_3\,a_3 = \frac{\sigma(\nu\to\nu) - \sigma(\bar{\nu}\to\bar{\nu})}{\sigma(\nu\to\mu^-) - \sigma(\bar{\nu}\to\mu^+)} \tag{4.6.b}$$

where $\sigma(\nu\to\nu)$ stands for the cross section for $\nu+N \to \nu+$hadrons, etc ...

When there is also an isoscalar component, the neutral and charged currents are no longer related via simple isospin rotations. We must rely on models, viz, the quark parton model with valence quark dominance. The net result is to change (4.6.a) and (4.6.b) to :

$$\frac{1}{4}\,(v_3^2 + a_3^2) + \frac{1}{9}\,(v_s^2 + a_s^2) = \frac{\sigma(\nu\to\nu) + \sigma(\bar{\nu}\to\bar{\nu})}{\sigma(\nu\to\mu^-) + \sigma(\bar{\nu}\to\mu^+)} \tag{4.7.a}$$

$$\frac{1}{2}\,v_3\,a_3 + \frac{2}{9}\,v_s\,a_s = \frac{\sigma(\nu\to\nu) - \sigma(\bar{\nu}\to\bar{\nu})}{\sigma(\nu\to\mu^-) - \sigma(\bar{\nu}\to\mu^+)} \tag{4.7.b}$$

where the isoscalar constants v_s and a_s are defined by :

$$\mathcal{L}_{\text{isosc}} = (G/\sqrt{2})\; i\bar{\nu}\gamma_\lambda(1+\gamma_5)\,\nu\;(v_s\,j^s_\lambda + a_s\,j^s_{5\lambda}) \tag{4.8}$$

$$j^s_\lambda = \frac{i}{3}\,(\bar{u}\gamma_\lambda u + \bar{d}\gamma_\lambda d + \ldots) \tag{4.9.a}$$

$$j^s_{5\lambda} = \frac{i}{3}\,(\bar{u}\gamma_\lambda\gamma_5 u + \bar{d}\gamma_\lambda\gamma_5 d + \ldots) \tag{4.9.b}$$

I have tried to present a general framework for discussing the deep inelastic reactions without commitment to particular models. If we so desire, we can, of course, easily specialize to any of your favorite models. For example, for the one-parameter Weinberg-Salam model, just set :

$$\begin{aligned} v_3 &= 1 - 2\sin^2\theta_W \qquad & a_3 &= 1 \\ v_s &= -\sin^2\theta_W & a_s &= 0 \end{aligned} \tag{4.10}$$

When the data are analyzed under the assumption that the current is predominantly isovector, there is a solution - an "axial-vector dominant solution" such that :

$$|a_3| \simeq 1 \tag{4.11}$$

with a small vector part. This is often taken as evidence in favor of the Weinberg-Salam model, the simplest (one-parameter) version of which requires a_3 to be unity.

From a more general point of view, however, the same data also admit a "vector-dominant solution" such that :

$$|v_3| \simeq 1 \tag{4.12}$$

with a small axial-vector part. Using the inclusive data alone, it is impossible to tell whether the vector-dominant or the axial-vector-dominant solution is the correct one. To answer that question, we look at some exclusive channels - e.g. diffractive production of A_1 and ρ, to which I'll come back later. Another way is to look for a low energy transition which selects A or V only. For instance, the reaction :

$$\bar{\nu} + D \to \bar{\nu} + n + p \tag{4.13}$$

at low (reactor) energies directly measures the strength of the isovector axial part of the neutral current.

There are now several models that predict that the neutral currents are pure vector. I wish to emphasize that to test the pure V (or pure A) hypothesis we need not necessarily look at the inclusive data. We simply test :

$$d\sigma(\nu+I \to \nu+F) = d\sigma(\bar{\nu}+I \to \bar{\nu}+F) \tag{4.14}$$

between any pair of initial and final states. The target I need not be isoscalar ; the reaction can be exclusive or inclusive ; the cross section can be differential or integrated ; you may apply any angular or energy cut as long as the same cuts are applied to both sides. The equality (4.14) is a rigorous consequence of Hermiticity and absence of VA interference. Obviously the fact that such an equality relation is satisfied for some reaction does not prove that the interaction is pure vector or pure axial vector. It is most informative to test this kind of equality in reactions where the analogous charged current reactions are known to exhibit VA interference.

QUESTION 5 : WHAT ARE THE ISOSPIN AND SU(3) [... SU(n)] PROPERTIES OF THE HADRONIC NEUTRAL CURRENT ?

The hadronic part of the neutral currents is nonstrange (S = 0) ; in addition Q = B = 0, of course. So just from the Gell-Mann-Niahijima rule

we have :

$$I_3 = Q - \frac{S+B}{2} = 0 \tag{5.1}$$

which leaves us with the following possibilities :

$$I = 0, 1, 2, \ldots \tag{5.2}$$

We are prejudiced against I = 2 or higher because (i) it is difficult to make a bilinear current with $I \geq 2$ using quark fields, and (ii) there is no evidence for $I \geq 2$ currents in the electromagnetic interactions nor in the charged-current weak interactions. In the following I assume that the current is isovector (I = 1) and/or isoscalar (I = 0).

The classical way to determine the isospin properties of the current is to study single pion production :

$$\begin{aligned} &\nu + p \to \nu + \pi^\circ + p, \ \nu + \pi^+ + n \\ &\nu + n \to \nu + \pi^\circ + n, \ \nu + \pi^- + p \end{aligned} \tag{5.3}$$

If the current is pure isoscalar, only I = 1/2 πN final states are possible. So we expect :

$$\sigma(\pi^\circ p) \ : \ \sigma(\pi^+ n) \ : \ \sigma(\pi^\circ n) \ : \ \sigma(\pi^- p) = 1 : 2 : 1 : 2 \tag{5.4}$$

If the current is isovector, both I = 1/2 and I = 3/2 final states are possible. However, if we work in the $W \simeq 1236$ MeV region, it may be reasonable to expect that the reactions (5.3) are dominated by $\Delta(1236)$ provided, of course, that the current is predominantly isovector. We then expect :

$$\sigma(\pi^\circ p) \ : \ \sigma(\pi^+ n) \ : \ \sigma(\pi^\circ n) \ : \ \sigma(\pi^- p) = 2 : 1 : 2 : 1 \tag{5.5}$$

in sharp contrast with (5.4)

Experimentally there was data from the ANL bubble chamber group favoring isovector, but that result was not regarded as conclusive evidence against pure isoscalar. More recently, the Gargamelle Collaboration has stud-ied the π^--to-π° ratio in single pion production. If we have a pure isoscalar current on an isoscalar target, the π^+-to-π^--to-π° ratios must be 1 : 1 : 1 ; this is clear because we have no preferred direction in isospin space to start with. Furthermore, this conclusion holds even in the presence of

final state interactions among nucleons and pions since the nuclear charge exchange corrections are expected to obey charge independence. The high π°-to-π ratio reported by Mme Brisson at this meeting shows that the pure isoscalar hypothesis is ruled out. We are forced to conclude that there must be a substantial amount of isovector.

There is, however, one final check to be made before a firm conclusion is to be reached. If the neutral current is predominantly (if not purely) isovector, there must be a strong Δ signal in the neutral current reactions (5.3). This is an inevitable consequence of isospin invariance because a Δ signal shows up strongly in both charged-current single pion production and single pion electroproduction. The $\pi^\circ p$ mass distributions observed by both the Columbia-Illinois-Rockefeller Collaboration and the Gargamelle Collaboration are inconclusive in this respect (see Goulianos' report), and this may have to do with the fact that the target used is Al or CF_3Br_2. Obviously it is desirable to look for a clean Δ signal in the $\pi^- p$ combination using D_2 targets.

In any case, it appears now from the Gargamelle data that the current is not pure isoscalar. The next natural question is : is it pure isovector ? To answer this question we must study isovector-isoscalar interference. For definiteness let us take pion inclusive reactions :

$$\nu + N \to \nu + \pi^{\pm,o} + X \tag{5.6}$$

where, as usual, N stands for the nucleon averaged over equal numbers of protons and neutrons. For a pure isoscalar current we obviously expect :

$$\sigma(\pi^+) \;:\; \sigma(\pi^\circ) \;:\; \sigma(\pi^-) = 1 : 1 : 1 \tag{5.7}$$

which relation, according to the Aachen side of the Gargamelle Collaboration, is also in difficulty, while the combination :

$$\sigma(\pi^+) + \sigma(\pi^-) - 2\,\sigma(\pi^\circ) \tag{5.8}$$

isolates the isovector contribution. Isoscalar-isovector interference can be obtained by looking at :

$$\begin{aligned} A_\nu &\equiv \sigma(\nu N \to \nu\pi^+ X) - \sigma(\nu N \to \nu\pi^- X) \\ A_{\bar\nu} &\equiv \sigma(\bar\nu N \to \bar\nu\pi^+ X) - \sigma(\bar\nu N \to \bar\nu\pi^- X) \end{aligned} \tag{5.9}$$

The sum and the difference of A_ν and $A_{\bar{\nu}}$ are proportional to products of isoscalar and isovector constants as follows :

$$A_\nu + A_{\bar{\nu}} \propto v_3 v_s,\ a_3 a_s$$
$$A_\nu - A_{\bar{\nu}} \propto v_3 a_s,\ v_s a_3 \qquad (5.10)$$

If we have separate data on proton and neutron targets (e.g. H_2 and D_2 bubble chamber experiments), we may study isovector-isoscalar interference in the following manner. If the current is isospin pure, i.e. pure I=1 or pure I=0, we, of course, expect :

$$\sigma(\nu p \to \nu X^+) = \sigma(\nu n \to \nu X^\circ)$$
$$\sigma(\bar{\nu} p \to \bar{\nu} X^+) = \sigma(\bar{\nu} n \to \bar{\nu} X^\circ) \qquad (5.11)$$

where X may be any hadronic state, exclusive or inclusive.

Deviations from these equality relations would provide conclusive evidence for the presence of isovector-isoscalar interference.

If an isoscalar piece is indeed present, we may examine its SU(3) (or SU(4), etc ...) properties. Even in the days when it was believed that there were only three flavors, we could consider two independent isoscalars :

$$\frac{1}{3}(\bar{u}u + \bar{d}d) - \frac{2}{3}\bar{s}s$$
$$\frac{1}{3}(\bar{u}u + \bar{d}d + \bar{s}s) \qquad (5.12)$$

The first transforms like the eight component of an SU(3) octet (e.g. the isoscalar part of the electromagnetic current) while the second transforms like a unitary singlet (e.g. the baryon current). The difference is $\bar{s}s$, a ϕ like piece. This is unfortunate. Within the framework of naive quark models which visualize the nucleon as being made up of three valence quarks, the deep inelastic inclusive reactions are insensitive to the presence or absence of a ϕ like piece. Resonance excitation (N^* production) does not help either because $\phi N \to N^*$ is forbidden by the Zweig (or Okubo-Iizuka) rule. To isolate a ϕ like component, we must look at Pomeron exchange reactions that violate the Zweig rule, e.g. diffractive ω and ϕ production. We'll come back to this point later.

If we start adding quarks of more exotic flavors - $\bar{c}c(\psi/J$ like), $\bar{t}t$, $\bar{b}b$, ... - the situation becomes even more involved. It seems practically impossible to propose an experiment to determine, for instance, the amount of

a $\bar{t}t$ component in the neutral currents.

QUESTION 6 : WHY STUDY EXCLUSIVE REACTIONS ?

One of the most important exclusive reactions is elastic p scattering :

$$\nu + p \to \nu + p \tag{6.1}$$

In a certain sense this reaction is as fundamental as neutron beta decay. At $q^2 = 0$ various models give simple and definitive predictions :

$$R_{el}\Big|_{q^2=0} \equiv \left.\frac{\frac{d\sigma}{dq^2}(\nu p \to \nu p)}{\frac{d\sigma}{dq^2}(\nu n \to \mu^- p)}\right|_{q^2=0}$$

$$= \begin{cases} \dfrac{v_3^2 + (1.25)^2 a_3^2}{4\left[1 + (1.25)^2\right]} & , \text{ pure isovector} \\ \dfrac{(1 - 4\sin^2\theta_W)^2 + (1.25)^2}{4\left[1 + (1.25)^2\right]} & , \text{ Weinberg Salam} \\ \dfrac{v_s^2}{1 + (1.25)^2} & , \text{ isoscalar vector} \end{cases} \tag{6.2}$$

As we go away from $q^2=0$, the predictions become more complicated because of form factors and also because of VA interference which depends both on q^2 and E. This is unfortunate ; experimentally low q^2 events are difficult to study because (i) the recoil kinetic energy of the proton is low, and (ii) the neutron background is most serious when q^2 is small. Despite these difficulties we are pleased to hear at this meeting that the Columbia-Illinois-Rockefeller Collaboration now has positive evidence for the elastic reaction (6.1) with q^2 between 0.3 GeV^2 and 1 GeV^2 (c.f. Goulianos' report).

Going up in the hadronic mass W, the next channel we encounter is π+N. The soft-pion techniques developed in the sixties enable us to relate single pion production near threshold to elastic νp scattering. Earlier attempts to compare the experimental data and the soft-pion predictions caused a great deal of excitement because the measured cross section for :

$$\nu+n \rightarrow \nu+\pi^- +p \qquad (6.3)$$

near threshold was an order of magnitude higher than the soft-pion expectations with any combination of V and A. Fortunately, or unfortunately, the data showing threshold enhancement, which stimulated many interesting speculations - SPT, second-class V, A etc ..., - have subsequently been withdrawn.

A great deal of theoretical work has been done on $\Delta(1236)$ production ; however, I won't discuss it here. Let me instead turn to diffractive production of vector and/or axial vector mesons. We first recall that in photoproduction and also in low q^2 electroproduction, the reactions :

$$\gamma(\text{real or virtual}) + p \rightarrow (\rho^\circ, \omega, \phi) + p \qquad (6.4)$$

are extremely important. Furthermore these vector meson states, having the same quantum numbers as the proton ($J^{PC} = 1^{--}$), are produced with all the features we expect from "diffraction" - energy independent cross sections, diffraction slopes characteristic of elastic scattering, sharp coherent peaks when nuclear targets are used, etc ... Likewise we expect that in neutrino reactions :

$$\nu+N \rightarrow \nu + (\rho^\circ, \omega, \phi, A_1^\circ, \ldots) + N \qquad (6.5)$$

the states with the same quantum numbers as the current get filtered out :

ρ for isovector vector
ω and ϕ for isoscalar vector
A_1 for isovector axial vector

There have been many calculations on these diffractive processes based on vector (and axial vector) meson dominance. Such estimates may not be too reliable in quantitative details. Fortunately various model uncertainties cancel when comparisons are made with the analogous charged current processes, e. g. :

$$\left.\frac{\sigma(\nu+N \rightarrow \nu+\rho^\circ+N)}{\sigma(\nu+N \rightarrow \mu^-+\rho^++N)}\right|_{\text{diff.}} = \frac{1}{2} v_3^2 \overset{SW}{=} \frac{1}{2}(1 - 2\sin^2\theta_W)^2 \qquad (6.6.a)$$

$$\left.\frac{\sigma(\nu+N \rightarrow \nu+A_1^\circ+N)}{\sigma(\nu+N \rightarrow \mu^-+A_1^++N)}\right|_{\text{diff.}} = \frac{1}{2} a_3^2 \overset{SW}{=} \frac{1}{2} \qquad (6.6.b)$$

where SW stands for Salam-Weinberg. Notice, in particular, that we can examine whether the vector dominant or axial-vector dominant solution is the right one. As for ω and ϕ, a careful study would in principle determine whether the isoscalar vector part of the neutral currents is an SU(3) singlet or belongs to the same SU(3) octet as the isovector part.

Finally I wish to mention coherent scattering off nuclei :

$$\nu + A \rightarrow \nu + A$$

where A stands for some complex nucleus. A coherent effect is expected when the contributions from the various nucleons add up in the amplitude, and in our case this is possible only through the isoscalar vector piece of the neutral currents. Much importance has been attached to this process because it might provide a mechanism for triggering a supernova explosion. Detailed calculations show, however, that in models with predominantly axial vector couplings such as the Weinberg-Salam model with $\sin^2 \theta_W \simeq 0.35$, it is unlikely that the νFe scattering cross section predicted is of sufficient strength to blow off the outer layer of a collapsed stellar object.

QUESTION 7 : WHAT CAN WE LEARN FROM NEUTRINO-ELECTRON SCATTERING ?

Let us now turn to neutrino-electron scattering. There are four reactions of interest :

$$\nu_e + e^- \rightarrow \nu_e + e^- \qquad (7.1.a)$$

$$\bar{\nu}_e + e^- \rightarrow \bar{\nu}_e + e^- \qquad (7.1.b)$$

$$\nu_\mu + e^- \rightarrow \nu_\mu + e^- \qquad (7.1.c)$$

$$\bar{\nu}_\mu + e^- \rightarrow \bar{\nu}_\mu + e^- \qquad (7.1.d)$$

Of these (7.1.c) and (7.1.d) are allowed only by the neutral-current interactions while (7.1.a) and (7.1.b) are allowed even in the old V-A charged-current theory which permits the appearance of the current in the u and the s channel, respectively. So observation of (7.1.c) or (7.1.d) can be taken as firm evidence for the existence of neutral currents whereas to establish neutral current effects in (7.1.a) and (7.1.b) detailed studies of the rate and the spectrum shape are needed.

There are now three events of $\bar{\nu}_\mu e$ scattering reported by the

Gargamelle Collaboration. The cross section corresponding to the observed three events is of the order of 10^{-42} cm^2 E (E in GeV). Perhaps the most important conclusion we can draw from the data is that the effective strength of the $\bar{\nu}_\mu e^-$ interaction is not too different from that of the semileptonic neutral current interactions. An $\bar{\nu}e$ cross section of 10^{-42} cm^2 E corresponds to a cross section of 0.06 G^2s/π ; in comparison, for hadronic final states, the observed neutral current inclusive cross sections for ν and $\bar{\nu}$ are typically in the range (0.04 - 0.06) G^2s/π per nucleon. So, independently of any detailed theory, we can conclude that the coupling strength of $\bar{e}e$ to $\bar{\nu}_\mu \nu_\mu$ is not too different from that of $\bar{q}q$ to $\bar{\nu}_\mu \nu_\mu$. In other words we have rough "universality", at least.

For a more quantitative formulation of universality, we must, of course, specify the group structure of the leptonic and hadronic currents. Definite predictions on the vector and axial vector coupling constants for $\nu_\mu e$, $\bar{\nu}_\mu e$ scattering can then be made. For example, in the (one-parameter) Weinberg-Salam model based on SU(2) $\otimes$ U(1) the coupling constants g_V and g_A defined by :

$$\mathcal{L} = - (G/\sqrt{2})\, \bar{\nu}_\mu \gamma_\lambda (1+\gamma_5)\, \nu_\mu\, \bar{e} \gamma_\lambda\, (g_V + g_A \gamma_5) e \qquad (7.2)$$

are given by :

$$g_V = - \frac{1}{2} + 2 \sin^2 \theta_W \,, \quad g_A = - \frac{1}{2} \qquad (7.3)$$

with $\sin^2 \theta_W$ already determined from the semileptonic data to be ~ 0.35.

I'll not present a detailed comparison between the data and various theoretical models except to emphasize that it is desirable to design an experiment that determines both g_V and g_A <u>separately</u>. When one compares the data with the (one-parameter) Weinberg-Salam model, one is, in effect, asking : What is the value of g_V when g_A is constrained to be - 1/2 ? The most objective way to show the experimental results is to display the constraints imposed by the data on a g_V-g_A plane. Such a plot is presented at this meeting by Mme Brisson.

QUESTION 8 : CAN WE DETECT NEUTRAL-CURRENT EFFECTS IN PROCESSES NOT INVOLVING NEUTRINOS ?

Even though we know from comparison between $\bar{\nu}_\mu e$ scattering and semileptonic inelastic reactions that $\bar{q}q$ and $\bar{\ell}\ell$ (ℓ = e and presumably also μ by μe universality) enter in the neutral currents with similar strength, we cannot

yet conclude that $\bar{\nu}\nu$ enters with similar strength. We can conceive of a crazy model in which the coefficients in front of $\bar{q}q$ and $\bar{\ell}\ell$ are both enhanced by a factor of r compared to models based on nomal universality while that in front of $\bar{\nu}\nu$ is down by $1/r$. To eliminate such a possibility it is essential that we detect neutral current effects in at least one reaction not involving neutrinos.

The most spectacular effect of neutral currents along this line would be the direct formation of a weak neutral boson Z in electron-positron collisions. In normal models based on universality the partial decay width of Z into e^+e^- goes as :

$$\Gamma(Z \to e^+e^-) \sim G\, m_Z^3 \tag{8.1}$$

just from dimensional considerations. Recall that even though we now know that ψ is a hadron, the leptonic decay width of ψ is about what one would expect for a weak boson of mass $\sim m_\psi$. This means that a higher mass weak boson would give rise to an effect even more spectacular than the ψ peak that shook the world.

Even if the Z boson turns out to be too massive (as in the Weinberg-Salam model) to be produced directly in electron-positron collisions in the near future, we are likely to start detecting neutral current effects in :

$$e^+ + e^- \to \mu^+ + \mu^- \tag{8.2}$$

in the kind of colliding beam machines now under construction.

With a Z mass much higher than the center-of-mass energy of the e^+e^- system, denoted by $\sqrt{s}$, the ratio of the weak amplitude to the electromagnetic amplitude goes roughly as :

$$A_{NC}/A_{EM} \sim G/(e^2/s) \sim 10^{-4}s \qquad (s \text{ in GeV}^2) \tag{8.3}$$

Thus, at sufficiently high energies, the weak amplitude becomes comparable to the electromagnetic amplitude. Even at moderate energies, say, $s \sim 10^3$ GeV^2, we may be able to detect significant interference effects.

To be quantitative let us write down the most general interaction with μe universality :

$$\mathcal{L} = -(G/\sqrt{2})\,[h_{VV}\,(\bar{e}\gamma_\lambda e + \bar{\mu}\gamma_\lambda \mu)(\bar{e}\gamma_\lambda e + \bar{\mu}\gamma_\lambda \mu)$$

$$+ 2\,h_{VA}\,(\bar{e}\gamma_\lambda e + \bar{\mu}\gamma_\lambda \mu)(\bar{e}\gamma_\lambda \gamma_5 e + \bar{\mu}\gamma_\lambda \gamma_5 \mu) \qquad (8.4)$$

$$+ h_{AA}\,(\bar{e}\gamma_\lambda \gamma_5 e + \bar{\mu}\gamma_\lambda \gamma_5 \mu)(\bar{e}\gamma_\lambda \gamma_5 e + \bar{\mu}\gamma_\lambda \gamma_5 \mu)]$$

where I have assumed $m_Z \gg \sqrt{s}$. If the interaction arises from the exhange of a single weak boson, then we must have :

$$h_{VA}^2 = h_{VV} h_{AA} \qquad (8.5)$$

However, if there are several intermediate bosons, all we can say is :

$$0 \leqslant h_{VA}^2 < h_{VV} h_{AA} \qquad (8.6)$$

So it is desirable to devise experiments that test each of the three terms separately. Various theoretical models give definite predictions on h_{VV}, h_{VA}, h_{AA}. For example, in the Weinberg-Salam model :

$$h_{VV} = \frac{1}{4}\,(1 - \sin^2\theta_W)^2$$

$$h_{VA} = \frac{1}{4}\,(1 - \sin^2\theta_W) \qquad (8.7)$$

$$h_{AA} = \frac{1}{4}$$

Weak current effects in muon pair production can be tested in three places :

(i) The magnitude and s dependence of the total cross section (sensitive to h_{VV}).

(ii) Forward-backward asymmetry (sensitive to h_{AA}).

(iii) Longitudinal polarization of the muon (sensitive to h_{VA}).

The relevant formulas are :

$$\frac{\Delta\sigma}{\sigma_{QED}} = (G/\sqrt{2}\,\pi\alpha)\,s\,h_{VV} \qquad (8.8.a)$$

$$A(\theta) \quad \frac{\sigma(\theta) - \sigma(\pi-\theta)}{\sigma(\theta) + \sigma(\pi-\theta)} = (G/\sqrt{2}\,\pi\alpha)s\, h_{AA} \left(\frac{2\cos\theta}{1+\cos^2\theta}\right) \qquad (8.8.b)$$

$$P_{\mu^+} = -P_{\mu^-} = (G/\sqrt{2}\,\pi\alpha) h_{VA}\, s \left[1 + \frac{2\cos\theta}{1+\cos^2\theta}\right] \qquad (8.8.c)$$

Just to give an order of magnitude, $(G/\sqrt{2}\,\pi\alpha)s\, h_{AA}$ is about 0.08 at $s \simeq 900$ GeV^2 in the Weinberg-Salam model (independent of θ_W) ; so forward-backward asymmetry should be comfortably measurable with a colliding beam apparatus of $E \simeq 15$ GeV each. In pure vector models h_{AA} and h_{VA} vanish, but h_{VV} is expected to be large ; so we are likely to see deviations from the QED predictions in the magnitude and the energy dependence of the muon pair cross section. It is amusing that from QED tests already performed at SPEAR energies we can already conclude :

$$h_{VV} < 6 \qquad (90\ \%\ \text{CL}) \qquad (8.9)$$

The main point I wish to emphasize is that, as long as we have rough universality, we are guaranteed to observe weak-electromagnetic interference effects at PETRA or PEP regardless of whether the interaction is predominantly axial-vector (as in the Weinberg-Salam model) or pure vector. In the 1981 Rencontre de Moriond we look forward to hearing about the first experiment to detect neutral current effects in electron-positron annihilation into muon pairs.

Neutral current effects without neutrinos can also be looked for by studying possible parity violation in atomic physics and in inelastic $\mu^{\pm}p$ scattering . However, I'll not treat them here.

oo0oo

It has been nearly three years since the dramatic discovery of neutral currents was announced by the Gargamelle Collaboration. We have to admit that the progress in this field has been rather slow when compared to the spectacular progress we made in the field of new particle spectroscopy since that fateful Sunday, November 10, 1974. Perhaps we have to be a little patient. It took twenty five years to show that nuclear beta decay interactions involve V and A.

The history of weak interaction physics has been characterized by (i) wrong experiments, and (ii) bad theoretical models based on wrong data. Let us hope that history won't repeat itself.

oo0oo

MORIOND PROCEEDINGS AVAILABLE

N° 1	First Rencontre de Moriond	: 2 vol (1966)
N° 2	Second Rencontre de Moriond	: 2 vol (1967)
N° 3	Third Rencontre de Moriond	: 2 vol (1968)
N° 4	Fourth Rencontre de Moriond	: 1 vol (1969)
N° 5	Fifth Rencontre de Moriond	: 1 vol (1970)
N° 6	Electromagnetic and Weak Interactions	: (1971)
N° 7	High-Energy Phenomenology	: (1971)
N° 8	Two Body Collisions	: (1972)
N° 9	Multiparticle phenomene and inclusive reactions	: (1972)
N° 10	Electromagnetic and Weak Interactions	: (1973)
N° 11	The Pomeron	: (1973)
N° 12	High energy hadronic interactions	: (1974)
N° 13	High energy leptonic interactions	: (1974)
N° 14	Phenomenology of hadronic Structure	: (1975)
N° 15	Charm, Color and the J	: (1975)
N° 16	New fields in hadronic physics	: (1976)
N° 17	Weak Interactions and neutrino physics	: (1976)
N° 18	Storage Ring Physics	: (1976)

All order should be sent to
Rencontre de Moriond
Laboratoire de Physique Théorique et Particules Elémentaires
Bâtiment 211 - Université Paris Sud
91405 ORSAY (France)

13 HIGH ENERGY LEPTONIC INTERACTIONS

Proceedings of the second session of the Ninth Rencontre de Moriond
3-15 March 1974

CONTENTS

I - Weak charged currents

M. Gourdin, Inclusive neutrino and antineutrino reactions and chargel currents ; B. Degrange, Tests of scale invariance in the " Gargamelle " neutrino-experiment ; A. Benvenuti, Recent results on ν, ν charged current interactions at NAL.

II - Weak neutral currents

P. Fayet, Introduction to weak neutral currents ; L. Kluberg, Neutral currents in Gargamelle ; D.D. Reeder, The status of the search for muonless events in the broad band neutrino beam at NAL.

III - Electron-Positron annihilation

H.L. Lynch, Preliminary results on hadron production in electron positron collisions at spear ; C.H. Llewellyn Smith, Remarks on e^+e^- annihilation ; H.R. Rubinstein, e^+e^-: six or more pions in search of a theory ; F. Renard, Vector mesons and e^+e^- annihilation ; M. Greco, The possible role of two photon processes in high energy colliding beam experiments ; M. Krammer, Electromagnetic properties of hadrons in a relativistic quark model.

IV - Inclusive photoproduction and electroproduction

J. Gandsman, Inclusive photoproduction and the triple Regge formula ; H. Nagel, Electroproduction in a streamer chamber : multiplicities, inclusive cross sections and vector meson production ; A.J. HEY, What do we learn from deep inelastic scattering with polarized targets ? ; F.E. Close, Why polarized electroproduction is interesting ; S. Kitakado, Dual quarks and parton quarks.

14 PHENOMENOLOGY OF HADRONIC STRUCTURE

CONTENTS

I - DIFFRACTION AND ELASTIC SCATTERING

G. Goggi, Single and double diffraction dissociation at FNAL and ISR energies ; **P. Strolin,** Diffractive production of the $p\pi^+\pi^-$ system at the ISR ; **S.L. Olsen,** Coherent diffraction dissociation of protons on deuterium at high energies ; **G. Goggi,** Preliminary results on double diffraction dissociation ; **E. Nagy,** Experimental results on large angle elastic pp scattering at the CERN ISR ; **A. Capella,** Elastic scattering in the Reggeon calculus at ISR energies ; **C.E. De Tar,** How can we trust the Reggeon calculus ? ; **R. Savit,** High energy scattering as a critical phenomena ; **J.S. Ball,** Seft consistent diffraction in the multiperipheral model ; **U. Maor,** Comments on the systematics of Pomeron exchange reactions ; **P. Kroll,** Geometrical scaling in proton scattering ; **A. Martin,** Does the Pomeron obey geometrical scaling ? ; **N.G. Antoniou,** Effects of the inclusive dipole Pomeron to exclusive processes.

II - TWO BODY SCATTERING

A. Yokosawa, pp scattering amplitude measurements with polarized beam and polarized targets at 2 to 6 GeV/c ; **A. Contogouris,** The structure of amplitudes of two-body reactions ; **F. Schrempp,** Towards a solution for the helicity dependence of scattering amplitudes ; **B. Schrempp,** Geometrical versus constituent interpretation of large angle exclusive scattering.

III - MULTIPARTICLE PRODUCTION

F. Sannes, Inclusive cross sections for $p+n \to p+X$ between 50 and 400 GeV ; **G. Jarlskog,** Results on inclusive charged particle production in the central region at the CERN ISR ; **R. Castaldi,** Measurements on two-particle correlations at the CERN ISR ; **A. Menzione,** Semi-inclusive correlations at the CERN ISR and cluster interpretation of results ; **A. Dar,** Multiparticle production in particle-nucleus collisions at high energies ; **E.H. de Groot,** Independent cluster production and the KNO scaling function ; **P. Schubelin,** Final state characteristics of central pp collisions at 28.5 GeV/c ; **L. Mandelli,** Meson spectroscopy with the Omega spectrometer ; **A. Krzywicki,** Local compensation of quantum number and shadow scattering ; **C. Michael,** Impact parameter structure of multi-body processes; **N. Sakai,** Helicity structure of the triple Regge formula.

IV - MISCELLANEOUS

E.J. Squires, Hadronic interactions in bag models ; **G.L. Kane,** Does it matter that the A1 does not exist ? ; **H. Moreno,** A stationary phase approach to high energy hadronic scattering ; **M.M. Islam,** Impact parameter representation without high energy, small-angle limitation ; **G.R. Farrar,** How to learn about hadron dynamics from an underlying quark-gluon field theory.

V. - CONCLUSIONS

A. Yokosawa, Conclusions and outlook.

15 CHARM, COLOR AND THE $\mathcal{Y}$

CONTENTS

J. TRAN THANH VAN : INTRODUCTION

I. - NEW RESONANCES, CHARM AND COLOR

U. Becker, Discovery of J (3.1) in lepton production by hadrons collisions ; **M. Breidenbach,** The ψ (3.1) and the search for other narrow resonances of SPEAR ; **J.A. Kadyk,** Some properties of the ψ (3.7) resonance ; **B.H. Wiik,** The experimental program at DORIS and a first look at the new resonances ; **G. Penso** and **M. Piccolo,** Status report on ψ (3.1) resonance from Adone ; **F.E. Close,** Charmless colourful models of the new mesons ; **D. Schildknecht,** Color and the new particles : A brief review ; **M.K. Gaillard,** Charm ; **G. Altarelli,** On weak decays of charmed hadrons ; **T. Inami,** Pomeron coupling to charmed particles ; **M. Teper,** The SU (4) character of the Pomeron ; **J. Kuti,** Extended particle model with quark confinement and charmonium spectroscopy ; **M. Gourdin,** Mass formulae and mixing in SU (4) symmetry ; **M.M. Nussbaum,** Preliminary results of our charm search ; **C.A. Heusch,** The experimental search for charmed hadrons.

II. - MISCELLANEOUS

G. Goggi, Inclusive hadron production at high momentum at SPEAR I ; **F.M. Renard,** Theoretical studies for lepton production in hadronic collisions ; **K. Schilling,** Jet structure and approach to scaling in e^+e^- annihilation ; **G.W. London,** Comment concerning the conservation of lepton number ; **J.C. Raynal,** SU (6) strong breaking, structure functions and static properties of the nucleon.

III - NEUTRINO REACTIONS

P. Musset, Review of the experimental status of neutral current reactions in GARGAMELLE ; **Nguyen Khac Ung,** Neutrino and antineutrino interactions in GARGAMELLE ; **F. Merritt,** Recent neutral current experiments in the Fermilab narrow band beam ; **E. Paschos,** Neutral currents in semileptonic reactions.

IV - CONCLUSIONS

J. Kuti, Conclusions.

16 NEW FIELDS IN HADRONIC PHYSICS

CONTENTS

I - NEW PARTICLES

J.J. Aubert, « A new particle in hadron interactions » ; D.I. Meyer, « Hadron production of the new particles at FNAL » ; P.G.O. Freund, « New approaches to unified theory » ; D. Sivers, « Where has all the charm gone ? » ;

II - MESON AND BARYON SPECTROSCOPY

Ph. Gavillet, « New results in meson spectroscopy » ; S.M. Flatte, « An unconventional view of meson resonances » ; N.M. Cason, « Evidence for a new scalar meson » ; L. Montanet, « Search for high mass mesons coupled to the NN system » ; P.J. Litchfield, « Baryon spectroscopy » ; J.O. Dickey, « Resonance background predictions and their application to phase shift analysis » ; A.D. Martin, « Analyticity and $\varrho' \to \pi\pi$ » ; A.G.H. Hey, « Meson spectroscopy and quark models » ; H. Lipkin, « Who undestands the Zweig-Iizuka rule ? » ; R.L. Jaffe, « Some spectroscopic problems in the bag theory of quark confinement » ; N.S. Craigie, « Structure of hadronic final states and confined quarks ».

III - MISCELLANEOUS

F. Wagner, « The additive quark model for Δ and Y* reactions » ; P.V. Landshoff, « Jets in large-p_T reactions » ; A. Dar, « Cumulative enhancement of J/ψ production in hadron nucleus collisions » ; K.J.M. Moriarty, « Inclusive production of ψ in the fragmentation region ».

IV - PHYSICS WITH HYPERON BEAMS

G. Sauvage, « Total cross sections and elastic scattering with hyperon beams » ; W.E. Cleland, « Inelastic hyperon-induced interactions » ; O.E. Overseth, « Experiments in neutral hyperon beams ; R.M. Brown, « Future counter experiments with charged hyperon beams » ; J.M. Gaillard, « Hyperon decays » ; H. Lipkin, « Who needs hyperon beams ? ».

V - CONCLUSIONS

R. Blankenbecler.

17 WEAK INTERACTIONS AND NEUTRINO PHYSICS

CONTENTS

I - DEEP INELASTIC SCATTERING

O. Nachtmann, « The parton model revisited » ; W.S.C. Williams, « Deep inelastic muon scattering » ; W.S.C. Williams, « Hadron production in inelastic muon scattering at 147 GeV » ; G. Coignet, « Experimental program planned at S.P.S. by the European Muon Collaboration » ; G. Parisi, « An introduction to scaling violations ».

II - NEUTRINO INTERACTIONS

M. Jaffre, « Charmed particle search in the Gargamelle neutrino experiment » ; D.C. Cundy, « The production of μ^-e+ events in high energy neutrino interactions » ; D.C. Cundy, « A study of inclusive strange particle production by neutrinos interacting in hydrogen at FNAL » ; R.N. Diamond, « Recent results on ν^-p and ν (H_2 - Ne) Interactions in the Fermilab 15' Bubble Chamber » ; M.K. Gaillard, « Aspects of charm ».

III - MISCELLANEOUS

A. Dar, « How to investigate future energy domains of particle physics with present accelerators ? » ; C.A. Dominguez, « Modified Adler sum rule and violation of charge symmetry » ; D.V. Nanopoulos, « CP violation, Heavy fermions and all that » ; A. Giazotto, « Latest results on the axial vector form factor » ; F. Hayot, « More than four quark flavors and vector-like models » ; K. Kang, « Five quark model with flavour-changing neutral current and dimuon events ».

IV - NEUTRAL CURRENTS

V. Brisson, « Neutral currents in Gargamelle » ; A. Bodek, « Experimental studies of neutral currents with the Fermilab narrow band neutrino beam » ; K. Goulianos, « Experimental study of exclusive neutral current reactions and search for μe-pairs at BNL » ; J.J. Sakurai, « Eight questions you may ask on neutral currents ».

18 STORAGE RING PHYSICS

CONTENTS

I - INTRODUCTION

J. Perez-Y-Jorba, « A short history of e+e- storage rings » ; J. Iliopoulos, « Great years ».

II - ELECTRON POSITION ANNIHILATION

B. Jean-Marie, « Multihadronic decays of ψ (3095) and ψ' (3684) » ; G. Wolf, « Radiative decays and a review of two-body hadronic decays and inclusive decay spectra of J / ψ and ψ' » ; J.S. Whitaker, « New states in the decays of ψ (3095) and ψ (3684) » ; T.F. Walsh, « A short Psion tour » ; G.F. Feldman, «Non resonant multibody production by e+e- annihilation»; F. Saltz. « Jet structure in strong and electromagnetic multihadron production » ; G. Parrour, « Electron positron annihilation at low energy ($\sqrt{s} < 1.1$ GeV)» ; F.E. Close, « Theoretical aspects of electron positron annihilation below 3 GeV » ; D.G. Coyne, « A γ-spectrometer experiment at Spear II ».

III - ISR PHYSICS

M. Jacob, « In s physics at the ISR. Definition. Knowledge and problems » ; M. Jacob, « Large p_T phenomena : Recent developpements » ; F.L. Navarria, « Teasing jets in p-p collisions at ISR energies » ; B.G. Pope, « Lepton production in hadronic reactions ».

IV - SEARCHES OF NEW PARTICLES

L.M. Lederman, « Observation of high mass e+e- pairs at Fermilab » ; K. Pretzl, « Dimuon production in proton nucleon collisions at 300 GeV/c » ; M.L. Perl, « Anamolous lepton production in e+e- annihilation » ; C.C. Morehouse, « Search for charm at e+e- storage ring » ; M. Cavalli Sforza, « Inclusive muon production at SPEAR and the hypothesis of heavy leptons » ; P. Musset, « Results of the charm search in Gargamelle » ; D.D. Reeder, « Characteristics of the muon-electron events produced in high energy neutrino interactions » ; A.K. Mann, « Evidence for a new family of hadronic matter from high energy neutrino interactions » ; S.C.C. Ting, « Search for new particles ».

V - THEORIES

J. Ellis, « Charmonium and Gauge theories » ; G. Altarelli, « Scale breaking from asymptotic freedom and neutrino scattering » ; D. Schildknecht, « Large ω scaling violations in deep inelastic scattering and new hadronic degrees of freedom » ; J. Kuti, « Bag model with pointlike quarks and the string limit » ; J. Nuyts, « A SU(2) x U(1) x U(1) gauge model of weak and electromagnetic interactions ».

VI - NEW PROJECTS

D. Trines, « PETRA » ; B.W. Montague, « Future european proton storage ring facilities » ; B. Richter, « Very high energy electron-positron colliding beams for the study of the weak interactions » ; U. Amaldi, « Linear accelerators to obtain e+e- collisions at many hundreds of GeV ».

VII - CONCLUSIONS

H. Harari, « How many quarks are there ? » ; G. Belletini, « The Flaine Meeting on Storage Ring Physics ».

IMPRIMÉ EN FRANCE